Phylogenetics and biogeography of soil invertebrates across Gondwana

A DISSERTATION PRESENTED

BY

CAITLIN BAKER

TO

THE DEPARTMENT OF ORGANISMIC AND EVOLUTIONARY BIOLOGY

IN PARTIAL FULFILLMENT OF THE REQUIREMENTS

FOR THE DEGREE OF

DOCTOR OF PHILOSOPHY

IN THE SUBJECT OF

BIOLOGY

HARVARD UNIVERSITY

CAMBRIDGE, MASSACHUSETTS

APRIL 2020

Phylogenetics and biogeography of soil invertebrates across Gondwana

ABSTRACT

Since the acceptance of plate tectonics, no topic in historical biogeography has attracted so much interest as the breakup of the former Southern Hemisphere supercontinent Gondwana. As it separated, it was thought that widely-distributed low vagility organisms passively rafted apart on the continental fragments – an idea known as Gondwanan vicariance. In this dissertation, I explore the extent to which vicariance explains biogeographic patterns in multiple groups of soil invertebrates. In **Chapter 1**, I resolve relationships in the mite harvestman family Pettalidae using RNA sequencing and phylogenomic analysis, specifically interrogating the position of an unstable taxon whose position differed in concatenation and coalescence methods. I also infer divergence times and characterize diversification patterns in the family, and find multiple instances of likely Gondwanan vicariance. In **Chapter 2**, I generate the first molecular phylogeny focused on the armored harvestman family Triaenonychidae using Sanger DNA sequencing and infer divergence times for the group. I similarly find that Triaenonychidae retains signatures of Pangaean and Gondwanan breakup, though I find at least one incidence of trans-oceanic dispersal, to New Caledonia. In **Chapter 3**, I reconstruct the evolutionary and biogeographic history of the phylum Onychophora (velvet worms) using transcriptomic analyses and divergence dating. In the temperate family Peripatopsidae, I again find signatures of Gondwanan vicariance. In the tropical family Peripatidae, though, I infer multiple instances of over-water dispersal, and hypothesize that their unique reproductive mode of placentotrophic viviparity could have enabled their colonization of oceanic islands in the Caribbean. Finally, **Chapter 4** narrows in scope to focus on a clade of triaenonychid harvestmen from New Zealand, the sister genera *Karamea* and *Sorensenella*. Using ultraconserved element sequencing, I reconstruct phylogenetic relationships, delimit species using traditional genetic and unsupervised machine learning approaches, characterize genetic diversity of the different species, and infer divergence times. My results support the existence of multiple species, many of which are undescribed and one of which is likely parthenogenetic, and find that the group retains signatures of multiple geologic and climatic events in New Zealand's history, such as the Oligocene marine transgression.

Contents

Acknowledgements

When I meet new people and tell them I study creepy-crawly soil invertebrates, reactions tend to fall into a handful of fixed categories. The most common response is, simply, "Ew, why?" But nearly as often people say, "Cool! I didn't even know that was a job that existed."

I am so unbelievably lucky to have had the opportunity to do this thesis. I've been given the time and space (and money) to think about whatever I find interesting. I got paid to leave New England in January and fly to New Zealand so I could walk around in beautiful forests looking for my animals. Twice. I spend my days surrounded by interesting and beautiful objects in the Museum of Comparative Zoology, and by interesting and beautiful people in OEB.

I have to start by thanking all of the people who have overlapped with me in the Giribet lab over the last six years. My fellow grad students Beka Buckman, Julia Cosgrove, Tauana Cunha, Vanessa Knutson, and Shoyo Sato saw me at my loopiest and lowest points, and always helped me get back on my feet. You all taught me so much about systematics, invertebrates, board games, crafting, photography, mental health, and more. A veritable army of postdocs not only helped to train me in molecular methods and bioinformatics, but also helped me strategize my thesis and career trajectories, including Ligia Benavides, David Combosch, Shahan Derkarabetian, Rosa Fernandez, Aaron Hartmann, Sarah Lemer, Juan Moles, Dennis Persson, and Martin Schwentner. I had the privilege of working with two fantastic undergraduates, Nina Armstrong and Ella Frigyik, whose enthusiasm was the perfect antidote to my mid-thesis slump and reminded me why I fell in love with arachnology and systematics in the first place. Erin McIntyre and Kate Sheridan helped me generate sequence data and organize an unholy number of harvestman specimens. And everyone down in the Invertebrate Zoology collections – Adam Baldinger, Penny Benson, Jennifer Goldstein, Sarah Kariko, Laura Leibensperger, Erin Polka, and Jennifer Trimble – not only helped me navigate

the collections and deal with paperwork, but constantly encouraged me and reminded me to keep up a life outside of the lab.

I am grateful to my committee members, Chuck Davis, Brian Farrell, and Robin Hopkins, for consistently providing me feedback on my work in spite of their hectic, jam-packed schedules. I am also thankful to all of the people outside of Harvard who chatted with me about my research at various points (or who perhaps simply tolerated my rambling on about harvestmen, or velvet worms, or systematics, or my constant referral to "Gondwana" as if it still existed), including Miquel Arnedo, Sarah Boyer, Danielle de Carle, Lauren Esposito, Guilherme Gainett, Vanessa Gonzalez, Gustavo Hormiga, Bob Kallal, Sebastian Kvist, Chris Laumer, Gustavo Miranda, Rina Morisawa, Andrew Ontano, Ricardo Pinto da Rocha, Mike Rix, Cristiano Sampaio Costa, Emily Setton, Prashant Sharma, Pietro Tardelli Canedo, and almost certainly more people that I am forgetting. There are also so many people at Harvard who have helped me, including Mary Sears, Ronnie Broadfoot, and Dorothy Barr at the Ernst Mayr Library, everyone in the Bauer Core (Jennifer Couget, Christian Daly, Patrick Dennett, Nicole El-Ali, Claire Reardon, and Emma White), Tim Sackton and the team at Research Computing, Breda Zimkus in the MCZ Cryogenic collection, Bruno de Medeiros, Anthony Geneva, Nikki Hughes, Marc Mapalo, Bridget Power, and my fellow Phylogenetics Journal Club members. Last but most certainly not least, I thank all of the inspiring, brilliant, kind people in my cohort.

I was able to go to the field not once but three times over the course of my thesis. Jean-Jérôme Cassan at the Direction du Développement Economique et de l'Environnement aided in acquiring collecting permits in Province Nord in New Caledonia, and I was funded by a Museum of Comparative Zoology Putnam Expedition Grant. Gonzalo Giribet was an excellent field assistant in New Caledonia and didn't even complain when we had to hike up a mountain after dark. Fieldwork in New Zealand was made possible by the Department of Conservation, who provided extensive

collecting permits, and was funded by multiple NSF grants to Gonzalo and a Putnam Expedition Grant to Rosa Fernandez, who graciously took me as a field assistant in 2016. I had the absolute best field season in New Zealand in 2019, first with Sarah Boyer, Rina Morisawa, Eliza Pessereau, and Pietro Tardelli Canedo from Macalester College, and then with my partner Ben Snawder, all of whom are excellent harvestman hunters.

Apart from my own collecting, I was able to draw on the extensive harvestman and velvet worm collections in the Museum of Comparative Zoology. So many people collected specimens that I used in this thesis that if I mentioned them all by name it would fill a page on its own. But I especially thank Michael Branstetter and Cristiano Sampaio Costa, who donated most of the Neotropical velvet worms for Chapter 3. I am also grateful to Jan Beccaloni (The Natural History Museum, London), Nikolaj Scharff (Natural History Museum of Denmark, University of Copenhagen), Phil Sirvid (Museum of New Zealand Te Papa Tongarewa), and Cor Vink (Canterbury Museum in New Zealand), all of whom sent me key triaenonychid specimens that made Chapters 2 and 4 possible.

To my family, thank you for always encouraging me to embrace my weird interests from a young age—you were onto something when you made that daddy long legs Christmas tree ornament for me back in 2001. To Ben, you've been a more supportive partner than I knew was possible. I knew you were special when I showed you a picture of my insect collection on our first date and you not only didn't end the date immediately, but also sent me a picture of a katydid the next day.

To everyone on Team Harvestman, you are my people. Sarah Boyer got me started studying harvestmen as a bright-eyed undergraduate, was the first person who made me think I could be a real scientist, and continues to be an outstanding mentor. Shahan Derkarabetian generously trained me in UCE protocols, was always eager to help me identify specimens, and provided many helpful discussions about species delimitation, biogeography, and all things harvestmen. Prashant Sharma

was my source for so much guidance on methodology and helped talk me out of one of the lowest points of my thesis, and I'm so excited to continue learning about harvestmen from him as a postdoc. Finally, Gonzalo. It's hard to put into words how much you've done for me and how much I've learned from you. You've been exceedingly generous with your time, from helping me identify specimens under the microscope when you knew I was down on my research to somehow always turning around manuscript drafts with your comments in less than a day. You kept me sane in New Caledonia even after a dog bit me and our car got stuck in a ditch on top of a mountain and we went nine days before finally finding triaenonychids. And you ensured there was always money to do whatever I wanted to do in lab. Thank you for making me confident in my abilities as a scientist through your positive feedback and justified criticisms alike, and thanks for always finding the formatting errors in my EndNote citations.

Introduction

Why do organisms live where they do? On its face, this is a simple question, but setting out to answer it can be surprisingly complicated. Explanations may include ecological answers – an organism might prefer a certain temperature range, or may not be able to compete with other species in a particular habitat. But such proximate answers may overlook important historical context – maybe an organism once lived elsewhere, and its current range only reflects a fragment of its former distribution. Conversely, perhaps an organism's preferred habitat suddenly, rapidly expanded, allowing it to quickly broaden its range. What if far-flung landmasses were once connected to each other, allowing organisms to more freely disperse between them? Such questions fall in the purview of biogeography, a field of study that seeks to integrate ecological and historical explanations for why the world's diversity exists where it does.

Perhaps no topic in biogeography has fascinated researchers as much as the breakup of the former supercontinent Gondwana. This landmass was an amalgamation of the Southern Hemisphere continents of South America, Africa, the Indian subcontinent, Antarctica, Australia, and Zealandia (containing New Zealand and New Caledonia). After the breakup of Pangaea into a northern Laurasia and a southern Gondwana *ca.* 220 Mya, Gondwana persisted until it, too, began breaking apart starting around 170 Mya (Ali & Aitchison, 2008; McLoughlin, 2001; Scotese, 2004). As it rifted, initially into West Gondwana (South America and Africa) and East Gondwana (Antarctica, Madagascar, India, Australia, and Zealandia), it was believed that organisms with limited dispersal abilities passively rafted along on the resulting continental fragments, thereby achieving disjunct distributions across the Southern Hemisphere. This idea, known as Gondwanan vicariance, dominated historical biogeographical explanations following the widespread acceptance of plate tectonics—that is, until the ascent of molecular phylogenetics and divergence dating methods (Sanmartín & Ronquist, 2004).

As biogeographers reconstructed evolutionary relationships and estimated divergence times between taxa with Southern Hemisphere distributions, they found many cases in which the resulting phylogenies had topologies that did not match the order of continental separation, or the intercontinental divergences post-dated tectonic rifting, or both. Former icons of Gondwanan vicariance, such as ratite birds, chironomid midges, and *Nothofagus* beech trees (now classified in four genera), are now believed to have achieved their disjunct distributions through not just geologic separation, but also via a combination of *trans*-oceanic dispersal, extinction, and *in situ* diversification (Cook & Crisp, 2005; Heenan & Smissen, 2013; Krosch, Baker, Mather, & Cranston, 2011; Mitchell et al., 2014; Sanmartín & Ronquist, 2004). As a result, some have questioned whether a strict vicariance scenario is a useful model for any biogeographical pattern across former Gondwanan landmasses.

More recently, though, Gondwanan vicariance has found a new set of champions: soil invertebrates. These small, cryptic animals are characterized by being extremely poor dispersers, typically unable to colonize Darwinian islands (*sensu* Gillespie & Roderick, 2002). They also constitute evolutionarily ancient lineages, with estimated ages that predate the breakup of Gondwana (and in some cases Pangaea), thereby allowing their distributions to have been influenced by its fragmentation. These taxa also tend to have high habitat fidelity and persistence, being able to survive in extremely small patches of forest and unlikely to move outside of those preferred environments, a behavior that could obscure ancient biogeographic signal. Exemplars include centipedes (Edgecombe & Giribet, 2008; Giribet & Edgecombe, 2006), millipedes (Wesener, Raupach, & Decker, 2011; Wesener, Raupach, & Sierwald, 2010), earthworms (Buckley et al., 2011), certain groups of spiders (Chousou-Polydouri et al., 2019; Wood, Matzke, Gillespie, & Griswold, 2013), velvet worms (Allwood et al., 2010; Giribet et al., 2018; Murienne, Daniels, Buckley, Mayer, &

Giribet, 2014), and harvestmen (Boyer et al., 2007; Fernández, Sharma, Tourinho, & Giribet, 2017; Sharma & Giribet, 2011).

Following the definition laid out by Sanmartín & Ronquist (2004), to qualify as a Gondwanan vicariant lineage, a group must (1) have a phylogeny in which divergences between taxa from different areas correspond to the order in which Gondwanan areas broke apart, and (2) have divergence times that coincide with the relevant geologic event. Unfortunately, many groups of soil invertebrates have poorly resolved phylogenies and/or limited fossil records, both of which preclude the ability to test the hypothesis of Gondwanan rifting as a driver of cladogenesis. However, the recent application of high-throughput sequencing data to phylogenetics has successfully resolved many previously recalcitrant evolutionary relationships across the tree of life, particularly within Arthropoda (e.g. Fernández, Edgecombe, & Giribet, 2018; Lozano-Fernandez et al., 2019; Misof et al., 2014; Schwentner, Combosch, Pakes Nelson, & Giribet, 2017). Likewise, the recent discovery of new fossil material, paired with thorough morphological examinations of new and old material using techniques such as μ-CT scanning, has clarified the timing of evolution in many lineages of soil invertebrates (e.g. Garwood et al., 2016; Garwood, Sharma, Dunlop, & Giribet, 2014; Huang et al., 2018; Oliveira et al., 2016; Selden, Dunlop, Giribet, Zhang, & Ren, 2016; Wang et al., 2018).

To that end, in this dissertation I use high-throughput sequencing techniques and/or large taxon sampling to produce molecular phylogenies for multiple groups of soil invertebrates with Southern Hemisphere distributions. I also generate chronograms for each of these lineages, most of which are calibrated using the ages of newly described fossil material, in order to determine the extent to which historical events, including Gondwanan breakup, explain their biogeographic patterns. Chapter 1 is a reprint of an article published in the Journal of Biogeography (Baker, Boyer, & Giribet, 2020). In this chapter, I generate transcriptomic data for sixteen species in the mite harvestman family Pettalidae, spanning nine (of ten) genera. I then perform a series of phylogenetic

analyses to resolve the relationships between genera, including a thorough exploration of the position of the genus *Pettalus*, which differed between concatenation and coalescence methods. Upon finding stronger support for the concatenation topology, I then explore biogeographic patterns in the family using a species-level chronogram based on Sanger sequencing data. Using the ancestral range inference program BioGeoBEARS, I find no evidence for *trans*-oceanic dispersal in the family, and identify multiple places where Gondwanan breakup likely contributed to cladogenesis. I also perform a speciation–extinction analysis in the program BAMM, which finds no evidence for mass extinction in Pettalidae, but does suggest the family initially diversified rapidly in the Late Triassic–Early Jurassic, with diversification continuously slowing down over time.

Chapter 2 corresponds to an article currently in review in *Invertebrate Systematics* (Baker et al., in review). Here, I generate the first molecular phylogeny focused on the armored harvestman family Triaenonychidae, the fourth most diverse family of harvestmen. Sequencing three loci (18S rRNA, 28S rRNA, and cytochrome *c* oxidase subunit I [COI]) for 300 ingroup specimens, I find that the family as traditionally defined is diphyletic, and accordingly transfer the genus *Lomanella* out of the family to maintain its monophyly. I also find that all landmasses from which triaenonychids are known contain non-monophyletic assemblages of taxa (with the exception of the United States and Sardinia, each of which contain relictual monotypic genera). A chronogram of the family demonstrates its ancient age, with an estimated origin in the Permian that predates the breakup of Pangaea. Though I was unable to resolve many of the relationships along the backbone of the phylogeny, I was able to demonstrate that the age of diversification in the family is largely consistent with Gondwanan vicariance. However, a strict vicariance scenario is insufficient to explain the presence of triaenonychids on New Caledonia, where dispersal from New Zealand to the island of Grande Terre after its re-emergence under oceanic crust *ca.* 37 Mya (Cluzel, Maurizot, Collot, & Sevin, 2012) is instead supported.

In Chapter 3, I generate a phylogeny of the phylum Onychophora using transcriptomic data, and infer divergence times in the group using calibrations derived from fossil ages. Unlike pettalid and triaenonychid harvestmen, which are restricted to temperate forests across the Southern Hemisphere (excluding the two relictual Laurasian representatives of Triaenonychidae), Onychophora is divided into two families. The family Peripatopsidae is co-distributed with pettalids and triaenonychids in these temperate forests; the family Peripatidae, however, is found in tropical forests around the world. In this chapter, I recover a well-resolved and stable topology for the temperate Peripatopsidae, which similarly contains multiple places in its phylogeny where Gondwanan breakup likely contributed to cladogenesis. However, the Neotropical lineage of Peripatidae shows evidence of a rapid radiation occurring in the Late Cretaceous–early Paleogene, potentially the result of a bolide impact in the Yucatán Peninsula associated with the K–P extinction (Hedges, 2006). And while phylogenetic analysis using translated amino acid data produce a largely unresolved phylogeny of the clade, analyses using nucleotide sequence data resolve many more relationships and suggest that peripatids have colonized oceanic islands in the Caribbean multiple times via over-water dispersal. I therefore propose a hypothesis to explain the differential dispersal capabilities of these two lineages of Onychophora based on the unique reproductive mode and life history strategy of the Neotropical peripatids.

Finally, in Chapter 4 I narrow my focus from looking at biogeographic patterns across all of Gondwana to looking at just one of its constituent landmass: New Zealand. New Zealand has been the subject of a well-known biogeographic debate in which some authors propose that all of its endemic biota is the result of recent dispersal to the archipelago following a complete marine inundation in the Oligocene (Trewick, Paterson, & Campbell, 2006), while others argue that Gondwanan-derived taxa persisted through this period on small island refugia (Giribet & Boyer, 2010; Wallis & Jorge, 2018). Apart from this marine transgression, the archipelago has also had a

turbulent geologic and climatic history marked by events such as the uplift of the Southern Alps in the Miocene and extensive glaciation in the Pleistocene (Trewick & Bland, 2012; Wallis & Trewick, 2009). In this chapter, I reveal the signatures these events left on the phylogenetic and genetic diversity of two sister genera of New Zealand-endemic triaenonychid harvestmen, *Sorensenella* and *Karamea*. Using ultraconserved element (UCE) sequencing, I reconstruct a well-resolved phylogeny for the clade. Additionally, I recover COI sequences for all specimens and use them to generate a chronogram using multiple published substitution rates for arthropods. I also extract SNPs from the UCE dataset and use them to delimit species using traditional genetic clustering methods (STRUCTURE and PCA) and an unsupervised machine learning approach (variational autoencoder, VAE). I find evidence for the existence of multiple species, several of which are undescribed and one of which is likely parthenogenetic, and then characterize the genetic diversity of these species in the context of New Zealand's history. In all, *Sorensenella* and *Karamea* show a reduced diversification rate coinciding with the Oligocene marine transgression, increased cladogenesis of lineages found in the Southern Alps coinciding with that period of orogenesis, and rapid expansion across the central North Island following the regression of a sea strait in the Pliocene.

Throughout this thesis, I find evidence for the effects of various historical geologic and climatic events on distantly related groups of soil invertebrates, including a pattern of Gondwanan vicariance. However, in both triaenonychid harvestmen and Neotropical velvet worms, vicariance does not tell the whole story. These studies underscore the importance of generating well-resolved, densely sampled phylogenies and obtaining accurate divergence time estimates when interpreting biogeographic histories, and showcase the outstanding ability of soil invertebrates to retain signatures of ancient events in their phylogenetic and genetic diversity patterns.

Chapter 1

A well-resolved transcriptomic phylogeny of the mite harvestman family Pettalidae (Arachnida, Opiliones, Cyphophthalmi) reveals signatures of Gondwanan vicariance

Published article:

Baker, C. M., Boyer, S. L., & Giribet, G. (2020). A well-resolved transcriptomic phylogeny of the mite harvestman family Pettalidae (Arachnida, Opiliones, Cyphophthalmi) reveals signatures of Gondwanan vicariance. *Journal of Biogeography, 47*. doi:10.1111/jbi.13828

Supplementary materials are hosted in Harvard Dataverse: http://doi.org/10.7910/DVN/89DHPH

Received: 6 June 2019 | Revised: 24 January 2020 | Accepted: 3 February 2020

DOI: 10.1111/jbi.13828

RESEARCH PAPER

Journal of Biogeography | WILEY

A well-resolved transcriptomic phylogeny of the mite harvestman family Pettalidae (Arachnida, Opiliones, Cyphophthalmi) reveals signatures of Gondwanan vicariance

Caitlin M. Baker[1] | Sarah L. Boyer[2] | Gonzalo Giribet[1]

[1]Museum of Comparative Zoology, Department of Organismic and Evolutionary Biology, Harvard University, Cambridge, MA, USA

[2]Biology Department, Macalester College, St. Paul, MN, USA

Correspondence
Caitlin M. Baker, Museum of Comparative Zoology, Department of Organismic and Evolutionary Biology, Harvard University, 26 Oxford Street, Cambridge, MA 02138, USA.
Email: baker02@g.harvard.edu

Funding information
NSF, Grant/Award Number: DEB-1457539, DEB-1754278 and DEB-1020809

Handling Editor: Isabel Sanmartín

Abstract

Aim: We explored the extent to which Gondwanan vicariance contributed to the circum-Antarctic distribution of the mite harvestman family Pettalidae, a group of small, dispersal-limited arachnids whose phylogeny has been poorly resolved, precluding rigorous biogeographic hypothesis testing.

Location: Continental landmasses of former temperate Gondwana (Chile, South Africa, Sri Lanka, Australia and New Zealand).

Taxon: Pettalidae, Opiliones.

Methods: We generated transcriptomes for a phylogeny of 16 pettalids, spanning 9 genera. Data were analysed using maximum likelihood, Bayesian inference and coalescence methods. The phylogenetic position of the Sri Lankan genus *Pettalus* was further explored using quartet likelihood mapping and changes in gene likelihood scores. We also estimated divergence times and looked for signatures of extinction across Antarctica and central Australia using previously published phylogenies with near-complete species sampling constrained to match our transcriptomic results. Finally, we estimated ancestral ranges and inferred instances of vicariance.

Results: We recovered a well-supported topology with a division between taxa from landmasses that made up East Gondwana, and a grade of taxa from West Gondwana. *Pettalus* was resolved either as the sister group of the Queensland-endemic *Austropurcellia*, or as the sister group to a larger clade from East Gondwana, though favouring *Pettalus* + *Austropurcellia*. Divergence times for multiple vicariance events coincided with Gondwana's breakup. Speciation–extinction analysis found one diversification process for the family: an initial burst of cladogenesis that slowed down through time.

Main Conclusions: Given that the order of cladogenesis corresponds to the order in which Gondwana fragmented, and the concurrent timing of vicariance and rifting, Gondwanan breakup explains major biogeographic patterns in Pettalidae. Some divergences predate initial rifting, but there is no evidence of *trans*-oceanic dispersal. The Sri Lanka–eastern Australia relationship makes sense in the light of large-scale

extinction across Antarctica and central Australia; however, we find no clear signatures of mass extinction.

KEYWORDS

Arachnida, Cyphophthalmi, Gondwana, Pettalidae, phylogenetic incongruence, phylogeny, transcriptomics, vicariance biogeography

1 | INTRODUCTION

Since the acceptance of plate tectonics, no topic in historical biogeography has attracted so much interest as the breakup of the former supercontinent Gondwana. Gondwana, which formed the southern part of Pangaea until *ca*. 220 Mya, began rifting apart starting ~170 Mya, first into West Gondwana (South America–Africa) and East Gondwana (Antarctica–India–Madagascar–Australia–New Zealand; Ali & Aitchison, 2008; Jokat, Boebel, König, & Meyer, 2003; McLoughlin, 2001). These landmasses continued breaking apart over the course of the Mesozoic, and while there has been debate over the precise timing (and in some cases, the order) of fragmentation, the commonly accepted pattern is as follows: South America separated from Africa starting ~150–120 Mya; India–Madagascar split from Antarctica–Australia–New Zealand ~130 Mya; New Zealand rifted away from Antarctica–Australia starting ~80 Mya; finally, Australia separated from Antarctica (and by very distant proxy, South America, which was connected to Antarctica via the Antarctic Peninsula) ~50–41 Mya, eventually resulting in the continental configuration seen today in the southern hemisphere (Ali & Aitchison, 2008; Eagles, 2007; Jokat et al., 2003; Sanmartín & Ronquist, 2004; Scotese, 2004; Upchurch, 2008; Wei, 2004).

As the supercontinent rifted, it was thought that low vagility organisms with widespread distributions across Gondwana rafted passively along on the continental fragments, thereby developing disjunct distributions – an idea known as Gondwanan vicariance. Commonly upheld examples of this phenomenon included ratite birds (Mitchell et al., 2014), *Nothofagus* beech trees (Cook & Crisp, 2005) and chironomid midges (Krosch, Baker, Mather, & Cranston, 2011).

However, as researchers searched for evidence supporting this hypothesis in different putative Gondwanan groups using time-calibrated molecular phylogenies, nearly all the resultant cladograms had topologies that did not match the order of Gondwana's breakup, or their cladogenetic splits were far younger than the period of rifting that supposedly drove their divergence, or both (Sanmartín & Ronquist, 2004). The predominant narrative now suggests that most of these groups diversified as a result not only of geological separation but also by a combination of *trans*-oceanic dispersal, extinction and in situ diversification.

Despite this, there are still a handful of putative Gondwanan vicariant lineages (e.g. Chousou-Polydouri et al., 2019; Murienne, Daniels, Buckley, Mayer, & Giribet, 2014). One notable example is the mite harvestman family Pettalidae (Arachnida, Opiliones, Cyphophthalmi; Boyer & Giribet, 2007; Giribet et al., 2016; Shear, 1980). Mite harvestmen are small (1- to 4-mm-long) arachnids that live in damp, dark environments such as leaf litter, caves and rotting logs. Like many other saproxylic animals, they are poor dispersers, thought to be unable to cross even small oceanic barriers (although see Clouse & Giribet, 2007), and are therefore found only on continents or islands of continental origin. They are also thought to be an ancient group: while the oldest Cyphophthalmi fossil is *ca*. 100 Ma from Burmese amber (Poinar, 2008), there are fossils of non-cyphophthalmid Opiliones that date to the early Devonian (*ca*. 411 Ma; Dunlop, Anderson, Kerp, & Hass, 2004), and previously published dated phylogenies of Opiliones suggest Cyphophthalmi may already have been diversifying in the Permian or Carboniferous (Fernández, Sharma, Tourinho, & Giribet, 2017; Oberski et al., 2018; Sharma & Giribet, 2014). Together, these characteristics (narrow habitat requirements, low vagility, old age predating Pangean and Gondwanan breakup) make mite harvestmen an excellent system for studying historical biogeography (e.g. Boyer et al., 2007).

Pettalidae has a classic temperate Gondwanan distribution, with representatives in Chile, South Africa, Madagascar,[1] Sri Lanka, Australia and New Zealand (Figure 1). After more than a decade of taxonomic study of the family, using both morphology and traditional molecular markers, systematists have settled on 10 accepted monophyletic genera in the family, each of which is restricted to one geographically cohesive landmass of former Gondwana (Boyer & Giribet, 2007; Giribet et al., 2012, 2016). However, while the monophyly of each genus has been well established using traditional Sanger sequencing markers, the relationships between genera remain largely unresolved, with the exception of the South African genus *Parapurcellia* being the sister group to all other genera. It has been hypothesized that this lack of signal is the result of saturation due to ancient, rapid diversification in the family coupled with large-scale extinction events as the temperate forests disappeared across Gondwana due to climate change in the Oligocene and Miocene, notably in Antarctica and central Australia (Cantrill & Poole, 2012; Kemp, 1978; Martin, 2006). However, failure to resolve relationships could also be a result of the limited molecular data available through Sanger-based approaches.

Without a fully resolved, time-calibrated phylogeny, it remains impossible to critically assess the idea that pettalids are a

[1]There are two monotypic Cyphophthalmi genera described from Madagascar (Shear & Gruber, 1996). While the only known specimens of these genera are not suitable for molecular work, the genus *Manangotria* is likely a member of Pettalidae based on a morphological cladistic analysis, though the genus *Ankaratra* remains *incertae sedis* (Giribet et al. 2012).

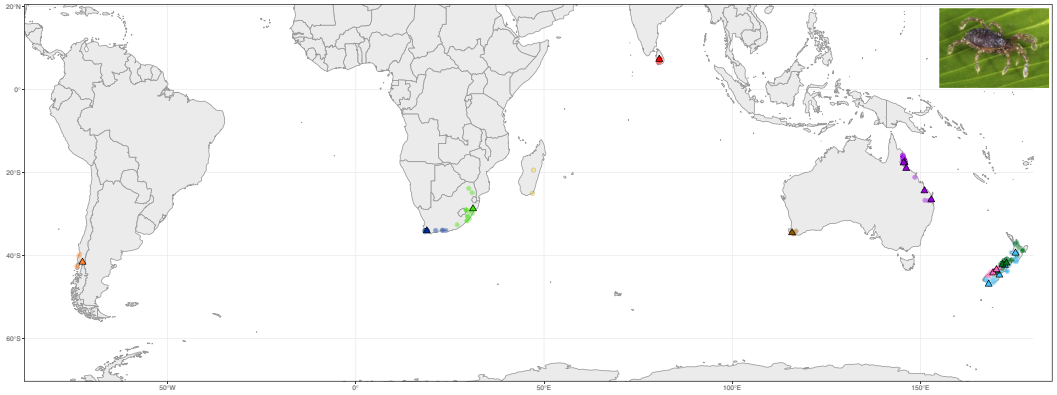

FIGURE 1 A map of the distribution of genera in Pettalidae. Circles show known localities for animals, with localities of transcriptome samples indicated by triangles. Each genus shown in a different colour: *Chileogovea* (orange), *Purcellia* (navy blue), *Parapurcellia* (light green), *Manangotria* (yellow; not sampled), *Pettalus* (red), *Karripurcellia* (brown), *Austropurcellia* (purple), *Neopurcellia* (pink), *Aoraki* (dark green) and *Rakaia* (light blue). Inset figure: *Neopurcellia salmoni* (IZ-152129) from New Zealand

vicariant Gondwanan lineage. We thus aim to test whether genomic approaches allow us to resolve the phylogeny of Pettalidae, as phylogenetic analyses of densely sampled transcriptomes have successfully resolved many phylogenies across the tree of life where the use of a handful of traditional markers has failed, including within arachnids (e.g. Benavides, Cosgrove, Harvey, & Giribet, 2019; Fernández & Giribet, 2015; Fernández, Hormiga, & Giribet, 2014; Hedin, Starrett, Akhter, Schonhofer, & Shultz, 2012; Sharma, Fernández, Esposito, González-Santillán, & Monod, 2015). To that end, we generated a transcriptomic phylogeny of the family, including at least one member of each of the nine genera for which we had molecular-quality specimens. We then performed a molecular dating analysis using fossil calibrations and assessed how closely the timing of the divergences between genera matched the breakup of Gondwana.

2 | MATERIALS AND METHODS

2.1 | Sample collection and molecular techniques

Specimens of 16 species representing 9 pettalid genera were newly collected and sequenced for this study. Information on sampling localities and accession numbers in the NCBI Sequence Read Archive (SRA) database for each transcriptome can be found in Table 1. In addition, three pettalids from a previously published study (Fernández et al., 2017) were included. The following taxa were used as outgroups: a horseshoe crab (*Limulus polyphemus*), a scorpion (*Centruroiudes sculpturatus*), a spider (*Liphistius malayanus*) and eight non-pettalid harvestmen (*Synthetonychia glacialis*, *Acropsopilio neozealandiae*, *Forsteropsalis pureora*, *Siro boyerae*, *Miopsalis* sp., *Metasiro savannahensis*, *Brasilogovea microphaga* and *Metagovea oviformis*). Previously published transcriptomes were downloaded from SRA (see Table S1). Specimens were initially preserved in RNA*later* and later flash frozen in liquid nitrogen and stored at −80°C. They are deposited in the Invertebrate Zoology collection of the Museum of Comparative Zoology (MCZ), Harvard University.

Illumina sequencing followed standard protocols developed in our laboratories (Fernández, Edgecombe, & Giribet, 2016; Fernández, Laumer, et al., 2014; Riesgo et al., 2012). Briefly, total RNA was extracted from single individuals and purified for mRNA, then converted into cDNA on an Apollo 324 (Wafergen Biosystems). Quality of the mRNA and the cDNA libraries was checked on an Agilent 2100 Bioanalyzer (Agilent Technologies) using the RNA pico assay and the HSDNA assay respectively. Libraries were then amplified (8–18 PCR cycles) and individually indexed with 1 of 12 indices of the PrepX mRNA library preparation kit for Illumina, to allow for multiplexing. Kapa Library Quantification kits (Kapa Biosystems) were then used to assess individual library concentrations. Equimolar multiplexed libraries were sequenced as 150 bp paired-end reads on an Illumina HiSeq 2500 at the Bauer Core Facility at Harvard University.

2.2 | Transcriptome assembly and orthology prediction

Demultiplexed raw FASTQ reads were error corrected using Rcorrector v 1.0.2 (Song & Florea, 2015) and quality filtered and trimmed using Trim Galore! v 0.4.1 (Krueger, 2015) to remove adapters, bases with Phred scores below 30 and reads shorter than 75 bp. Post-trimming quality was assessed with FastQC. rRNA and mtDNA reads were filtered out using Bowtie2 v2.2.9 (Langmead & Salzberg, 2012), using custom-built Panarthropoda databases of rRNA from SILVA (18S and 28S rRNA; Yilmaz et al., 2014) and GenBank (5S and 5.8S rRNA), and mtDNA from AMiGA (Feijão, Neiva, de

TABLE 1 Collection and accession information for pettalid specimens used in this study

Taxon name	MCZ Accession #	SRR number	Orthogroups in M3	BUSCO % complete	Latitude	Longitude	Collection date
***Aoraki denticulata* "Northern"**	**IZ-141172**	**SRR9611067**	**3,699**	**94.00%**	**−42.15621**	**171.79275**	**16-Jan-2016**
***Aoraki denticulata* "Southern"**	**IZ-141173**	**SRR9611066**	**3,639**	**92.12%**	**−41.80598**	**172.84351**	**16-Jan-2016**
Aoraki longitarsa	IZ-137238	SRR5181387	2,104	56.29%	−43.737936	170.095493	20-Jan-2014
Austropurcellia acuta	**IZ-44060**	**SRR9611068**	**3,172**	**81.43%**	**−26.55778**	**152.8661**	**23-May-2014**
Austropurcellia alata	**IZ-141418**	**SRR9611069**	**2,170**	**54.03%**	**−17.68475**	**145.52281**	**1-Jun-2015**
Austropurcellia* cf. *acuta	**IZ-141419**	**SRR9611062**	**2,757**	**68.86%**	**−24.41302**	**151.03873**	**25-May-2015**
Austropurcellia clousei	**IZ-141420**	**SRR9611063**	**3,625**	**92.78%**	**−19.01176**	**146.20552**	**29-May-2015**
Austropurcellia despectata	**IZ-141417**	**SRR9611064**	**3,785**	**95.68%**	**−17.59547**	**145.75577**	**31-May-2015**
Chileogovea oedipus	**IZ-138106**	**SRR9611065**	**3,472**	**88.09%**	**−41.59351**	**−72.59359**	**15-Oct-2014**
Karripurcellia peckorum	**IZ-49989**	**SRR9611060**	**3,245**	**80.77%**	**−34.533333**	**116.020556**	**23-Nov-2014**
Neopurcellia salmoni	IZ-29310	SRR5181448	3,543	84.80%	−44.16771398	169.274167	19-Jan-2014
Neopurcellia salmoni	**IZ-144625**	**SRR9611061**	**3,320**	**82.18%**	**−43.41156**	**170.17742**	**17-Jan-2016**
Parapurcellia silvicola	**IZ-134743**	**SRR9611070**	**3,201**	**90.71%**	**−28.74421301**	**31.13762699**	**4-Apr-2001**
Pettalus thwaitesi	**IZ-132349**	**SRR9611071**	**741**	**20.54%**	**7.272507995**	**80.59333004**	**17-Jun-2004**
***Purcellia* n. sp. "Helderberg"**	**IZ-49518**	**SRR9611072**	**3,267**	**82.08%**	**−34.04235**	**18.87395**	**16-Dec-2014**
Rakaia magna australis	IZ-29212	SRR5181449	2,436	62.57%	−42.37968698	172.401185	17-Jan-2014
Rakaia minutissima	**IZ-143240**	**SRR9611073**	**3,504**	**88.56%**	**−39.4164**	**175.21866**	**13-Jan-2016**
Rakaia pauli	**IZ-144621**	**SRR9611074**	**3,289**	**83.49%**	**−44.70055**	**170.96715**	**23-Jan-2016**
Rakaia stewartiensis	**IZ-49801**	**SRR9611075**	**2,649**	**75.42%**	**−46.89424901**	**168.104017**	**17-Feb-2008**

Note: Newly sequenced samples are shown in bold. M3 refers to matrix 3 (see Table 2). BUSCO completeness scores are for the Arthropoda database.

TABLE 2 Information on matrices used for phylogenetic inference

	Orthogroups	Sites	Description
Matrix 1	464	123,809	90% occupancy
Matrix 2	1,298	369,462	75% occupancy
Matrix 3	4,054	1,348,829	50% occupancy
Matrix 4	739	160,576	All orthogroups with *Pettalus* represented from Matrix 3
Matrix 5	643	133,226	Homogeneous orthogroups from Matrix 4
Matrix 6	444	99,389	Fastest and slowest 20% of genes excluded from Matrix 4

Note: See Section 2 for details.

Azeredo-Espin, & Lessinger, 2006) and GenBank. This was done because all contigs were eventually translated into amino acid sequences, and mtDNA uses a different translation code while rRNA is not translated. All sequences in these custom databases were manually checked for taxonomic mislabelling or contamination using the top 20 BLAST matches as confirmation of identity. Filtered reads were then de novo assembled, accounting for strand specificity, in Trinity v 2.4.0 (Grabherr et al., 2011; Haas et al., 2013). Assembled reads were again checked for rRNA and mtDNA sequences using Bowtie2, to ensure that only nuclear mRNA was included in the assembly. Redundancy within each individual assembly was collapsed using the program CD-HIT-EST v4.6.4 (Fu, Niu, Zhu, Wu, & Li, 2012) with a 98% similarity cut-off, to remove highly similar contigs. Retained contigs were then translated from nucleotide sequences to amino acid sequences with TransDecoder v3.0 (Haas et al., 2013), which looks for open reading frames (ORF). Predicted peptides were then filtered to select only one peptide per putative gene by choosing the longest ORF using a Python script from Laumer, Hejnol, and Giribet (2015). The completeness of each assembly was evaluated with BUSCO by comparison with the Arthropoda database (Simão, Waterhouse, Ioannidis, Kriventseva, & Zdobnov, 2015).

Orthologous genes were predicted across all samples using the Orthologous Matrix Algorithm, OMA standalone v1.0.6 (Altenhoff et al., 2015), an all-by-all graph-based Markov clustering method with high precision in identifying orthologous genes as opposed to paralogs, an important consideration in phylogenomic analyses (Altenhoff et al., 2016). All computations were run on the Odyssey cluster supported by the FAS Division of Science, Harvard University.

2.3 | Matrix assembly

Each OMA-generated orthogroup was aligned individually with MUSCLE v3.8.31 (Edgar, 2004), using default parameters. To reduce alignment uncertainty, we also ran Zorro (Wu, Chatterji, & Eisen, 2012) on each aligned orthogroup, discarding all sites with a probability score below 5.

We then constructed six matrices, accommodating for different potential systematic biases (Table 2). Matrices 1–3 allowed for varying amounts of missing data: 90%, 75% and 50% occupancy respectively. Occupancy was defined as all the orthogroups present in at least that percentage of taxa (i.e. the 90% occupancy matrix contained all the orthogroups present in at least 90% of taxa analysed). We further refined our data by making matrix 4, which included all the orthogroups from matrix 3 that had sequence data for *Pettalus thwaitesi* (the most degraded, poorly sampled transcriptome in this study and the only representative of a biogeographically key lineage from Sri Lanka). Matrix 5 was composed of all the orthogroups from matrix 4 that passed a test of amino acid compositional homogeneity, as implemented in the simulation-based Python package p4 (Foster, 2004, 2018) and run using a script from Cunha and Giribet (2019) with a p-value of 0.1. Finally, to account for the possibility of extreme evolutionary rates biasing phylogenetic reconstruction, matrix 6 was created by removing 20% of the fastest- and slowest-evolving orthogroups from matrix 4. Orthogroup evolutionary rate was calculated in TrimAl (Capella-Gutiérrez, Silla-Martínez, & Gabaldón, 2009). Selected orthogroups were concatenated into matrices using Phyutility (Smith & Dunn, 2008).

We also ran additional analyses on a dataset that only included Opiliones (27 taxa total) to minimize the potential effect of long-branch attraction due to highly distant outgroups (see Figure S1.1). However, including the distantly related non-opilionid outgroup taxa (*Limulus polyphemus*, *Centruroiudes sculpturatus* and *Liphistius malayanus*) was necessary for placing fossil calibrations in the dating analysis.

2.4 | Phylogenetic analysis

For each of the first three matrices, we performed a series of phylogenetic analyses, covering Bayesian inference (BI), maximum likelihood and species tree methods. BI was performed in ExaBayes 1.3 (Aberer, Kobert, & Stamatakis, 2014) using two runs of two chains and up to 2 million generations, until the average standard deviation of split frequencies was below 5%. A consensus of both runs was created, discarding the first 25% of trees as burn-in. Maximum likelihood tree searches were run in IQ-TREE-MPI v1.5.5 (Nguyen, Schmidt, von Haeseler, & Minh, 2015) using two methods: an orthogroup-partitioned analysis, incorporating model and partition selection tests ("IQTREE-part", Kalyaanamoorthy, Minh, Wong, von Haeseler, & Jermiin, 2017), including LG4 mixture models; and a non-partitioned analysis with model and partition selection tests, including the 10–60 class profile mixture models (maximum likelihood implementations of the Bayesian CAT model, "IQ-TREE-cat"). We also used the concatenation-free coalescence (species tree) program ASTRAL 4.10.12 (Mirarab et al., 2014) to account for the potential biasing effect of concatenating loci with conflicting gene genealogies. ASTRAL requires individual gene trees as input; these

were generated for each orthogroup in RAxML v8.2.11 (Stamatakis, 2014) using the PROTGAMMAAUTO model selection feature. Finally, we performed a BI analysis on Matrix 1 (the smallest matrix) using the CAT + GTR site-heterogeneous mixture model as implemented in PhyloBayes-MPI v1.7a (Lartillot, Rodrigue, Stubbs, & Richer, 2013), as this model has been shown to better describe the substitutional heterogeneity of large matrices compared with stationary models (Lartillot & Philippe, 2004). Two chains were run in parallel until they reached convergence, as assessed with the bpcomp and tracecomp commands, discarding the first 25% of trees as burn-in. PhyloBayes was not run on other matrices due to computational limitations.

Given the results of our phylogenetic analyses on matrices 1–3, wherein the position of *Pettalus* differed in concatenation versus coalescence methods, we performed further tests on matrices 4–6, which had 100% gene occupancy for that taxon. For these matrices, we inferred trees with IQ-TREE using both the partitioned and non-partitioned strategies described above. We also ran ASTRAL on the set of gene trees comprising each of these matrices.

Because the discordance between ASTRAL and concatenation methods persisted in the more refined matrices 4–6, we performed a quartet likelihood mapping approach (Strimmer & von Haeseler, 1997) as implemented in IQ-TREE to interrogate whether our dataset was able to resolve the position of *Pettalus* at all. Clusters were defined for the clades *Pettalus*, *Austropurcellia*, *Rakaia* and *Neopurcellia* + *Karripurcellia* + *Aoraki*, with all other terminals ignored. The mapping was done on the concatenated matrix 4, using all available quartets.

To determine whether the difference in concatenation versus coalescence topologies was due to conflicting signal among individual orthogroups, we also computed the difference in gene-wise log-likelihood score (ΔGLS) for all orthogroups in matrix 4, as described in Shen, Hittinger, and Rokas (2017). For this, we first ran an unconstrained tree search ("T1") in RAxML and a constrained tree search (using the -g option) in which we forced the topology to follow (*Rakaia*, (*Pettalus*, (*Austropurcellia*, (*Neopurcellia*, *Karripurcellia*, *Aoraki*)))) on the concatenated matrix (i.e. the topology recovered by ASTRAL, "T2"). All other terminals in the tree, including the other pettalid genera, were left unconstrained for the T2 search. For both tree searches, the matrix was partitioned by orthogroup, deriving the substitution model for each orthogroup from the results of PROTGAMMAAUTO on our individual gene trees. We then used the -f G flag in RAxML to calculate site-wise log-likelihood scores for T1 and T2, and used a script provided in Shen et al. (2017) to sum the log-likelihood scores for each gene (gene-wise likelihood score, or GLS) and calculate the difference between GLS for T1 and T2 (ΔGLS).

2.5 | Molecular dating

To estimate the timing of divergences within Pettalidae and assess whether they corresponded to the breakup of Gondwana, a molecular clock analysis was performed with PhyloBayes v4.1 (Lartillot, Lepage, & Blanquart, 2009), as it can accommodate genomic-scale data. However, to be able to do so the program requires a constrained input tree to reduce calculation time, so we used the topology from our concatenated analyses. To infer branch lengths, we used Matrix 1, the smallest and most complete matrix that includes all outgroups. By choosing the most complete matrix, we hoped to minimize the potential negative effects that missing data can have on branch lengths.

Because we were attempting to determine whether tectonic breakup coincided with cladogenesis, we avoided using geologic calibration points and instead used four fossil-derived calibrations (Kodandaramaiah, 2011). We placed all our calibration points on outgroup nodes, as there are no known pettalid fossils. Given the taxonomic sampling in our transcriptomic phylogeny, uniform priors with soft bounds were chosen to accommodate the inherently imprecise relationship between phylogenetic placement of the calibrations and their corresponding divergence times (Heath, 2012; Ho & Phillips, 2009). We erred on the side of vague, uninformative priors, preferring wider posterior credibility intervals to the possibility of recovering narrow but inaccurate estimates.

Largely following the methods of Sharma and Giribet (2014) and Sharma et al. (2018), we constrained the following nodes: (1) The Cyphophthalmi–Phalangida split was constrained to a minimum age of 411 Ma with no maximum age, based on the placement of the extinct order Tetrophthalmi (*Hastocularis argus* + *Eophalangium sheari*) as sister group to Cyphophthalmi (Dunlop et al., 2004; Garwood, Sharma, Dunlop, & Giribet, 2014; Sharma & Giribet, 2014). Tetrophthalmi contains the oldest known Opiliones fossil, *Eophalangium sheari*, from the Rhynie Chert, which is radiometrically dated to *ca*. 411 Ma (Dunlop et al., 2004). (2) The minimum age of Palpatores was set to 305 Ma with no maximum age, based on the fossils *Ameticos scolos* (Dyspnoi) and *Macrogyion cronus* (Eupnoi), both of which come from the Montceau-les-Mines Lagerstätte, the upper limit of which is biostratigraphically dated to *ca*. 305 Ma (Garwood, Dunlop, Giribet, & Sutton, 2011). The fossils used to calibrate nodes (1) and (2) have all been taxonomically verified in a total-evidence phylogenetic analysis (Sharma & Giribet, 2014). (3) The Araneae–Scorpiones split was given a minimum age of 430 Ma with no upper limit based on the oldest known fossil scorpion with modern appendages, *Eramoscorpius brucensis*, from the Eramosa formation, which has a stratigraphic date range of 430–433 Ma (Waddington, Rudkin, & Dunlop, 2015). (4) The root of the tree, corresponding to Euchelicerata, was constrained using a gamma prior with a mean of 550 Ma and a standard deviation of 20 (Figure 2; Sharma et al., 2018; Wolfe, Daley, Legg, & Edgecombe, 2016). We did not use the oldest Cyphophthalmi fossil, *Palaeosiro burmanicum* (Stylocellidae), known from Burmese amber (Giribet et al., 2012; Poinar, 2008), as it represents a derived stylocellid, we only had a single terminal representing that family in our tree, and constraining the minimum age of Cyphophthalmi to 100 Ma would not be informative given the much older age of the other Opiliones fossils used for calibration.

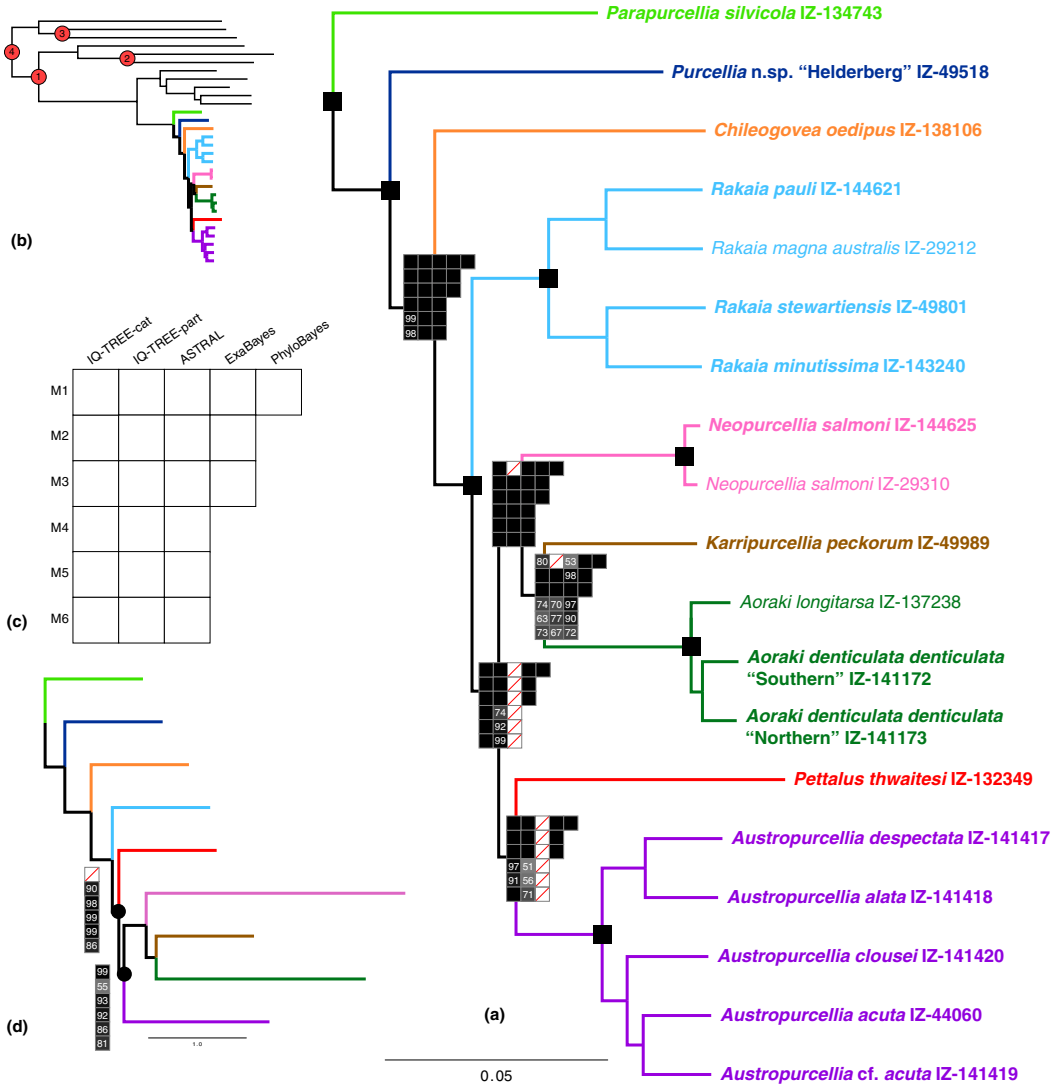

FIGURE 2 Pettalidae phylogeny inferred from the largest matrix (M3) using IQ-TREE's CAT-like profile mixture model ("IQTREE-cat"). (a) Small black squares represent nodes which received maximal support in all analyses, and nodes in which at least one analysis did not give full support are shown with a plot, coloured in grey scale by strength of support. Squares with red lines indicate analyses which did not recover the topology shown here. Branches and terminals coloured by genus, as in Figure 1. Transcriptomes newly sequenced for this study are shown in bold. (b) Phylogeny with outgroups, with ingroup branches coloured as in (a). Red circles denote nodes constrained in divergence time estimation, with numbers corresponding to fossils described in the main text. (c) Explanation of nodal support plot, as shown in (a). (d) Pettalid phylogeny inferred from M3 in ASTRAL, with branches collapsed and coloured as in (a). Support plots shown for the two nodes that conflict with the topology of (a), marked with black circles

Divergence times were estimated under an autocorrelated lognormal clock, implementing the site-heterogeneous CAT + GTR model. Four independent chains were run for 8,679–11,183 cycles. Despite running for 6 months, PhyloBayes' tracecomp command indicated that none of the chains converged. This is likely due to both the large size of our alignment and the limited availability of relevant fossil calibrations for our phylogeny, causing branch lengths to expand and contract, and results in large error bars on our final chronogram.

2.6 | Speciation–extinction analysis

We further explored the role of Gondwanan vicariance in the biogeography of Pettalidae by taking previously published Sanger-based phylogenies with dense taxon sampling (Giribet et al., 2016; Oberski et al., 2018) and re-estimating divergence times under a birth–death tree prior in BEAST 2.4.3 (Bouckaert et al., 2014). We included one exemplar of each extant species for which we have molecular data, including known but undescribed species, resulting in 96 ingroup terminals (there are currently 76 described species and subspecies within Pettalidae (Giribet et al., 2016)). We constrained the relationships between the genera to match our concatenated transcriptomic topology (cf. Wheeler et al., 2017). Five genes were used: two nuclear ribosomal genes (18S and 28S rRNA), one nuclear protein coding gene (histone H3), one mitochondrial protein coding gene (COI) and one mitochondrial ribosomal gene (16S rRNA). The analysis was partitioned by gene, with each partition given a unique model of sequence evolution as specified in jModelTest (Posada, 2008). We used an expanded outgroup sampling of 93 taxa to incorporate additional fossil calibration points, all under uniform distributions so as to be relatively uninformative: (a) Opiliones was constrained to be a minimum of 411 Ma (see above for justification, Dunlop et al., 2004); (b) Eupnoi was constrained to be a minimum of 305 Ma (see above, Garwood et al., 2011); (c) Epedanidae was constrained to be a minimum of 105 Ma based on the age of *Petrobunoides sharmai*, a fossil from Upper Cretaceous Burmese amber (Selden, Dunlop, Giribet, Zhang, & Ren, 2016); (d) Stylocellidae was constrained to be a minimum of 105 Ma (see above, Poinar, 2008). The maximum age for all calibrations was set to 500 Ma, corresponding to the minimum estimated age of the group Euchelicerata, based on a *Chasmataspis*-like resting trace fossil (Wolfe et al., 2016). We launched four runs of 200 million generations, which were combined post-burnin of 25%. Stationarity was confirmed in Tracer v1.6 (Rambaut & Drummond, 2009), with all ESS values >200.

Following phylogenetic inference, we pruned all outgroups from the resulting BEAST consensus phylogeny and ran a speciation–extinction analysis in BAMM v2.5.0 (Rabosky, 2014) to characterize shifts in net diversification rate. We believe that the ancient sister-group relationship between *Pettalus* and *Austropurcellia* would make sense if there had been several other lineages in this clade endemic to Antarctica and central Australia that had since gone extinct as those continents cooled and aridified, respectively, throughout the Cenozoic (Cantrill & Poole, 2012; Martin, 2006). In the absence of a fossil record for this group of small invertebrates, we wanted to see if we could detect a signal of mass extinction that might explain this geographically distant sister-group relationship, and having as close to complete extant species sampling as possible is critical for determining diversification dynamics, to avoid artificially skewing inferred speciation or extinction rates. BAMM was run using four chains for 50 million generations and a global sampling fraction of 0.96 (reflecting the near-complete species sampling), with priors determined by the R package BAMMtools. All post-MCMC analyses were also performed using BAMMtools.

2.7 | Ancestral range estimation

Finally, in an attempt to more explicitly assess the extent to which Gondwanan breakup may have led to divergences within Pettalidae, we used our species-level chronogram inferred in BEAST to perform ancestral range estimations under the DEC model (Ree & Smith, 2008) and the DIVA-like model (Ronquist, 1997) in the R package "BioGeoBEARS" (Matzke, 2013). We chose these two models as they both model types of vicariance. They differ in that the DEC model allows subset sympatry, whereas DIVA does not, and DIVA allows widespread vicariance, unlike the DEC model (Ronquist & Sanmartín, 2011).

We defined our geographic areas as (a) Chile, (b) South Africa, (c) Sri Lanka, (d) Western Australia, (e) Eastern Australia and (f) New Zealand. Western and Eastern Australia were designated as separate regions because the large distance and desert conditions across Australia act as an effective barrier for dispersal-limited animals (Giribet & Edgecombe, 2006). The maximum range size was constrained to three areas to speed up computations and because pettalid species have narrow ranges, typically under 50km across, and allowing an ancestral range to span six areas seemed biologically implausible.

We ran both models in an unconstrained framework and in a stratified framework in which we included information about the connectivity between the landmasses of Gondwana throughout its breakup (Table 3). In cases where the timing of a geologic event is more uncertain, such as the opening of the Atlantic Ocean, we set our stratification breaks to be on the earlier side of the estimated date range, as Cyphophthalmi tend to be unable to cross even small

TABLE 3 Stratification times for geological events used in "BioGeoBEARS" analysis

50 Mya	Australia splits from Antarctica–South America (opening of the Tasmanian Gateway)	Wei (2004)
80 Mya	New Zealand splits from Australia–Antarctica (opening of the Tasman Sea)	McLoughlin (2001)
130 Mya	Madagascar–India split from Australia–Antarctica–New Zealand	Ali and Aitchison (2008); McLoughlin (2001)
140 Mya	South America splits from Africa (opening of southern Atlantic Ocean)	Eagles (2007)
170 Mya	West Gondwana (South America–Africa) and East Gondwana (India–Madagascar–Antarctica–Australia–New Zealand) split	Ali and Aitchison (2008)

barriers such as rivers. We ran this stratified analysis twice, using different values in the manual dispersal multipliers matrix (Table S2). In one configuration ("lenient"), the dispersal multipliers ranged from 0.1 to 1, in line with other studies that have looked for signals of Gondwanan vicariance (e.g. Beaulieu, Tank, & Donoghue, 2013; Mao et al., 2012). For the second configuration ("strict"), we set the manual dispersal multipliers to vary from 0.01 to 1 and made the connectivity between different areas more restrictive, as we felt this better reflected the biology of pettalids. Finally, to accommodate the uncertainty of our inferred phylogenetic divergence times, we took 100 random trees from the posterior distribution of the BEAST analysis, ran the DEC and DIVA-like models on each of them, and averaged their results. This resulted in six permutations of ancestral range inference ("DIVA-unconstrained", "DIVA-lenient", "DIVA-strict", "DEC-unconstrained", "DEC-lenient" and "DEC-strict").

3 | RESULTS

3.1 | Phylogenetic relationships in Pettalidae

We recovered the monophyly of Pettalidae in all analyses with maximal support. Furthermore, we found a nearly fully resolved, well-supported topology with respect to intergeneric relationships that was stable when accounting for the most common sources of systematic error, including inference method, matrix completeness, compositional heterogeneity, evolutionary rate variation, and outgroup composition (Figure 2a and Figure S1.1).

We found the South African genus *Parapurcellia* to be the sister group to all other genera, consistent with results from previously published Sanger-based phylogenies (Boyer & Giribet, 2007; Giribet et al., 2016). Furthermore, in all our analyses, we recovered a clear split between a clade of taxa from former Eastern Gondwana (i.e. Australia [*Austropurcellia*, *Karripurcellia*], New Zealand [*Aoraki*, *Neopurcellia*, *Rakaia*], and the Indian subcontinent [*Pettalus*]), and an earlier-branching grade of taxa from Western Gondwana (i.e. Africa [*Parapurcellia*, *Purcellia*] and South America [*Chileogovea*]).

There were two places where results varied between analyses: (a) Matrix 1 placed the New Zealand genera *Aoraki* and *Neopurcellia* as sister taxa to the exclusion of the Western Australian genus *Karripurcellia* in the partitioned IQ-TREE analysis (71% bootstrap support), whereas all other analyses found *Aoraki* + *Karripurcellia*, to the exclusion of *Neopurcellia* (Figure S1.2). Given that this was our smallest matrix, and that it recovered a relatively low bootstrap support value, we believe this is an artefact of limited gene sampling and feel more confident with the grouping of *Aoraki* + *Karripurcellia*, supported by the larger matrices. (b) In our concatenated analyses, the Sri Lankan genus *Pettalus* always resolved as the sister group of the eastern Australian genus *Austropurcellia*, typically with high support. However, in 5/6 of our ASTRAL analyses, *Pettalus* came out as the sister group to a larger clade of the genera *Austropurcellia*, *Neopurcellia*, *Karripurcellia* and *Aoraki* (all from Australia and New Zealand) with high support (Figure 2d). The ASTRAL analysis of matrix 1 placed *Pettalus* as the sister group of all the other eastern Gondwanan genera, with 83% support (Figure S1.3).

3.2 | Interrogating the position of *Pettalus*

Inconsistency in results of concatenation and coalescence methods is a well-known problem in systematics, with numerous papers arguing for the application of certain methods over others depending on biases in data. Those who favour coalescence methods tout their ability to account for gene tree heterogeneity due to, for example, incomplete lineage sorting (Liu, Yu, Kubatko, Pearl, & Edwards, 2009). Advocates of concatenation methods, on the other hand, point to the ability of concatenation to reveal weak but consistent phylogenetic signal across genes that might be obscured in coalescence methods (Gatesy & Baker, 2005; Gatesy & Springer, 2014). Resolving the position of the sole lineage from the Indian subcontinent is critical for understanding the biogeographic history of this family in former East Gondwana. Given the differing placement of *Pettalus* in our phylogeny with concatenation and coalescence methods, we took additional steps to explore our data to see what might be driving this result.

We used quartet likelihood mapping to assess the phylogenetic information content of our matrix 4 alignment with respect to resolving the position of *Pettalus* (Figure 3). Quartet mapping allows one to visualize the tree likeness of all quartets (i.e. comparisons of four taxa) into a single graph; points that fall in the centre of the triangle represent quartets that show star-like evolution and are therefore unsuitable for resolving between alternative topology hypotheses. Points that fall in one of the corners of the triangle support a well-resolved phylogeny. Our likelihood mapping analysis of all 120 quartets from our alignment placed all points in corners: 70% (84/120) support *Pettalus* + *Austropurcellia*, 5% (6/120) support *Pettalus* + (*Neopurcellia*, *Karripurcellia* and *Aoraki*) and 25% (30/120) support *Pettalus* + *Rakaia*.

We also calculated the ΔGLS metric of Shen et al. (2017) to assess how much conflicting signal we had in our data for the concatenated versus coalescent topology (Figure S1.4). This analysis allows one to determine where in a dataset the support for differing topologies is located, and how strong that support is. Our results showed that the vast majority of orthogroups only weakly support either topology (T1 mean = 1.492, max = 12.22; T2 mean = −1.496, max = −20.56), although slightly more orthogroups support T1 (411/739) versus T2 (328/739). These results help explain the underlying reason for the divergent results of concatenation methods and ASTRAL for our data; stochastic errors in individual gene trees, arising from short genes with limited phylogenetic signal, can cause species tree estimation errors in summary coalescence methods such as ASTRAL. In this circumstance, concatenation methods will resolve relationships with weak but consistent phylogenetic signal across genes (i.e. "hidden support", Gatesy & Baker, 2005; Gatesy & Springer, 2014). Indeed, the average length of orthogroups in matrix 4 (optimizing signal for *Pettalus*) is significantly shorter than the average length of orthogroups in matrix 3, from which it is derived (M3 = 333 AAs, M4 = 217 AAs; *p*-value = 2.2e-16),

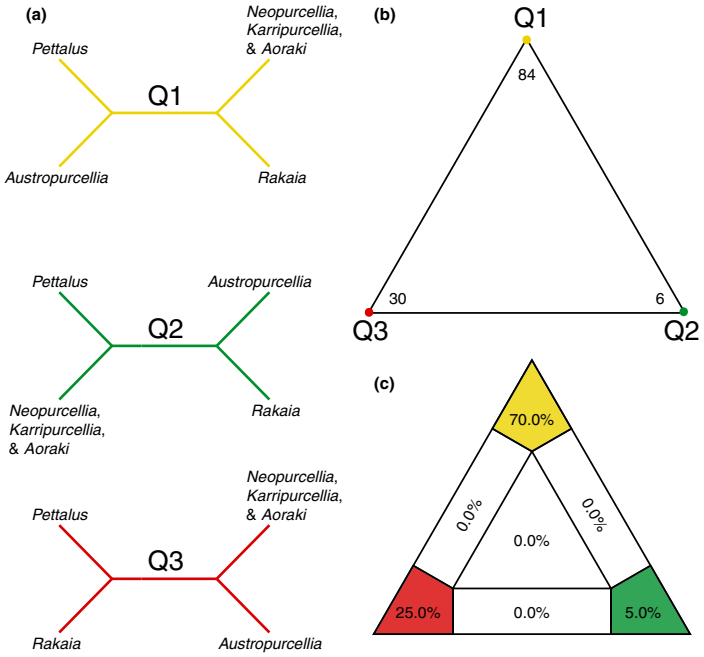

FIGURE 3 Results of the quartet likelihood mapping analysis performed on M4. (a) The three possible topologies for our four predefined groups from East Gondwana (see Section 2 for details). (b) Number of quartets that support each of the three possible topologies. Colours as in (a). (c) Percentage of quartets that support each of the possible topologies, with regions of the graph differentiated according to how well a quartet falling in that region can answer a phylogenetic hypothesis

suggesting that there is simply limited signal to be drawn from the transcriptomic data of this older, highly degraded specimen.

Based on the stronger signal for *Pettalus* + *Austropurcellia* (T1) in the likelihood mapping analysis, and the consistently ambiguous support for either topology based on ΔGLS, we felt more confident in our concatenated topology, and used that as the framework for our biogeographic hypothesis testing.

3.3 | Diversification analyses

In our time-calibrated phylogeny of transcriptomic data, the age of Pettalidae is estimated to be 212 Ma (95% highest posterior density [HPD]: 267–160 Ma). The East Gondwanan taxa (*Rakaia*, *Pettalus*, *Austropurcellia*, *Neopurcellia*, *Karripurcellia* and *Aoraki*) diverged from the West Gondwanan taxa (*Parapurcellia*, *Purcellia* and *Chileogovea*) 151 Mya (95% HPD: 196–110 Mya). Within West Gondwana, the South American genus *Chileogovea* diverged from the South African genera 162 Mya (95% HPD: 209–119 Mya). *Rakaia* diverged from the other East Gondwanan taxa 151 Mya (95% HPD: 196–110 Mya). *Neopurcellia* diverged from *Aoraki* and *Karripurcellia* 126 Mya (95% HPD: 167–91 Ma), and *Aoraki* and *Karripurcellia* diverged 114 Mya (95% HPD: 153–81 Mya). *Pettalus* and *Austropurcellia* diverged from each other 130 Mya (95% HPD: 172–93 Mya). These times, inclusive of the 95% confidence intervals, largely concord with the dates inferred in our densely sampled Sanger-based diversification analysis as well (Figure 4). Indeed, the only two inferred ages that do not overlap are the age of the genus *Austropurcellia* and the age of the *Aoraki denticulata* clade (we compared the times in just this subclade because our transcriptomic sampling for *Aoraki* did not cover the full taxonomic range of the genus, see Figure 4).

Our speciation–extinction analysis in BAMM found one distinct shift configuration, corresponding to zero core shifts in net diversification rate through time (p = 1.0, Figure S1.5). We had expected to find at least one shift in net diversification rate, corresponding to the extinction of lineages in Antarctica and Australia as those continents lost suitable habitat due to cooling and aridification in the Cenozoic. Instead, we found a relatively constant net diversification rate through time, although qualitatively looking at the LTT plot it does appear that the majority of cladogenesis occurred at the base of the tree, with an apparent slowdown in the Cenozoic (Figure 4). This trend is also reflected in a γ value of −6.00578 for our tree (Pybus & Harvey, 2000). It is possible that this apparent slowdown in net diversification could be due to extinction across Antarctica and Australia, although the process appears to be constant over the entire tree and not just restricted to the clade of *Pettalus* + *Austropurcellia*, or even only the East Gondwanan clade. Programs explicitly developed to detect time-simultaneous shifts in extinction rates, such as CoMET (May, Höhna, Moore, & Cooper, 2016), could be used in the future to further test this hypothesis of uniform mass extinction across Pettalidae in the Cenozoic.

3.4 | Ancestral range estimation

Analyses under both the DEC and DIVA-like models gave very similar results for the ancestral range estimation of Pettalidae. All six

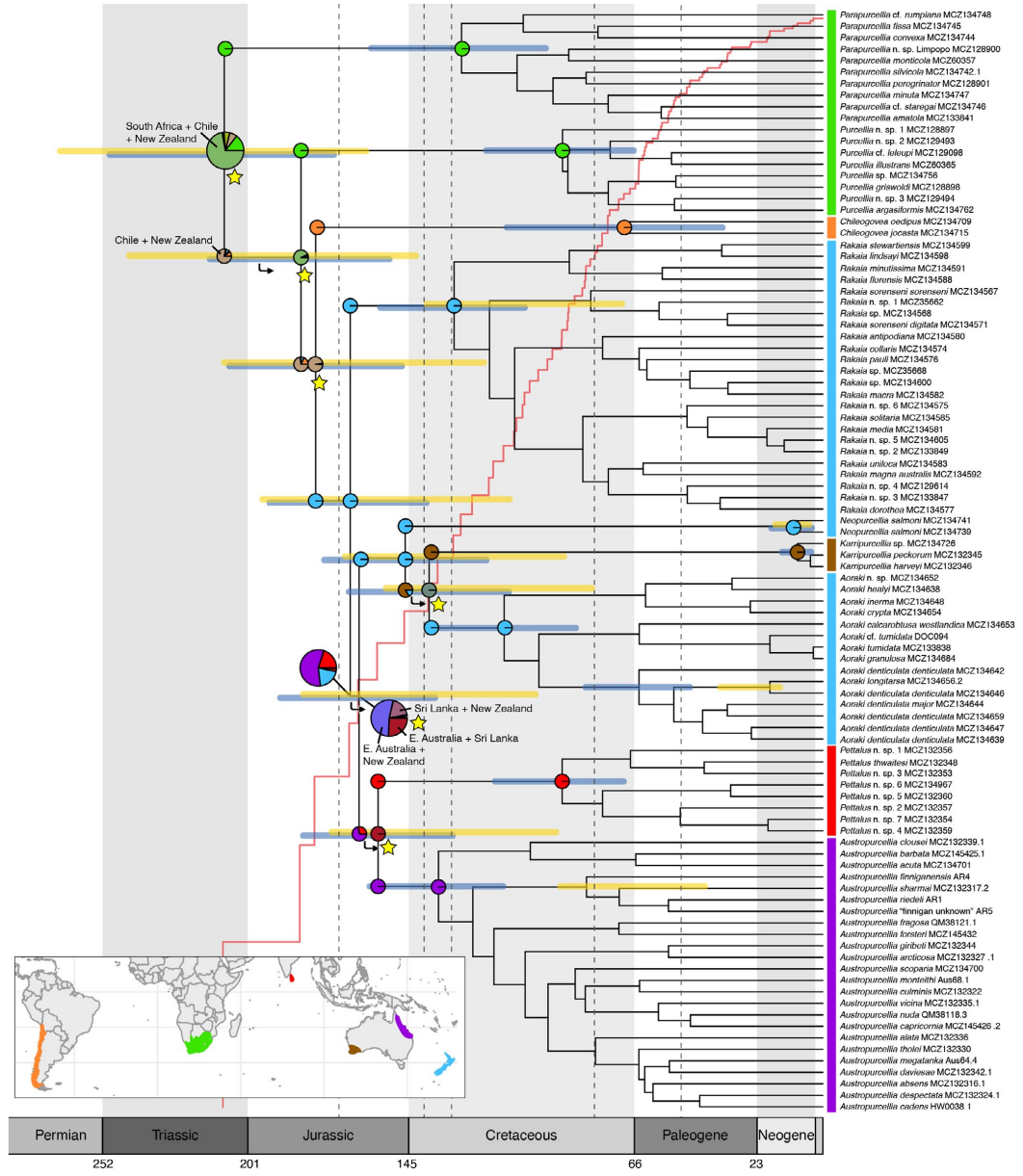

FIGURE 4 Dated phylogeny of 96 pettalid terminals inferred in BEAST with the topology constrained to follow the intergeneric relationships of the T1 concatenated topology. Yellow bars correspond to 95% HPD regions of the transcriptomic dating analysis done in PhyloBayes, blue bars correspond in 95% HPD regions of the BEAST dating analysis. Terminals coloured according to geographic region, as shown in inset map. Pie charts at nodes show relative probabilities of estimated ancestral ranges as inferred by the "DIVA-strict" analysis (highest likelihood result). Certain pie charts enlarged to show detail. Yellow stars indicate nodes where vicariance is inferred; black arrows indicate branches along which range expansion occurred. Vertical dotted lines correspond to major events in Gondwanan rifting included in the "BioGeoBEARS" stratified models. Red line shows the LTT plot for Pettalidae, scaled according to geologic time. HPD, highest posterior density

permutations of the analysis estimated low rates of dispersal (d = 1e-04–1.6e-03), and an extinction rate of 0. The analysis with the highest likelihood was the "DIVA-strict" model (Ln*L* = −28.78 averaged across 100 posterior trees), whereas the lowest likelihood analysis was the "DEC-unconstrained" model (Ln*L* = −35.21). Interestingly, under both the DEC model and the DIVA model, we recovered higher likelihoods for our stratified analyses compared with the unconstrained analyses, suggesting a negligible role for overwater long-distance dispersal.

For each of the six analyses, the reconstructed ranges were nearly identical at all nodes (Figures S2.1–S2.6). That is, regardless of the model of biogeographic range evolution, or the stringency of stratification (or lack thereof), we recover a consistent pattern of range evolution in pettalids (see Figure 4). The ancestral range of all pettalids was estimated to be Chile + New Zealand + South Africa, which vicariantly split into a lineage that remained in South Africa (*Parapurcellia*) and another lineage that persisted in Chile + New Zealand in the DIVA-strict reconstruction. That lineage then dispersed back into South Africa and went through another round of vicariance in which one lineage remained in South Africa (*Purcellia*) and the other lineage persisted in Chile + New Zealand. The clade in Chile + New Zealand underwent another round of vicariance, with one lineage leading to *Chileogovea* and the other persisting in New Zealand and leading to the East Gondwanan clade. Within that clade, the different biogeographic analyses reconstruct similar sequences of dispersal and vicariance events, although the probability of any one particular range reconstruction is often fairly low, especially at the corner and node leading to *Neopurcellia*, *Karripurcellia*, *Aoraki*, *Pettalus* and *Austropurcellia*. Notably, this is the same node that was particularly difficult to resolve phylogenetically.

In total, we inferred six vicariance events and four dispersal events within Pettalidae. Importantly, all of the reconstructed dispersal events occurred while the relevant landmasses were still connected, suggesting contiguous terrestrial range expansion. This was true even in the unconstrained analyses.

4 | DISCUSSION

4.1 | Pettalidae is a Gondwanan vicariant lineage

While it has previously been demonstrated that the timing of diversification within Pettalidae was consistent with the timing of Gondwanan breakup (Giribet et al., 2012; Oberski et al., 2018), the relationships between genera had remained recalcitrant until now, precluding explicit biogeographic analysis. We find here that not only is the timing of diversification within the family consistent with a scenario of Gondwanan vicariance, but the order of cladogenesis also corresponds to the manner in which the supercontinent broke apart, corroborating its status as a textbook example of Gondwanan vicariance (Zimmer, 2010).

Furthermore, we can point to specific inferences of vicariance in our tree that occurred at approximately the same time as when the relevant landmasses were separating. For example, the timing of the divergence between *Chileogovea* (Chile) and *Parapurcellia* and *Purcellia* (South Africa) has a 95% HPD range 209–119 Mya, inclusive of both divergence analyses, which overlaps with the initial opening of the southern Atlantic Ocean ~150–120 Mya (Figure 4). In addition, the divergence between *Austropurcellia* (eastern Australia) and *Pettalus* (Sri Lanka) has a total range 182–93 Mya inclusive of both dating analyses, which overlaps with the timing of India–Madagascar rifting from Australia–Antarctica–New Zealand *ca*. 130 Mya. Also, the timing of the divergence between *Purcellia* (South Africa) and the rest of the family (except *Parapurcellia*) has a 95% HDP range 242–142 Mya inclusive of both analyses, which overlaps with the initial divergence between West Gondwana and East Gondwana ~170 Mya. Although this bipartition is not between those two landmasses exactly, it is well accepted that South America remained connected to East Gondwana via the Antarctic Peninsula, and many geological reconstructions specify the split between Africa and Antarctica, corresponding to the opening of the Weddell Sea, as the first Gondwanan rifting event (e.g. Jokat et al., 2003).

Some of the divergences predate any Gondwanan rifting, such as the first split of *Parapurcellia* and the rest of the family. In addition, the genera from New Zealand (*Rakaia*, *Neopurcellia* and *Aoraki*) are inferred to have diverged from their sister groups before New Zealand separated from Australia–Antarctica *ca*. 80 Mya. In the case of the diverse genera *Rakaia* and *Aoraki*, the BEAST analysis even recovers 95% CIs around their initial diversification that completely predate New Zealand's separation from mainland Gondwana. While non-monophyly in these landmasses (e.g. South Africa, New Zealand) seems contrary to the idea of Gondwanan vicariance, the ancient ages of the constituent genera show that their origination predates Gondwanan breakup, instead implying multiple colonizations of major areas or ancestral cladogenesis while landmasses were still connected. Indeed, this same pattern wherein Gondwanan landmasses contain non-monophyletic assemblages of taxa is also found in other groups of organisms with ancient ages, such as onychophorans (Murienne et al., 2014), orsolobid spiders (Chousou-Polydouri et al., 2019), freshwater mussels (Graf, Jones, Geneva, Pfeiffer, & Klunzinger, 2015) and earthworms (Buckley et al., 2011), potentially suggesting common mechanisms driving cladogenesis in distantly related groups.

This pattern becomes even more impressive when compared against various sources of geological evidence from temperate Gondwana, such as the palynological record and glacial deposits. These suggest that in the Triassic and Jurassic, as pettalids were first diversifying and expanding across the supercontinent, floristic provincialism across high latitudes was likely low, marked by cosmopolitan species and widespread vegetation types (McLoughlin, 2001). With continuous expanses of forest, pettalids likely experienced few barriers to terrestrial migration within these temperate regions. However, the Cretaceous was marked by floristic turnovers corresponding to the rise of angiosperms and increased provincialism caused by differentiation along latitudinal clines, continental fragmentation and substantial marine incursions, especially across Australasia (McLoughlin & Kear, 2010). Four major subprovinces are recognized within southern Gondwana at this time:

Patagonia–Palmer (southern South America–Antarctic Peninsula), South Africa, Indo-Eromanga (India–northern Australia) and Tasman (south-eastern Australia and New Zealand; McLoughlin, 2001). Amazingly, these four areas of endemism described for plants almost perfectly correlate with the major clades we recover in Pettalidae at the same time (Figure 4). Subsequent cladogenesis and extinction was likely further promoted by climate-related habitat heterogeneity and fragmentation. Importantly, despite the fact that some cladogenesis was not driven by Gondwanan breakup per se, there is no evidence that long-distance, *trans*-oceanic dispersal played any role in the biogeographic history of the family.

4.2 | East Gondwanan relationships and diversification dynamics

While the ancient age of the *Pettalus–Austropurcellia* divergence is congruent with the timing of tectonic breakup of their respective landmasses, their sister-group relationship is unexpected, especially given that the Western Australian genus *Karripurcellia* was geographically much closer to the Indian subcontinent than eastern Australia ever was. However, *Karripurcellia* always groups with two genera from New Zealand, *Aoraki* and *Neopurcellia*, with strong support. Our difficulty in resolving the position of *Pettalus*, while no doubt hampered by the poor quality of the transcriptome, may also have been confounded by missing lineages in our study. There are two monotypic mite harvestman genera from Madagascar, at least one of which falls within Pettalidae, but these species have not been found since their initial discovery in 1969 (Giribet et al., 2012; Shear & Gruber, 1996), despite great efforts in sampling leaf-litter arthropods in Madagascar in the past decade, and therefore are necessarily missing from our molecular analysis. In addition, it is very likely that pettalids once lived in the temperate rainforests that covered Antarctica and central Australia, but given the improbability of (a) a mite harvestman fossilizing and (b) finding one of those fossils, the presence of those lineages is completely speculative and may never be known for certain. Still, the sheer amount of land area in Antarctica and central Australia makes it possible that there were several distinct lineages of pettalids there that subsequently went extinct. Likewise, *Pettalus* is the only genus known from the Indian subcontinent, and they are restricted to Sri Lanka, on its southernmost tip, but it is likely that additional pettalid diversity lived in the Indian subcontinent and that it went extinct after colliding with Eurasia. This phenomenon could have contributed to the difficulty in resolving intergeneric relationships using standard Sanger markers, and in placing *Pettalus* using transcriptomes specifically.

While it is difficult to prove extinction in the absence of a fossil record, we tested for signal of extinction using a time-calibrated phylogeny with near-complete extant species sampling. Our speciation–extinction analysis in BAMM found no place in our phylogeny where net diversification rates were significantly different. Qualitative assessment of our LTT plot does reveal an apparent slowdown in net diversification starting in the Oligocene (*ca.* 33 Mya). However, in a quantitative framework, we find no evidence for mass extinction in the Cenozoic (or at any time) that could correspond to lineages going extinct as central Australia aridified and Antarctica glaciated.

4.3 | A note on the role of taxonomy in diversification analyses

The species delimitation criteria favoured by taxonomists undoubtedly have great influence on the ability of any method to infer diversification from phylogenies. Taxonomy in Pettalidae has been well-characterized using modern, integrative methods (e.g. pairing molecular phylogenetics with detailed microscopic examination to detect cryptic species) and has been worked on almost exclusively by our research groups, so we feel confident that species concepts have been consistently applied across the entire family. That being said, in Sri Lanka there are only four described species of *Pettalus* and a much larger number of undescribed species, half of which were discovered during a single field excursion by SLB and GG. Given the short-range endemic nature of mite harvestmen, further fieldwork would very likely uncover new species, which in turn could further clarify the diversification dynamics of Pettalidae, especially in East Gondwana.

5 | CONCLUSION

Using a combination of transcriptome sequencing and species-level sampling of Sanger loci, we have resolved the phylogenetic relationships between genera in Pettalidae and found signatures of Gondwanan vicariance in the biogeographic history of the family. The topology and divergence times together tell a compelling story of early Mesozoic diversification and range expansion, contemporaneous with the expansion of temperate forests across southern Gondwana, followed by allopatric speciation due to tectonic breakup and climatic differentiation.

It is worth noting that to meet the temporal standard of vicariance, one must have fairly precise date estimations, and as such it is easier to accept a hypothesis of transoceanic dispersal or non-Gondwanan vicariance (Upchurch, 2008). Despite our limited fossil record and resultantly large error bars in divergence dating, we find three places in our phylogeny in which biogeographic range models infer vicariance and the estimated time of that cladogenetic event overlaps with the relevant geologic event. While we do not take this to mean necessarily that the geologic event caused such cladogenesis, it does suggest that the taxa were in approximately the right place at approximately the right time to have been influenced by Gondwanan breakup. Indeed, the entire concept of continental breakup driving speciation is somewhat removed from how we believe speciation actually occurs in pettalids; rather, it seems more biologically plausible that Gondwanan fragmentation reinforced divergences between clades that were already under way, preventing re-colonization of areas once they become isolated. Despite all this, we believe that

there is still ample evidence that Pettalidae retains signatures of Gondwanan breakup, a remarkable feat for such an ancient event.

ACKNOWLEDGEMENTS

This study would not have been possible without Fernando Álvarez Padilla, Miquel Arnedo, Michelle Coblens, Ron Clouse, Savel R. Daniels, Rosa Fernández, Sophie Harrison, Mark Harvey, Gustavo Hormiga, Katya Jay, Joanne Johnson, Bob Kallal, Indika Karunarathna, Jill Oberski, Christine Palmer, Abel Pérez-González, Mike Rix, Prashant Sharma and Sebastián Vélez, all of whom helped collect specimens for this project. All specimens were collected under valid permits (New Zealand multiple permits [38002-RES]; Australia [QLD #WITK13653913, #WITK08381010; WA Permits #OF000190, #CE000648, #SF004565]; Chile [Autorización #026/2014]; South Africa [Eastern Cape permits #CRO 108/11CR and CRO 109/11CR; KZN #OP 4085/2011] and Western Cape Permit # AAA007-00344-0035). We thank Rosa Fernández and Martin Schwentner for their help in teaching molecular and computational methods involved in RNA sequencing. Adam Baldinger and Breda Zimkus provided collections support at the MCZ. Computations for this project were done on the Odyssey cluster, supported by the FAS Division of Science at Harvard University. Shahan Derkarabetian, Vanessa Knutson, Shoyo Sato and Prashant Sharma provided helpful discussion of this project. Field work was supported by multiple Putnam Expedition Grants from the MCZ. This work was supported by an NSF GRFP to CMB, by NSF Grants DEB-1457539, DEB-1754278 to GG, and DEB-1020809 to SLB. Editor Isabel Sanmartín and two anonymous reviewers provided comments that helped to improve this study.

CONFLICT OF INTEREST

The authors have no conflicts of interest to report.

DATA AVAILABILITY STATEMENT

All alignments and resulting Newick-format phylogenies, the BEAST xml file, and the input trees and results of the ΔGLS calculations have been uploaded to the Harvard Dataverse (https://doi.org/10.7910/DVN/89DHPH). Sequence data are available from the NCBI Sequence Read Archive (SRA) database under PRJNA547831 (SRR11735076–SRR11735091). Specimen information (as shown in Table 1 and Table S1) is available online through the Museum of Comparative Zoology's database, MCZBase (http://mczbase.mcz.harvard.edu).

ORCID

Caitlin M. Baker https://orcid.org/0000-0002-9782-4959
Sarah L. Boyer https://orcid.org/0000-0003-1414-4489
Gonzalo Giribet https://orcid.org/0000-0002-5467-8429

REFERENCES

Aberer, A. J., Kobert, K., & Stamatakis, A. (2014). ExaBayes: Massively parallel Bayesian tree inference for the whole-genome era. *Molecular Biology and Evolution*, *31*(10), 2553–2556. https://doi.org/10.1093/molbev/msu236

Ali, J. R., & Aitchison, J. C. (2008). Gondwana to Asia: Plate tectonics, paleogeography and the biological connectivity of the Indian sub-continent from the Middle Jurassic through latest Eocene (166–35 Ma). *Earth-Science Reviews*, *88*(3–4), 145–166. https://doi.org/10.1016/j.earscirev.2008.01.007

Altenhoff, A. M., Boeckmann, B., Capella-Gutierrez, S., Dalquen, D. A., DeLuca, T., Forslund, K., … Dessimoz, C. (2016). Standardized benchmarking in the quest for orthologs. *Nature Methods*, *13*(5), 425–430. https://doi.org/10.1038/nmeth.3830

Altenhoff, A. M., Skunca, N., Glover, N., Train, C. M., Sueki, A., Pilizota, I., Dessimoz, C. (2015). The OMA orthology database in 2015: function predictions, better plant support, synteny view and other improvements. *Nucleic Acids Research*, *43*(Database issue), D240–D249. https://doi.org/10.1093/nar/gku1158

Beaulieu, J. M., Tank, D. C., & Donoghue, M. J. (2013). A Southern hemisphere origin for campanulid angiosperms, with traces of the break-up of Gondwana. *BMC Evolutionary Biology*, *13*, 80. https://doi.org/10.1186/1471-2148-13-80

Benavides, L. R., Cosgrove, J. G., Harvey, M. S., & Giribet, G. (2019). Phylogenomic interrogation resolves the backbone of the Pseudoscorpiones Tree of Life. *Molecular Phylogenetics and Evolution*, *139*, 106509. https://doi.org/10.1016/j.ympev.2019.05.023

Bouckaert, R., Heled, J., Kühnert, D., Vaughan, T., Wu, C.-H., Xie, D., … Drummond, A. J. (2014). BEAST 2: A software platform for Bayesian evolutionary analysis. *PLOS Computational Biology*, *10*(4), e1003537. https://doi.org/10.1371/journal.pcbi.1003537

Boyer, S. L., Clouse, R. M., Benavides, L. R., Sharma, P. P., Schwendinger, P. J., Karunarathna, I., & Giribet, G. (2007). Biogeography of the world: A case study from cyphophthalmid Opiliones, a globally distributed group of arachnids. *Journal of Biogeography*, *34*(12), 2070–2085. https://doi.org/10.1111/j.1365-2699.2007.01755.x

Boyer, S. L., & Giribet, G. (2007). A new model Gondwanan taxon: Systematics and biogeography of the harvestman family Pettalidae (Arachnida, Opiliones, Cyphophthalmi), with a taxonomic revision of genera from Australia and New Zealand. *Cladistics*, *23*(4), 337–361. https://doi.org/10.1111/j.1096-0031.2007.00149.x

Buckley, T. R., James, S., Allwood, J., Bartlam, S., Howitt, R., & Prada, D. (2011). Phylogenetic analysis of New Zealand earthworms (Oligochaeta: Megascolecidae) reveals ancient clades and cryptic taxonomic diversity. *Molecular Phylogenetics and Evolution*, *58*(1), 85–96. https://doi.org/10.1016/j.ympev.2010.09.024

Cantrill, D. J., & Poole, I. (2012). After the heat: late Eocene to Pliocene climatic cooling and modification of the Antarctic vegetation. In *The Vegetation of Antarctica through Geological Time* (pp. 390–457). Cambridge: Cambridge University Press. https://doi.org/10.1017/CBO9781139024990.009

Capella-Gutiérrez, S., Silla-Martínez, J. M., & Gabaldón, T. (2009). trimAl: A tool for automated alignment trimming in large-scale phylogenetic analyses. *Bioinformatics*, *25*(15), 1972–1973. https://doi.org/10.1093/bioinformatics/btp348

Chousou-Polydouri, N., Carmichael, A., Szűts, T., Saucedo, A., Gillespie, R., Griswold, C., & Wood, H. M. (2019). Giant Goblins above the waves at the southern end of the world: The biogeography of the spider family Orsolobidae (Araneae, Dysderoidea). *Journal of Biogeography*, *46*(2), 332–342. https://doi.org/10.1111/jbi.13487

Clouse, R. M., & Giribet, G. (2007). Across Lydekker's Line – first report of mite harvestmen (Opiliones : Cyphophthalmi : Stylocellidae) from New Guinea. *Invertebrate Systematics*, *21*(3), 207. https://doi.org/10.1071/is06046

Cook, L. G., & Crisp, M. D. (2005). Not so ancient: The extant crown group of *Nothofagus* represents a post-Gondwanan radiation. *Proceedings of the Royal Society B: Biological Sciences*, *272*(1580), 2535–2544. https://doi.org/10.1098/rspb.2005.3219

Cunha, T. J., & Giribet, G. (2019). A congruent topology for deep gastropod relationships. *Proceedings of the Royal Society B: Biological*

Sciences, *286*(1898), 20182776. https://doi.org/10.1098/rspb.2018.2776

Dunlop, J. A., Anderson, L. I., Kerp, H., & Hass, H. (2004). A harvestman (Arachnida: Opiliones) from the Early Devonian Rhynie cherts, Aberdeenshire, Scotland. *Transactions of the Royal Society of Edinburgh: Earth Sciences*, *94*(04), 341–354. https://doi.org/10.1017/s0263593300000730

Eagles, G. (2007). New angles on South Atlantic opening. *Geophysical Journal International*, *168*(1), 353–361. https://doi.org/10.1111/j.1365-246X.2006.03206.x

Edgar, R. C. (2004). MUSCLE: Multiple sequence alignment with high accuracy and high throughput. *Nucleic Acids Research*, *32*(5), 1792–1797. https://doi.org/10.1093/nar/gkh340

Feijão, P. C., Neiva, L. S., de Azeredo-Espin, A. M., & Lessinger, A. C. (2006). AMiGA: The arthropodan mitochondrial genomes accessible database. *Bioinformatics*, *22*(7), 902–903. https://doi.org/10.1093/bioinformatics/btl021

Fernández, R., Edgecombe, G. D., & Giribet, G. (2016). Exploring phylogenetic relationships within Myriapoda and the effects of matrix composition and occupancy on phylogenomic reconstruction. *Systematic Biology*, *65*(5), 871–889. https://doi.org/10.1093/sysbio/syw041

Fernández, R., & Giribet, G. (2015). Unnoticed in the tropics: Phylogenomic resolution of the poorly known arachnid order Ricinulei (Arachnida). *Royal Society Open Science*, *2*(6), 150065. https://doi.org/10.1098/rsos.150065

Fernández, R., Hormiga, G., & Giribet, G. (2014). Phylogenomic analysis of spiders reveals nonmonophyly of orb weavers. *Current Biology*, *24*(15), 1772–1777. https://doi.org/10.1016/j.cub.2014.06.035

Fernández, R., Laumer, C. E., Vahtera, V., Libro, S., Kaluziak, S., Sharma, P. P., … Giribet, G. (2014). Evaluating topological conflict in centipede phylogeny using transcriptomic data sets. *Molecular Biology and Evolution*, *31*(6), 1500–1513. https://doi.org/10.1093/molbev/msu108

Fernández, R., Sharma, P. P., Tourinho, A. L., & Giribet, G. (2017). The Opiliones tree of life: shedding light on harvestmen relationships through transcriptomics. *Proceedings of the Royal Society of London B*, *284*(1849). https://doi.org/10.1098/rspb.2016.2340

Foster, P. G. (2004). Modeling compositional heterogeneity. *Systematic Biology*, *53*(3), 485–495. https://doi.org/10.1080/10635150490445779

Foster, P. G. (2018). p4 (Python package). Program and documentation. Available at http://p4.nhm.ac.uk/tutorial/tut_compo.html

Fu, L., Niu, B., Zhu, Z., Wu, S., & Li, W. (2012). CD-HIT: Accelerated for clustering the next-generation sequencing data. *Bioinformatics*, *28*(23), 3150–3152. https://doi.org/10.1093/bioinformatics/bts565

Garwood, R. J., Dunlop, J. A., Giribet, G., & Sutton, M. D. (2011). Anatomically modern Carboniferous harvestmen demonstrate early cladogenesis and stasis in Opiliones. *Nature Communications*, *2*, 444. https://doi.org/10.1038/ncomms1458

Garwood, R. J., Sharma, P. P., Dunlop, J. A., & Giribet, G. (2014). A Paleozoic stem group to mite harvestmen revealed through integration of phylogenetics and development. *Current Biology*, *24*(9), 1017–1023. https://doi.org/10.1016/j.cub.2014.03.039

Gatesy, J., & Baker, R. H. (2005). Hidden likelihood support in genomic data: Can forty-five wrongs make a right? *Systematic Biology*, *54*(3), 483–492. https://doi.org/10.1080/10635150590945368

Gatesy, J., & Springer, M. S. (2014). Phylogenetic analysis at deep timescales: Unreliable gene trees, bypassed hidden support, and the coalescence/concatalescence conundrum. *Molecular Phylogenetics and Evolution*, *80*, 231–266. https://doi.org/10.1016/j.ympev.2014.08.013

Giribet, G., Boyer, S. L., Baker, C. M., Fernández, R., Sharma, P. P., de Bivort, B. L., … Griswold, C. E. (2016). A molecular phylogeny of the temperate Gondwanan family Pettalidae (Arachnida, Opiliones, Cyphophthalmi) and the limits of taxonomic sampling. *Zoological Journal of the Linnean Society*, *178*(3), 523–545. https://doi.org/10.1111/zoj.12419

Giribet, G., & Edgecombe, G. D. (2006). The importance of looking at small-scale patterns when inferring Gondwanan biogeography: A case study of the centipede *Paralamyctes* (Chilopoda, Lithobiomorpha, Henicopidae). *Biological Journal of the Linnean Society*, *89*(1), 65–78. https://doi.org/10.1111/j.1095-8312.2006.00658.x

Giribet, G., Sharma, P. P., Benavides, L. R., Boyer, S. L., Clouse, R. M., De bivort, B. L., … Schwendinger, P. J. (2012). Evolutionary and biogeographical history of an ancient and global group of arachnids (Arachnida: Opiliones: Cyphophthalmi) with a new taxonomic arrangement. *Biological Journal of the Linnean Society*, *105*(1), 92–130. https://doi.org/10.1111/j.1095-8312.2011.01774.x

Grabherr, M. G., Haas, B. J., Yassour, M., Levin, J. Z., Thompson, D. A., Amit, I., … Regev, A. (2011). Full-length transcriptome assembly from RNA-Seq data without a reference genome. *Nature Biotechnology*, *29*(7), 644–652. https://doi.org/10.1038/nbt.1883

Graf, D. L., Jones, H., Geneva, A. J., Pfeiffer, J. M. 3rd, & Klunzinger, M. W. (2015). Molecular phylogenetic analysis supports a Gondwanan origin of the Hyriidae (Mollusca: Bivalvia: Unionida) and the paraphyly of Australasian taxa. *Molecular Phylogenetics and Evolution*, *85*, 1–9. https://doi.org/10.1016/j.ympev.2015.01.012

Haas, B. J., Papanicolaou, A., Yassour, M., Grabherr, M., Blood, P. D., Bowden, J., … Regev, A. (2013). *De novo* transcript sequence reconstruction from RNA-seq using the Trinity platform for reference generation and analysis. *Nature Protocols*, *8*(8), 1494–1512. https://doi.org/10.1038/nprot.2013.084

Heath, T. A. (2012). A hierarchical Bayesian model for calibrating estimates of species divergence times. *Systematic Biology*, *61*(5), 793–809. https://doi.org/10.1093/sysbio/sys032

Hedin, M., Starrett, J., Akhter, S., Schonhofer, A. L., & Shultz, J. W. (2012). Phylogenomic resolution of paleozoic divergences in harvestmen (Arachnida, Opiliones) via analysis of next-generation transcriptome data. *PLoS ONE*, *7*(8), e42888. https://doi.org/10.1371/journal.pone.0042888

Ho, S. Y., & Phillips, M. J. (2009). Accounting for calibration uncertainty in phylogenetic estimation of evolutionary divergence times. *Systematic Biology*, *58*(3), 367–380. https://doi.org/10.1093/sysbio/syp035

Jokat, W., Boebel, T., König, M., & Meyer, U. (2003). Timing and geometry of early Gondwana breakup. *Journal of Geophysical Research: Solid Earth*, *108*(B9), https://doi.org/10.1029/2002jb001802

Kalyaanamoorthy, S., Minh, B. Q., Wong, T. K. F., von Haeseler, A., & Jermiin, L. S. (2017). ModelFinder: Fast model selection for accurate phylogenetic estimates. *Nature Methods*, *14*(6), 587–589. https://doi.org/10.1038/nmeth.4285

Kemp, E. M. (1978). Tertiary climatic evolution and vegetation history in the Southeast Indian Ocean region. *Palaeogeography, Palaeoclimatology, Palaeoecology*, *24*(3), 169–208. https://doi.org/10.1016/0031-0182(78)90042-1

Kodandaramaiah, U. (2011). Tectonic calibrations in molecular dating. *Current Zoology*, *57*(1), 116–124. https://doi.org/10.1093/czoolo/57.1.116

Krosch, M. N., Baker, A. M., Mather, P. B., & Cranston, P. S. (2011). Systematics and biogeography of the Gondwanan Orthocladiinae (Diptera: Chironomidae). *Molecular Phylogenetics and Evolution*, *59*(2), 458–468. https://doi.org/10.1016/j.ympev.2011.03.003

Krueger, F. (2015). Trim Galore v 0.4.1. Program and documentation. Available at https://www.bioinformatics.babraham.ac.uk/projects/trim_galore/

Langmead, B., & Salzberg, S. L. (2012). Fast gapped-read alignment with Bowtie 2. *Nature Methods*, *9*(4), 357–359. https://doi.org/10.1038/nmeth.1923

Lartillot, N., Lepage, T., & Blanquart, S. (2009). PhyloBayes 3: A Bayesian software package for phylogenetic reconstruction and molecular

dating. *Bioinformatics*, *25*(17), 2286–2288. https://doi.org/10.1093/bioinformatics/btp368

Lartillot, N., & Philippe, H. (2004). A Bayesian mixture model for across-site heterogeneities in the amino-acid replacement process. *Molecular Biology and Evolution*, *21*(6), 1095–1109. https://doi.org/10.1093/molbev/msh112

Lartillot, N., Rodrigue, N., Stubbs, D., & Richer, J. (2013). PhyloBayes MPI: Phylogenetic reconstruction with infinite mixtures of profiles in a parallel environment. *Systematic Biology*, *62*(4), 611–615. https://doi.org/10.1093/sysbio/syt022

Laumer, C. E., Hejnol, A., & Giribet, G. (2015). Nuclear genomic signals of the 'microturbellarian' roots of platyhelminth evolutionary innovation. *Elife*, *4*, https://doi.org/10.7554/eLife.05503

Liu, L., Yu, L., Kubatko, L., Pearl, D. K., & Edwards, S. V. (2009). Coalescent methods for estimating phylogenetic trees. *Molecular Phylogenetics and Evolution*, *53*(1), 320–328. https://doi.org/10.1016/j.ympev.2009.05.033

Mao, K., Milne, R. I., Zhang, L., Peng, Y., Liu, J., Thomas, P., … Renner, S. S. (2012). Distribution of living Cupressaceae reflects the breakup of Pangea. *Proceedings of the National Academy of Sciences*, *109*(20), 7793–7798. https://doi.org/10.1073/pnas.1114319109

Martin, H. A. (2006). Cenozoic climatic change and the development of the arid vegetation in Australia. *Journal of Arid Environments*, *66*(3), 533–563. https://doi.org/10.1016/j.jaridenv.2006.01.009

Matzke, N. J. (2013). Probabilistic historical biogeography: New models for founder-event speciation, imperfect detection, and fossils allow improved accuracy and model-testing. *Frontiers of Biogeography*, *5*(4), 242–248. https://doi.org/10.21425/F55419694

May, M. R., Höhna, S., Moore, B. R., & Cooper, N. (2016). A Bayesian approach for detecting the impact of mass-extinction events on molecular phylogenies when rates of lineage diversification may vary. *Methods in Ecology and Evolution*, *7*(8), 947–959. https://doi.org/10.1111/2041-210x.12563

McLoughlin, S. (2001). The breakup history of Gondwana and its impact on pre-Cenozoic floristic provincialism. *Australian Journal of Botany*, *49*(3), 271–300. https://doi.org/10.1071/bt00023

McLoughlin, S., & Kear, B. P. (2010). The Australasian Cretaceous scene. *Alcheringa: an Australasian Journal of Palaeontology*, *34*(3), 197–203. https://doi.org/10.1080/03115518.2010.497264

Mirarab, S., Reaz, R., Bayzid, M. S., Zimmermann, T., Swenson, M. S., & Warnow, T. (2014). ASTRAL: Genome-scale coalescent-based species tree estimation. *Bioinformatics*, *30*(17), i541–i548. https://doi.org/10.1093/bioinformatics/btu462

Mitchell, K. J., Llamas, B., Soubrier, J., Rawlence, N. J., Worthy, T. H., Wood, J., … Cooper, A. (2014). Ancient DNA reveals elephant birds and kiwi are sister taxa and clarifies ratite bird evolution. *Science*, *344*(6186), 898–900. https://doi.org/10.1126/science.1251981

Murienne, J., Daniels, S. R., Buckley, T. R., Mayer, G., & Giribet, G. (2014). A living fossil tale of Pangaean biogeography. *Proceedings of the Royal Society B: Biological Sciences*, *281*(1775), 20132648. https://doi.org/10.1098/rspb.2013.2648

Nguyen, L.-T., Schmidt, H. A., von Haeseler, A., & Minh, B. Q. (2015). IQ-TREE: A fast and effective stochastic algorithm for estimating maximum-likelihood phylogenies. *Molecular Biology and Evolution*, *32*(1), 268–274. https://doi.org/10.1093/molbev/msu300

Oberski, J. T., Sharma, P. P., Jay, K. R., Coblens, M. J., Lemon, K. A., Johnson, J. E., & Boyer, S. L. (2018). A dated molecular phylogeny of mite harvestmen (Arachnida: Opiliones: Cyphophthalmi) elucidates ancient diversification dynamics in the Australian Wet Tropics. *Molecular Phylogenetics and Evolution*, *127*, 813–822. https://doi.org/10.1016/j.ympev.2018.06.029

Poinar, G. (2008). *Palaeosiro burmanicum* n. gen., n. sp., a fossil Cyphophthalmi (Arachnida: Opiliones: Sironidae) in Early Cretaceous Burmese amber. In S. E. Makarov, & R. N. Dimitrijevic (Eds.), *Advances in Arachnology and Developmental Biology. Papers dedicated to Prof. Dr. Bozidar Curic*. (pp. 267–274). Vienna, Belgrade, Sofia: Faculty of Life Sciences, University of Vienna, and Serbian Academy of Sciences and Arts.

Posada, D. (2008). jModelTest: Phylogenetic model averaging. *Molecular Biology and Evolution*, *25*(7), 1253–1256. https://doi.org/10.1093/molbev/msn083

Pybus, O. G., & Harvey, P. H. (2000). Testing macro-evolutionary models using incomplete molecular phylogenies. *Proceedings of the Royal Society B: Biological Sciences*, *267*(1459), 2267–2272. https://doi.org/10.1098/rspb.2000.1278

Rabosky, D. L. (2014). Automatic detection of key innovations, rate shifts, and diversity-dependence on phylogenetic trees. *PLoS ONE*, *9*(2), e89543. https://doi.org/10.1371/journal.pone.0089543

Rambaut, A., & Drummond, A. J. (2009). Tracer v. 1.6. Program and documentation. Available at http://tree.bio.ed.ac.uk/software/tracer/

Ree, R. H., & Smith, S. A. (2008). Maximum likelihood inference of geographic range evolution by dispersal, local extinction, and cladogenesis. *Systematic Biology*, *57*(1), 4–14. https://doi.org/10.1080/10635150701883881

Riesgo, A., Andrade, S. C. S., Sharma, P. P., Novo, M., Pérez-Porro, A. R., Vahtera, V., … Giribet, G. (2012). Comparative description of ten transcriptomes of newly sequenced invertebrates and efficiency estimation of genomic sampling in non-model taxa. *Frontiers in Zoology*, *9*, 33. https://doi.org/10.1186/1742-9994-9-33

Ronquist, F. (1997). Dispersal-vicariance analysis: A new approach to the quantification of historical biogeography. *Systematic Biology*, *46*(1), 195–203. https://doi.org/10.1093/sysbio/46.1.195

Ronquist, F., & Sanmartín, I. (2011). Phylogenetic methods in biogeography. *Annual Review of Ecology, Evolution, and Systematics*, *42*(1), 441–464. https://doi.org/10.1146/annurev-ecolsys-102209-144710

Sanmartín, I., & Ronquist, F. (2004). Southern hemisphere biogeography inferred by event-based models: Plant versus animal patterns. *Systematic Biology*, *53*(2), 216–243. https://doi.org/10.1080/10635150490423430

Scotese, C. R. (2004). A continental drift flipbook. *The Journal of Geology*, *112*(6), 729–741. https://doi.org/10.1086/424867

Selden, P. A., Dunlop, J. A., Giribet, G., Zhang, W., & Ren, D. (2016). The oldest armoured harvestman (Arachnida: Opiliones: Laniatores), from Upper Cretaceous Myanmar amber. *Cretaceous Research*, *65*, 206–212. https://doi.org/10.1016/j.cretres.2016.05.004

Sharma, P. P., Baker, C. M., Cosgrove, J. G., Johnson, J. E., Oberski, J. T., Raven, R. J., … Giribet, G. (2018). A revised dated phylogeny of scorpions: Phylogenomic support for ancient divergence of the temperate Gondwanan family Bothriuridae. *Molecular Phylogenetics and Evolution*, *122*, 37–45. https://doi.org/10.1016/j.ympev.2018.01.003

Sharma, P. P., Fernández, R., Esposito, L. A., González-Santillán, E., & Monod, L. (2015). Phylogenomic resolution of scorpions reveals multilevel discordance with morphological phylogenetic signal. *Proceedings of the Royal Society B: Biological Sciences*, *282*(1804), 20142953. https://doi.org/10.1098/rspb.2014.2953

Sharma, P. P., & Giribet, G. (2014). A revised dated phylogeny of the arachnid order Opiliones. *Frontiers in Genetics*, *5*, 255. https://doi.org/10.3389/fgene.2014.00255

Shear, W. A. (1980). A review of the Cyphophthalmi of the United States and Mexico, with a proposed reclassification of the suborder (Arachnida, Opiliones). *American Museum Novitates*, *2705*, 1–34.

Shear, W. A., & Gruber, J. (1996). Cyphophthalmid opilionids new to Madagascar: Two new genera (Opiliones, Cyphophthalmi, ?Pettalidae). *Bulletin of the British Arachnological Society*, *10*(5), 181–186.

Shen, X.-X., Hittinger, C. T., & Rokas, A. (2017). Contentious relationships in phylogenomic studies can be driven by a handful of genes. *Nature Ecology & Evolution*, *1*(5), 0126. https://doi.org/10.1038/s41559-017-0126

Simão, F. A., Waterhouse, R. M., Ioannidis, P., Kriventseva, E. V., & Zdobnov, E. M. (2015). BUSCO: Assessing genome assembly and

annotation completeness with single-copy orthologs. *Bioinformatics*, *31*(19), 3210–3212. https://doi.org/10.1093/bioinformatics/btv351
Smith, S. A., & Dunn, C. W. (2008). Phyutility: A phyloinformatics tool for trees, alignments and molecular data. *Bioinformatics*, *24*(5), 715–716. https://doi.org/10.1093/bioinformatics/btm619
Song, L., & Florea, L. (2015). Rcorrector: Efficient and accurate error correction for Illumina RNA-seq reads. *GigaScience*, *4*, 48. https://doi.org/10.1186/s13742-015-0089-y
Stamatakis, A. (2014). RAxML version 8: A tool for phylogenetic analysis and post-analysis of large phylogenies. *Bioinformatics*, *30*(9), 1312–1313. https://doi.org/10.1093/bioinformatics/btu033
Strimmer, K., & von Haeseler, A. (1997). Likelihood-mapping: A simple method to visualize phylogenetic content of a sequence alignment. *Proceedings of the National Academy of Sciences*, *94*(13), 6815–6819. https://doi.org/10.1073/pnas.94.13.6815
Upchurch, P. (2008). Gondwanan break-up: Legacies of a lost world? *Trends in Ecology & Evolution*, *23*(4), 229–236. https://doi.org/10.1016/j.tree.2007.11.006
Waddington, J., Rudkin, D. M., & Dunlop, J. A. (2015). A new mid-Silurian aquatic scorpion-one step closer to land? *Biology Letters*, *11*(1), 20140815. https://doi.org/10.1098/rsbl.2014.0815
Wei, W. (2004). Opening of the Australia-Antarctica Gateway as dated by nannofossils. *Marine Micropaleontology*, *52*(1–4), 133–152. https://doi.org/10.1016/j.marmicro.2004.04.008
Wheeler, W. C., Coddington, J. A., Crowley, L. M., Dimitrov, D., Goloboff, P. A., Griswold, C. E., … Zhang, J. (2017). The spider tree of life: Phylogeny of Araneae based on target-gene analyses from an extensive taxon sampling. *Cladistics*, *33*(6), 574–616. https://doi.org/10.1111/cla.12182
Wolfe, J. M., Daley, A. C., Legg, D. A., & Edgecombe, G. D. (2016). Fossil calibrations for the arthropod Tree of Life. *Earth-Science Reviews*, *160*, 43–110. https://doi.org/10.1016/j.earscirev.2016.06.008
Wu, M., Chatterji, S., & Eisen, J. A. (2012). Accounting for alignment uncertainty in phylogenomics. *PLoS ONE*, *7*(1), e30288. https://doi.org/10.1371/journal.pone.0030288
Yilmaz, P., Parfrey, L. W., Yarza, P., Gerken, J., Pruesse, E., Quast, C., … Glöckner, F. O. (2014). The SILVA and "All-species Living Tree Project (LTP)" taxonomic frameworks. *Nucleic Acids Research*, *42*(Database issue), D643–D648. https://doi.org/10.1093/nar/gkt1209
Zimmer, C. (2010). *The Tangled Bank: An introduction to evolution* (1st ed.). Greenwood Village, Colorado: Roberts and Co.

BIOSKETCH

Caitlin M. Baker is a PhD candidate in the Museum of Comparative Zoology at Harvard University. She is interested in the systematics and biogeography of soil invertebrates in the southern hemisphere, particularly harvestmen and velvet worms.

Author contributions: C.M.B., G.G. and S.L.B. conceived the study. C.M.B. conducted laboratory work, analyses and wrote the manuscript. G.G. and S.L.B. provided comments.

SUPPORTING INFORMATION

Additional supporting information may be found online in the Supporting Information section.

How to cite this article: Baker CM, Boyer SL, Giribet G. A well-resolved transcriptomic phylogeny of the mite harvestman family Pettalidae (Arachnida, Opiliones, Cyphophthalmi) reveals signatures of Gondwanan vicariance. *J Biogeogr.* 2020;00:1–17. https://doi.org/10.1111/jbi.13828

Chapter 2

Molecular phylogeny and biogeography of the temperate Gondwanan family Triaenonychidae (Opiliones: Laniatores) reveals pre-Gondwanan regionalization, common vicariance, and rare dispersal

In revision as:

Baker, C.M., Sheridan, K., Derkarabetian, S., Pérez-González, A., Vélez, S., & Giribet, G. Molecular phylogeny and biogeography of the temperate Gondwanan family Triaenonychidae (Opiliones: Laniatores) reveals pre-Gondwanan regionalization, common vicariance, and rare dispersal. *Invertebrate Systematics*.

Abstract

Triaenonychidae Sørensen *in* L. Koch, 1886 is a large family of Opiliones with *ca.* 480 described species broadly distributed across temperate forests in the Southern Hemisphere. However, it remains poorly understood taxonomically, as no comprehensive phylogenetic work has ever been undertaken. In this study we capitalize on samples largely collected by us during the last two decades

and use Sanger DNA-sequencing techniques to produce a large phylogenetic tree with 300 triaenonychid terminals representing nearly 50% of triaenonychid genera and including representatives from all the major geographic areas from which they are known, with the exception of the Crozet Islands and Sardinia. Phylogenetic analyses using maximum likelihood and Bayesian inference methods recover the family as diphyletic, placing *Lomanella* Pocock, 1903 as the sister group to the New Zealand endemic family Synthetonychiidae Forster, 1954. With the exception of the Laurasian representatives of the family, all landmasses contain non-monophyletic assemblages of taxa. To determine whether this non-monophyly was the result of Gondwanan vicariance, ancient cladogenesis due to habitat regionalization, or more recent over-water dispersal, we inferred divergence times. We found that most divergence times between landmasses predate Gondwanan breakup, though there has been at least one instance of *trans*-oceanic dispersal—to New Caledonia. In all, we identify multiple places in the phylogeny where taxonomic revision is needed, and transfer *Lomanella* outside of Triaenonychidae in order to maintain monophyly of the family.

2.1 Introduction

Triaenonychidae Sørensen *in* L. Koch, 1886, is the fourth most diverse family of Opiliones, with *ca.* 480 described species and subspecies (Kury, Mendes, & Souza, 2014). They can be readily identified by their trident-shaped tarsal claws of the third and fourth legs, and as with most Laniatores, their robust, armoured pedipalps that are much larger than the chelicerae. All triaenonychids have similar basic habitat requirements, living in cool, dark, humid environments such as leaf litter, rotting logs, and caves. They are nocturnal predators, and like most harvestmen, are believed to be dispersal-limited. Despite sharing these characteristics, the family contains remarkable morphological and behavioural diversity, with body sizes that range from ~2–10 mm in length, variable levels of armature, striking colour pattern variation, both sexual dimorphism and male polymorphism, and

even a documented instance of paternal care (Machado, 2007) (Figure 2.1).

Figure 2.1. Live habitus of members of Triaenonychidae. (a) *Fumontana deprehendor* MCZ IZ-46881 (b) *Pristobunus heterus* MCZ IZ-133243 (c) *Lomanella* sp. MCZ IZ-152652 (d) *Karamea lobata* MCZ IZ-152313 (e) *Glyptobunus ornatus* (f) new genus MCZ IZ-138076 (g) *Hickmanoxyomma* sp. (h) *Austromontia* sp. MCZ IZ-49523 (i) *Triconobunus horridus* MCZ IZ-151590 (j) *Nuncia* sp. MCZ IZ-152266 (k) *Larifuga* sp. MCZ IZ-132879 (l) "*Nuncia*" *verrucosa* MCZ IZ-138139. Photos a, b, f, h, k, and l by Gonzalo Giribet; photo c by Shahan Derkarabetian; photos d, i, and j by Caitlin Baker; photos e and g by Marshal Hedin.

Together with the New Zealand-endemic family Synthetonychiidae Forster, 1954 (14 species), Triaenonychidae is traditionally placed in the superfamily Triaenonychoidea. This group in turn is classified with the superfamily Travunioidea Absolon & Kratochvíl, 1932 (*ca.* 78 species and subspecies) in the infraorder Insidiatores Loman, 1901, one of the two main lineages within Laniatores Thorell, 1876 (Derkarabetian et al., 2018; Kury et al., 2014). Despite this traditional classification scheme, the monophyly of Insidiatores has been inconsistently recovered. While a recent phylogenetic analysis using transcriptomic data did find a monophyletic Insidiatores (Fernández, Sharma, Tourinho, & Giribet, 2017), other phylogenies based on Sanger DNA-sequencing data (Giribet, Vogt, González, Sharma, & Kury, 2010; Sharma & Giribet, 2011) and UCE sequencing (Derkarabetian et al., 2018) instead found either Synthetonychiidae or Travunioidea to be the sister group to all other Laniatores, rendering Insidiatores paraphyletic. It has been postulated that the limited taxonomic sampling of Triaenonychidae in these previous studies (each included no more than eight exemplars of the family) may have contributed to the inability to resolve these phylogenetic relationships (Sharma & Giribet, 2011).

In addition to the uncertain placement of Triaenonychidae within Insidiatores, the phylogenetic relationships within the family are also subject to debate. Genera within the family are traditionally classified in four subfamilies. Adaeinae Pocock, 1903 (40 species), is diagnosed by having a sub-triangular or wedge-shaped sternum and primarily contains genera from South Africa, as well as a monotypic genus from Western Australia (*Dingupa* Forster, 1952). Members of the subfamily Sorensenellinae Forster, 1954 (16 species and subspecies) all have tarsal claws on the third and fourth legs in which the lateral prongs are longer than the median prong. Sorensenellinae is composed of two genera from New Zealand (*Sorensenella* Pocock, 1903 and *Karamea* Forster, 1954) and two monotypic genera from South Africa (*Lawrencella* Strand, 1932 and *Speleomontia* Lawrence, 1931), but the putative synapomorphy of the family is also found in the Tasmanian genus

Tasmanonyx Hickman, 1958, classified in Triaenonychinae. The subfamily Triaenobuninae Pocock, 1903 (69 species and subspecies) is also diagnosed by the shape of the sternum, which is wide and crescent-shaped on its posterior margin. It contains multiple genera from New Zealand and Australia, as well as two monotypic genera from Chile (*Americobunus* Muñoz-Cuevas, 1972 and *Araucanobunus* Muñoz-Cuevas, 1973) and the genus *Ankaratrix* Lawrence, 1959, from Madagascar. Finally, the bulk of diversity is classified in the subfamily Triaenonychinae Sørensen, 1886 (354 species and subspecies), all of which have a long, arrow-shaped sternum. However, this subfamily has been treated as a "catch-all" clade, and as such it demands phylogenetic investigation.

To date, only a few studies have addressed phylogenetic relationships within Triaenonychidae, most of which used morphological data only for a subset of species, and focused on specific landmasses (Hunt, 1996; Mendes & Kury, 2008). In an unpublished Ph.D. thesis, Mendes (2009) addressed the broader Insidiatores phylogeny using morphological data. Although none of the taxonomic actions proposed there have validity, she placed the Tasmanian/South Australian *Lomanella* Pocock, 1903 and the Tasmanian monotypic genus *Pyenganella* Hickman, 1958 in a "new" family, Lomanellidae (*nomen nudum*), which then formed a clade with Synthetonychiidae, but this result was only obtained under implied weights; in other analyses they nested within Triaenonychidae. Hunt (1996) also found *Lomanella* (but not *Pyenganella*) to be the sister group to all other Australian triaenonychids, whether using equal weights or successive weighting, but as this analysis lacked representatives outside of Australia it is hard to compare with other analyses. Phylogenetic relationships in the family were also addressed using Sanger DNA sequencing in another unpublished thesis (Vélez, 2011) that focused on the New Zealand taxa and provided a dated chronogram in order to test the Oligocene drowning hypothesis (Giribet & Boyer, 2010; Landis et al., 2008).

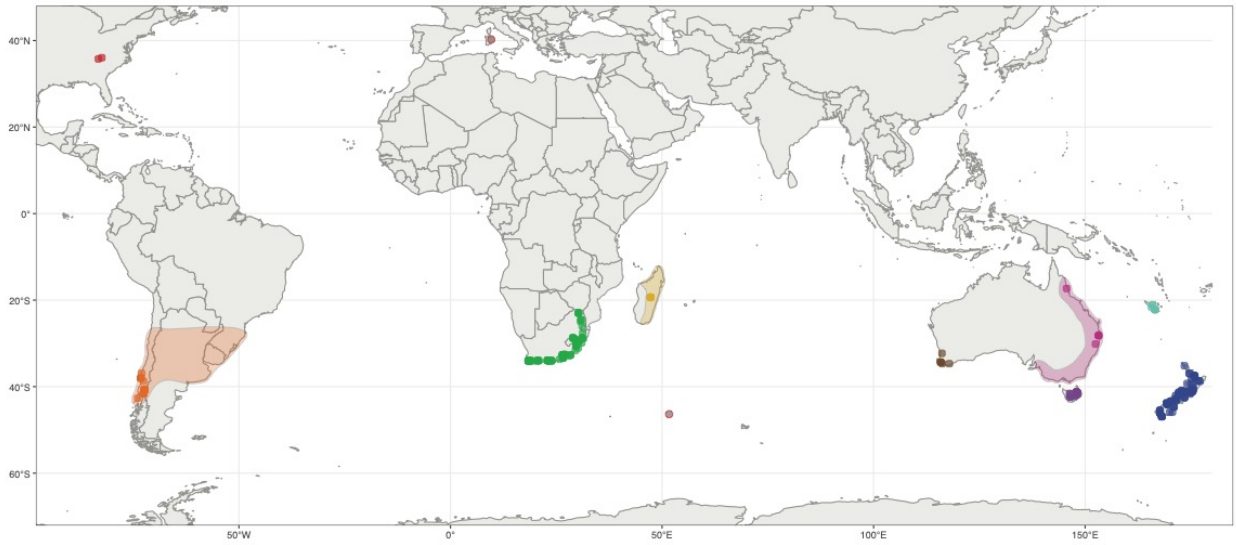

Figure 2.2. Map showing the distribution of Triaenonychidae samples used in the present study, with points coloured by region. Outlined shapes in South America, Madagascar, and eastern Australia reflect the known distribution of Triaenonychidae on those landmasses that extends beyond our study's sampling. Grey points with red outlines correspond to the phylogenetically and biogeographically important, but unsampled, lineages of *Buemarinoa patrizii* (Sardinia) and *Promecostethus unifalculatus* (Crozet Islands).

The vast majority of triaenonychid diversity is found in the Southern Hemisphere, across South America, southern Africa, Madagascar, Australia, and New Zealand (Figure 2.2). This geographic pattern reflects a classic temperate Gondwanan distribution, inviting biogeographic comparisons to other groups such as Pettalidae Shear, 1980 (Opiliones) (Baker, Boyer, & Giribet, 2020; Boyer & Giribet, 2007; Giribet et al., 2016; Shear, 1980), Neopilionidae Lawrence, 1931 (Opiliones) (Taylor, 2011; Vélez, Fernández, & Giribet, 2014), Peripatopsidae Bouvier, 1907 (Onychophora) (Giribet et al., 2018; Murienne, Daniels, Buckley, Mayer, & Giribet, 2014), Orsolobidae Cooke,1965 (Araneae) (Chousou-Polydouri et al., 2019), and Bothriuridae Simon, 1880 (Scorpiones) (Sharma et al., 2018). However, along with its temperate Gondwanan members, the family also contains monotypic genera in eastern North America, *Fumontana deprehendor* Shear, 1977 (Thomas & Hedin, 2008), and Sardinia, *Buemarinoa patrizii* Roewer, 1956 (see Karaman, 2019), a species from the oceanic Crozet Islands in the Southern Ocean, *Promecostethus unifalculatus* Enderlein,

1909, and two species from Grande Terre in New Caledonia, *Triconobunus horridus* Roewer, 1914 and *Diaenobunus armatus* Roewer, 1915. Grande Terre's basement geology is derived from Gondwanan terranes, but subsequently experienced long periods of marine inundation, and is therefore more accurately thought of as a functionally Darwinian island (though see discussion in Giribet & Baker, 2019; Grandcolas et al., 2008).

Given this largely temperate Gondwanan distribution, Triaenonychidae has been suggested as another example of a Gondwanan vicariant group, comparable to the examples listed above. Nevertheless, their presence in the Northern Hemisphere, the morphological affinities of those Northern Hemisphere species to the genus *Flavonuncia* Lawrence, 1959 from Madagascar (Karaman, 2019), and their occurrence on multiple Darwinian islands suggest either ancient relictualism or else more recent dispersal to these areas. It is also unknown whether the different continental landmasses contain monophyletic assemblages of taxa, as one might expect under a Gondwanan vicariant scenario. None of these biogeographic hypotheses have been interrogated using time-calibrated molecular phylogenetics. However, the limited triaenonychid sampling in the dated phylogenies of Giribet et al. (2010), Vélez (2011), Sharma and Giribet (2011), and Fernández et al. (2017) estimated the family's origin at some point between the Cretaceous and the Permian, suggesting an ancient origin for the group.

To address these gaps in our knowledge of a major lineage within Opiliones, we herein present a densely sampled time-calibrated molecular phylogeny of Triaenonychidae. This marks the first phylogeny focused on the family using broad molecular data, and allows us to evaluate both the taxonomy and major biogeographic patterns of the group.

Table 2.1. Collection information and GenBank accession numbers for specimens used in this study, including outgroups. Sequences newly generated for this study are bolded.

Species	Accession #	"subfamily"	Region	18S rRNA	28S rRNA	COI	Lat.	Long.
Equitius doriae	MCZ-134630	Triaenonychinae	Australia (NSW)	U37003	GQ912788	EF108590	–	–
Holonuncia sp.	MCZ-134219	Triaenonychinae	Australia (QLD)	**MT224370**	**MT224762**	**MT240352**	-28.194	153.1869
Triaenobunus armstrongi	MCZ-134473	Triaenobuninae	Australia (NSW)	GQ912724	GQ912794	**MT240354**	–	–
Triaenobunus armstrongi	MCZ-58944	Triaenobuninae	Australia (QLD)	**MT224527**	**MT224671**		-17.3109	145.6263
Triaenobunus bicarinatus	MCZ-134879	Triaenobuninae	Australia (NSW)	GQ912724	GQ912795	GQ912878	-30.1475	152.4439
Triaenobunus minutus	MCZ-134218	Triaenobuninae	Australia (QLD)	**MT224369**	**MT224761**		-28.194	153.1869
Triaenobunus minutus	MCZ-134220	Triaenobuninae	Australia (QLD)	**MT224371**	**MT224763**	**MT240353**	-28.194	153.1869
Glyptobunus ornatus	WSU-10076	Triaenobuninae	Australia (TAS)	**MT224610**	**MT224656**	**MT240476**	-41.6406	148.2417
Glyptobunus ornatus	WSU-10077	Triaenobuninae	Australia (TAS)	**MT224611**	**MT224657**	**MT240477**	-41.6406	148.2417
Glyptobunus ornatus	WSU-10090	Triaenobuninae	Australia (TAS)	**MT224614**	**MT224660**		-41.3223	148.1319
Glyptobunus signatus	WSU-10028	Triaenobuninae	Australia (TAS)	**MT224598**	**MT224644**		-41.3083	147.9389
Glyptobunus signatus	WSU-10049	Triaenobuninae	Australia (TAS)	**MT224605**	**MT224651**		-41.3214	147.9247
Glyptobunus signatus	WSU-10050	Triaenobuninae	Australia (TAS)	**MT224606**	**MT224652**	**MT240472**	-41.3214	147.9247
Glyptobunus sp.	WSU-10008	Triaenobuninae	Australia (TAS)	**MT224584**	**MT224630**		-41.2245	147.9689
Glyptobunus sp.	WSU-10026	Triaenobuninae	Australia (TAS)	**MT224596**	**MT224642**		-41.9483	147.8742
Glyptobunus sp.	WSU-10044	Triaenobuninae	Australia (TAS)	**MT224601**	**MT224647**	**MT240468**	-42.2867	146.4569
Rhynchobunus arrogans	WSU-10001	Triaenobuninae	Australia (TAS)	**MT224580**	**MT224626**	**MT240457**	-41.624	148.2556
Triaenobunus asper	WSU-10006	Triaenobuninae	Australia (TAS)	**MT224582**	**MT224628**	**MT240458**	-41.624	148.2556
Triaenobunus asper	WSU-10016	Triaenobuninae	Australia (TAS)	**MT224589**	**MT224635**	**MT240460**	-41.9483	147.8742
Triaenobunus asper	WSU-10017	Triaenobuninae	Australia (TAS)	**MT224590**	**MT224636**	**MT240461**	-41.9483	147.8742
Triaenobunus asper	WSU-10020	Triaenobuninae	Australia (TAS)	**MT224592**	**MT224638**	**MT240462**	-41.9483	147.8742
Triaenobunus asper	WSU-10021	Triaenobuninae	Australia (TAS)	**MT224593**	**MT224639**	**MT240463**	-41.9483	147.8742
Triaenobunus asper	WSU-10023	Triaenobuninae	Australia (TAS)	**MT224594**	**MT224640**	**MT240464**	-41.9483	147.8742
Triaenobunus asper	WSU-10024	Triaenobuninae	Australia (TAS)	**MT224595**	**MT224641**	**MT240465**	-41.9483	147.8742
Triaenobunus asper	WSU-10060	Triaenobuninae	Australia (TAS)	**MT224607**	**MT224653**	**MT240473**	-42.0042	147.8517
Triaenobunus asper	WSU-10069	Triaenobuninae	Australia (TAS)	**MT224608**	**MT224654**	**MT240474**	-41.6406	148.2417
Triaenobunus asper	WSU-10070	Triaenobuninae	Australia (TAS)	**MT224609**	**MT224655**	**MT240475**	-41.6406	148.2417
Hickmanoxyomma gibbergunyar	MCZ-134907	Triaenonychinae	Australia (TAS)	**MT224374**	**MT224767**		-41.5803	146.3439
Hickmanoxyomma gibbergunyar	MCZ-135687	Triaenonychinae	Australia (TAS)	**MT224407**	**MT224800**		-41.5994	146.4053
Hickmanoxyomma cf. *tasmanicum*	WSU-10005	Triaenonychinae	Australia (TAS)	**MT224581**	**MT224627**		-41.624	148.2556
Hickmanoxyomma cf. *tasmanicum*	WSU-10032	Triaenonychinae	Australia (TAS)	**MT224599**	**MT224645**	**MT240466**	-41.5344	148.1756
Hickmanoxyomma cf. *tasmanicum*	WSU-10082	Triaenonychinae	Australia (TAS)	**MT224612**	**MT224658**		-41.5608	148.095
Lomanella raniceps	WSU-10045	Triaenonychinae	Australia (TAS)	**MT224602**	**MT224648**	**MT240469**	-42.2867	146.4569
Lomanella raniceps	WSU-10046	Triaenonychinae	Australia (TAS)	**MT224603**	**MT224649**	**MT240470**	-42.2867	146.4569
Lomanella raniceps	WSU-10047	Triaenonychinae	Australia (TAS)	**MT224604**	**MT224650**	**MT240471**	-42.2867	146.4569
Lomanella sp.	WSU-10011	Triaenonychinae	Australia (TAS)	**MT224587**	**MT224633**		-41.2245	147.9689
Lomanella sp.	WSU-10038	Triaenonychinae	Australia (TAS)	**MT224600**	**MT224646**	**MT240467**	-41.5344	148.1756
Lomanella sp.	WSU-10089	Triaenonychinae	Australia (TAS)	**MT224613**	**MT224659**		-41.3223	148.1319
Nucina dispar	WSU-10018	Triaenonychinae	Australia (TAS)	**MT224591**	**MT224637**		-41.9483	147.8742
Nunciella tasmaniensis	WSU-10009	Triaenonychinae	Australia (TAS)	**MT224585**	**MT224631**		-41.2245	147.9689
Nunciella tasmaniensis	WSU-10010	Triaenonychinae	Australia (TAS)	**MT224586**	**MT224632**		-41.2245	147.9689
Nunciella tasmaniensis	WSU-10027	Triaenonychinae	Australia (TAS)	**MT224597**	**MT224643**		-41.3083	147.9389
Nunciella sp.	WSU-10014	Triaenonychinae	Australia (TAS)	**MT224588**	**MT224634**		-41.2245	147.9689
Odontonuncia saltuensis	WSU-10007	Triaenonychinae	Australia (TAS)	**MT224583**	**MT224629**	**MT240459**	-41.2245	147.9689
Calliuncus cf. *labyrinthus*	MCZ-132901	Triaenonychinae	Australia (WA)	**MT224352**	**MT224744**	**MT240343**	-34.3419	115.8619
Calliuncus cf. *labyrinthus*	MCZ-99185	Triaenonychinae	Australia (WA)	**MT224578**	**MT224721**	**MT240336**	-34.3419	115.8619

Table 2.1 (Continued)

Calliuncus cf. *labyrinthus*	MCZ-99220	Triaenonychinae	Australia (WA)	**MT224579**	**MT224722**	**MT240337**	-34.3905	115.8608
Nunciella karriensis	MCZ-132904	Triaenonychinae	Australia (WA)	**MT224353**	**MT224745**	**MT240344**	-34.6759	117.8717
Nunciella sp.	MCZ-132908	Triaenonychinae	Australia (WA)	**MT224354**	**MT224746**	**MT240345**	-32.2711	116.166
Nunciella sp.	MCZ-99182	Triaenonychinae	Australia (WA)	**MT224577**	**MT224720**		-34.7002	116.2223
Americobunus ringueleti	MCZ-138157	Triaenobuninae	Chile	**MT224504**	**MT224896**	**MT240440**	-38.7291	-72.59149
Diasia michaelsenii	MCZ-138126	Triaenonychinae	Chile	**MT224496**	**MT224888**		-40.7372	-72.31062
Diasia sp.	MCZ-138056	Triaenonychinae	Chile	**MT224480**	**MT224873**		-38.0126	-73.18517
Nuncia americana	MCZ-59011	Triaenonychinae	Chile	**MT224537**	**MT224681**	**MT240321**	-40.7372	-72.30647
Nuncia americana	MCZ-59016	Triaenonychinae	Chile	**MT224538**	**MT224682**	**MT240322**	-40.7372	-72.30647
Nuncia americana	MCZ-59020	Triaenonychinae	Chile	**MT224539**	**MT224683**	**MT240323**	-40.7372	-72.30647
Nuncia americana	MCZ-59021	Triaenonychinae	Chile	**MT224540**	**MT224684**	**MT240324**	-40.7372	-72.30647
Nuncia cf. *americana*	MCZ-138110	Triaenonychinae	Chile	**MT224490**	**MT224882**		-41.5935	-72.59359
Nuncia cf. *americana*	MCZ-138115	Triaenonychinae	Chile	**MT224491**	**MT224883**		-40.7355	-72.32894
Nuncia chilensis	MCZ-138133	Triaenonychinae	Chile	**MT224498**	**MT224890**	**MT240436**	-40.7135	-72.50297
Nuncia verrucosa	MCZ-138097	Triaenonychinae	Chile	**MT224488**	**MT224880**	**MT240432**	-41.5783	-72.55828
Nuncia verrucosa	MCZ-138122	Triaenonychinae	Chile	**MT224492**	**MT224884**	**MT240434**	-40.7372	-72.31062
Nuncia verrucosa	MCZ-138139	Triaenonychinae	Chile	**MT224500**	**MT224892**	**MT240437**	-40.7375	-72.30875
Nuncia sp.	MCZ-138091	Triaenonychinae	Chile	**MT224484**	**MT224877**	**MT240429**	-41.5881	-72.58122
Nuncia sp.	MCZ-138093	Triaenonychinae	Chile	**MT224485/ MT224486**	**MT224878**	**MT240430**	-41.5785	-72.55692
Nuncia sp.	MCZ-59030	Triaenonychinae	Chile	**MT224541**	**MT224685**		-42.662	-74.01062
Triaenonyx chilensis	MCZ-138132	Triaenonychinae	Chile	**MT224497**	**MT224889**	**MT240435**	-40.7135	-72.50297
Triaenonyx dispersus	MCZ-138125	Triaenonychinae	Chile	**MT224495**	**MT224887**		-40.7372	-72.31062
Triaenonyx sp.	MCZ-138029	Triaenonychinae	Chile	**MT224479**	**MT224872**		-36.876	-72.99386
Triaenonyx sp.	MCZ-138074	Triaenonychinae	Chile	**MT224481**	**MT224874**	**MT240426**	-38.0163	-73.17902
Triaenonyx sp.	MCZ-138096	Triaenonychinae	Chile	**MT224487**	**MT224879**	**MT240431**	-41.5783	-72.55828
Triaenonyx sp.	MCZ-138109	Triaenonychinae	Chile	**MT224489**	**MT224881**	**MT240433**	-41.5935	-72.59359
Triaenonyx sp.	MCZ-138124	Triaenonychinae	Chile	**MT224494**	**MT224886**		-40.7372	-72.31062
Triaenonyx sp.	MCZ-138140	Triaenonychinae	Chile	**MT224501**	**MT224893**	**MT240438**	-40.7375	-72.30875
cf. *Triaenonyx arrogans*	MCZ-138077	Triaenonychinae	Chile	**MT224483**	**MT224876**	**MT240428**	-38.0163	-73.17902
Valdivionyx crassipes	MCZ-138123	Triaenonychinae	Chile	**MT224493**	**MT224885**		-40.7372	-72.31062
Valdivionyx crassipes	MCZ-138138	Triaenonychinae	Chile	**MT224499**	**MT224891**		-40.7375	-72.30875
Valdivionyx crassipes	MCZ-138150	Triaenonychinae	Chile	**MT224502**	**MT224894**		-40.7381	-72.31139
Valdivionyx sp.	MCZ-138151	Triaenonychinae	Chile	**MT224503**	**MT224895**	**MT240439**	-40.7381	-72.31139
Triaenonychidae n. gen.	MCZ-138076	Triaenonychinae	Chile	**MT224482**	**MT224875**	**MT240427**	-38.0163	-73.17902
Acumontia sp. 2		Triaenonychinae	Madagascar	**MT224322**	**MT224615**		-19.3546	47.31128
Acumontia sp. 3		Triaenonychinae	Madagascar	**MT224323**	**MT224616**	**MT240451**	-19.3506	47.30402
Acumontia sp. 4		Triaenonychinae	Madagascar	**MT224324**	**MT224617**	**MT240452**	-19.3522	47.30753
Acumontia sp. 5		Triaenonychinae	Madagascar	**MT224325**	**MT224618**	**MT240453**	-19.3506	47.30402
Acumontia sp. 6		Triaenonychinae	Madagascar	**MT224326**		**MT240454**	-19.3506	47.30402
Acumontia sp. 7		Triaenonychinae	Madagascar	**MT224327**	**MT224619**	**MT240455**	-19.3506	47.30402
Acumontia sp. 8		Triaenonychinae	Madagascar	**MT224328**	**MT224620**		-19.3506	47.30402
Flavonuncia sp. 9		Triaenonychinae	Madagascar	**MT224329/ MT224330**	**MT224624**	**MT240456**	-19.3546	47.31128
Flavonuncia sp. 10		Triaenonychinae	Madagascar	**MT224319**	**MT224621**	**MT240450**	-19.3546	47.31128
Flavonuncia sp. 11		Triaenonychinae	Madagascar	**MT224320**	**MT224622**		-19.3546	47.31128
Flavonuncia sp. 12		Triaenonychinae	Madagascar	**MT224321**	**MT224623**		-19.3522	47.30753
Triaenonychidae sp. 1		Triaenonychinae	Madagascar	**MT224318**	**MT224625**	**MT240449**	-19.3522	47.30753
Diaenobunus armatus	MCZ-151609.1	Triaenonychinae	New Caledonia	**MT224512**	**MT224904**	**MT240444**	-22.1706	166.5086
Diaenobunus armatus	MCZ-151609.2	Triaenonychinae	New Caledonia	**MT224513**	**MT224905**	**MT240445**	-22.1706	166.5086
Diaenobunus armatus	MCZ-151609.3	Triaenonychinae	New Caledonia	**MT224514**	**MT224906**	**MT240446**	-22.1706	166.5086
Diaenobunus armatus	MCZ-151611.1	Triaenonychinae	New Caledonia	**MT224515**	**MT224907**	**MT240447**	-22.1708	166.5083

Table 2.1 (Continued)

Diaenobunus armatus	MCZ-151611.2	Triaenonychinae	New Caledonia	**MT224516**	**MT224908**	**MT240448**	-22.1708	166.5083
Diaenobunus sp.	MCZ-134884	Triaenonychinae	New Caledonia	**MT224372**	**MT224765**	**MT240355**	-21.6167	165.8833
Triconobunus horridus	MCZ-151590.1	Triaenonychinae	New Caledonia	**MT224510**	**MT224902**	**MT240442**	-21.1116	165.8787
Triconobunus horridus	MCZ-151590.2	Triaenonychinae	New Caledonia	**MT224511**	**MT224903**	**MT240443**	-21.1116	165.8787
Karamea lobata australis	MCZ-136031	Sorensenellinae	New Zealand	**MT224431**	**MT224824**	**MT240391**	-42.0369	171.3897
Karamea lobata lobata	MCZ-136011	Sorensenellinae	New Zealand	**MT224428**	**MT224821**	**MT240389**	-41.7967	172.0494
Karamea lobata lobata	MCZ-136012	Sorensenellinae	New Zealand	**MT224429**	**MT224822**	**MT240390**	-41.7967	172.0494
Karamea tricerata	MCZ-135504	Sorensenellinae	New Zealand	**MT224397**	**MT224790**	**MT240365**	-40.883	172.8108
Karamea tricerata	MCZ-135507	Sorensenellinae	New Zealand	**MT224398**	**MT224791**	**MT240366**	-40.883	172.8108
Sorensenella prehensor prehensor	MCZ-133201	Sorensenellinae	New Zealand	**MT224364**	**MT224756**		-36.9466	174.6101
Sorensenella rotara	MCZ-148131	Sorensenellinae	New Zealand	**MT224508**	**MT224900**		-38.6474	176.9079
Sorensenella n. sp.	MCZ-133130	Sorensenellinae	New Zealand	**MT224362**	**MT224754**		-35.1904	173.4556
Sorensenella n. sp.	MCZ-133380	Sorensenellinae	New Zealand	**MT224367**	**MT224759**		-39.4654	175.09
Sorensenella n. sp.	MCZ-133429	Sorensenellinae	New Zealand	**MT224368**	**MT224760**	**MT240350**	-38.26	175.0998
Cenefia cf. *adaeiformis*	MCZ-135771	Triaenobuninae	New Zealand	**MT224408**	**MT224801**		-41.0868	174.1381
Pristobonus henopoeus	MCZ-135974	Triaenobuninae	New Zealand	**MT224412**	**MT224805**		-41.3453	174.9317
Pristobunus acuminatus a cantheis	MCZ-136194	Triaenobuninae	New Zealand	**MT224465**	**MT224858**	**MT240415**	-40.6388	175.3224
Pristobunus heterus	MCZ-133351	Triaenobuninae	New Zealand	**MT224366**	**MT224758**		-40.2445	175.5421
Pristobunus sp.	MCZ-133205	Triaenobuninae	New Zealand	**MT224365**	**MT224757**	**MT240349**	-39.2738	174.0937
Pristobunus sp.	MCZ-135678	Triaenobuninae	New Zealand	**MT224406**	**MT224799**	**MT240372**	-41.1377	173.5168
Pristobunus sp.	MCZ-148111	Triaenobuninae	New Zealand	**MT224506**	**MT224898**		-43.2859	170.401
Triaenonychidae sp.	MCZ-136244	Triaenobuninae	New Zealand	**MT224469**	**MT224862**	**MT240418**	-46.897	168.0923
Algidia chiltoni chiltoni	MCZ-135458	Triaenonychinae	New Zealand	**MT224383**	**MT224776**	**MT240358**	-38.6757	176.699
Algidia chiltoni chiltoni	MCZ-136192	Triaenonychinae	New Zealand	**MT224464**	**MT224857**	**MT240414**	–	–
Algidia chiltoni longispinosa	MCZ-135437	Triaenonychinae	New Zealand	**MT224379**	**MT224772**	**MT240356**	-41.1133	175.3494
Algidia cuspidata multispinosa	MCZ-136151	Triaenonychinae	New Zealand	**MT224453**	**MT224846**	**MT240407**	-42.5421	173.4524
Algidia homerica	MCZ-135537	Triaenonychinae	New Zealand	**MT224400**	**MT224793**	**MT240368**	-43.4126	170.1772
Algidia cf. *homerica*	MCZ-136061	Triaenonychinae	New Zealand	**MT224437**	**MT224830**	**MT240397**	-43.4882	170.0326
Algidia interrupta interrupta	MCZ-136008	Triaenonychinae	New Zealand	**MT224427**	**MT224820**	**MT240388**	-41.7967	172.0494
Algidia marplesi	MCZ-135672	Triaenonychinae	New Zealand	**MT224405**	**MT224798**	**MT240371**	-45.8803	170.6102
Algidia nigriflava	MCZ-136171	Triaenonychinae	New Zealand	**MT224457**	**MT224850**	**MT240410**	-41.1558	174.9652
Algidia cf. *nigriflava*	MCZ-136202	Triaenonychinae	New Zealand	**MT224467**	**MT224860**	**MT240417**	-40.7213	175.2456
Algidia sp.	MCZ-148126	Triaenonychinae	New Zealand	**MT224507**	**MT224899**	**MT240441**	-41.348	174.9309
Hedwiga manubriata	MCZ-135637	Triaenonychinae	New Zealand	**MT224404**	**MT224797**	**MT240370**	-46.897	168.0923
Hedwiga manubriata	MCZ-136129	Triaenonychinae	New Zealand	**MT224450**	**MT224843**	**MT240404**	-46.8942	168.104
Hedwiga manubriata	MCZ-136258	Triaenonychinae	New Zealand	**MT224473**	**MT224866**	**MT240421**	-44.7006	170.9676
Hedwiga manubriata	MCZ-136259	Triaenonychinae	New Zealand	**MT224474**	**MT224867**	**MT240422**	-44.7006	170.9676
Hendea bucculenta	MCZ-136167	Triaenonychinae	New Zealand	**MT224454**	**MT224847**	**MT240408**	-41.1558	174.9652
Hendea maitaia	MCZ-135991	Triaenonychinae	New Zealand	**MT224421**	**MT224814**		-41.0867	174.1381
Hendea myersi	MCZ-135987	Triaenonychinae	New Zealand	**MT224418**	**MT224811**	**MT240380**	-41.7075	174.7861
Hendea myersi	MCZ-136170	Triaenonychinae	New Zealand	**MT224456**	**MT224849**	**MT240409**	-41.1558	174.9652
Hendea myersi	MCZ-136173	Triaenonychinae	New Zealand	**MT224459**	**MT224852**		-41.1558	174.9652
Hendea phillippsi	MCZ-136180	Triaenonychinae	New Zealand	**MT224460**	**MT224853**	**MT240411**	-41.0733	175.1463
Hendea sp.	MCZ-135543	Triaenonychinae	New Zealand	**MT224401**	**MT224794**		-43.7104	169.2671
Hendea sp.	MCZ-136005	Triaenonychinae	New Zealand	**MT224426**	**MT224819**	**MT240387**	-41.7956	172.5972
Hendea sp.	MCZ-136055	Triaenonychinae	New Zealand	**MT224436**	**MT224829**	**MT240396**	-43.4235	170.168
Nuncia arcuata aorangiensis	MCZ-136113	Triaenonychinae	New Zealand	**MT224447**	**MT224840**	**MT240402**	-46.1095	167.6903
Nuncia coriacea coriacea	MCZ-135438	Triaenonychinae	New Zealand	**MT224380**	**MT224773**		-41.065	175.3528

Table 2.1 (Continued)

Nuncia coriacea coriacea	MCZ-135486	Triaenonychinae	New Zealand	**MT224394**	**MT224787**		-41.065	175.3528
Nuncia coriacea coriacea	MCZ-136041	Triaenonychinae	New Zealand	**MT224433**	**MT224826**	**MT240393**	-43.0211	171.595
Nuncia coriacea coriacea	MCZ-136043	Triaenonychinae	New Zealand	**MT224434**	**MT224827**	**MT240394**	-43.0211	171.595
Nuncia coriacea coriacea	MCZ-136091	Triaenonychinae	New Zealand	**MT224443**	**MT224836**		-44.0769	169.3866
Nuncia coriacea coriacea	MCZ-58942	Triaenonychinae	New Zealand	**MT224525**	**MT224669**	**MT240316**	-42.5421	173.4524
Nuncia coriacea ovata	MCZ-136038	Triaenonychinae	New Zealand	**MT224432**	**MT224825**	**MT240392**	-43.0211	171.595
Nuncia dentifera	MCZ-135460	Triaenonychinae	New Zealand	**MT224384**	**MT224777**	**MT240359**	-37.5974	175.8616
Nuncia heteromorpha	MCZ-136049	Triaenonychinae	New Zealand	**MT224435**	**MT224828**	**MT240395**	-42.7145	171.245
Nuncia levis	MCZ-136022	Triaenonychinae	New Zealand	**MT224430**	**MT224823**		-41.4244	172.1056
Nuncia nigriflava parva	MCZ-135989	Triaenonychinae	New Zealand	**MT224419**	**MT224812**	**MT240381**	-41.0867	174.1381
Nuncia obesa grimmetti	MCZ-135970	Triaenonychinae	New Zealand	**MT224410**	**MT224803**	**MT240374**	-41.3475	174.9269
Nuncia obesa grimmetti	MCZ-135975	Triaenonychinae	New Zealand	**MT224413**	**MT224806**	**MT240376**	-41.2944	174.7513
Nuncia obesa grimmetti	MCZ-135980	Triaenonychinae	New Zealand	**MT224414**	**MT224807**	**MT240377**	-41.2656	174.7575
Nuncia obesa grimmetti	MCZ-135984	Triaenonychinae	New Zealand	**MT224416**	**MT224809**	**MT240378**	-41.2667	174.7583
Nuncia obesa grimmetti	MCZ-136198	Triaenonychinae	New Zealand	**MT224466**	**MT224859**	**MT240416**	-40.6388	175.3224
Nuncia obesa grimmetti	MCZ-136206	Triaenonychinae	New Zealand	**MT224468**	**MT224861**		-40.5755	175.4815
Nuncia obesa grimmetti	MCZ-136265	Triaenonychinae	New Zealand	**MT224476**	**MT224869**	**MT240423**	-41.2944	174.7513
Nuncia obesa obesa	MCZ-136076	Triaenonychinae	New Zealand	**MT224438**	**MT224831**	**MT240398**	-43.9381	169.2882
Nuncia obesa obesa	MCZ-136137	Triaenonychinae	New Zealand	**MT224451**	**MT224844**	**MT240405**	-45.9047	169.9878
Nuncia obesa obesa	MCZ-136169	Triaenonychinae	New Zealand	**MT224455**	**MT224848**		-41.1558	174.9652
Nuncia obesa rotunda	MCZ-136172	Triaenonychinae	New Zealand	**MT224458**	**MT224851**		-41.1558	174.9652
Nuncia cf. *obesa rotunda*	MCZ-149353	Triaenonychinae	New Zealand	**MT224509**	**MT224901**		-46.8985	168.1002
Nuncia oconnori paucispinosa	MCZ-135469	Triaenonychinae	New Zealand	**MT224388**	**MT224781**	**MT240362**	-37.4668	175.7713
Nuncia pallida	MCZ-136099	Triaenonychinae	New Zealand	**MT224444**	**MT224837**		-45.5733	167.6199
Nuncia roeweri demissa	MCZ-135439	Triaenonychinae	New Zealand	**MT224381**	**MT224774**		-41.065	175.3528
Nuncia roeweri gelida	MCZ-135468	Triaenonychinae	New Zealand	**MT224387**	**MT224780**		-37.4668	175.7713
Nuncia roeweri humilis	MCZ-135463	Triaenonychinae	New Zealand	**MT224385**	**MT224778**	**MT240360**	-37.5974	175.8616
Nuncia roeweri humilis	MCZ-135487	Triaenonychinae	New Zealand	**MT224395**	**MT224788**	**MT240364**	-37.5974	175.8616
Nuncia roeweri roeweri	MCZ-136116	Triaenonychinae	New Zealand	**MT224448**	**MT224841**		-46.8942	168.104
Nuncia roeweri roeweri	MCZ-136147	Triaenonychinae	New Zealand	**MT224452**	**MT224845**	**MT240406**	-44.7006	170.9675
Nuncia roeweri seditiosa	MCZ-136112	Triaenonychinae	New Zealand	**MT224446**	**MT224839**		-46.1095	167.6903
Nuncia smithi	MCZ-135436	Triaenonychinae	New Zealand	**MT224378**	**MT224771**		-41.065	175.3528
Nuncia smithi	MCZ-135479	Triaenonychinae	New Zealand	**MT224390**	**MT224783**		-40.722	175.6402
Nuncia smithi	MCZ-135484	Triaenonychinae	New Zealand	**MT224392**	**MT224785**	**MT240363**	-37.4668	175.7713
Nuncia stewartia stewartia	MCZ-136086	Triaenonychinae	New Zealand	**MT224440**	**MT224833**	**MT240399**	-43.9381	169.2882
Nuncia stewartia stewartia	MCZ-136087	Triaenonychinae	New Zealand	**MT224441**	**MT224834**	**MT240400**	-44.0769	169.3866
Nuncia stewartia stewartia	MCZ-136127	Triaenonychinae	New Zealand	**MT224449**	**MT224842**	**MT240403**	-46.8942	168.104
Nuncia stewartia tumosa	MCZ-136088	Triaenonychinae	New Zealand	**MT224442**	**MT224835**	**MT240401**	-44.0769	169.3866
Nuncia sublaevis	MCZ-135481	Triaenonychinae	New Zealand	**MT224391**	**MT224784**		-37.5974	175.8616
Nuncia sublaevis	MCZ-135485	Triaenonychinae	New Zealand	**MT224393**	**MT224786**		-37.4668	175.7713
Nuncia variegata delli	MCZ-135985	Triaenonychinae	New Zealand	**MT224417**	**MT224810**	**MT240379**	-41.2667	174.7583
Nuncia sp.	MCZ-134924	Triaenonychinae	New Zealand	**MT224375**	**MT224768**		-43.9381	169.2882
Nuncia sp.	MCZ-135475	Triaenonychinae	New Zealand	**MT224389**	**MT224782**		-40.6388	175.3224
Nuncia sp.	MCZ-135515	Triaenonychinae	New Zealand	**MT224399**	**MT224792**	**MT240367**	-41.27	172.1333
Nuncia sp.	MCZ-135610	Triaenonychinae	New Zealand	**MT224402**	**MT224795**	**MT240369**	-45.4511	167.6804
Nuncia sp.	MCZ-135973	Triaenonychinae	New Zealand	**MT224411**	**MT224804**	**MT240375**	-41.3478	174.9258
Nuncia sp.	MCZ-135983	Triaenonychinae	New Zealand	**MT224415**	**MT224808**		-41.2667	174.7583
Nuncia sp.	MCZ-135990	Triaenonychinae	New Zealand	**MT224420**	**MT224813**	**MT240382**	-41.0867	174.1381
Nuncia sp.	MCZ-135994	Triaenonychinae	New Zealand	**MT224422**	**MT224815**	**MT240383**	-41.0867	174.1381

Table 2.1 (Continued)

Nuncia sp.	MCZ-135998	Triaenonychinae	New Zealand	**MT224423**	**MT224816**	**MT240384**	-41.3003	173.5711
Nuncia sp.	MCZ-135999	Triaenonychinae	New Zealand	**MT224424**	**MT224817**	**MT240385**	-41.1892	172.7422
Nuncia sp.	MCZ-136000	Triaenonychinae	New Zealand	**MT224425**	**MT224818**	**MT240386**	-41.1892	172.7422
Nuncia sp.	MCZ-136079	Triaenonychinae	New Zealand	**MT224439**	**MT224832**		-43.9381	169.2882
Nuncia sp.	MCZ-136111	Triaenonychinae	New Zealand	**MT224445**	**MT224838**		-46.1095	167.6903
Nuncia sp.	MCZ-136182	Triaenonychinae	New Zealand	**MT224461**	**MT224854**		-41.0752	175.1467
Nuncia sp.	MCZ-136183	Triaenonychinae	New Zealand	**MT224462**	**MT224855**	**MT240412**	-41.0752	175.1467
Nuncia sp.	MCZ-136250	Triaenonychinae	New Zealand	**MT224470**	**MT224863**	**MT240419**	-43.0211	171.595
Nuncia sp.	MCZ-136251	Triaenonychinae	New Zealand	**MT224471**	**MT224864**		-44.0769	169.3866
Nuncia sp.	MCZ-136252	Triaenonychinae	New Zealand	**MT224472**	**MT224865**	**MT240420**	-42.5421	173.4524
Nuncia sp.	MCZ-136261	Triaenonychinae	New Zealand	**MT224475**	**MT224868**		-46.1095	167.6903
Prasma tuberculata mearosa	MCZ-136190	Triaenonychinae	New Zealand	**MT224463**	**MT224856**	**MT240413**	-40.6388	175.3224
Prasma sp.	MCZ-117475	Triaenonychinae	New Zealand	**MT224331**	**MT224723**	**MT240338**	-46.1106	167.6897
Prasma sp.	MCZ-133199	Triaenonychinae	New Zealand	**MT224363**	**MT224755**	**MT240348**	-36.9466	174.6101
Prasma sp.	MCZ-135491	Triaenonychinae	New Zealand	**MT224396**	**MT224789**		-41.1856	173.4877
Prasma sp.	MCZ-135614	Triaenonychinae	New Zealand	**MT224403**	**MT224796**		-45.4511	167.6804
Prasma sp.	MCZ-147580	Triaenonychinae	New Zealand	**MT224505**	**MT224897**		-39.3561	175.4764
Triregia fairburni fairburni	MCZ-135467	Triaenonychinae	New Zealand	**MT224386**	**MT224779**	**MT240361**	-37.4668	175.7713
Triregia fairburni fairburni	MCZ-135963	Triaenonychinae	New Zealand	**MT224409**	**MT224802**	**MT240373**	-37.8809	175.9115
Triregia fairburni grata	MCZ-135450	Triaenonychinae	New Zealand	**MT224382**	**MT224775**	**MT240357**	-38.7979	177.1237
Adaeulum areolatum	MCZ-30072.1	Adaeinae	South Africa	**MT224518**	**MT224662**	**MT240314**	-32.6823	26.49135
Adaeulum bicolor	MCZ-126991.2	Adaeinae	South Africa	**MT224332**	**MT224724**		-28.745	31.13596
Adaeulum godfreyi	MCZ-138019	Adaeinae	South Africa	**MT224478**	**MT224871**	**MT240425**	-32.889	28.05258
Adaeulum humifer	MCZ-59004	Adaeinae	South Africa	**MT224532**	**MT224676**		-22.996	30.26447
Adaeulum moruliferum	MCZ-138016	Adaeinae	South Africa	**MT224477**	**MT224870**	**MT240424**	-28.7117	28.9342
Adaeulum robustum	MCZ-132883	Adaeinae	South Africa	**MT224350**	**MT224742**	**MT240342**	-29.3221	30.26258
Adaeulum supervidens	MCZ-127214	Adaeinae	South Africa	**MT224336**	**MT224728**	**MT240340**	-30.6311	29.71596
Adaeum sp.	MCZ-73548.1	Adaeinae	South Africa	**MT224561**	**MT224705**	**MT240328**	-32.5704	26.9403
Adaeum sp.	MCZ-73548.2	Adaeinae	South Africa	**MT224562**	**MT224706**	**MT240329**	-32.5704	26.9403
Larifuga capensis	MCZ-133938	Adaeinae	South Africa		GQ912792	**MT240351**	-33.9792	18.45
Larifuga sp.	MCZ-127211.3	Adaeinae	South Africa	**MT224335**	**MT224727**	**MT240339**	-33.9521	22.91155
Larifuga sp.	MCZ-132879	Adaeinae	South Africa	**MT224347**	**MT224739**	**MT240341**	-33.9942	20.45868
Larifuga sp.	MCZ-132909.2	Adaeinae	South Africa	**MT224355**	**MT224747**		-33.9749	23.14712
Larifuga sp.	MCZ-49519	Adaeinae	South Africa	**MT224524**	**MT224668**	**MT240315**	-34.0424	18.87395
Larifuga sp.	MCZ-98386	Adaeinae	South Africa	**MT224574**	**MT224718**	**MT240335**	-34.0424	18.87395
Larifugella cf. *afra*	MCZ-132913	Adaeinae	South Africa	**MT224358**	**MT224750**	**MT240347**	-30.5326	29.68318
Larifugella cf. *afra*	MCZ-98385	Adaeinae	South Africa	**MT224573**	**MT224717**	**MT240334**	-30.5326	29.68318
Larifugella zuluana	MCZ-98906.5	Adaeinae	South Africa	**MT224575/ MT224576**	**MT224719**		-28.745	31.13596
cf. *Larifugella* sp.	MCZ-132921.1	Adaeinae	South Africa	**MT224361**	**MT224753**		-24.5697	30.86031
cf. *Larifugella* sp.	MCZ-30078	Adaeinae	South Africa	**MT224521**	**MT224665**		-32.6871	26.4937
Paradaeum sp.	MCZ-73504	Adaeinae	South Africa	**MT224551**	**MT224695**		-33.9839	20.82532
Speleomontia sp.	MCZ-132910.1	Sorensenellinae	South Africa	**MT224356**	**MT224748**	**MT240346**	-33.9856	18.40128
Amatola sp.	MCZ-127202	Triaenonychinae	South Africa	**MT224334**	**MT224726**		-29.6028	30.3464
Amatola sp.	MCZ-128699	Triaenonychinae	South Africa	**MT224346**	**MT224738**		-30.5326	29.68318
Amatola sp.	MCZ-132881	Triaenonychinae	South Africa	**MT224348**	**MT224740**		-29.8635	30.98691
Amatola sp.	MCZ-132882	Triaenonychinae	South Africa	**MT224349**	**MT224741**		-29.3221	30.26258
Amatola sp.	MCZ-73541.2	Triaenonychinae	South Africa	**MT224557**	**MT224701**		-32.6823	26.49135
Austromontia sp.	MCZ-127281.1	Triaenonychinae	South Africa	**MT224338**	**MT224730**		-33.9521	22.91155
Austromontia sp.	MCZ-127282.2	Triaenonychinae	South Africa	**MT224339**	**MT224731**		-33.9521	22.91155
Austromontia sp.	MCZ-127678	Triaenonychinae	South Africa	**MT224343**	**MT224735**		-33.9262	22.93821

Table 2.1 (Continued)

Austromontia sp.	MCZ-134926	Triaenonychinae	South Africa	**MT224376**	**MT224769**		-33.6858	25.8342
Austromontia sp.	MCZ-73450.3	Triaenonychinae	South Africa	**MT224545**	**MT224689**		-33.9673	18.94315
Austromontia sp.	MCZ-73484.3	Triaenonychinae	South Africa	**MT224547**	**MT224691**		-33.9749	23.14712
Austromontia sp.	MCZ-73488	Triaenonychinae	South Africa	**MT224549**	**MT224693**		-33.9876	18.40547
Austromontia sp.	MCZ-73505.2	Triaenonychinae	South Africa	**MT224552**	**MT224696**		-33.9839	20.82532
Austromontia sp.	MCZ-73525.3	Triaenonychinae	South Africa	**MT224555**	**MT224699**		-33.9657	23.9286
Austromontia sp.	MCZ-88579.1	Triaenonychinae	South Africa	**MT224571**	**MT224715**	**MT240332**	-34.0042	18.38316
Austromontia sp.	MCZ-88580	Triaenonychinae	South Africa	**MT224572**	**MT224716**	**MT240333**	-34.0042	18.38316
Biacumontia sp.	MCZ-127587	Triaenonychinae	South Africa	**MT224342**	**MT224734**		-34.0235	23.89033
Biacumontia sp.	MCZ-132917	Triaenonychinae	South Africa	**MT224359**	**MT224751**		-31.6061	29.5385
Biacumontia sp.	MCZ-73478.1	Triaenonychinae	South Africa	**MT224546**	**MT224690**		-33.9262	22.93821
Biacumontia sp.	MCZ-73512	Triaenonychinae	South Africa	**MT224554**	**MT224698**		-33.966	23.66401
Biacumontia sp.	MCZ-73544	Triaenonychinae	South Africa	**MT224560**	**MT224704**		-33.9749	23.14712
Biacumontia sp.	MCZ-87095.2	Triaenonychinae	South Africa	**MT224564**	**MT224708**		-33.9749	23.14712
Ceratomontia sp.	MCZ-127009	Triaenonychinae	South Africa	**MT224333**	**MT224725**		-31.0629	30.17422
Ceratomontia sp.	MCZ-135001.1	Triaenonychinae	South Africa	**MT224377**	**MT224770**		-33.3399	26.58824
Ceratomontia sp.	MCZ-30077.2	Triaenonychinae	South Africa	**MT224520**	**MT224664**		-32.6871	26.4937
Ceratomontia sp.	MCZ-58943.2	Triaenonychinae	South Africa	**MT224526**	**MT224670**	**MT240317**	-34.0235	23.89033
Ceratomontia sp.	MCZ-73543.1	Triaenonychinae	South Africa	**MT224559**	**MT224703**	**MT240327**	-32.6871	26.4937
Ceratomontia sp.	MCZ-88282	Triaenonychinae	South Africa	**MT224568**	**MT224712**		-33.3399	26.58824
cf. *Ceratomontia* sp.	MCZ-58945.1	Triaenonychinae	South Africa	**MT224528**	**MT224672**		-32.6868	28.37712
cf. *Ceratomontia* sp.	MCZ-58945.2	Triaenonychinae	South Africa	**MT224529**	**MT224673**	**MT240318**	-32.6868	28.37712
Graemontia sp.	MCZ-73486.1	Triaenonychinae	South Africa	**MT224548**	**MT224692**		-33.9749	23.14712
Graemontia sp.	MCZ-73506.2	Triaenonychinae	South Africa	**MT224553**	**MT224697**	**MT240326**	-33.9839	20.82532
Graemontia sp.	MCZ-73526	Triaenonychinae	South Africa	**MT224556**	**MT224700**		-33.9749	23.14712
Lizamontia sp.	MCZ-132885	Triaenonychinae	South Africa	**MT224351**	**MT224743**		-28.9602	29.22588
Mensamontia sp.	MCZ-127856	Triaenonychinae	South Africa	**MT224344**	**MT224736**		-33.9942	20.45868
Mensamontia sp.	MCZ-73445.1	Triaenonychinae	South Africa	**MT224544**	**MT224688**		-33.9679	18.94161
Micromontia sp.	MCZ-73542.2	Triaenonychinae	South Africa	**MT224558**	**MT224702**		-29.0535	29.38516
Monomontia sp.	MCZ-127314	Triaenonychinae	South Africa	**MT224340**	**MT224732**		-28.7435	31.13804
Monomontia sp.	MCZ-127324	Triaenonychinae	South Africa	**MT224341**	**MT224733**		-28.7316	28.91859
Monomontia sp.	MCZ-128564	Triaenonychinae	South Africa	**MT224345**	**MT224737**		-28.9602	29.22588
Monomontia sp.	MCZ-132918	Triaenonychinae	South Africa	**MT224360**	**MT224752**		-28.8882	31.37523
Monomontia sp.	MCZ-30065.2	Triaenonychinae	South Africa	**MT224517**	**MT224661**		-32.5704	26.9403
Monomontia sp.	MCZ-35537	Triaenonychinae	South Africa	**MT224522**	**MT224666**		-27.545	31.28185
Monomontia sp.	MCZ-58975.3	Triaenonychinae	South Africa	**MT224531**	**MT224675**		-22.996	30.26447
Monomontia sp.	MCZ-73245.2	Triaenonychinae	South Africa	**MT224542**	**MT224686**		-22.996	30.26447
Monomontia sp.	MCZ-73250	Triaenonychinae	South Africa	**MT224543**	**MT224687**		-22.996	30.26447
Monomontia sp.	MCZ-87149.3	Triaenonychinae	South Africa	**MT224565**	**MT224709**		-24.5697	30.86031
Monomontia sp.	MCZ-87608	Triaenonychinae	South Africa	**MT224567**	**MT224711**	**MT240331**	-30.5326	29.68318
Monomontia sp.	MCZ-88573.1	Triaenonychinae	South Africa	**MT224570**	**MT224714**		-25.997	31.11646
Planimontia sp.	MCZ-134889	Triaenonychinae	South Africa	**MT224373**	**MT224766**		-34.0042	18.38316
Planimontia sp.	MCZ-73493.3	Triaenonychinae	South Africa	**MT224550**	**MT224694**	**MT240325**	-29.0535	29.38516
Planimontia sp.	MCZ-88571	Triaenonychinae	South Africa	**MT224569**	**MT224713**		-34.0042	18.38316
Roewerania sp.	MCZ-127275.2	Triaenonychinae	South Africa	**MT224337**	**MT224729**		-28.7316	28.91859
Roewerania sp.	MCZ-30076.2	Triaenonychinae	South Africa	**MT224519**	**MT224663**		-32.6823	26.49135
Roewerania sp.	MCZ-84507.2	Triaenonychinae	South Africa	**MT224563**	**MT224707**		-32.6823	26.49135
Roewerania sp.	MCZ-87385.1	Triaenonychinae	South Africa	**MT224566**	**MT224710**	**MT240330**	-28.9602	29.22588
Rostromontia capensis	MCZ-133944	Triaenonychinae	South Africa	GQ912723	GQ912793		-33.9792	18.45
Rostromontia sp.	MCZ-132911	Triaenonychinae	South Africa	**MT224357**	**MT224749**		-33.9854	18.40135
Triaenonychidae sp.	MCZ-58974	Triaenonychinae	South Africa	**MT224530**	**MT224674**	**MT240319**	-24.8742	30.71744
Triaenonychidae sp.	MCZ-59007.1	Triaenonychinae	South Africa	**MT224533**	**MT224677**		-33.3399	26.58824
Triaenonychidae sp.	MCZ-59007.2	Triaenonychinae	South Africa	**MT224534**	**MT224678**		-33.3399	26.58824
Triaenonychidae sp.	MCZ-59008.1	Triaenonychinae	South Africa	**MT224535**	**MT224679**	**MT240320**	-33.3399	26.58824

Table 2.1 (Continued)

Triaenonychidae sp.	MCZ-59008.2	Triaenonychinae	South Africa	**MT224536**	**MT224680**		-33.3399	26.58824
Fumontana deprehendor	MCZ-134565	Triaenonychinae	United States	GQ912721	GQ912790/ **MT224764**	EU162780	36.04833	-82.4
Fumontana deprehendor	MCZ-46881	Triaenonychinae	United States	**MT224523**	**MT224667**	EU162788	35.75681	-83.21165
Outgroup taxa		**Family**	**Higher group**					
Acropsopilio chilensis		Acropsopilionidae	Dyspnoi	KF963305	KF955592	GQ912899		
Ceratolasma tricantha		Ischyropsalididae	Dyspnoi	AF124943	GQ912764	GQ912865		
Hesperonemastoma modestum		Taracidae	Dyspnoi	AF124942	EF108577	KU875193		
Caddo agilis		Caddidae	Eupnoi	KF963310	KF955597	MF816271		
Eurybunus brunneus		Sclerosomatidae	Eupnoi	JQ437010	JQ437102			
Alloepedanus sp.		Epedanidae	Grassatores	JF786480	JF786572			
Euepedanus sp.		Epedanidae	Grassatores	JF786479	JF786571			
Pseudobiantes japonicus		Epedanidae	Grassatores		LC176242	LC176240		
Pseudoepedanus dolensis		Epedanidae	Grassatores	GQ912731	GQ912807			
Acutisoma longipes		Gonyleptidae	Grassatores	GQ912736	GQ912815	JF786441		
Pachyloides thorellii		Gonyleptidae	Grassatores	PTU37007	U91508	KF726794		
Remyus sp.		Phalangodidae	Grassatores	JF786470	JF786608	JF786431		
Zalmoxis cardwellensis		Zalmoxidae	Grassatores	JN885755	JN885734	JN885769		
Synthetonychia sp.		Synthetonychiidae		GQ912720	GQ912787	GQ912875		
Synthetonychia sp.		Synthetonychiidae		KT302218	KT302254	KT302305		
Briggsus flavescens		Cladonychiidae	Travunioidea		HM056643	HM056726		
Erebomaster flavescens		Cladonychiidae	Travunioidea	GQ912716	GQ912781	HM056722		
Holoscotolemon jaqueti		Cladonychiidae	Travunioidea	GQ912717	GQ912783	GQ912873		
Peltonychia clavigera		Cladonychiidae	Travunioidea	FJ796479	GQ912785	FJ796491		
Speleonychia sengeri		Cladonychiidae	Travunioidea		GQ205667	HM056727		
Theromaster brunnea		Cladonychiidae	Travunioidea	GQ912718	GQ912784	HM056723		
Cryptomaster leviathan		Cryptomastridae	Travunioidea		HM056641	HM056724		
Speleomaster lexi		Cryptomastridae	Travunioidea		HM056642	HM056725		
Metanonychus setulus		Paranonychidae	Travunioidea		HM056649	HM056732		
Paranonychus brunneus		Paranonychidae	Travunioidea		HM056645	HM056728		
Sclerobunus nondimorphicus		Paranonychidae	Travunioidea		HM056659	GQ870663		
Zuma acuta		Paranonychidae	Travunioidea	AF124951	AF124978	EU162817		
Trojanella serbica		Travuniidae	Travunioidea	GQ912719	GQ912786	GQ912874		

2.2 Materials and methods

2.2.1 Taxon sampling

Specimens used in this study were collected mostly by the authors via leaf-litter sifting or direct hand collection between 2003 and 2018. Animals were immediately preserved in 95% ethanol and later stored at -20 ºC or -80 ºC. All specimens used in this work are stored at the Museum of Comparative Zoology (MCZ) or at Worcester State University (WSU), and locality data are available online through MCZBase (https://mczbase.mcz.harvard.edu) and Table 2.1. All specimens acquired by the authors for this project were collected under valid permits (New Zealand multiple permits

[38002-RES]; Australia [NSW #SL101324; QLD #WITK00845202; WA Permits #OF000190, #CE000648, #SF004565]; New Caledonia [#609011-75/2018]; Chile [Autorización #026/2014]; South Africa [Easter Cape permits #CRO 108/11CR and CRO 109/11CR; KZN #OP 4085/2011; Western Cape Permit # AAA007-00344-0035]; USA [Great Smoky Mts N.P. Permit #GRSM-2014-SCI-02335]) or by donation from local collectors and museums.

Taxonomic identification was done using light microscopy of somatic and genitalic characters, and specimens were then selected for molecular work, focusing our sampling on representing as many genera and species as possible. We also used multiple specimens per genus and species whenever possible so as to test the monophyly of those groups. Our sampling spans ~50% of all currently accepted genera (50/108 genera + 1 undescribed genus) and includes representatives from all the major geographic areas from which triaenonychids are known, with the exception of Sardinia and Crozet Islands. In total, our dataset includes 329 terminals, 300 of which are currently classified as triaenonychids. For our outgroup sampling, we included three Dyspnoi Hansen & Sørensen, 1904, three Eupnoi Hansen & Sørensen, 1904, eight Grassatores Kury *in* Giribet, Edgecombe, Wheeler & Babbitt, 2002, 13 Travunioidea, and two *Synthetonychia* Forster, 1954, an endemic New Zealand genus classified as a separate family, Synthetonychiidae (Table 2.1).

2.2.2 Molecular data generation

DNA extractions were done using Qiagen's DNeasy Blood & Tissue kit with an overnight incubation. We sequenced three markers, including two conserved nuclear ribosomal genes (18S and 28S rRNA) and the more variable mitochondrial gene cytochrome *c* oxidase subunit I (hereafter 'COI'), totalling to almost 4kb of sequence data. 18S rRNA was amplified in three fragments using primer pairs 1F–5R, 3F–18Sbi, and 18Sa2.0–9R (Giribet, Carranza, Baguñà, Riutort, & Ribera, 1996; Whiting, Carpenter, Wheeler, & Wheeler, 1997). 28S rRNA was sequenced in two fragments using

primer pairs 28Sa–28Srd5b and 28Srd4.8a–28Srd7bi. Some specimens were also amplified for the first fragment of 28S rRNA using primer pair 28Srd1a and rd4b, but due to difficulty getting clean sequences for this fragment, these were excluded from the final analysis (for details on the 28S rRNA primers see (Giribet & Shear, 2010)). COI was amplified with the primer pair LCO1490–HCO2198 (Folmer, Black, Hoeh, Lutz, & Vrujenhoek, 1994). PCR reactions were carried out with 1–2 μL DNA template, using either GoTaq DNA polymerase in a 25 μL reaction, Bioline Biolase in a 10 μL reaction, or with GE beads in a 25 μL reaction. Gel electrophoresis was used to visualize amplification reactions, and successful reactions were cleaned using ExoSAP in a 1:5 dilution. Cycle sequencing proceeded with 0.5 μL of BigDye, and final cycle sequencing products were sequenced on an ABI 3730 in the Bauer Core at Harvard University. New sequences are deposited in GenBank under accession numbers MT224318–MT224908 and MT240314–MT240477 (Table 2.1).

Sequence data were quality-checked, trimmed, and assembled in Geneious 10 (https://www.geneious.com), with additional outgroup sequences downloaded from GenBank. Each locus was then aligned in MAFFT (Katoh & Standley, 2014) via the Geneious plugin, with automatic model selection. The 28S rRNA alignment was further edited to remove long gaps at the ends of the alignment. Alignments were concatenated in SequenceMatrix (Vaidya, Lohman, & Meier, 2011) and the concatenated dataset was then subjected to phylogenetic analysis.

2.2.3 Phylogenetic inference

Model testing and phylogenetic analysis was initially performed in W-IQ-TREE v 1.6.9 (Nguyen, Schmidt, von Haeseler, & Minh, 2015), implementing the ModelFinder function (Kalyaanamoorthy, Minh, Wong, von Haeseler, & Jermiin, 2017) and partitioning by locus (Chernomor, von Haeseler, & Minh, 2016). Nodal support was assessed with Shimodaira–Hasegawa approximate likelihood ratio testing (SH-aLRT) and ultrafast bootstrap analysis (UFBoot) (Hoang, Chernomor, von

Haeseler, Minh, & Vinh, 2018), specifying 1000 replications for each measure. We also inferred a tree with RAxML-HPC v8 (Stamatakis, 2014) via the CIPRES Science Gateway v3.3 (https://www.phylo.org), partitioning by locus and using the GTR + Γ substitution model for all partitions. Nodal support in RAxML was assessed using both standard non-parametric bootstrapping (-b) and rapid bootstrapping (-x) mapped onto the best tree. Finally, we analysed our dataset in BEAST v 2.4.6 (Bouckaert et al., 2014), using the results of IQ-TREE's ModelFinder to define substitution models for each partition independently. In order to determine the best clock model and tree prior for our dataset, we used an iterative strategy using the stepping-stone Path sampler application in BEAST 2 (Xie, Lewis, Fan, Kuo, & Chen, 2011). First, we ran three path sampling analyses all under a Yule tree prior with 100 steps of 1 million generations, corresponding to a strict clock, an exponential relaxed clock, and a lognormal relaxed clock. Marginal likelihood estimates were compared using Bayes Factors to select the optimal clock model. We then ran another path sampling analysis under the optimal clock model, but using a birth-death tree prior. Again, marginal likelihood estimates for the two analysed tree priors were compared using Bayes Factors, and the optimal clock model and tree prior combination was used for lineage age inference.

BEAST chronograms were calibrated using known Opiliones fossils to constrain crown-group ages of specified nodes, all under uniform distributions with a maximum age for each calibration set to 514 Ma, corresponding to the age of the oldest fossil chelicerate *Wisangocaris barbarahardyae* Jago, García-Bellido & Gehling, 2016, from the Emu Bay Shale (Wolfe, Daley, Legg, & Edgecombe, 2016). The following nodes were calibrated: (1) Dyspnoi was constrained to a minimum age of 305 Ma, reflecting the age of the fossil *Ameticos scolos* Garwood, Dunlop, Giribet & Sutton, 2011, from the Montceau-les-Mines Lagerstätte, the upper limit of which is biostratigraphically dated to *ca.* 305 Ma (Garwood, Dunlop, Giribet, & Sutton, 2011); (2) The age of Eupnoi was constrained to a minimum of 305 Ma, reflecting the age of *Macrogyion cronus* Garwood,

Dunlop, Giribet & Sutton, 2011, also from the Montceau-les-Mines Lagerstätte (Garwood et al., 2011); (3) Epedanidae Sørensen, 1886, was constrained to a minimum age of 105 Ma, reflecting the age of *Petrobunoides sharmai* Selden, Dunlop, Giribet, Zhang & Ren, 2016, from Burmese amber from the lowermost Cenomanian (~100 Mya) (Selden, Dunlop, Giribet, Zhang, & Ren, 2016). While

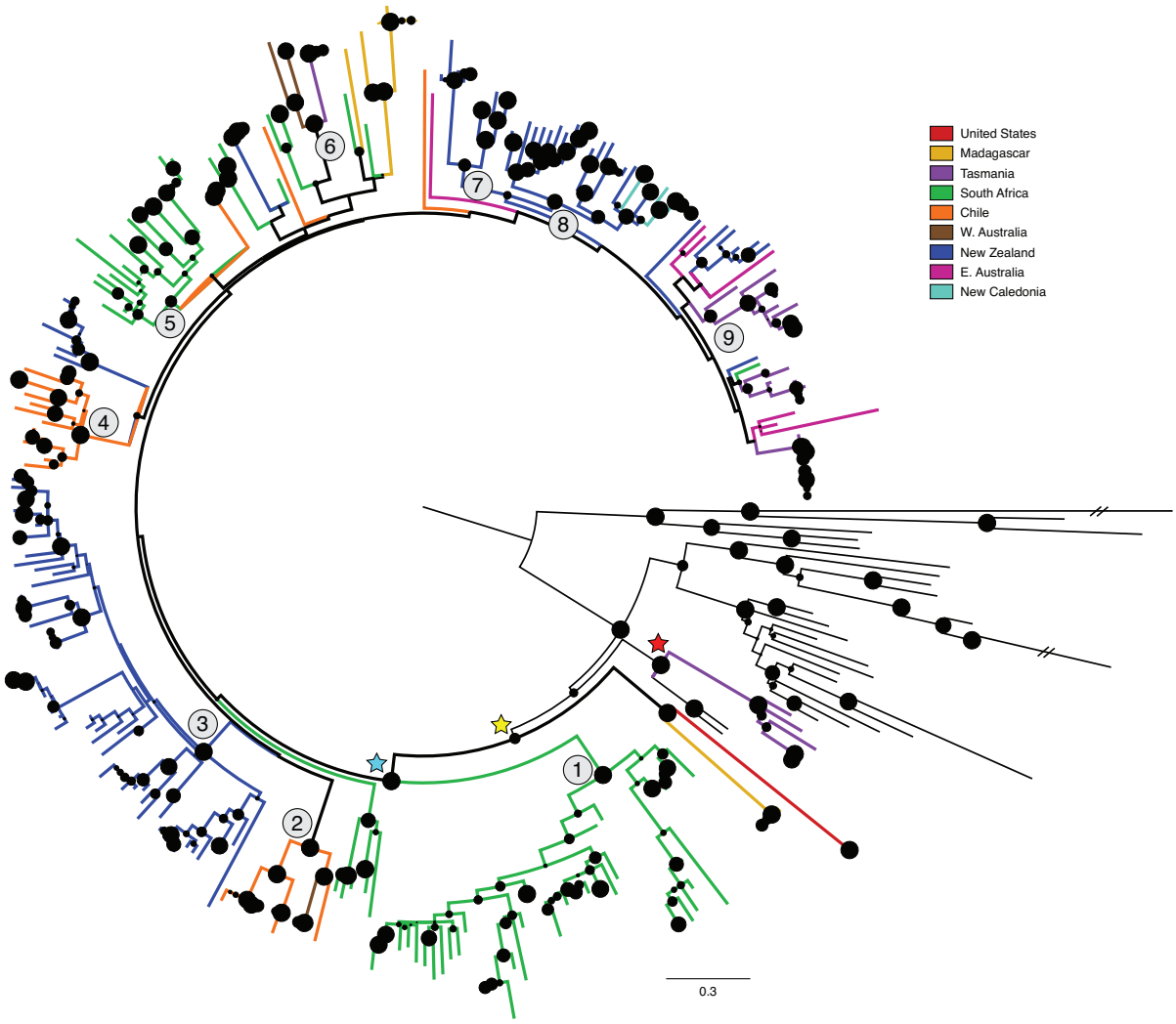

Figure 2.3. Result of RAxML analysis, partitioned by locus. Branches coloured by landmass as shown in the key and in Figure 2.2. Circles at nodes scaled according to rapid bootstrap support values. Red star denotes the clade of *Lomanella* + *Synthetonychia*. Yellow star denotes Triaenonychidae including *Fumontana* + *Flavonuncia*. Blue star shows Southern Hemisphere Triaenonychidae. Numbered nodes correspond to well-supported clades across all analyses (see Results and Discussion for details).

the placement of this fossil in Epedanidae has not been verified in the context of a total evidence phylogeny, unlike the other fossils used in our calibrations (Garwood, Sharma, Dunlop, & Giribet, 2014; Sharma & Giribet, 2014), its assignment to Epedanidae is based on multiple morphological characters such as its elongate, raptorial pedipalps, the tarsal formula, and the shape of the eyemound (Selden et al., 2016); (4) The root age of all Opiliones was constrained to a minimum of 405 Ma, corresponding to the age of the oldest known Opiliones fossil *Eophalangium sheari* Dunlop, Anderson, Kerp & Hass, 2004 (Dunlop, Anderson, Kerp, & Hass, 2004; Garwood et al., 2014). Four different BEAST analyses were run for 200 million generations each and combined post burn-in. Stationarity was confirmed in Tracer v 1.6 (Rambaut & Drummond, 2009), with all ESS values >200.

All individual gene alignments (in phylip format), concatenated tree and trees inferred from individual loci (in Newick format), and the BEAST xml file are available as supplementary information via the Harvard Dataverse (https://doi.org/10.7910/DVN/ULZIHT).

2.3 Results and discussion

2.3.1 Composition of Triaenonychidae and its position within Insidiatores

Analysis of our partitioned dataset recovered a non-monophyletic Triaenonychidae (Figures 2.3–2.6). Across all analyses with maximal support, we instead found a sister-group relationship between the Australian triaenonychid genus *Lomanella* and the New Zealand-endemic *Synthetonychia*, the only genus in the family Synthetonychiidae (red star in Figures 2.3–2.5). *Lomanella* and *Synthetonychia* share several morphological affinities, specifically in terms of their penis structure (both have reduced

dorsolateral plates along the truncus) and tarsal claws (many *Lomanella* species and all *Synthetonychia* species have a complex branching peltonychium rather than the typical triaenonychid trident claw), as previously discussed by Hunt and Hickman (1993), and in part supported by the work of Mendes

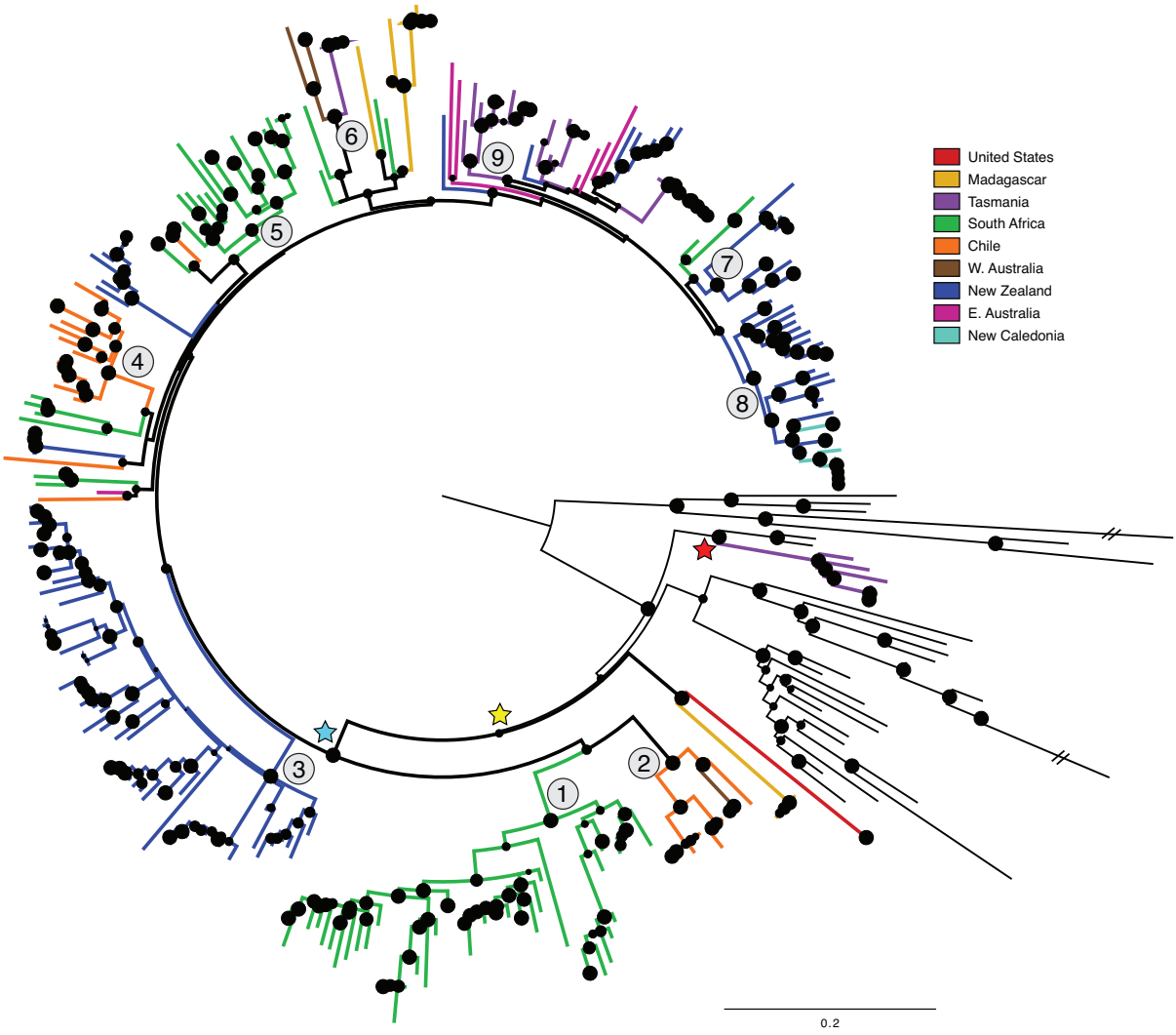

Figure 2.4. Result of IQ-TREE analysis, partitioned by locus. Branches coloured by landmass as indicated in the key, and in Figures 2.2 and 2.3. Circles at nodes scaled according to ultrafast bootstrap support values. Red star corresponds to *Synthetonychia* + *Lomanella*, yellow star corresponds to Triaenonychidae, and blue star corresponds to Southern Hemisphere Triaenonychidae. Numbered nodes correspond to well-supported clades across all analyses, as in Figure 2.3.

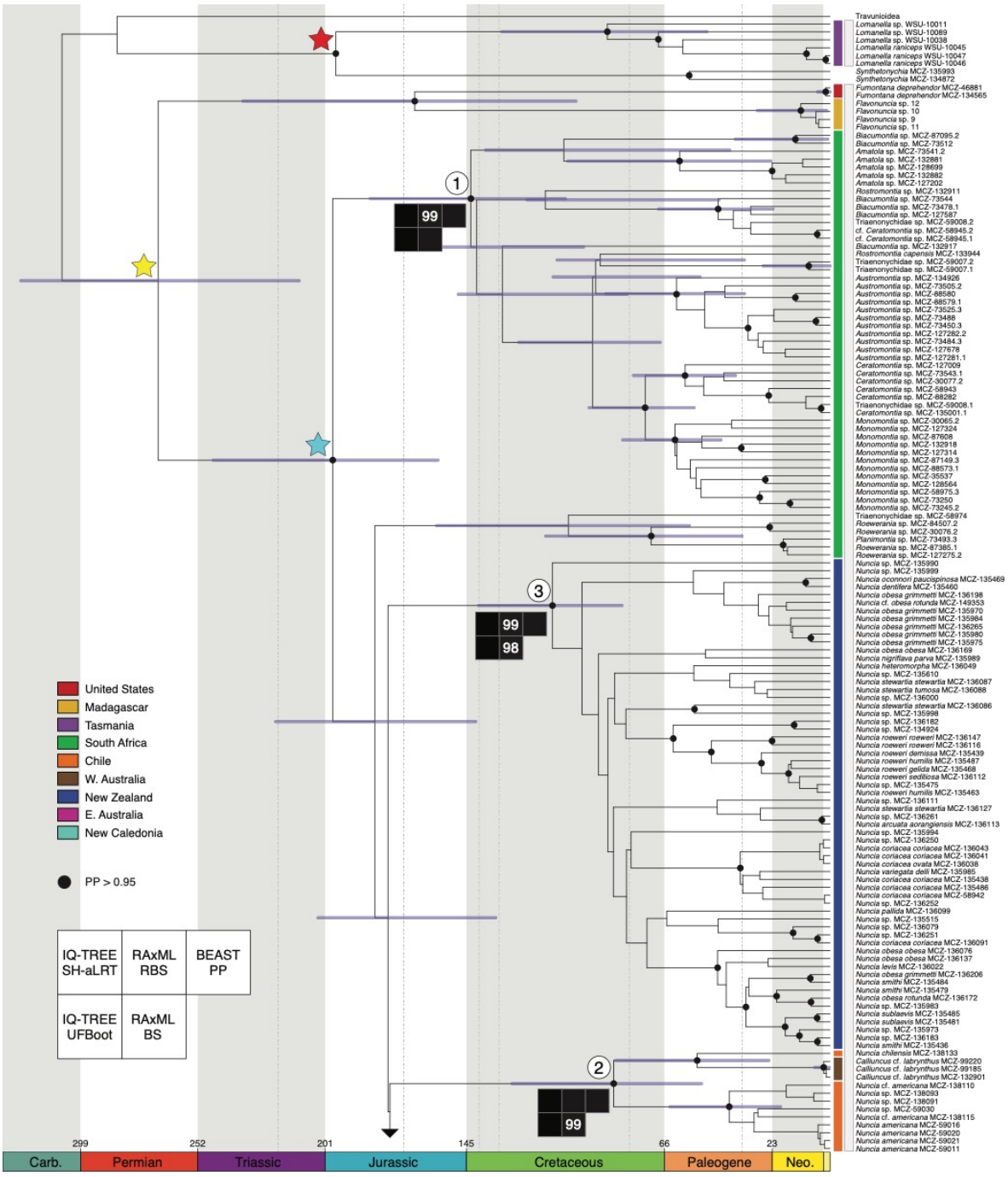

Figure 2.5. BEAST chronogram showing divergence time estimates for Triaenonychidae. Error bars at nodes show 95% highest probability densities of estimated divergence times. Left column next to terminals coloured by geographic area, as shown in the key and in Figures 2.2–2.4. Right column coloured by subfamily (white = Triaenonychinae; black = Sorensenellinae; light grey = Triaenobuninae; dark grey = Adaeinae). Red star corresponds to *Synthetonychia* + *Lomanella*, yellow star corresponds to Triaenonychidae, and blue star corresponds to Southern Hemisphere Triaenonychidae. Nodes with black circles correspond to well supported clades (posterior probability > 95%). Numbered nodes correspond to well-supported clades across all analyses, as in Figures 2.3 and

(Continued) 2.4. For these nodes, sensitivity plots showing support values for all analyses are included. Dotted vertical lines correspond to major tectonic events in the breakup of Gondwana: 220 Mya (Pangaea splits into Gondwana and Laurasia); 170 Mya (East–West Gondwana split); 140 Mya (South Atlantic ocean starts opening); 132 Mya (Madagascar–India separates from Australia–Antarctica–Zealandia); 80 Mya (Zealandia separates from Australia–Antarctica); 35 Mya (Antarctica disconnects from Australia and South America, New Caledonia re-emerges after marine transgression).

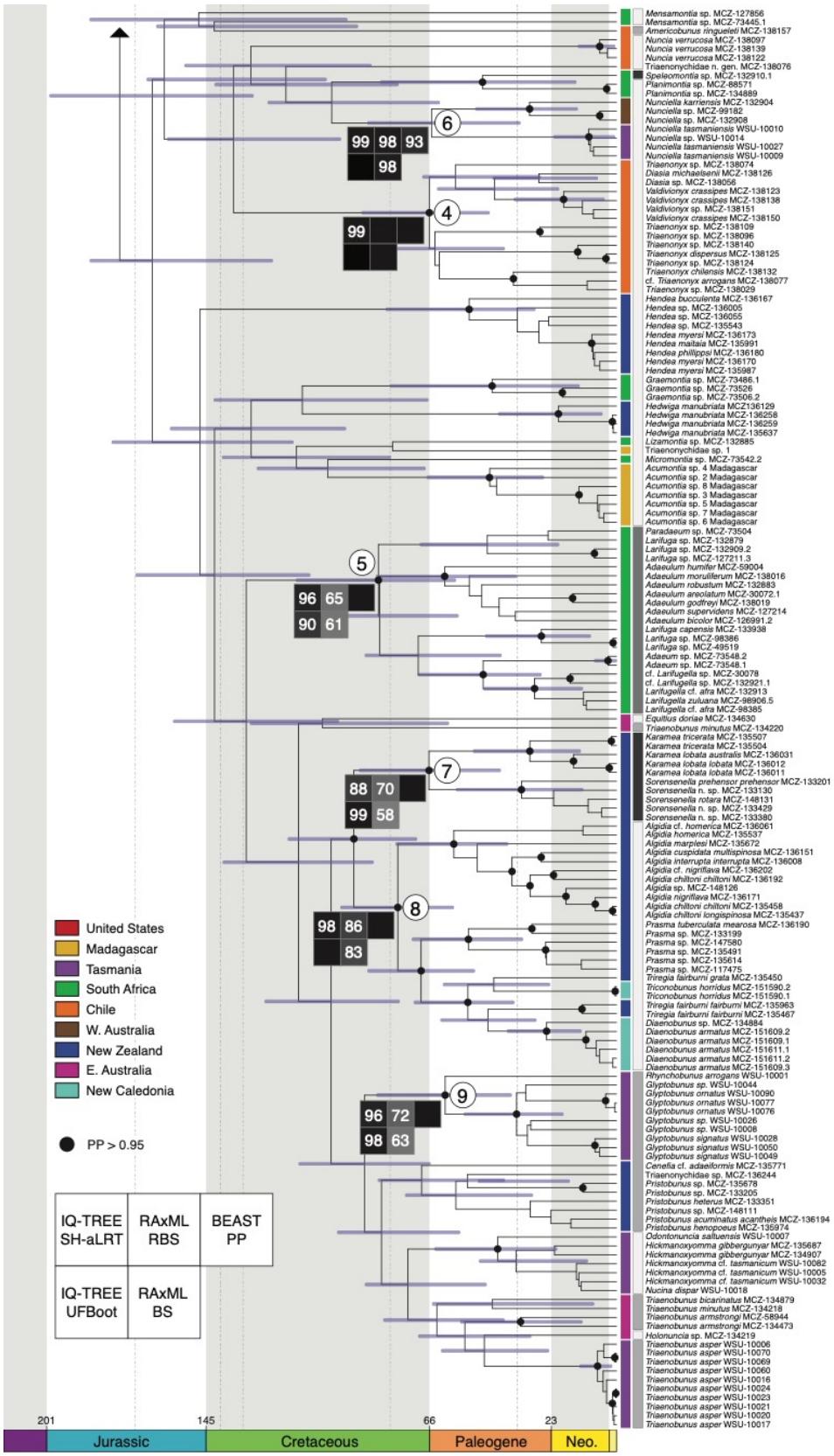

Figure 2.5 (Continued)

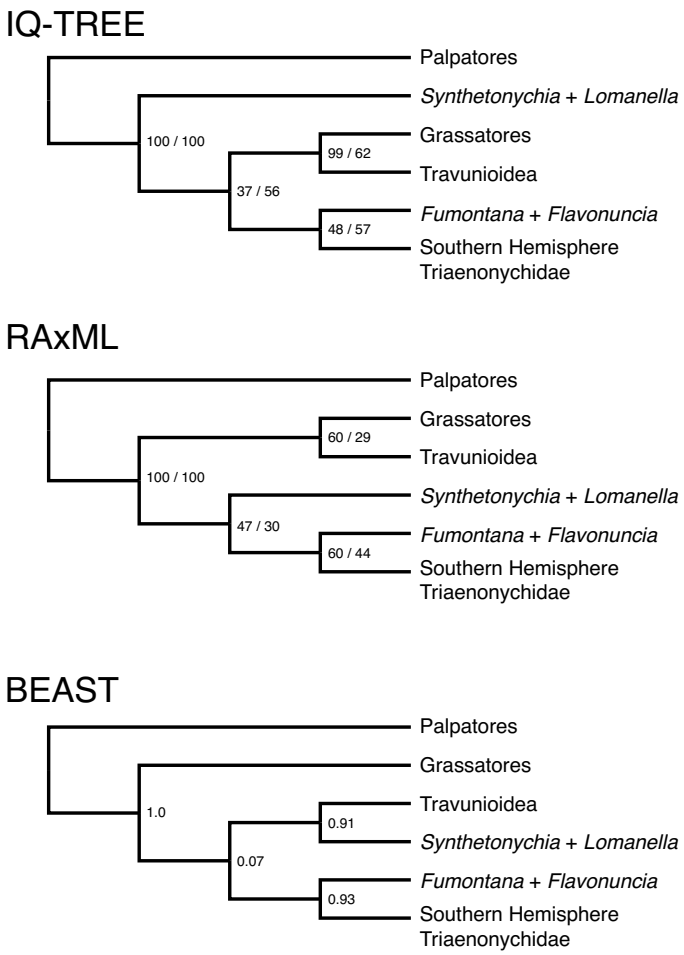

Figure 2.6. Summary of major relationships of Laniatores from three phylogenetic analyses. Numbers at nodes show support values for depicted relationships (IQ-TREE: SH-aLRT/UFBoot; RAxML: RBS/BS; BEAST: PP).

(2009) (although she also included *Pyenganella* in this clade). However, Hunt (1996) did not place *Pyenganella* with *Lomanella*, instead finding *Lomanella* as the sister group to all remaining Australian triaenonychids. The placement of this clade of *Lomanella* + *Synthetonychia*, however, was inconsistent across analyses (Figure 2.6). In our RAxML tree, it was recovered as the sister group to all other triaenonychids, albeit without support (47% rapid bootstrap support [RBS] and 30% standard bootstrap support [BS] in RAxML). In our BEAST tree, it was recovered as the sister group to Travunioidea, again without support (posterior probability [PP] 0.91) but consistent with the results of Fernández et al. (2017) (though that study did not include *Lomanella*). Finally, our IQ-TREE

phylogeny placed the group as the sister lineage to all other Laniatores (100% SH-aLRT and 100% UFBoot), in line with the results of Giribet et al. (2010) and Sharma and Giribet (2011), who found *Synthetonychia* (*Lomanella* was not sampled) to be the sister group to the remaining Laniatores. Given this low and inconsistent support for the relationship of *Lomanella* + *Synthetonychia* to other Triaenonychidae genera, and the fact that other studies have found *Synthetonychia* not to be related to other triaenonychids, even when using phylogenomics (Fernández *et al.* 2017), we believe this constitutes a unique and distinct evolutionary lineage, as proposed earlier by Mendes (2009). However, until *Pyenganella* is examined, we refrain from erecting new taxa, yet recognize that *Lomanella* should be moved out of Triaenonychidae.

We also failed to recover a monophyletic Insidiatores in two of three analyses, and instead found a sister group relationship between Grassatores and Travunioidea with variable levels of support in IQ-TREE (99% SH-aLRT, 62% UFBoot) and RAxML (60% RBS, 29% BS). This relationship contrasts with the results of previous analyses to include Travunioidea, Grassatores, and Triaenonychidae. For example, Derkarabetian et al. (2018) found a relationship of Grassatores + Triaenonychidae to the exclusion of Travunioidea in most analyses, and Sharma *et al.* (2011) found monophyly of Insidiatores except for *Synthetonychia*. Our BEAST analysis did recover a monophyletic Insidiatores, but with extremely low support (0.07 PP). This result was, however, recovered by Fernández *et al.* (2017) using transcriptomic data. Given the generally low nodal supports of our analyses and the limited number of loci used in our study, we prefer to leave this issue aside until additional data become available.

Triaenonychidae (excepting *Lomanella*, which we now consider to be the sister group of Synthetonychiidae) was monophyletic in all analyses, though with low support (IQ-TREE: 47% SH-aLRT, 57% UFBoot; RAxML: 60% RBS, 44% BS; BEAST: 0.93 PP). This poorly-supported bipartition corresponds to a split between two monotypic genera, the eastern North American

Fumontana deprehendor and *Flavonuncia pupilla* Lawrence, 1959, from Madagascar, and all other triaenonychids (herein "Southern Hemisphere Triaenonychidae"). The relationship of *Fumontana* + *Flavonuncia* received high support in all analyses, and together with the Sardinian monotypic genus *Buemarinoa* Roewer, 1956, has been proposed as a tribe of Triaenonychinae, Buemarinoini Karaman, 2019, on the basis of their similar male genital morphology (Karaman, 2019). While our data supported the clade Buemarinoini, they did not support its status as a tribe within Triaenonychinae. Likewise, the clade of the Southern Hemisphere Triaenonychidae received strong support in all analyses. We therefore accept the placement of *Fumontana* as a *bona fide* member of Triaenonychidae despite its geographic isolation. However, we acknowledge that given the low support for this relationship, *Fumontana* + *Flavonuncia* (= Buemarinoini) may represent a distinct evolutionary lineage, and its placement within the family should be further tested using more robust high-throughput sequencing methods, since the divergence between these two main lineages occurred between the Carboniferous and the Triassic (Figure 2.5).

2.3.2 Phylogenetic relationships within Southern Hemisphere Triaenonychidae

Within the Southern Hemisphere Triaenonychidae, nodal supports along the backbone of the phylogeny were uniformly low, though some smaller clades were recovered consistently with high support (Figures 2.3–2.5). These included (1) a clade of several South African genera classified in the subfamily Triaenonychinae (*Amatola* Lawrence, 1931, *Austromontia* Staręga, 1992, *Biacumontia* Staręga, 1992, *Ceratomontia* Roewer, 1915, *Monomontia* Staręga, 1992, and *Rostromontia* Staręga, 1992); (2) a clade of Chilean and Western Australian taxa (*Calliuncus* Roewer, 1931 and some *Nuncia* Loman, 1902 spp. with few spines; the South American *Nuncia* bear little morphological resemblance nor are closely phylogenetically related to the real *Nuncia* from New Zealand, as discussed below); (3) The New Zealand *Nuncia*; (4) a clade of some South American Triaenonychinae (*Diasia* Sørensen, 1902,

Triaenonyx Sørensen, 1886, *Valdivionyx* Maury, 1988); (5) the South African genera in the subfamily Adaeinae (*Adaeulum* Roewer, 1915, *Adaeum* Karsch, 1880, *Larifuga* Loman, 1898, *Larifugella* Staręga, 1992, *Paradeum* Lawrence, 1931); (6) the genus *Nunciella* Roewer, 1931, from both Western Australia and Tasmania; (7) the New Zealand Sorensenellinae genera *Sorensenella* and *Karamea*; (8) a clade of several spiny Triaenonychinae genera from New Zealand and the two genera from New Caledonia (*Algidia* Hogg, 1920, *Prasma* Roewer, 1931, *Triregia* Forster, 1948, *Triconobunus* and *Diaenobunus*); and (9) a clade comprised of two Tasmanian Triaenobuninae genera, *Glyptobunus* Roewer, 1915 and *Rhynchobunus* Hickman, 1958.

Regarding the subfamilies of Triaenonychidae, our results confirmed the polyphyletic "catch-all" status of Triaenonychinae, as well as the polyphyly of Triaenobuninae and Sorensenellinae. While we did recover a monophyletic Adaeinae in our trees, we were unable to include the Western Australian genus *Dingupa*, the only member of that subfamily found outside of South Africa. Mendes (2009) previously identified the inconsistency of these subfamilial classifications, instead proposing a division of the family into two subfamilies, Adaeinae and Triaenonychinae. However, the constituent taxa in her emended subfamilies were either not sampled by us or else not closely related to each other in our phylogenies, making comparison and reconciliation difficult, and indeed the most recent catalogue of Opiliones still uses the traditional subfamilies (Kury et al., 2014). All told, we find the current categorization of the four subfamilies to be uninformative at best and evolutionarily misleading at worst, and therefore recommend that their use be discontinued. However, we refrain from proposing any new classification scheme here given the low nodal support and inconsistent topology along the backbone of the tree.

2.3.4 New Zealand – New Caledonia

Wherever possible, we sequenced multiple individuals per genus so as to test their validity (*i.e.* monophyly). Of these, most genera from New Zealand were found to be monophyletic with high support in all analyses (*Hendea* Roewer, 1931, *Hedwiga* Roewer, 1931, *Algidia*, *Sorensenella*, *Karamea*, and *Prasma*). The New Zealand genus *Pristobunus* Roewer, 1931, was monophyletic in both IQ-TREE (96% SH-aLRT, 99% UFBoot) and RAxML (61% RBS, 49% BS) phylogenies, but potentially not in the BEAST tree, where one juvenile that could only be confidently identified to the subfamily "Triaenobuninae" (MCZ-136244) fell within the clade (72% PP). In contrast to the ambiguous monophyly of *Pristobunus*, the New Zealand genus *Triregia* was paraphyletic with respect to the two genera from New Caledonia (*Triconobunus* and *Diaenobunus*) in all cases. Furthermore, *Triconobunus* and *Diaenobunus* were never found to be sister taxa, though support values for these internal relationships are generally low. It is clear, however, that this clade requires a thorough revision, including the incorporation of the type species *Triregia monstrosa* Forster, 1948, from Three Kings Islands.

2.3.5 *Nuncia* and *Ceratomontia* – trans-oceanic genera?

Currently, *Nuncia* and *Ceratomontia* are the only genera in Triaenonychidae known from multiple landmasses. *Ceratomontia* has previously been shown to be non-monophyletic, with one clade in South America and a possible grade in South Africa that also includes other genera (*Austromontia*, *Monomontia*) (Mendes & Kury, 2008). We were not able to include South American *Ceratomontia* specimens in our study, so this hypothesis remains untested with molecular data, but our analyses showed that the South African *Ceratomontia* were deeply nested within a South African clade of triaenonychids.

Likewise, *Nuncia* was found in both New Zealand (which is home to the type species, *Nuncia sperata* Loman, 1902*,* jr. syn. of *Triaenonyx obesus* Simon, 1899) and South America, in Chile and

Argentina. *Nuncia* is by far the most diverse genus in the family, with 63 accepted species and subspecies (Kury et al., 2014), and it is characterized by a smooth carapace and a relative lack of spines and tubercles (see Figure 2.1j). Despite being defined more by a lack of features than the presence of any character in particular, all *Nuncia* from New Zealand constituted a clade with full support in all our analyses, unlike in the unpublished thesis of Vélez (2011). Lower-level relationships within the New Zealand *Nuncia*, though, indicate that many morphological species and subspecies are not valid, and this group requires substantial taxonomic revision.

The included *Nuncia* from South America were not at all closely related to the true New Zealand *Nuncia*, as suggested by a recent study of their genitalia (Porto & Pérez-Gonázlez, 2019), and indeed the South American species were found in two distinct places in the phylogeny. One of these clades corresponded to the species *Nuncia verrucosa* Maury, 1990 (and based on morphology, presumably *N. spinulosa* Maury, 1990, though this species was not available for this study), the "grupo *spinulosa*" of Maury (1990). As implied by their specific epithets, both of these species are replete with spines and tubercles (see Figure 2.1l and Figures I, III in Maury 1990), and in his original descriptions Maury (1990) noted that perhaps they should not be placed in *Nuncia* at all given their morphological dissimilarity to both the New Zealand *Nuncia* and the other South American *Nuncia* species. Our phylogenetic results validated this scepticism, and while redescribing these species under a new genus name is outside the scope of this paper, we recommend such a transfer. The other clade of *Nuncia* from South America contained the species *Nuncia americana* Roewer, 1961 and *Nuncia chilensis* (H. Soares, 1968) , as well as the species *Calliuncus* cf. *labyrinthus*, from Western Australia. While the members of this clade do lack spines and large tubercles and therefore superficially look similar to *Nuncia* from New Zealand, this clearly also constitutes a distinct evolutionary lineage. Again, without a thorough morphological examination of both *Calliuncus* (including its type species, *Calliuncus ferrugineus* Roewer, 1931) and the smooth-bodied

South American *Nuncia* species, we refrain from taking any nomenclatorial action here, but our phylogenetic results highlight the need for revision.

2.3.6 Chile

Apart from the *Nuncia* from South America in our tree, we also recovered a clade of several other genera from Chile. The genus *Valdivionyx* was monophyletic in all analyses with high support. The closely related genus *Diasia* was monophyletic in both the RAxML and BEAST trees, but paraphyletic with respect to *Valdivionyx* in the IQ-TREE result. These two genera were closely related to the genus *Triaenonyx* in all analyses, which was recovered as monophyletic in the IQ-TREE and RAxML phylogenies, but was paraphyletic with respect to *Valdivionyx* and *Diasia* in the BEAST tree. The monotypic genus *Americobunus* does appear to be a distinct evolutionary lineage in the family, as it sat on a long branch and resolved in different locations in each of the three trees. Furthermore, we included an exemplar of an animal that morphologically does not correspond to any described species (MCZ IZ-138076; Figure 2.1f). It too was recovered as a distinct evolutionary lineage, and together with its unique morphology corroborate its status as a new genus that will need to be described.

2.3.7 South Africa

Within South Africa, some genera were recovered as monophyletic in all analyses (*e.g.*, *Adaeum*, *Adaeulum*, *Amatola*, *Austromontia*, *Graemontia* Staręga, 1992, *Larifugella*, and *Monomontia*), but just as many were not (*e.g.*, *Biacumontia*, *Ceratomontia*, *Larifuga*, *Mensamontia* Staręga, 1992, *Planimontia* Kauri, 1961, *Roewerania* Lawrence, 1934, and *Rostromontia*). In addition, South African members appeared in 7–10 independent clades, some of them connected to Madagascar. Many genera as they are currently defined are extremely hard to distinguish based on morphology, and diagnostic characters at the

genus level show overlapping variability between genera. Future taxonomic work will certainly be needed to revise those genera, including looking for morphological characters that correspond to phylogenetic groups.

2.3.8 Madagascar

Our taxonomic sampling in Madagascar was restricted due to the limited availability of molecular-grade specimens from these landmasses in our collections. We therefore are unable to say much about the validity of those taxa, especially since its 35 species include several genera with only one or two species each (*Ankaratrix*, *Antogila* Roewer, 1931, *Decarynella* Fage, 1945, *Flavonuncia*, *Hovanuncia* Lawrence, 1959, *Ivohibea* Lawrence, 1959, *Millomontia* Lawrence, 1959, *Millotonyx* Lawrence, 1959, and *Paulianyx* Lawrence, 1959) plus the more diverse *Acumontia* Loman, 1898, with 22 described species (Kury et al., 2014). Even more unfortunately, the animals from Madagascar used in this study were consumed during DNA extraction and no vouchers remain for morphological analysis. However, we did recover multiple distinct lineages on the island, including the relictual *Flavonuncia*, a clade of specimens corresponding to *Acumontia*, and an unidentified species that groups with *Lizamontia* Kury, 2004 sp. from South Africa in all analyses. Further sampling of Madagascar species with techniques that allow using historical museum samples (e.g. Derkarabetian, Benavides, & Giribet, 2019) should help resolve this mystery.

2.3.9 Australia

We similarly had few exemplars from mainland Australia, which reflects the relatively unexamined triaenonychid diversity of the continent. The majority of our specimens, and indeed the majority of described species in the country, came from Tasmania, which we treated as a separate region. (While we often discuss Tasmania as a distinct region, it cannot be considered a separate landmass from

Australia given continental land bridge connections during the Quaternary (Lambeck & Chappell, 2001)). Given the large part of Australia without suitable recent habitat, we also treated Western Australia as separate from the east, a distributional pattern that is not uncommon in short-range saproxylic animals (Giribet & Edgecombe, 2006; Rix et al., 2015).

Here, we recovered a monophyletic *Glyptobunus* and found as its sister group the genus *Rhynchobunus*, also from Tasmania. However, some of our morphospecies were not monophyletic or had very old divergences, probably reflecting the poor taxonomy of the group. We also recovered a monophyletic *Nunciella*, which contained two reciprocally monophyletic lineages that corresponded to a group in Western Australia and a group in Tasmania. In contrast, we did not recover the monophyly of the genus *Triaenobunus* Sørensen, 1886, which is known from eastern and southeastern mainland Australia as well as Tasmania. Similarly, the charismatic Tasmanian genus *Hickmanoxyomma* Hunt, 1990, which is easily identified by its extremely tall and pointed eyemound (Figure 2.1g), was not recovered as a monophyletic group. Instead, we found two other Tasmanian species nested within the genus, *Nucina dispar* Hickman, 1958 and *Odontonuncia saltuensis* Hickman, 1958, neither of which have especially large spines on their eyemounds (though in the BEAST tree *O. salutensis* formed the sister group to this clade rather than nesting within it). The close relationship between *Hickmanoxyomma* and *Odontonuncia* was previously hypothesized by Hunt (1990). Lastly, as discussed above, the Western Australian genus *Calliuncus* was monophyletic in all analyses, and nested within the smooth-bodied clade of South American *Nuncia*.

Clearly, many different lineages within Triaenonychidae are in need of revision. Future work must focus on areas with significant taxonomic and phylogenetic discrepancies, such as the South American *Nuncia*, the many para- and polyphyletic South African genera, the clade containing *Triregia* plus the New Caledonian triaenonychids, and the genus *Triaenobunus* in Australia.

Furthermore, given the low nodal support along the backbone of our trees, future work should focus on resolving higher-level phylogenetic relationships using high-throughput sequencing techniques, including more genera, and whenever possible, the type species of such genera.

2.3.10 Biogeographic results

With the exception of North America, which only contains the monotypic genus *Fumontana*, and Sardinia, with *Buemarinoa*, no major landmass on which triaenonychids are found contains a monophyletic assemblage of taxa. This result holds even accounting for the low nodal support values along the backbone of our tree. Indeed, even the two genera from New Caledonia were not recovered as sister taxa; instead, both nested within the New Zealand genus *Triregia* as discussed above. In order to determine whether the non-monophyly of taxa in these Southern Hemisphere landmasses was attributable to ancient cladogenesis prior to Gondwanan breakup or more recent *trans*-oceanic dispersal, and to look for possible instances of Gondwanan vicariance, we performed a divergence dating analysis.

Comparison of marginal *L* estimates with Bayes Factors identified an exponential relaxed clock and a Yule tree prior as the optimal model for the dataset, with decisive support from Bayes Factors (BF = 15.59 compared to the next-highest model's marginal *L* estimate). The use of a Yule tree prior on our dataset, which includes both inter- and intraspecific divergences, is a theoretical violation of that speciation model and as such could bias divergence time estimates. However, simulation-based analysis of mixed inter- and intraspecific datasets in a Bayesian dating framework has shown that in sampling schemes such as ours, where the majority of nodes correspond to interspecies divergences, estimates of node times were robust to tree prior choice, and that model selection procedures such as ours were effective in rejecting models likely to cause highly inaccurate node time estimates (Ritchie, Lo, & Ho, 2017).

2.3.11 Initial diversification of Triaenonychidae predates Pangaean and Gondwanan breakup

Our divergence dating results recovered an ancient origin for Triaenonychidae, with a mean age in the Permian, at 268 Ma (95% confidence interval [CI]: 323–212 Ma) (Figure 2.5). While the lower limit of the 95% CI did not quite predate the initial breakup of Pangaea *ca.* 220 Mya (Ali & Aitchison, 2008), for the most part these dates suggest the family was diversifying before Pangaea began breaking up into the northern landmass of Laurasia and the southern landmass of Gondwana. The estimated age of the North America–Madagascar divergence, corresponding to the split between *Fumontana* and *Flavonuncia*, ranged from 234–101 Ma, with a mean age of 166 Ma, in the Jurassic. This age range roughly coincides with the timing of separation between Laurasia and Gondwana, and therefore implies that *Fumontana* is a relictual lineage in North America, just as *Buemarinoa* remains a relict in Western Europe. This parallels a similar pattern seen in other groups of arachnids, such as the oribatid mite family Malaconothridae Berlese, 1916, which has a cosmopolitan distribution and an estimated age of 333 Ma (Colloff, 2013), as well as the dispersal-limited pseudoscorpion families Pseudotyrannochthoniidae Beier, 1932 and Pseudogarypidae Chamberlin, 1923, which have representatives in both temperate Australia and the Holarctic (though the ages of these families have not been estimated using molecular dating methods, their divergence from their sister group are Palaeozoic for the first and early Mesozoic for the latter) (Benavides, Cosgrove, Harvey, & Giribet, 2019; Harvey et al., 2017). Similar signatures of Pangaean breakup have also been detected in multiple groups of plants (Beaulieu, Tank, & Donoghue, 2013; Mao et al., 2012) and amphibians (Pyron, 2014).

The mean age of the Southern Hemisphere Triaenonychidae was estimated to be 198 Ma (95% CI: 246–156 Ma), in the Early Jurassic. Again, these dates suggest the family was already diversifying well before Gondwana began breaking apart (initial rifting started in the Middle Jurassic,

~170 Mya) (Ali & Aitchison, 2008), and allows for the possibility that triaenonychids were able to colonize extensive continental areas via over-land dispersal before continents separated. Palynological and isotopic records from this period suggest that during the Triassic and Jurassic, southern Gondwana experienced less climatic differentiation and a greater floristic uniformity dominated by lycophytes, ferns, and tree ferns (Cantrill & Poole, 2012; McLoughlin, 2001). Given the large-scale biotic turnovers that followed the end-Permian extinction and the subsequent expansion of continuous stretches of suitable vegetation, over-land expansion of Triaenonychidae during this period seems highly plausible, and would therefore follow a pattern seen in other saproxylic taxa such as pettalid harvestmen (Baker et al., 2020) and peripatopsid velvet worms (Giribet et al., 2018; Murienne et al., 2014).

2.3.12 Relationships of taxa from disjunct landmasses

The Cretaceous period saw major rifting events, including the opening of the southern Atlantic Ocean, the separation of Madagascar–India from Australia–Antarctica–Zealandia, and the start of Zealandia's isolation (Ali & Aitchison, 2008; McLoughlin, 2001). Coinciding with this increased tectonism was the rise of angiosperms, and with it large-scale floristic turnovers and increased provincialism (McLoughlin, 2001; McLoughlin & Kear, 2010). All of these factors likely contributed to the inferred increase in cladogenesis of triaenonychids starting in the Cretaceous and continuing into the Paleogene (Figure 2.5), as suitable forest habitat became more fragmented and populations in turn became more isolated. This may also have contributed to our difficulty resolving relationships between many clades in our phylogeny.

Because there was limited support for relationships between genera from different landmasses, we refrained from employing any explicit biogeographic models of range evolution. Despite those limitations, we still found a few places in the tree that were well-supported and that

corresponded to divergences between taxa from different landmasses. For example, *Calliuncus* (Western Australia) and *Nuncia chilensis* (Chile), (clade 2 in Figures 2.3–2.5) had an estimated divergence time of 25–85 Mya, with a mean date of 53 Mya. As Australia and Chile were connected via Antarctica until ~35–40 Mya, when Tasmania and Antarctica separated (McLoughlin, 2001; Wei, 2004), this divergence time is consistent with the process of Gondwanan vicariance, though we cannot rule out *trans*-oceanic dispersal, as its lower age estimate post-dates continental separation by ~10 Ma. Interestingly, *Nuncia chilensis* was originally described as *Parattahia chilensis* H. Soares, 1968, making it the second species in the genus erected for the Tasmanian species *Parattahia usignata* Roewer, 1915. The similarity between *Parattahia* and *Calliuncus* was recognized by Hunt (1996), who suspected *Calliuncus* to be a junior synonym of *Parattahia* (though without explicit morphological justification). While *Parattahia chilensis* was later transferred to *Nuncia* by Maury (1990), our results bolster the hypothesis of H. Soares (1968), who recognized the affiliation between the species from Chile and Tasmania. Sampling *P. usignata* and *Calliuncus ferrugineus* Roewer 1931 (the type species of *Calliuncus*) will be useful in further clarifying the potential trans-Antarctic nature of this clade.

Nearly all divergences between taxa from different landmasses in the family were estimated to have occurred before the end of the Mesozoic (66 Mya), though the lower limits of several 95% CIs post-dated this boundary. Similarly, the majority of Gondwanan rifting events took place during the Mesozoic, from the initial split into East and West Gondwana *ca.* 170 Mya to the separation of Zealandia from East Gondwana *ca.* 80 Mya. The only major separation events that occurred in the Cainozoic were the disconnection of Australia and South America from Antarctica, which occurred ~35–40 Mya and ~30–35 Mya, respectively (McLoughlin, 2001; Wei, 2004). This underscores the idea that the common mode of range expansion and diversification in Triaenonychidae was over-land dispersal followed by subsequent isolation as continental blocks separated.

A well-known biogeographic debate exists surrounding the source of New Zealand's terrestrial biota. Briefly, the controversy suggests that following the separation of Zealandia (*i.e.* the small continent that contains New Zealand and New Caledonia (Mortimer et al., 2017)) from Australia–Antarctica *ca.* 80 Mya, New Zealand experienced a prolonged marine transgression (often called the "Oligocene drowning") (see Giribet & Boyer, 2010). This period lasted from ~36 to ~23 Mya, and at its peak (23 Mya) land area was reduced to ~18% of its current area (Cooper & Cooper, 1995; Wallis & Jorge, 2018). However, some authors have gone so far as to say the archipelago was completely inundated, which extirpated any relicts of Gondwanan origin; the implication then is that all of New Zealand's modern biota is the result of more recent dispersals that post-date 23 Mya (Trewick, Paterson, & Campbell, 2006). We find at least three clades of taxa from New Zealand whose 95% CIs completely pre-date the peak of the Oligocene drowning period: (1) The New Zealand *Nuncia* (mean age: 110 Ma; 95% CI: 83–140 Ma), (2) *Hendea* (mean age: 52 Ma; 95% CI: 29–81 Ma), and (3) a clade composed of *Sorensenella*, *Karamea*, *Algidia*, *Prasma*, *Triregia*, and the New Caledonian *Diaenobunus* and *Triconobunus* (mean age: 93 Ma; 95% CI: 71–116 Ma). Triaenonychids therefore serve as yet another source of examples refuting the hypothesis of New Zealand's total submersion during the Oligocene, as suspected by earlier workers (Giribet & Boyer, 2010).

While most divergences in the family concorded with Gondwanan vicariance or potentially pre-Gondwanan cladogenesis, there is at least one likely case of dispersal in the family: to New Caledonia. As stated previously, New Caledonia (specifically the main island of Grande Terre) is part of the small continent Zealandia, which separated from the eastern margin of Gondwana ~80 Mya (McLoughlin, 2001). Despite being part of the same crustal block, New Zealand and New Caledonia have never shared a terrestrial connection with each other. Unlike in New Zealand, where the geologic evidence for total submersion is inconclusive at best, there is strong geologic evidence that New Caledonia was submerged thousands of meters underwater during the Palaeocene, and

subsequently thrust under oceanic crust during the Eocene, finally re-emerging ~37 Mya (Cluzel, Maurizot, Collot, & Sevin, 2012; Grandcolas et al., 2008; Sutherland et al., 2020). New Caledonia is therefore functionally a Darwinian island, and accordingly, most endemic taxa that have been studied using time-calibrated molecular phylogenetics are found to have arrived to the island no earlier than 37 Mya (though see Giribet & Baker, 2019; Nattier et al., 2017). In the case of Triaenonychidae, we found both New Caledonian genera (*Diaenobunus* and *Triconobunus*) to be clearly nested within the New Zealand genus *Triregia*, which was in turn a part of a larger clade of New Zealand-endemic taxa (clade 8 in Figures 2.3–2.5). While we only had specimens of *Triconobunus* from a single locality and therefore cannot make any inferences about its origination and diversification time on the island, we did have sequence data for *Diaenobunus* from two different localities, separated by a linear distance of 16 km and constituting two putative species (although the genus remains monotypic). The estimated diversification time of *Diaenobunus* was 25 Mya (95% CI: 13–38 Mya), consistent with the idea that the genus dispersed from New Zealand and started diversifying on the island after its re-emergence ~37 Mya. While nodal supports within this clade were relatively low across all analyses, they were consistent, so if these results do reflect the true topology it implies that triaenonychids dispersed from New Zealand to New Caledonia twice. It is also worth noting that the upper limit of the 95% CI for this diversification at 38 Mya allows us to reject the hypothesis that these animals are a Gondwanan relict, as this post-dates Zealandia's split from Gondwana in the Late Cretaceous, ~80 Mya.

2.4 Conclusions

We generated the first molecular phylogeny focused on Triaenonychidae, the fourth most speciose family of Opiliones, and inferred divergence times using fossil-derived calibrations. We found that the family as traditionally defined is not monophyletic, and transferred *Lomanella* out of

Triaenonychidae, as it is the sister group to Synthetonychiidae, and this clade is not always related to the other triaenonychids. We also support *Fumontana* and *Flavonuncia* as a clade (*Buemarinoa* would be related to these, but was not sampled), which is the sister group to all other temperate Gondwanan triaenonychids. Despite low nodal support for relationships between many taxa, our results do highlight many places in which taxonomy does not reflect phylogeny, and which should therefore be revised. Complementary work by our group is already underway to resolve higher-level relationships using UCE (ultraconserved elements) sequencing (Faircloth et al., 2012). A well-resolved phylogeny of this nature will be critical for further addressing evolutionary questions in the family, such as those about morphological stasis and disparity, sexual and male dimorphism, parental care strategies, niche conservatism, and diversification dynamics through time.

Through our divergence dating analysis, we also found that Triaenonychidae is an ancient family that predates Pangaean and Gondwanan rifting, therein explaining their widespread but disjunct distribution across the Southern Hemisphere and North America and Western Europe. Indeed, nearly all divergences of taxa from different landmasses predate or coincide with Gondwanan tectonic events. However, we find at least one irrefutable case of dispersal, to the island of Grande Terre in New Caledonia. We suggest this is another example of "common vicariance and rare dispersal" in Opiliones (Hedin & McCormack, 2017). There have likely been multiple dispersal events in the family, as evidenced by their presence in the oceanic Crozet Islands and on far offshore islands in New Zealand, such as the Chatham and Auckland Islands (Enderlein, 1909; Forster, 1954). Future work will also be necessary to incorporate specimens from these islands into a phylogenetic framework so as to understand their biogeographic history and the capacity for dispersal within the family.

Chapter 3

It's the cute ones you have to watch out for: phylotranscriptomic analysis of velvet worms (phylum Onychophora) and the continued recalcitrance of Peripatidae

Caitlin M. Baker, Rebecca S. Buckman-Young, and Gonzalo Giribet

Note: Supplementary materials are included in Appendix A.

Abstract

Onychophora ("velvet worms" or "peripatus") are charismatic soil invertebrates known to biologists for their status as a "living fossil", their phylogenetic affiliation to arthropods, and their distinctive biogeographic patterns. However, several aspects of their internal phylogenetic relationships remain unresolved, limiting our understanding of the group's evolutionary history particularly with regard to changes in reproductive mode and their dispersal ability. To address these gaps, we used RNA sequencing and phylogenomic analysis of transcriptomes to reconstruct evolutionary relationships and infer divergence times within the phylum. We recovered a fully resolved and well supported phylogeny for the circum-Antarctic family Peripatopsidae, which retains signals of ancient Gondwanan vicariance and showcases the evolutionary lability of reproductive mode in the family.

Within the Neotropical clade of Peripatidae, though, we found that amino acid-translated sequence data masked nearly all phylogenetic signal, resulting in highly unstable and poorly supported relationships. Analyses using nucleotide sequence data were able to resolve many more relationships, though we still saw discordant phylogenetic signal between genes, indicative of a rapid, Late Cretaceous–early Paleogene radiation in the group. Finally, we hypothesize that the unique reproductive mode of placentotrophic viviparity within the Neotropical peripatids may have facilitated the multiple inferred instances of over-water dispersal and establishment on oceanic islands.

3.1 Introduction

Onychophora (Grube, 1853), commonly referred to as "velvet worms" or "peripatus", is a terrestrial phylum of invertebrates that lives in humid, dark microhabitats such as rotting logs, leaf litter detritus, and caves (Figure 3.1). These charismatic animals have attracted the attention of biologists for a multitude of reasons, such as their status as a "living fossil" (Ghiselin, 1984; Werth & Shear, 2014) and their unique prey-capture and defense mechanism of ejecting a glue-like substance from oral slime papillae (Benkendorff, Beardmore, Gooley, Packer, & Tait, 1999; Concha et al., 2015). They also have a striking geographic distribution, which recent work has demonstrated is largely the result of ancient Pangaean and Gondwanan vicariance (Giribet et al., 2018; Murienne, Daniels, Buckley, Mayer, & Giribet, 2014).

Onychophora are traditionally united with Arthropoda and Tardigrada in the clade Panarthropoda, one of the major lineages of Ecdysozoa (Aguinaldo et al., 1997; Giribet & Edgecombe, 2017). While the internal relationships of Panarthropoda (and even its validity) are still

Figure 3.1. Live habitus of Onychophora. (a) *Epiperipatus* sp. MCZ-131442 (Peripatidae) from Brazil (Roraima) displaying the unique prey-capture method of shooting glue out of slime glands. (b) *Macroperipatus torquatus* MCZ-143928 (Peripatidae), a placentotrophic viviparous adult female from Trinidad with recently birthed juvenile. (c) *Ooperipatellus* sp. MCZ-152165 (Peripatopsidae), an oviparous female from New Zealand with a visible ovipositor. (d) *Peripatoides novaezealandiae* MCZ-152262 (Peripatopsidae), a viviparous species endemic to New Zealand. (e) *Peripatopsis alba* (not collected; Peripatopsidae), an endangered troglobitic species endemic to South Africa. (f) *Epiperipatus* sp. MCZ-136557 (Peripatidae) from Brazil (Amazonas), a rogue taxon in our phylogenetic analyses.

actively debated (Giribet & Edgecombe, 2017; Ortega-Hernández, 2016; M. R. Smith & Ortega-Hernández, 2014), many studies have recovered Onychophora as the sister group of arthropods (Borner, Rehm, Schill, Ebersberger, & Burmester, 2014; Hejnol et al., 2009; Laumer et al., 2019; Rota-Stabelli, Daley, & Pisani, 2013). As the putative sister group to the most diverse animal phylum, their modest sum of ~180 described species (Oliveira, Read, & Mayer, 2012) raises macroevolutionary questions about the nature of morphological and genetic radiations and stasis (e.g. Lee, Soubrier, & Edgecombe, 2013). This phylogenetic position also makes them a key lineage for understanding the evolutionary development of arthropods, particularly the so-called "arthropod head problem" (Mayer, Whitington, Sunnucks, & Pfluger, 2010). But in spite of the widespread interest in onychophorans across many fields of biology, much of their basic natural history, including several aspects of the internal phylogeny, remains poorly understood (Mayer, Franke, Treffkorn, Gross, & de Sena Oliveira, 2015).

There are two extant families within Onychophora. The family Peripatidae has a circum-tropical distribution, with representatives in Southeast Asia, West Africa, and the Neotropics, the last of which holds the vast majority of the family's diversity. The other family, Peripatopsidae, has a circum-Antarctic distribution with representatives in Chile, South Africa, and Australasia (Figure 3.2). The validity of these families has previously been confirmed using Sanger DNA sequencing (Giribet et al., 2018; Murienne et al., 2014), and they are supported by a suite of morphological characters (e.g. the position of the gonopore between the penultimate pair of limbs in Peripatidae or behind the last pair of limbs in Peripatopsidae; the solubility of pigments in ethanol in Peripatidae or not in Peripatopsidae; the presence of a diastema on the inner mandible blade in Peripatidae and its absence in Peripatopsidae) (Reid, 1996).

Figure 3.2. Map showing the distribution of samples used in this analysis, colored according to geographic area and clade identity, as in Figures 3.3–3.5. Peripatidae shown in orange tones, Peripatopsidae shown in blue tones. General distributions of Peripatidae indicated by white circles with orange outlines; Peripatopsidae distribution indicated by white circles with blue outlines.

Phylogenetic relationships within these families, however, are in many cases poorly supported or unresolved, particularly within the Neotropical lineage of Peripatidae (Giribet et al., 2018; Sampaio Costa, 2016). Systematic and taxonomic work in the group is stymied by several factors. For one, despite the morphological diversity seen in stem-group onychophoran fossils (Yang et al., 2015), extant velvet worms are highly morphologically conserved, with all species sharing the same general body pattern of a head, a segmented trunk with a variable number of paired limbs, and an anal cone (Mayer et al., 2015). Because of this limited morphological disparity, taxonomy requires careful examination of characters to differentiate species, often using scanning electron microscopy (SEM) (Daniels, Dambire, Klaus, & Sharma, 2016; Oliveira, Franke, et al., 2012; Reid, 1996; Ruhberg, 1985); even so, consistent morphological differences may not be detected (e.g. Sampaio Costa, 2016; Sato, Buckman-Young, Harvey, & Giribet, 2018). Additionally, a number of monotypic genera have been erected on the basis of autapomorphic characters, but these species have subsequently been found to nest within other genera (Giribet et al., 2018). In the case of one genus

(*Macroperipatus*), its diagnostic trait is even suspected to be an artefact of fixation in ethanol for at least some of its constituent described species (Oliveira, Wieloch, & Mayer, 2010).

The application of molecular data to onychophoran systematics has been revolutionary, providing increased phylogenetic resolution, particularly within Peripatopsidae, and elucidating a large number of cryptic species (Allwood et al., 2010; Briscoe & Tait, 1995; Bull et al., 2013; Daniels et al., 2016; Daniels, Picker, Cowlin, & Hamer, 2009; Giribet et al., 2018; Gleeson, Rowell, Tait, Briscoe, & Higgins, 1998; Murienne et al., 2014; Oliveira & Mayer, 2017; Oliveira, Ruhberg, Rowell, & Mayer, 2018; Oliveira et al., 2013; Sato et al., 2018; Tait & Briscoe, 1995; Trewick, 1998, 2000). However, onychophorans have notoriously challenging molecular characteristics, with extremely large nuclear genomes that are suspected to contain a lot of repetitive elements (Jeffery, Oliveira, Gregory, Rowell, & Mayer, 2012), low GC content (Mora, Herrera, & León, 1994), highly variable mitochondrial genomes showing gene rearrangements and pseudogenes (Braband, Cameron, Podsiadlowski, Daniels, & Mayer, 2010; Braband, Podsiadlowski, Cameron, Daniels, & Mayer, 2010; Podsiadlowski, Braband, & Mayer, 2008), and novel insertions in variable regions of 18S rRNA (Giribet & Wheeler, 2001). Together, these factors make the generation of large, multilocus PCR-based Sanger sequencing datasets onerous as many universal primers do not amplify and many data sets have considerable amounts of missing data, which contributes to the limited resolution in the group.

To add to these challenges, the animals themselves, with a few notable exceptions, are hard to find, as they live in cryptic environments and in most places exhibit low population densities (Daniels et al., 2016). As such, gathering enough specimens to diagnose inter- or intraspecific differences, or to comprehensively sample across their known geographic and taxonomic spectrum, requires extensive collecting efforts.

Over the past decade, we have been fortunate enough to collect and receive donations of onychophoran tissues suitable for RNA sequencing from nearly all the major landmasses from which they are known (Figure 3.2). Transcriptome sequencing is particularly promising for the study of onychophoran systematics because it circumvents the limitations of PCR amplification to generate large amounts of sequence data for each individual. Furthermore, as a reduced-representation genomic sequencing method, it bypasses the need to sequence the extremely large and presumably repetitive nuclear genomes of onychophorans, and its implementation requires no prior genomic knowledge. Given that transcriptome sequencing has successfully resolved evolutionary relationships across the animal tree of life (Dunn et al., 2008; Kocot et al., 2017; Laumer et al., 2019; Rota-Stabelli et al., 2013), and within Arthropoda in particular (Fernández, Edgecombe, & Giribet, 2018; Lozano-Fernandez et al., 2019; Misof et al., 2014; Schwentner, Combosch, Pakes Nelson, & Giribet, 2017; Sharma et al., 2018), we therefore sequenced transcriptomes of species from both families of Onychophora in an attempt to clarify evolutionary relationships and biogeographic patterns in the phylum, particularly within the Neotropical clade of Peripatidae—a clade known as Neopatida.

3.2 Methods

3.2.1 Sample collection and molecular methods

Specimens of 25 onychophorans, representing eight peripatopsids and 17 peripatids, were newly sequenced for this study. Additionally, we included six onychophorans from previously published studies, all of which were downloaded from the NCBI Sequence Read Archive (SRA) (Table 3.1). Sampling within Peripatopsidae covered all major landmasses from which they are known, with the exception of New Guinea (and some outlying islands) and Tasmania. Sampling within Peripatidae was restricted to the Neotropics (i.e. Neopatida, *sensu* Oliveira et al., 2016), as we did not have RNA-

Table 3.1. Collection and accession information for onychophoran specimens used in this study. Newly sequenced samples are shown in bold. M3 refers to matrix 3 (see Table 3.2). BUSCO completeness scores are for the Metazoa database.

Species	Catalog no.	SRA number	Country	BUSCO	Loci in M3	Latitude	Longitude	Source
Family Peripatidae								
Epiperipatus sp.	MCZ-136557	SRR8627713	Brazil (Amazonas)	38.45%	993	-2.9295	-59.9756	Laumer et al. 2019
Peripatidae sp.	**MCZ-141132**		**Brazil (Mato Grosso)**	**42.02%**	**844**	**-15.4488**	**-55.7727**	**this study**
***Epiperipatus* sp.**	**MCZ-141131**		**Brazil (Rio de Janeiro)**	**42.84%**	**947**	**-22.4101**	**-42.7355**	**this study**
Peripatidae sp.	**MCZ-141458**		**Colombia**	**68.61%**	**1016**	**5.8806**	**-73.0640**	**this study**
Macroperipatus valerioi	**MCZ-130841**		**Costa Rica**	**39.78%**	**962**	**9.4885**	**-83.9568**	**this study**
Macroperipatus valerioi	**MCZ-130842**		**Costa Rica**	**14.83%**	**436**	**9.4838**	**-83.9396**	**this study**
Peripatus solorzanoi	**MCZ-130840**		**Costa Rica**	**40.18%**	**829**	**9.6731**	**-83.0243**	**this study**
***Oroperipatus* sp.**	**MCZ-133614**		**Galapagos**	**9.82%**	**410**	**-0.6249**	**-90.3855**	**this study**
***Peripatus* sp.**	**MCZ-46445**		**Guyana**	**10.53%**	**617**	**4.1514**	**-58.2146**	**this study**
Oroperipatus eisenii	**MCZ-74293**		**Mexico**	**46.63%**	**836**	**21.4794**	**-105.0776**	**this study**
Epiperipatus* cf. *edwardsii	**MCZ-49455**		**Panama**	**14.01%**	**725**	**8.7916**	**-78.4524**	**this study**
Epiperipatus sp.	MCZ-141126	SRR8320992	Panama	77.61%	936	8.7467	-82.4189	Mapalo et al. 2020
Epiperipatus vagans	**MCZ-141130**		**Panama**	**67.48%**	**1046**	**9.0836**	**-79.6632**	**this study**
Peripatidae sp.	**MCZ-141128**		**Panama**	**64.72%**	**904**	**8.4332**	**-82.4519**	**this study**
Peripatus juanensis	**MCZ-133571**		**Puerto Rico**	**6.65%**	**579**	**18.1720**	**-67.0445**	**this study**
Peripatus juanensis	**MCZ-133572**		**Puerto Rico**	**9.61%**	**658**	**18.3232**	**-65.8155**	**this study**
Epiperipatus broadwayi	**MCZ-143935**		**Trinidad & Tobago (Tobago)**	**67.69%**	**975**	**11.2869**	**-60.6101**	**this study**
Epiperipatus trinidadensis	**MCZ-143926**		**Trinidad & Tobago (Trinidad)**	**69.02%**	**1048**	**10.7051**	**-61.2898**	**this study**
Macroperipatus torquatus	**MCZ-143928**		**Trinidad & Tobago (Trinidad)**	**62.78%**	**1013**	**10.7459**	**-61.2554**	**this study**
Family Peripatopsidae								
Euperipatoides kanangrensis	**MCZ-131395**		**Australia (NSW)**	**16.87%**	**178**	**-33.9833**	**150.1333**	**this study**
Peripatopsidae sp.	**MCZ-141470**		**Australia (QLD)**	**61.25%**	**898**	**-27.3917**	**152.9236**	**this study**
Peripatopsidae sp.	**MCZ-141416**		**Australia (QLD)**	**67.28%**	**1008**	**-24.4130**	**151.0387**	**this study**
Kumbadjena occidentalis	**MCZ-141468**		**Australia (WA)**	**42.43%**	**551**	**-33.9078**	**115.0136**	**this study**
Occiperipatoides gilesii	**MCZ-141469**		**Australia (WA)**	**48.16%**	**846**	**-31.8667**	**116.0667**	**this study**
Metaperipatus inae	**MCZ-138078**		**Chile**	**75.87%**	**1037**	**-38.0163**	**-73.1790**	**this study**
Ooperipatellus viridimaculatus	MCZ-29203	SRR8627697	New Zealand	33.23%	708	-44.4876	168.7874	Laumer et al. 2019
Peripatoides aurorbis	MCZ-29204	SRR8627695	New Zealand	47.24%	867	-37.8419	174.7734	Laumer et al. 2019
Opisthopatus kwazululandi	MCZ-131434	SRR8318947	South Africa	82.62%	1025	-24.9370	31.3752	Mapalo et al. 2020
Opisthopatus highveldi	**MCZ-131328**		**South Africa**	**21.17%**	**257**	**-28.7442**	**31.1376**	**this study**
Peripatopsis bolandi	**MCZ-49527**		**South Africa**	**79.75%**	**1005**	**-34.0047**	**18.9944**	**this study**
Peripatopsis overbergiensis	MCZ-131372	SRR1145776	South Africa	51.94%	963	-33.9819	20.8231	Sharma et al. 2014

quality material from the monotypic genus *Mesoperipatus* from West Africa or from the Southeast Asian genera *Typhloperipatus* (monotypic) and *Eoperipatus* (with four described species).

Transcriptomes of the following taxa were downloaded as raw data from SRA or as assemblies in Dryad and used as ecdysozoan outgroups: a priapulan (*Priapulus caudatus*) (Kocot et al., 2017), a nematomorph (*Nectonema munidae* [SRR8618616]) (Laumer et al., 2019), two tardigrades (*Echiniscus testudo* [SAMN10601501–SAMN10601521] (Mapalo et al., 2020), *Hypsibius dujardini* (Yoshida et al., 2017)), and three arthropods (*Scutigera coleoptrata* [SRR1158078] (Fernández et al., 2014), *Limulus polyphemus* [SRR1145732] (Sharma et al., 2014), and *Anoplodactylus insignis* [SRR5237777] (Fernández, Edgecombe, & Giribet, 2016)). Information on sampling localities and accession numbers for onychophorans used in this study are included in Table 3.1. Specimens were initially preserved in RNA*later* and later flash frozen in liquid nitrogen and stored at –80ºC. All newly sequenced specimens from this study are deposited in the Invertebrate Zoology collection of the Museum of Comparative Zoology (MCZ), Harvard University and can be accessioned through the online portal MCZbase (https://mczbase.mcz.harvard.edu). Illumina sequencing of transcriptomes followed the protocols of Baker, Boyer, and Giribet (2020), with all samples sequenced as 150bp paired-end reads on an Illumina HiSeq 2500 at the Bauer Core Facility at Harvard University.

3.2.2 Data sanitation and orthogroup inference

Quality filtering, trimming of reads, and strand-specific assembly of transcriptomes largely followed the methods of Baker et al. (2020). mRNA contigs were translated from nucleotide sequences to amino acid sequences with TransDecoder v 3.0 (Haas et al., 2013), and predicted peptide (.pep) files were filtered to select only one peptide per putative gene by choosing the longest open reading frame (ORF) using a Python script from Laumer, Hejnol, and Giribet (2015). Due to limited phylogenetic signal within Neopatida, we also ran additional analyses for this clade using the coding

sequences (.cds) produced in TransDecoder, again selecting only one sequence per orthogroup by choosing the longest ORF. The completeness of each assembly was evaluated with BUSCO by comparison with the Metazoa database (Simão, Waterhouse, Ioannidis, Kriventseva, & Zdobnov, 2015).

Orthologous genes were predicted across all samples, for both amino acid and codon datasets, using the all-by-all graph-based clustering method Orthologous Matrix Algorithm, OMA standalone v 2.2.0 (Altenhoff et al., 2018). Each OMA-generated amino acid (AA) orthogroup was aligned individually with MAFFT v 7.309 (Katoh & Standley, 2014). To reduce alignment uncertainty, we also ran Zorro (Wu, Chatterji, & Eisen, 2012) on each aligned orthogroup, discarding all sites with a probability score below 5. For the codon-level orthogroups, each locus was aligned individually using the reading frame-aware aligner MACSE v 2.03 (Ranwez, Harispe, Delsuc, & Douzery, 2011), specifying the standard genetic code and discarding all stop codons at alignment ends. All orthogroups that contained frameshifts or that lacked parsimony informative sites were excluded from downstream analyses. To reduce alignment uncertainty of the codon-level orthogroups, we used the trimAlignment function of MACSE to remove alignment ends until at least 30% of sequences included nucleotide data at that site.

Table 3.2. Information on matrices used for phylogenetic inference. See section 3.2.2 for details.

	Orthogroups	Sites	Description
Matrix 1	1,032	257,477	50% occupancy, AA, Ecdysozoan outgroups
Matrix 2	181	41,491	75% occupancy, AA, Ecdysozoan outgroups
Matrix 3	1,219	311,947	50% occupancy, AA, Onychophora only
Matrix 4	290	67,345	75% occupancy, AA, Onychophora only
Matrix 5	1,147	931,677	50% occupancy, DNA, Peripatidae only
Matrix 6	160	114,561	75% occupancy, DNA, Peripatidae only
Matrix 7	1,107	871,881	Homogeneous orthogroups from M5
Matrix 8	689	570,657	Fastest and slowest 20% of orthogroups excluded from M5

3.2.3 Matrix construction

We constructed a series of data matrices to accommodate different potential systematic biases (Table 3.2). Matrices 1 and 2 corresponded to amino acid orthogroup matrices containing all onychophorans and outgroup taxa with 50% and 75% taxon occupancy, respectively. Taxon occupancy was defined as the orthogroups present in at least that percentage of taxa. To minimize the potential effect of long-branch attraction, we created matrices 3 and 4 by removing all non-onychophoran taxa and including orthogroups with 50% and 75% taxon occupancy, respectively.

Because of the limited phylogenetic signal in our data for Peripatidae—something also seen with earlier Sanger-based data—we also constructed a series of matrices using the untranslated amino acid sequences from TransDecoder (see above). Matrices 5 and 6 contained only the samples in Peripatidae (i.e. all the Neotropical specimens) and orthogroups with 50% and 75% taxon occupancy, respectively. We further refined matrix 5 (50% taxon occupancy in Peripatidae, DNA sequence data) by performing a chi-square test of compositional homogeneity in the program BaCoCa (Kuck & Struck, 2014) and removing all loci with a p-value < 0.99 (matrix 6). Finally, we removed the fastest- and slowest-evolving 20% loci from matrix 5 so as to account for the potential biasing effect of extreme evolutionary rates (matrix 7). Evolutionary rate was calculated in the program TrimAl (Capella-Gutiérrez, Silla-Martínez, & Gabaldón, 2009). Selected orthogroups were concatenated into matrices using Phyutility (S. A. Smith & Dunn, 2008) for subsequent phylogenetic analysis.

3.2.4 Phylogenetic analysis

For all matrices we performed a series of phylogenetic analyses, covering maximum likelihood (ML), Bayesian inference (BI), and species tree methods. ML tree searches were performed in IQ-TREE-MPI v 1.6.10 (Nguyen, Schmidt, von Haeseler, & Minh, 2015). For the amino acid matrices (M1–

M4), we used the ML implementation of the Bayesian CAT model, a non-partitioned analysis that included the 10–60 class profile mixture models, as well as model and partition selection tests in ModelFinder (-m MFP+MERGE) (Kalyaanamoorthy, Minh, Wong, von Haeseler, & Jermiin, 2017). For the untranslated DNA sequence matrices (M5–M8), analyses were partitioned by orthogroup (Chernomor, von Haeseler, & Minh, 2016), specifying codon models. Model and partition testing were performed using ModelFinder, and each partition was allowed its own set of branch lengths to account for heterotachy (-sp flag). For all ML analyses, nodal support was assessed using 1500 ultrafast bootstrap replicates (Hoang, Chernomor, von Haeseler, Minh, & Vinh, 2018). BI tree searches were run in ExaBayes 1.5 (Aberer, Kobert, & Stamatakis, 2014) using two runs of two chains and up to 5 million generations, until the average standard deviation of split frequencies was below 5%. A consensus of both runs was created, discarding the first 25% of trees as burn-in. We also used ASTRAL 4.10.12 (Mirarab et al., 2014) as a concatenation-free species tree inference method. Individual gene trees for ASTRAL input were generated in RAxML for M1–M4, using the model selection feature PROTGAMMAAUTO, and in IQ-TREE for M5–M8, using ModelFinder for codon models. Finally, we performed a BI analysis on M4 and M6 in PhyloBayes-MPI v 1.7a (Lartillot, Rodrigue, Stubbs, & Richer, 2013) using the CAT+GTR site-heterogeneous mixture model. PhyloBayes was only run on these matrices due to computational limitations, as they represent some of the smallest matrices constructed from AA and codon sequence data, respectively. For each matrix, two chains were run in parallel until at they reached convergence, assessed using the bpcomp and tracecomp commands, and discarding the first 25% of trees as burn-in.

Due to the inconsistent placement of the Amazonian *Epiperipatus* sp. (MCZ-136557), we performed additional analyses to explore the strength of support for different topologies within Neopatida. First, we visualized incongruence between the ML gene trees computed in IQ-TREE

using the program SuperQ v 1.1 (Grünewald, Spillner, Bastkowski, Bogershausen, & Moulton, 2013), which breaks down gene trees into quartets and generates "supernetworks" in which edge lengths are scaled according to quartet frequencies (that is, longer lines indicate stronger support for a bipartition across a set of gene trees). We generated a supernetwork for M5 and visualized the resulting NEXUS file in SplitsTree v 4.14.2 (Huson & Bryant, 2006), filtering out the two specimens of *Oroperipatus* for visual clarity.

Additionally, we performed a quartet likelihood mapping analysis (Strimmer & von Haeseler, 1997) as implemented in IQ-TREE to interrogate whether the orthogroups in M5 were capable of resolving the position of the specimen from Amazonas. Clusters were defined as follows: (1) Trinidad & Tobago (*Macroperipatus torquatus*, *Epiperipatus trinidadensis*, *Epiperipatus broadwayi*); (2) Amazonas (*Epiperipatus* sp. MCZ-136557); (3) Puerto Rico–Guyana–Brazil (both specimens of *Peripatus juanensis*, *Peripatus* sp. MCZ-46445, *Epiperipatus* sp. MCZ-141131, and Peripatidae sp. MCZ-141132); (4) Central America (*Epiperipatus vagans*, *Epiperipatus* cf. *edwardsii*, *Epiperipatus* sp. MCZ-141126, *Peripatus solorzanoi*, Peripatidae sp. MCZ-141128, and both specimens of *Macroperipatus valerioi*). All other terminals were ignored, and all available quartets were mapped.

Data sanitation, transcriptome assembly, orthogroup inference, and all phylogenetic analyses were run on the Odyssey and Cannon clusters, supported by the FAS Division of Science, Harvard University.

3.2.5 Molecular dating

To estimate the timing of divergences within Onychophora and interpret its biogeographic history, we performed a molecular divergence dating analysis in PhyloBayes v 4.1 (Lartillot, Lepage, & Blanquart, 2009). We used this program as it can accommodate genomic-scale data, which is facilitated by the use of a fixed guide tree. For the input tree, we used the topology recovered from

PhyloBayes analysis of M4 to specify ingroup relationships, and the topology of the outgroups was constrained to match the result of IQ-TREE analysis of M1. We used the alignment of M2 to infer branch lengths, as it was the smallest and most complete matrix that included Ecdysozoan outgroups, where we placed several calibrations based on fossil specimen ages, and to minimize the effect of missing data on branch length inference.

We constrained the following outgroup nodes, all of which followed the recommendations of Wolfe, Daley, Legg, and Edgecombe (2016): (1) the Priapulida–Nematomorpha split was set to a maximum age of 636 Ma (corresponding to the maximum age of the Lantian biota) and a minimum age of 529 Ma (the age of strata containing *Rusophycus* trace fossils). (2) The Arthropoda–Onychophora divergence was constrained to a minimum age of 529 Ma with no maximum age, again corresponding to the age of *Rusophycus*. (3) The Mandibulata–Chelicerata split (i.e. crown Arthropoda) was set to a minimum age of 514 Ma based on the age of *Yicaris dianensis*, and no maximum age was set. (4) The Pycnogonida–Euchelicerata split (i.e. Chelicerata) was set to a minimum age of 509 Ma, corresponding to the age of the shale in which *Wisangocaris barbarahardyae* is found. All calibrations were set under uniform priors so as to be as uninformative as possible. Additionally, we constrained the maximum age of Onychophora to be 300 Ma with no minimum, again under a uniform distribution. The oldest onychophoran fossil, *Antennipatus montceauensis*, is from the Montceau-Les-Mines Lagerstätte, which dates to the Stephanian (the European stage of the Gzhelian, upper boundary of 299 Ma) (Garwood et al., 2016). However, the fossil lacks any features that would allow one to assign it to stem-group Onychophora, stem-group Peripatidae, stem-group Peripatopsidae, or crown-group Peripatidae or Peripatopsidae. As such, we conservatively treated it as a stem-group onychophoran (following the strategy of Giribet et al., 2018), thereby requiring the group to be younger than its age. Finally, we constrained Peripatidae to a minimum age of 100 Ma

with no maximum, reflecting the age of the peripatid fossil *Cretoperipatus burmiticus* from Burmese amber (Grimaldi, Engel, & Nascimbene, 2002; Oliveira et al., 2016).

Divergence times were estimated under an autocorrelated lognormal clock and implementing the site-heterogeneous CAT+GTR model. Four independent chains were run for 5736–7839 cycles, with convergence and stationarity assessed using the tracecomp command of PhyloBayes.

3.3 Results and discussion

3.3.1 Phylogenetic relationships of Peripatopsidae

We recovered the monophyly of Onychophora, as well as the reciprocal monophyly of both families, with full support across all analyses (Figure 3.3). This result is consistent with previous analyses based on Sanger sequencing data that included non-onychophoran outgroups (Giribet et al., 2018; Murienne et al., 2014). We also recovered Arthropoda as the sister group to Onychophora with high support in all but one analysis (IQ-TREE analysis of M2, which recovered Onychophora + Tardigrada to the exclusion of Arthropoda) (Figure A.1).

Within Peripatopsidae, we recovered a well-supported and stable topology across our analyses (Figure 3.3). The family was composed of two main clades, one of which contained taxa from South Africa and Chile, and the other from Australia and New Zealand, again in line with results of previous studies (Giribet et al., 2018; Murienne et al., 2014; Oliveira et al., 2018).

The clade corresponding to South Africa and Chile found a monophyletic South Africa (*Opisthopatus* and *Peripatopsis*) to the exclusion of *Metaperipatus* from Chile in all but one analysis. The deviant result (ASTRAL analysis of M2) instead recovered a sister-group relationship between *Metaperipatus* and *Peripatopsis*, albeit with marginal support (Figure A.2). Our main tree topology contradicts the results of previous studies that have included all three of these genera, all of which recovered *Peripatopsis* + *Metaperipatus*, though with variable support (61% bootstrap support [BS] in

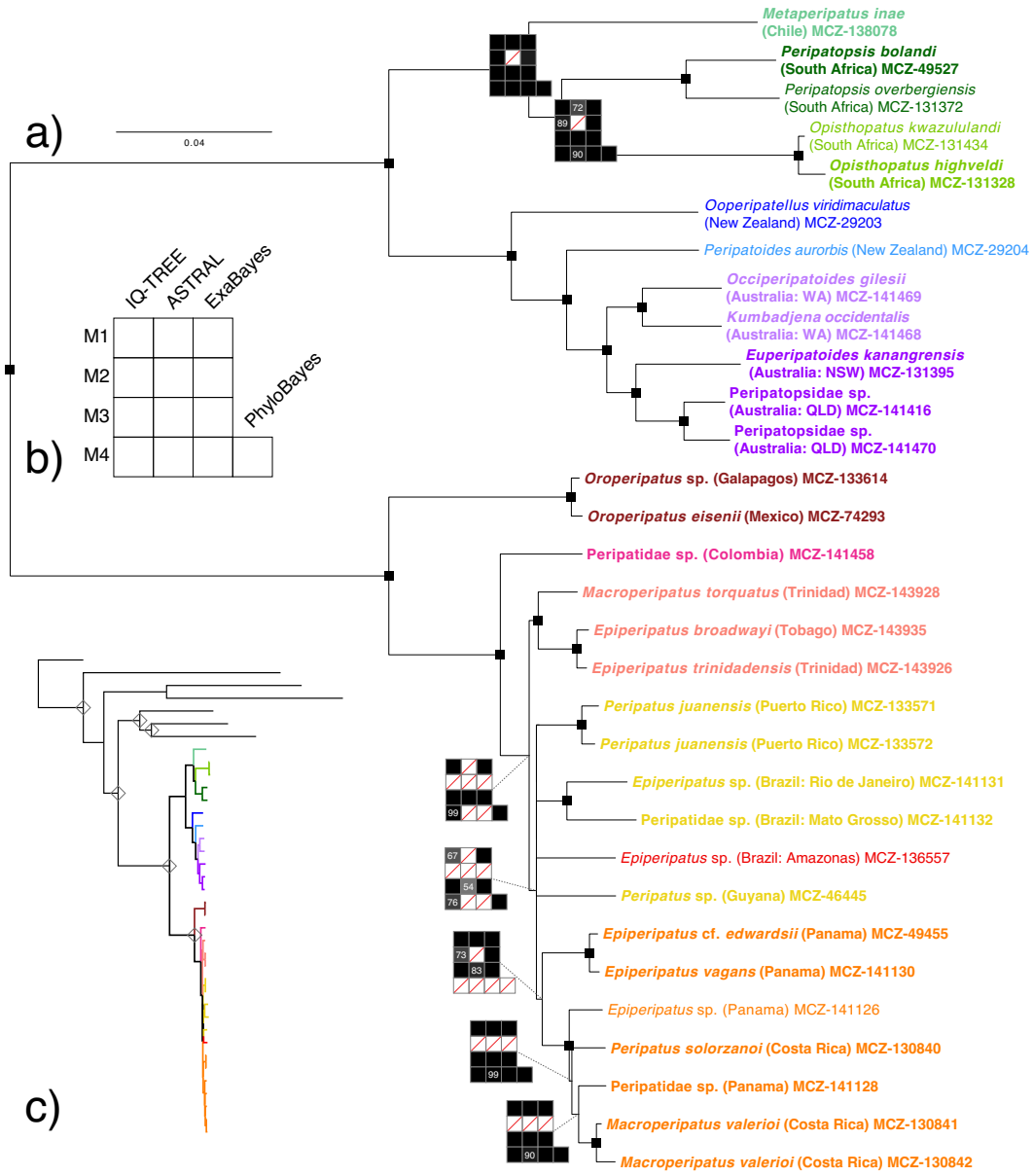

Figure 3.3. (a) Phylogeny of Onychophora inferred from M3 in IQ-TREE (amino acid sequence data). Terminals colored according to geographic area and clade identity, as in Figure 3.2 (Peripatopsidae in blue tones, Peripatidae in orange tones). Small black squares indicate nodes that were recovered in all analyses with strong support (IQ-TREE and ASTRAL > 90, ExaBayes and PhyloBayes > 0.95). Nodes that were recovered in fewer than 50% of analyses are collapsed. Support plots are drawn at nodes recovered in > 50% of analyses but which did not receive high support across all analyses. White squares with red lines through them indicate node was not recovered in that analysis. (b) Explanation of support plot, as shown in (a). (c) Outline of full phylogeny, including outgroups. Ingroup branches colored as in (a). Grey diamonds show the locations of calibrated nodes in the divergence dating analysis.

Allwood et al. (2010); 0.52 posterior probability [PP] in Murienne et al. (2014); 84% BS in Giribet et al. (2018)). Because we recovered the grouping of *Opisthopatus* + *Peripatopsis* with high support in nearly all our analyses, we therefore trust that relationship and interpret previous confidence of South African paraphyly to be overstated and the result of limited character sampling. However, we note that we were unable to include representatives of the monotypic Chilean genus *Paropisthopatus*, which has been hypothesized to be closely related to *Opisthopatus* (Daniels et al., 2016), and as such these results could change with the inclusion of that lineage. Notably, all members of this clade utilize the reproductive mode of matrotrophic viviparity, a potential synapomorphy for the group (though this is also found in the genus *Paraperipatus*, from New Guinea; see below for comment on this genus) (Mayer et al., 2015).

Within the Australian and New Zealand clade, the first lineage to diverge was recovered as *Ooperipatellus*, an oviparous genus found in both New Zealand and Tasmania. Previous studies have demonstrated that within this genus, the taxa from those landmasses are reciprocally monophyletic with strong support (Giribet et al., 2018; Murienne et al., 2014; Oliveira & Mayer, 2017). The viviparous[1] New Zealand-endemic genus *Peripatoides* was recovered as the next lineage to diverge in our analyses. Similar to *Ooperipatellus*, previous phylogenetic analyses found that *Peripatoides* is closely related to a suite of viviparous taxa from Tasmania (*Diemenipatus*, *Leucopatus*, *Tasmanipatus*) with strong support (Giribet et al., 2018; Murienne et al., 2014; Oliveira et al., 2018). Interestingly, Murienne et al. (2014) and Giribet et al. (2018) recovered these two *trans*-Tasman Sea clades as each other's sister group (0.99 PP in the former, 71% BS in the latter); however, Oliveira and Mayer

[1] Oliveira et al. (2018) noted that the use of the term "ovoviviparous" within Peripatopsidae is an oversimplification, as it encompasses several different reproductive modes including matrotrophic viviparity (in which the eggs have little or no yolk and the mother provides nutrients to embryos, though not via a placenta), lecithotrophic viviparity (in which the eggs contain substantial amounts of yolk and the mother does not provide nutrients to embryos), and combined matrotrophic and lecithotrophic viviparity (eggs have yolk, but mother provides additional nourishment). In the absence of detailed studies of embryonic development in most species, we use the generic term "viviparous".

(2017) and Oliveira et al. (2018) recovered *Ooperipatellus* as the sister group to a clade of mainland Australian taxa with low support. Our results unequivocally contradict all of these studies, placing *Peripatoides* (and presumably the viviparous genera from Tasmania) as the sister group to a clade of taxa from mainland Australia.

In the clade from mainland Australia, we found a division between taxa from Western Australia and Eastern Australia. The two genera from Western Australia (*Kumbadjena* and *Occiperipatoides*), both of which are viviparous, formed a clade, a relationship that has been found in many previous analyses based on molecular and morphological data (Giribet et al., 2018; Murienne et al., 2014; Oliveira & Mayer, 2017; Oliveira et al., 2018; Reid, 1996). We also recovered a monophyletic group of taxa from Eastern Australia, which was represented in our phylogeny by three specimens. Of these, two (*Euperipatoides kanangrensis* and Peripatopsidae sp. MCZ-141470) were viviparous, and the other (Peripatopsidae sp. MCZ-141416) was oviparous. Eastern Australia is home to a great diversity of velvet worms, currently organized into 36 genera with 41 species total, and as such our sampling is far from comprehensive (Reid, 1996). Despite those limitations, our results underscore the evolutionary lability of reproductive mode in Peripatopsidae (Mayer et al., 2015; Oliveira & Mayer, 2017). They also highlight the promise of using transcriptomics to sort out the taxonomy in this group so as to better characterize the full extent of Australian peripatopsid diversity. Finally, while we lack representatives of the genus *Paraperipatus* from New Guinea and Indonesia, this genus was found to be the sister group to all other peripatopsids from Australia and New Zealand in Giribet et al. (2018) with 100% BS. It therefore is likely that this genus would come out as the first diverging lineage in the Australia–New Zealand clade, before *Ooperipatellus*, though future work should test this hypothesis should tissue suitable for RNA sequencing become available.

3.3.2 Phylogenetic relationships in Peripatidae

Our sampling within Peripatidae was restricted to the Neotropical clade (Neopatida). However, previous phylogenetic studies have demonstrated that the first two divergences within the family correspond to *Eoperipatus* (from Southeast Asia), followed by *Mesoperipatus* (from West Africa), which is then sister group to the diverse clade of Neopatida (Giribet et al., 2018; Murienne et al., 2014). No phylogenetic analysis has yet included the Indian genus *Typhloperipatus*, but this has been proposed to be related to the other Southeast Asian genus (Oliveira et al., 2016). Despite sequencing over 80 Neopatida specimens from across an extensive geographic range, Giribet et al. (2018) found the evolutionary relationships within this clade to be extremely poorly supported, with a few exceptions. They were able to recover the monophyly of taxa from specific islands or smaller continental areas (e.g. Jamaica [100% BS], Trinidad & Tobago [99% BS], Puerto Rico [97% BS], certain species from Costa Rica and Panama [97% BS]), but relationships between those areas were poorly supported (BS 24%–79%). Additionally, they found strong support for an initial divergence in Neopatida between *Oroperipatus* (from west of the Andes, including the Galapagos, and into Mexico) and the rest of the group, followed by a split between a clade from Colombia and Ecuador and the remaining taxa (from Central America, the Caribbean, and South America east of the Andes, hereafter the "Eastern clade"). The recalcitrance of this Eastern clade has been noted by many previous authors as well (Cunha et al., 2017; Murienne et al., 2014; Oliveira, Lacorte, Fonseca, Wieloch, & Mayer, 2011; Oliveira et al., 2014; Sampaio Costa, 2016).

Unfortunately, our results only moderately improved resolution in this group. Analyses of amino acid data (M1–M4) were stunningly inconsistent, recovering nine distinct topologies for the 19 taxa across 13 treatments, usually with low support (Figure 3.3, Figures A.2–A.14). There were some consistently well-supported relationships: we found the same three clades of Neopatida as in Giribet et al. (2018), corresponding to (1) *Oroperipatus*, (2) a lineage from the Colombian Andes (here

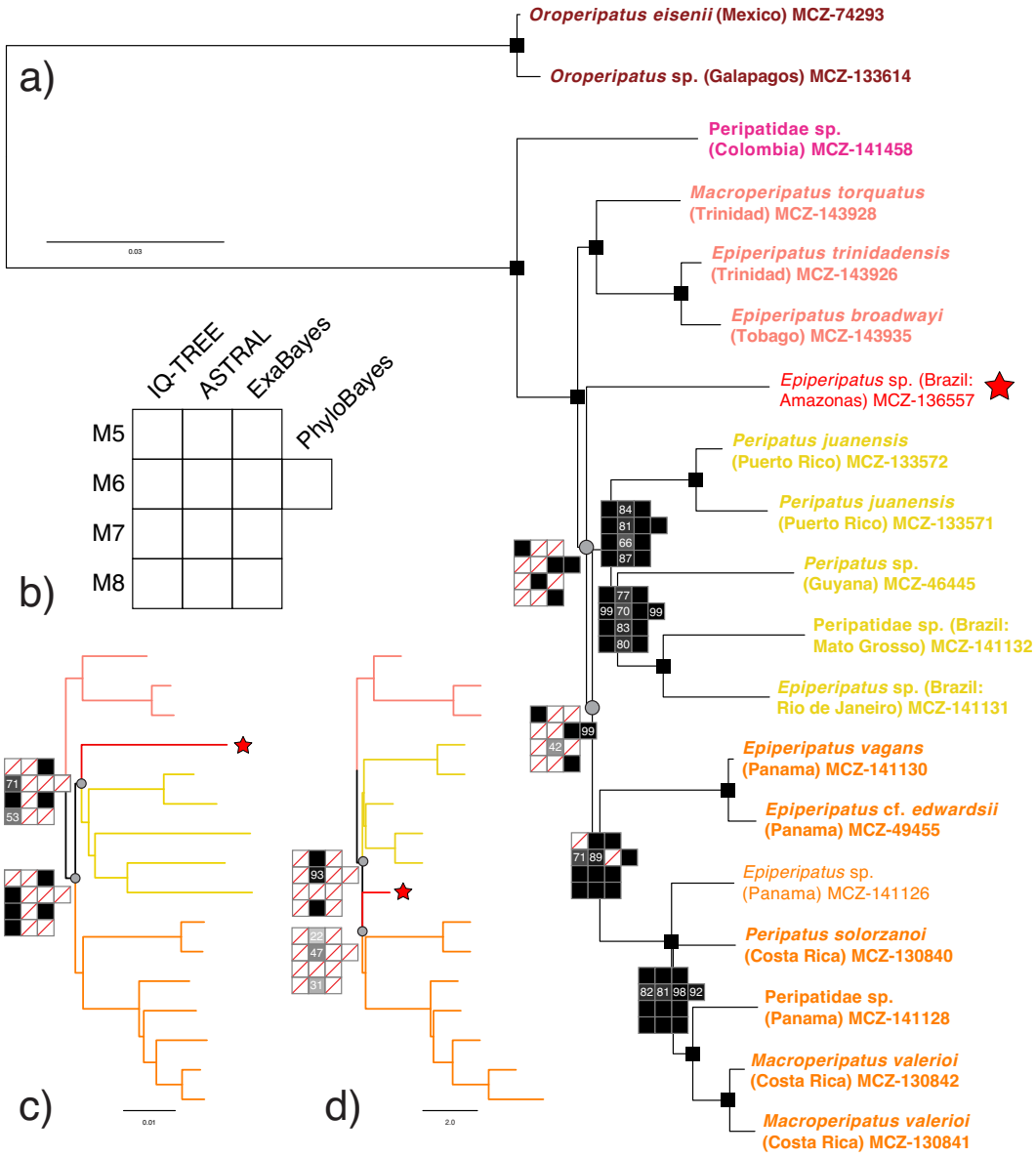

Figure 3.4. (a) Phylogeny of Neopatida inferred from M6 in PhyloBayes (codon sequence data). Small black squares indicate nodes that were recovered in all analyses with strong support (IQ-TREE and ASTRAL > 90, ExaBayes and PhyloBayes > 0.95). Terminals colored by clade identity, as in Figures 3.2 and 3.3: *Oroperipatus* (dark red); Colombia (hot pink); Trinidad & Tobago (salmon); Amazonas (red); Puerto Rico–Guyana–Brazil (yellow); Central America (orange). Support plots are drawn at nodes that did not receive high support across all analyses, as in Figure 3.3. Red star denotes the rogue taxon *Epiperipatus* sp. (MCZ-136557) from Amazonas. Grey circles drawn at node leading to the specimen from Amazonas and the clade of composed of (Amazonas + Central America + Puerto Rico–Guyana–Brazil). (b) Explanation of nodal support plot, as shown in (a), (c), and (d). (c, d) Alternative topologies of Neopatida showing different possible placements of the sample from Amazonas. Branch colors, support plots, red star, and grey circles as in (a). Topology of (c) derived from ExaBayes analysis of M5; topology of (d) derived from ASTRAL analysis of M5.

represented by a single species), and (3) the Eastern clade (from Central America, the Caribbean, and the rest of South America). Within the Eastern clade, we also recovered the monophyly of taxa from specific geographic areas, such as Trinidad and Tobago, Puerto Rico, and Central America, and in seven of the 13 treatments, the taxa from Trinidad and Tobago were recovered as the sister group to all other members. But beyond that, very few relationships could be discerned with any confidence.

We then generated a third set of matrices that contained only the peripatid taxa. The average pairwise identity of the recovered amino acid orthogroups was very high (94.5%), suggesting that the observed incongruence in this clade could be due to limited phylogenetic signal. We therefore went back to the untranslated nucleotide sequences to perform additional analyses, believing they would harbor increased signal (Figure 3.4, Figures A.15–A.27). This approach yielded better resolution, universally recovering the clade from Trinidad and Tobago (colored in salmon in Figure 3.4) as the sister group to the remaining members of the Eastern clade with full support. We also found support for a clade of taxa from the Brazilian Cerrado (MCZ-14132) and Atlantic Rainforest (MCZ-131131), Guyana (MCZ-46445), and Puerto Rico (MCZ-133572 and MCZ-133571) across all treatments (yellow in Figure 3.4). A clade from Central America (specimens from Costa Rica and Panama) was recovered in 11 out of 13 analyses, a relationship we also recovered in eight out of 13 analyses with M1–M4 (orange in Figure 3.4). However, a specimen of *Epiperipatus* from Amazonas (MCZ-136557, pictured in Figure 3.1f, colored in red and denoted by a star in Figure 3.4) was highly unstable, coming out either as the sister group to the Central American and Puerto Rico–Guyana–Brazil clades (Figure 3.4a), the sister group to the Puerto Rico–Guyana–Brazil clade alone (Figure 3.4c), or else the sister group to the Central American clade alone (Figure 3.4d), each with variable support.

3.3.3 Interrogating the position of *Epiperipatus* sp. from Amazonas

Given the instability of *Epiperipatus* sp. from Amazonas, we performed a quartet likelihood mapping analysis using all the orthogroups in M5 to determine whether our data were capable of resolving between these three different phylogenetic hypotheses (Figure 3.5). We found that almost all quartets (99%) showed strong resolving power (i.e. fell in one of the corners of the triangle), and a slight majority (50.5%) supported a topology in which the specimen from Amazonas was the sister group to the Central American and Puerto Rico–Guyana–Brazil clades (Q2, consistent with the topology of Figure 3.4a). However, one third of the quartets instead supported the topology of Figure 3.4c, in which the Amazonas specimen was the sister group to only the clade from Puerto Rico–Guyana–Brazil, obfuscating any clear placement for this species.

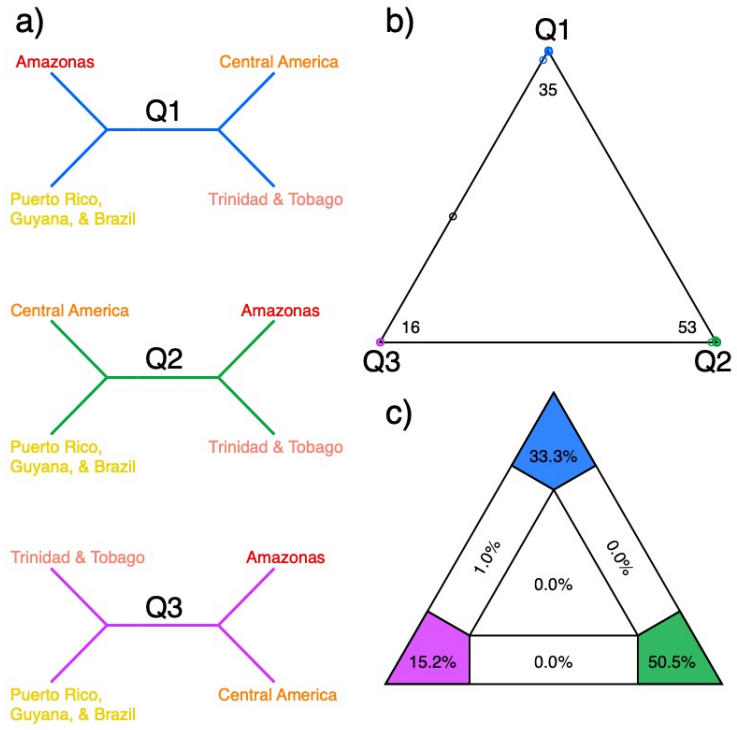

Figure 3.5. Results of the likelihood quartet mapping analysis performed on M5. (a) The three possible topologies for our four predefined groups from the Neotropics. (b) Number of quartets that support each of the three possible topologies. Points colored by which topology they support, colored as in (a). (c) Percentage of quartets that support each of the possible topologies, with regions of the graph differentiated according to how well a quartet falling in that region can answer a phylogenetic hypothesis.

Furthermore, the SuperQ network of M5 gene trees (Figure 3.6) showed a predominantly radial pattern, displaying high levels of reticulation between the well-supported clades in our phylogeny and indicating extensive gene tree conflict. In particular, the specimen from Amazonas showed no strong affinity to any of the other taxa, substantiating its rogue behavior across our different phylogenetic treatments. This instability was not attributable to missing data, as it was represented in no fewer than 73% of orthogroups across all matrices (Table A.1). Also, while this specimen only had 38.5% of complete BUSCOs (Table 3.1), BUSCO scores were generally low across Peripatidae (family average = 41.8%), and other taxa with lower BUSCO scores and higher amounts of missing data were reliably placed (e.g. *Oroperipatus* sp. Galapagos, both specimens of *Peripatus juanensis*). This star-like supernetwork may therefore reflect a history in which peripatids rapidly radiated across the Neotropics, a scenario that could explain the genetic (and morphological) similarity of Neopatida (as measured by orthogroup pairwise identity), the extremely short basal internodes in the clade, and our overall difficulty resolving relationships.

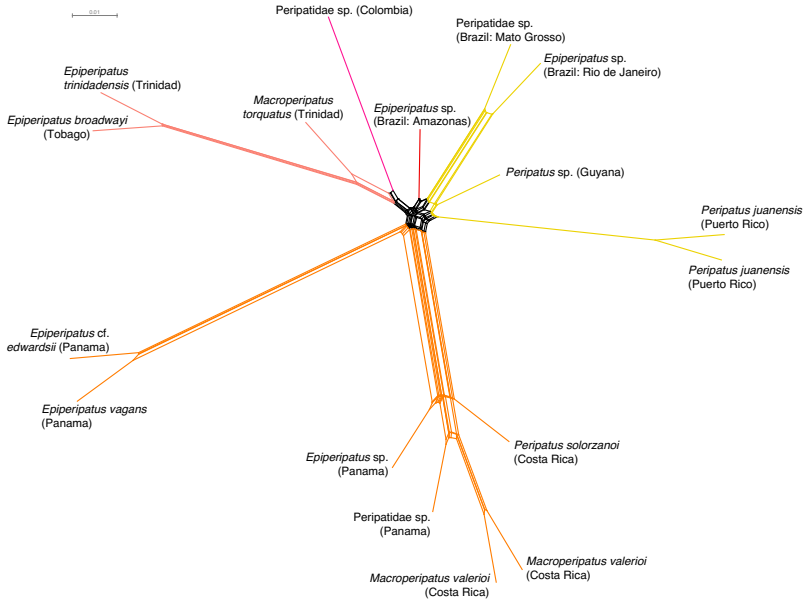

Figure 3.6. Quartet supernetwork built from 1,147 individual gene trees (M5) in SuperQ, showing conflicting signal between genes. *Oroperipatus eisenii* and *Oroperipatus* sp. Galapagos filtered out for visual clarity. Edges scaled according to bipartition frequency, with specific edges colored according to clade identity as in Figures 3.2–3.5.

3.3.4 Biogeographic patterns in Peripatopsidae

Divergence dating of Onychophora resulted in an estimated age for the phylum of 297 Ma (95% highest probability density [HPD] 287–300 Ma) (Figure 3.7). Peripatopsidae was found to be 198 Ma (95% HPD: 168–232 Ma), corresponding to the split between the South Africa–Chile clade and the Australia–New Zealand clade. This age closely concorded with the dates found in Giribet et al. (2018) and Murienne et al. (2014), which found Peripatopsidae to be ~187 Ma and ~182 Ma, respectively. As discussed extensively in those papers, this division reflects the initial breakup of the former supercontinent Gondwana into West Gondwana (South America and Africa) and East Gondwana (Australia, New Zealand, India, and Antarctica) *ca.* 170 Mya (Ali & Aitchison, 2008; McLoughlin, 2001). Additionally, the divergence between *Metaperipatus* from Chile and *Opisthopatus* + *Peripatopsis* from South Africa was estimated at 146 Mya (95% HPD: 105–189 Mya), closely coinciding with the opening of the southern Atlantic Ocean *ca.* 140–130 Mya (Eagles, 2007; McLoughlin, 2001). This parallels Gondwanan vicariant patterns seen in other groups of animals, such as pettalid harvestmen (Baker et al., 2020; Giribet et al., 2012), sphaerodactyl geckos (Gamble, Bauer, Greenbaum, & Jackman, 2008), caecilians (Kamei et al., 2012), and potentially water scavenger beetles (Toussaint, Bloom, & Short, 2017).

Because we only had one exemplar from each of the New Zealand genera, and also did not have representatives of their Tasmanian counterparts, our chronogram gave little insight into the biogeography of those taxa. However, the estimated divergence times for both *Ooperipatellus* and *Peripatoides* from their sister clades, inclusive of 95% HPD intervals, predated the separation of New Zealand from Eastern Gondwana *ca.* 80 Mya, a result consistent with previous studies that demonstrated the persistence of these taxa in New Zealand need not invoke *trans*-oceanic dispersal (Allwood et al., 2010; Giribet et al., 2018; Murienne et al., 2014). Finally, within the Australian clade we recovered an estimated divergence time between Western and Eastern Australia in the mid-

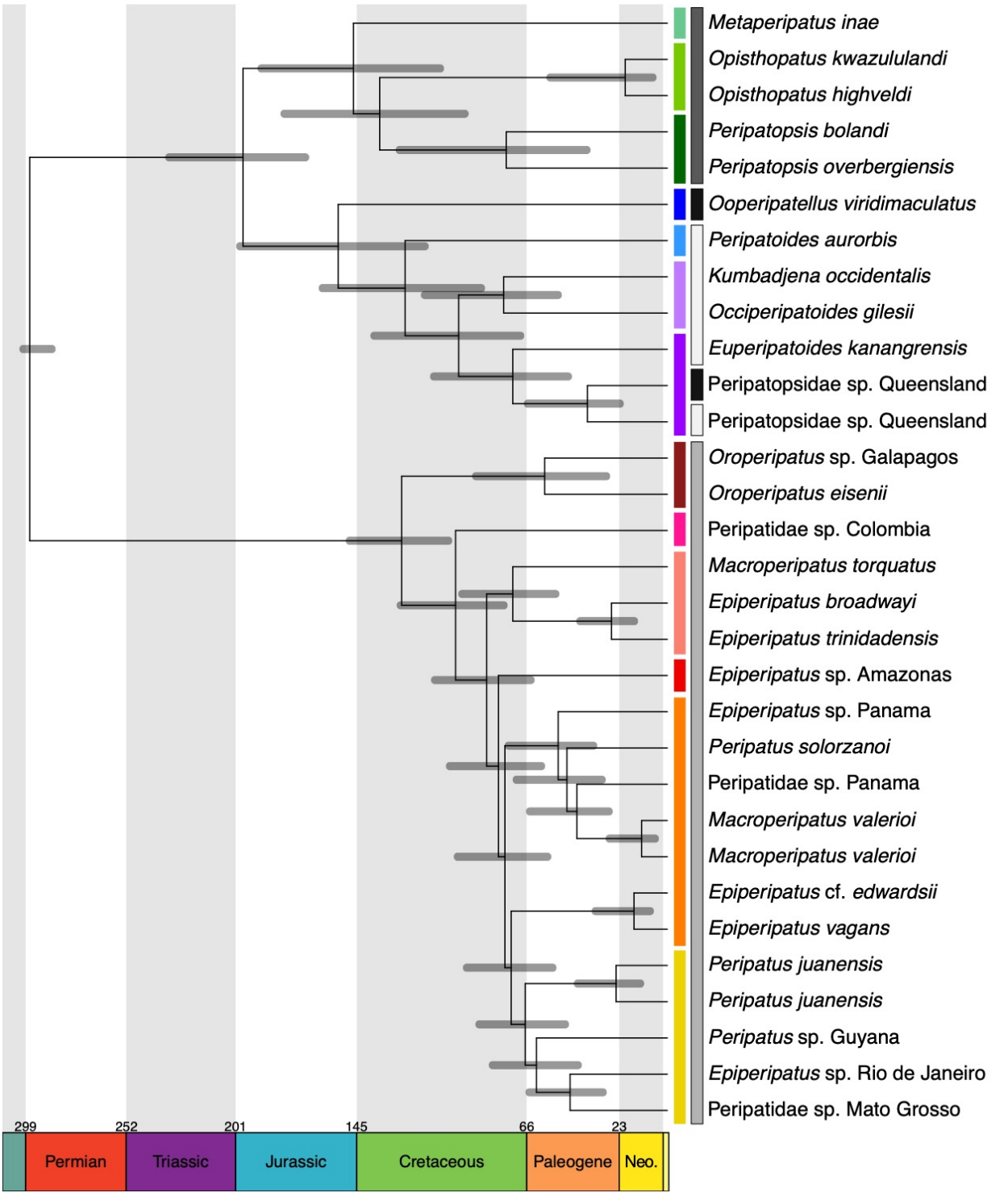

Figure 3.7. Chronogram of Onychophora inferred in PhyloBayes. 95% highest probability density (HPD) intervals for divergence times are shown at nodes and colored in grey. Lefthand colored bars correspond to clade identities as in Figures 3.2–3.6, righthand grey bars correspond to reproductive mode (black = oviparity, dark grey = matrotrophic viviparity, white = lecithotrophic viviparity or combined lecithotrophic/matrotrophic viviparity, light grey = placentrotrophic viviparity).

Cretaceous, about 97 Mya (95% HPD: 68–136 Mya). This reflects an ancient separation that may be attributable to the formation of an extensive seaway across central Australia in the Cretaceous (McLoughlin & Kear, 2010). Divergences within Eastern Australia far predated Miocene aridification in Australia (Martin, 2006), a process hypothesized to have driven diversification in other Australian taxa (e.g. Rix & Harvey, 2012). Indeed, the divergence between the two unidentified specimens of Peripatopsidae from Queensland almost completely predated the start of the Miocene at 23 Ma (estimated divergence at 37 Ma, 95% HPD: 21–64 Ma). However, the inclusion of additional taxonomic and geographic diversity from Eastern Australia will be critical for determining whether Miocene aridification played any role in the group's diversification.

3.3.5 Biogeographic patterns in Peripatidae

The initial diversification of Neopatida (the only lineage sampled within Peripatidae here) was dated to the Early Cretaceous *ca.* 124 Mya (95% HPD: 101–147 Mya), a somewhat younger estimate than was recovered by Murienne et al. (2014) (~172 Ma) and Giribet et al. (2018) (~167 Ma). This corresponded to the divergence between *Oroperipatus* and the rest of Neopatida. Divergences between major groups in the Eastern clade were estimated to have occurred in the Late Cretaceous to early Paleogene, with mean ages ranging between 66 and 84 Ma (95% HPD inclusive of all backbone nodes: 47–108 Ma). Despite our slightly younger estimated age of Neopatida, the timing of the Eastern clade's radiation corresponded closely with that of Murienne et al. (2014) (which recovered the diversification at ~62–95 Ma) and Giribet et al. (2018) (rapid cladogenesis of the group spanning ~70–120 Ma). This repeated cladogenesis that occurred nearly simultaneously further bolsters the hypothesis that the Neotropical peripatids represent a true evolutionary radiation, in accordance with the extensive gene tree conflict apparent in the SuperQ network

(Figure 3.6) and the extremely short and poorly supported internodes in the ASTRAL trees of Peripatidae (Figure 3.4d).

The geologic history of the Neotropics is complex and marked by major events in Earth's history, including the impact of a bolide near the Yucatán Peninsula *ca.* 66 Mya, which is associated with the Cretaceous–Paleogene extinction (Hedges, 2006; Hedges, Hass, & Maxson, 1992). It also was affected by the subduction of the Pacific-Farallon plate below the Caribbean and South American plates, which led to the formation of the Panama volcanic arc *ca.* 73 Mya; it also contributed to the formation of the Lesser Antilles, and eventually resulted in the formation of a continuous Panamanian land bridge between North and South America ~2.6 Mya (Ali, 2012; Bacon et al., 2015; Buchs, Arculus, Baumgartner, Baumgartner-Mora, & Ulianov, 2010; O'Dea et al., 2016). Additionally, the uplift of the Andes, which commenced in the Mesozoic, drastically affected the evolution of the Neotropical biota (Antonelli, Nylander, Persson, & Sanmartín, 2009; Chen, Wu, & Suppe, 2019). Remarkably, Neopatida appears to retain signatures of several of these important historical events.

With an estimated diversification time of ~124 Mya, Neopatida represents an ancient lineage in the Neotropics, particularly compared to the vertebrate fauna (Hedges, 2006). This old age implies that onychophorans survived the K–P extinction *in situ*, despite the proximity of the bolide impact and its resulting indirect effects (e.g. debris clouds, tsunamis). It is possible that their restriction to sheltered, often subterranean microhabitats such as leaf litter, rotting logs, and caves facilitated their survival, and that following the mass extinction they were able to radiate in newly open niches. Unfortunately, the current understanding of Neotropical onychophoran biodiversity is highly incomplete (Oliveira, Read, et al., 2012) and the lack of a proper taxonomic and systematic framework for the group precludes testing these hypotheses using modern macroevolutionary comparative methods (e.g. May, Höhna, Moore, & Cooper, 2016; Rabosky, 2014). Future work

should continue to focus on the description of new species using integrative taxonomy (e.g. detailed morphological examination of multiple individuals per population paired with high-throughput molecular data analyzed in a phylogenetic framework) so that such hypotheses may eventually be tested.

Even with those taxonomic limitations, several biogeographic patterns are evident in Neopatida. For one, it is clear that a strict vicariance scenario is insufficient to explain their distribution across the Neotropics. This is obvious from their presence on oceanic islands such as the Galapagos, and while we were unable to include these lineages in our study, they are also known from several islands in the Lesser Antilles, such as Saint Vincent (home to the type species of Onychophora, *Peripatus juliformis*). Additionally, the divergence time between *Oroperipatus* and the other members of Neopatida *ca.* 124 Mya far predated the formation of a continuous land connection between North and South America (which was only established ~2.6 Mya (O'Dea et al., 2016)), and yet *Oroperipatus* is known from Mexico (*O. einsenii*; while our phylogeny only includes representatives of *Oroperipatus* from Mexico and the Galapagos, the genus is mainly found in Ecuador and Colombia). The timing of this divergence is not compatible with any geologically informed vicariance scenario, and instead suggests a history in which a lineage of *Oroperipatus* dispersed, perhaps via a stepping-stone or sweepstakes scenario, to Mexico. A similar stepping-stone scenario has also been proposed to explain the dispersal of land vertebrates between North and South America in the late Cretaceous (Ortiz-Juareguizar & Pascual, 2011).

Furthermore, our chronogram indicates that peripatids have been diversifying on Puerto Rico since ~24 Mya (95% HPD: 12–41 Mya), and our phylogenetic analyses indicate that they share common ancestry with taxa from the Guiana Shield and Brazil. Interestingly, taking into account the 95% HPD interval, this reconstructed history concords with the controversial GAARlandia hypothesis of Iturralde-Vinent and MacPhee (1999), who suggested that a semi-continuous walkway

existed between 33–35 Mya connecting South America to the Greater Antilles atop the Aves Ridge. This land bridge was proposed as an explanation for the presence of non-volant vertebrates in the Greater Antilles that were closely related to species from South America. However, there is scant geologic evidence for such a walkway (Ali, 2012), and indeed the general pattern of movement from South America to the West Indies follows the direction of water currents in the Caribbean Sea, as well as the path taken by nearly all hurricanes in the region (Hedges, 2006). We therefore conclude that the most likely mechanism by which onychophorans colonized Puerto Rico (and other islands in the West Indies from which they are known but which were not included in this study, such as Jamaica and Hispaniola) was not over-land dispersal via GAARlandia, but rather by rafting via a sweepstakes scenario, possibly as a result of tropical storms. This dispersal scenario for Caribbean peripatids was likewise proposed by Monge-Nájera (1995).

Finally, the uplift of the Andes is well-understood to have affected diversification rates and distribution patterns in many groups endemic to the Neotropics (e.g. Antonelli et al., 2009; Elias et al., 2009; Lagomarsino, Condamine, Antonelli, Mulch, & Davis, 2016; McGuire et al., 2014). Given that Neopatida is estimated to have started diversifying in the early Cretaceous, it is therefore likely that Andean orogeny, which started in the Jurassic or Cretaceous and continues to the present (Antonelli et al., 2009; Chen et al., 2019), likely shaped the diversification of Neopatida. This is perhaps most evident in the initial divergence between *Oroperipatus*, which is found west of the Andes, and the rest of Neopatida, which predominantly is found east of the Andes. But again, in the absence of a well-characterized taxonomic framework, a dense sampling of Andean taxa, and a comprehensive understanding of their geographic range, we cannot draw any pointed conclusions about whether or not Andean orogeny affected cladogenesis or extinction rates in the group.

3.3.6 Relative dispersal abilities in Peripatidae and Peripatopsidae

There are multiple places in the phylogeny of Peripatopsidae that reflect a history of Gondwanan vicariance, and indeed there is little evidence of *trans*-oceanic dispersal in the family. This fact has contributed to Onychophora being heralded as a short-range endemic taxon, characterized by low dispersal abilities and high population structure (Harvey, 2002). But within Neopatida, over-water dispersal—at least over moderately short distances—seems to have occurred multiple times in many of the Caribbean islands and probably to the Galapagos (although some have argued that the occurrence of the Galapagos species is a human introduction, no one has demonstrated it (Espinasa et al., 2015)). This discrepancy is striking and begs for a biological explanation, which remains elusive given the generally limited understanding of many basic aspects of onychophoran biology, such as survival ability in sea water (see Monge-Nájera, Barrientos, & Aguilar, 1993; Monge-Nájera, 1995).

One possible avenue of future interrogation, though, could be reproductive mode, which is surprisingly variable across the phylum (Figure 3.7). Neopatida is the only lineage within Onychophora that utilizes placentotrophic viviparity, characterized by small, yolkless eggs that receive nourishment exclusively from the mother via a "placenta". In contrast, members of Peripatopsidae have a variety of reproductive modes, including oviparity, matrotrophic viviparity, lecithotrophic viviparity, and a combination of matrotrophic and lecithotrophic viviparity (see section 3.1) (Mayer et al., 2015). Even within Peripatidae, the Southeast Asian genus *Eoperipatus* exhibits lecithotrophic viviparity (though the reproductive mode of the West African genus *Mesoperipatus* is unknown beyond "viviparity").

All modes of viviparity necessitate increased maternal investment in offspring development compared to oviparity, which Monge-Nájera (1995) hypothesized could be a result of evolutionary pressures from parasites or predators. However, a female onychophoran with multiple internally

developing embryos that survived a period of over-water rafting, perhaps in a rotting log or vegetative mat, may hypothetically be able to establish a population upon reaching an island. Placentotrophic viviparity could therefore be an exaptation that allowed neopatids to colonize oceanic islands after a period of rafting. Furthermore, peripatid females have been shown to mate when very young and subsequently retain sperm long-term in seminal receptacles for later fertilization, another trait that could aid in the establishment of new populations; by contrast, the seminal receptacles of peripatopsid females are believed to function only as short-term sperm stores (Mayer, 2007 and references therein). Future research into the ecological tolerances of different onychophoran species, characterization of the relative contribution of maternal investment in species with different reproductive modes, and a more comprehensive resolved phylogeny of Neopatida that clarifies exactly how many lineages have established as a result of over-water dispersal will all be useful in testing this hypothesis.

3.4 Conclusions

Onychophora is an ancient phylum that retains biogeographic signatures of many major events in Earth's history, from the breakup of Pangaea and Gondwana to a putative radiation following the K–P extinction. We also recovered distinct biogeographic patterns between Peripatopsidae and Peripatidae that reflect different dispersal capabilities in the two families, and propose that divergent life history strategies and reproductive modes may be related to these differential abilities. Furthermore, we showed that phylogenomic analysis of transcriptomic data is a promising avenue for future taxonomic and systematic work in the group, as it was able to resolve several previously unknown relationships, particularly in Neopatida when analyzed at the nucleotide (instead of amino acid) level. However, rogue behavior of specific taxa paired with the rapid cladogenesis of the Neotropical species in the Late Cretaceous–early Paleogene may reflect a polytomy, a scenario with

thorny taxonomic implications. Currently, Neopatida comprises a handful of "catch-all" genera (e.g. *Peripatus*, *Epiperipatus*, *Macroperipatus*), and series of monotypic genera (e.g. *Plicatoperipatus*, *Principapillatus*, *Speleoperipatus*), all of which have questionable validity (Giribet et al., 2018, this study). In their paper, Giribet et al. (2018) proposed, but did not enact, a drastic solution – reverting to the classification scheme of Bouvier (1899a, b) by dividing Neopatida into two genera, one corresponding to the "Péripates andicoles", i.e. *Oroperipatus*, and placing the rest of the taxa into a second, highly diverse genus corresponding to the "Péripates caraïbes". While we likewise do not advocate for this taxonomic change, the results of our analyses underscore the flaws of the current system, and suggest that the work of erecting new, valid genera will require more extensive and informative sequence data beyond a handful of Sanger sequencing loci, as well as a thorough reexamination of morphology, karyotype, and/or behavior to find synapomorphies for phylogenetic groups.

Chapter 4

Species delimitation and biogeographic history of the New Zealand-endemic harvestmen *Sorensenella* and *Karamea* (Arachnida: Opiliones: Triaenonychidae) through the Cenozoic

Caitlin M. Baker and Gonzalo Giribet

Note: Supplementary materials are included in Appendix B.

Abstract

New Zealand harbors some of the most unique biota on Earth, but the question of how and why its endemic biota has evolved and responded to geologic and climatic events remains an active area of research. In this study, we explored the biogeographic history of two New Zealand-endemic harvestman genera, *Sorensenella* and *Karamea* (Opiliones, Laniatores, Triaenonychidae), using data derived from ultraconserved element (UCE) sequencing. Phylogenetic analysis of UCE loci confirmed the reciprocal monophyly of both genera as well as the existence of multiple previously unrecognized genetic lineages. Species delimitation analyses, including both standard genetic clustering and an unsupervised machine learning approach, corroborated the status of these lineages as distinct species. Divergence dating of lineages paired with genetic diversity statistics indicated that

Sorensenella and *Karamea* have been diversifying in New Zealand since before the Oligocene marine transgression, and that the subsequent land expansion and mountain building due to the activation of the Alpine fault led to an increase in diversification in both lineages. Pliocene sea-strait flooding across the central North Island and glacial cycles in the Pleistocene likely caused a reduction in genetic diversity in some *Sorensenella* species, and may have been a factor leading to the evolution of parthenogenesis in the species *S. rotara*.

4.1 Introduction

New Zealand has long fascinated biogeographers due to its unique flora and fauna. The archipelago was once thought to be a haven for relictual Gondwanan taxa following the archipelago's separation from that supercontinent *ca.* 80 mya (McLoughlin, 2001), with ever stranger forms evolving on the isolated landmass (McGlone, 2005). However, it is now generally accepted that a substantial proportion of New Zealand's distinctive biota is the result of more recent dispersal to the continent following a widespread marine incursion in the Oligocene, which peaked *ca.* 23 mya (Landis et al., 2008; Wallis & Jorge, 2018). Despite this emerging consensus, there are still many relictual Gondwanan lineages in New Zealand that survived the Oligocene marine transgression (OMT), especially when one looks at soil invertebrate communities (Buckley, Krosch, & Leschen, 2015; Giribet & Boyer, 2010; Wallis & Jorge, 2018).

Following the OMT, activation of the Alpine Fault between the Australian and Pacific plates led to rapid crustal uplift and the formation of the Southern Alps on the South Island *ca.* 10–5 mya (Cooper & Cooper, 1995). This orogenesis created a strong precipitation gradient across the South Island, with low levels of rain on the eastern side of the mountain range and increased rainfall on the West coast (Gellatly, Chinn, & Rothlisberger, 1988). The tectonic forces that generated the Southern Alps also affected the North Island, promoting extensive volcanism, mountain building, and basin

formation across the island during the late Miocene (McGlone, 1985). In the Pliocene, strike-slip movement in the central North Island eventually led to flooding and creation of a seaway across the south and central areas of the island, which persisted until the Pleistocene, when it retreated progressively southward (Ellis et al., 2015; Lewis, Carter, & Davey, 1994). More recently, glacial-interglacial cycles in the Pleistocene caused forests all across New Zealand to expand and contract, likely leading to allopatric speciation as well as extinction of many forest-dwelling lineages (Bunce et

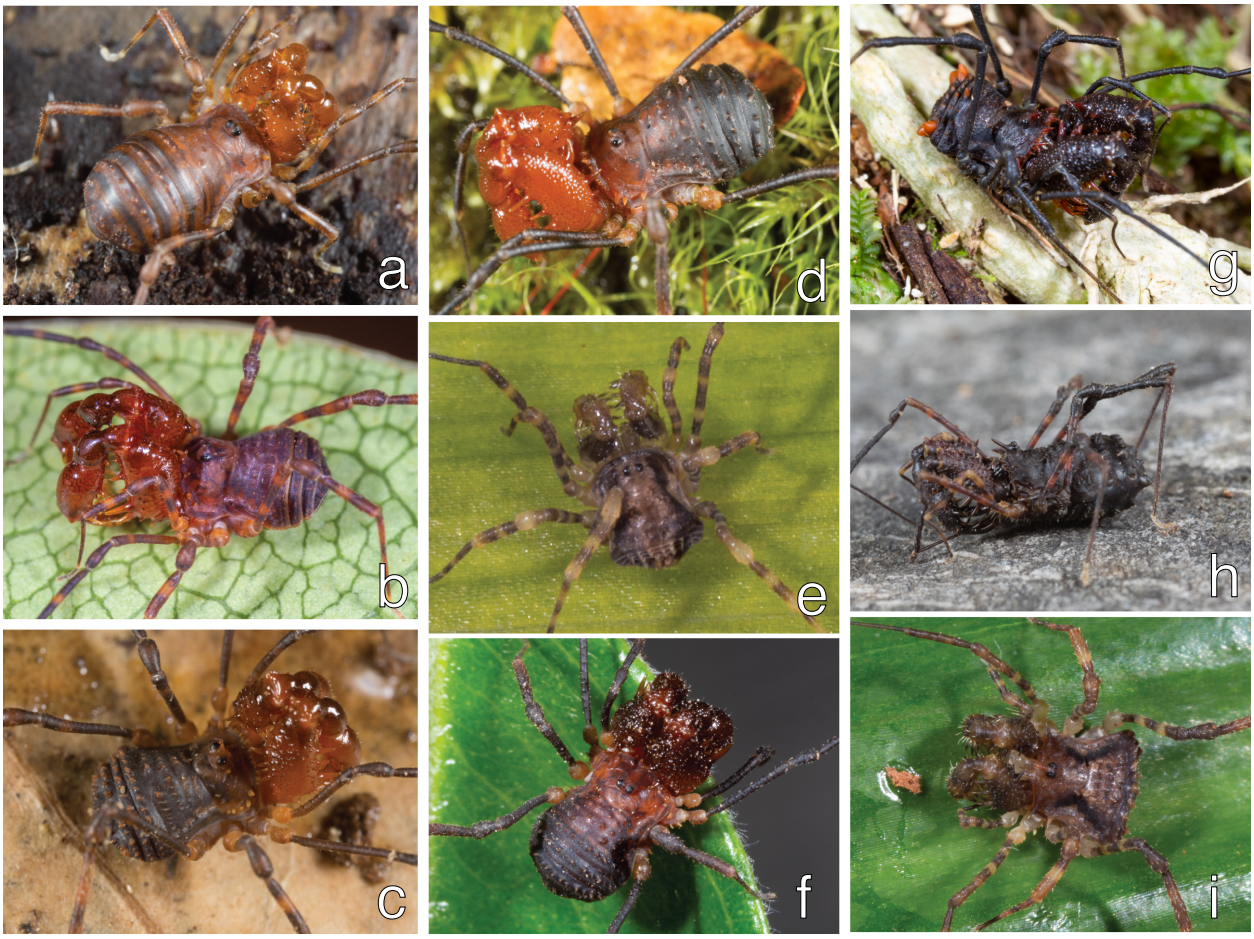

Figure 4.1 Live habitus of members of *Sorensenella* and *Karamea*. (a) *S. prehensor prehensor* MCZ-132838 (b) *S. prehensor prehensor* (*obesa*) MCZ-152217 (c) *Sorensenella* n. sp. "Mangamuka" MCZ-132850 (d) *Sorensenella* n. sp. "Central" MCZ-133368 (e) *S. rotara* MCZ-152234 (f) *S. prehensor nitida* MCZ-152237 (g) *K. lobata lobata* MCZ-152313 (h) *K. lobata australis* MCZ-152033 (i) *K. tricerata* MCZ-152285. Photos a, c, d, and h by Gonzalo Giribet; photos b, e, f, g, and i by Caitlin Baker.

al., 2009; McGlone, 1985). How New Zealand's biota has responded to this long and turbulent geologic and climatic history is an active area of research (e.g. Buckley et al., 2015; Ellis et al., 2015; Marske, Leschen, & Buckley, 2011).

Across New Zealand, armored harvestmen in the family Triaenonychidae Sørensen, 1886 (Arachnida, Opiliones, Laniatores) constitute one of the most commonly encountered leaf litter taxa. Triaenonychidae is the fourth most speciose family of harvestmen (Kury, Mendes, & Souza, 2014), and one third of its described species are endemic to New Zealand (155/480 species and subspecies). Recent systematic and biogeographic work on the family has demonstrated that the New Zealand triaenonychids are not a monophyletic assemblage of taxa, but rather part of a large, ancient clade of temperate Gondwana-derived taxa that are found across southern South America, South Africa, Madagascar, Australia, New Caledonia, and New Zealand (Chapter 2).

The sister genera *Sorensenella*[1] Pocock, 1903b and *Karamea* Forster, 1954 are two of the most charismatic groups of New Zealand's triaenonychids, and are widespread across much of the North and South Islands, respectively (Figures 4.1 and 4.2). They are part of a diverse group of New Zealand-endemic triaenonychids that have been diversifying since *ca.* 93 Ma, and therefore represent a lineage that survived the OMT (Chapter 2). They are easily identified by their grossly enlarged and spine-laden pedipalps (especially in the males), having tarsal claws on legs III and IV with lateral prongs that are equal in length to or longer than the median prong, and having a prominent spine on their eyemound that is directed straight up (*Sorensenella*) or forward (*Karamea*). They are also the only clade within Triaenonychidae with demonstrated paternal care (Machado, 2007). There are currently seven described species and subspecies within *Sorensenella*: *S. prehensor prehensor* Pocock, 1903b, *S. prehensor obesa* Forster, 1954, *S. prehensor nitida* Forster, 1954, *S. rotara* Phillipps & Grimmett, 1932, *S.*

[1] Though often reported as *Soerensenella* (e.g. Forster, 1954), *Sorensenella* is the correct spelling for this genus (see Kury, 2017 for justification).

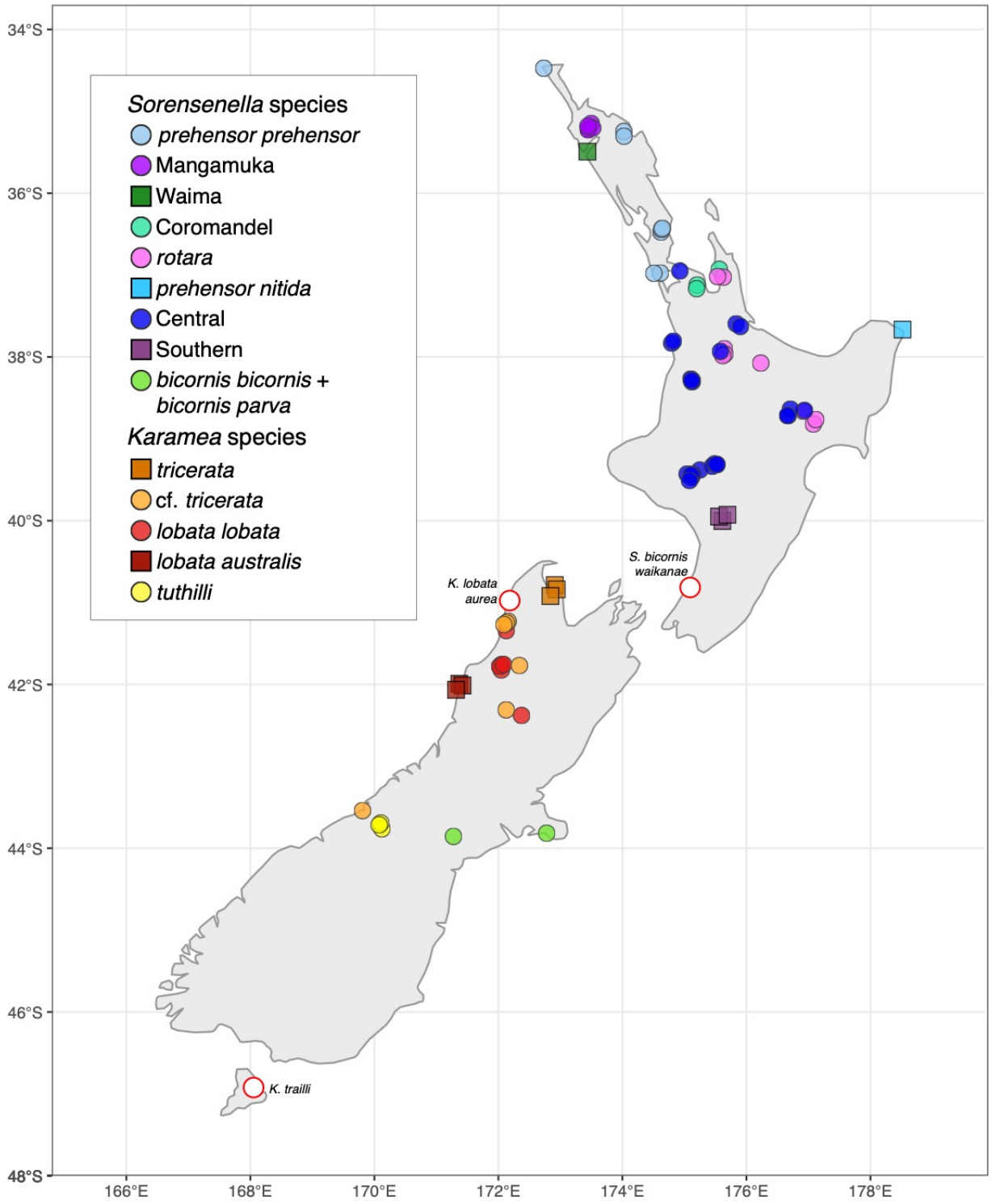

Figure 4.2 Map showing sampling localities of specimens used in this study. Points colored by species. Type localities of the three unsampled morphospecies are indicated by white points with red outlines.

bicornis bicornis Pocock, 1903a, *S. bicornis parva* Forster, 1954, and *S. bicornis waikanae* Forster, 1954. Within *Karamea*, there are six described species and subspecies: *K. lobata lobata* Forster, 1954, *K. lobata aurea* Forster, 1954, *K. lobata australis* Forster, 1954, *K. trailli* (Hogg, 1920), *K. tricerata* Forster, 1954, and *K. tuthilli* Forster, 1954. However, no taxonomic work has been done on this group since 1954 (Forster, 1954), and as a result all the species designations are based exclusively on morphology, having never been tested in any phylogenetic framework using either morphological or molecular data.

Harvestmen are, on the whole, notoriously poor dispersers, with most species being unable to cross even small oceanic and climatic barriers (Boyer, Markle, Baker, Luxbacher, & Kozak, 2016; Derkarabetian, Burns, Starrett, & Hedin, 2016). However, they also have extremely high habitat persistence, needing only small patches of humid forest to survive (down to ~30 meters across, authors' personal collecting experience). They therefore constitute an excellent system in which to ask questions of both historical and ecological biogeography, and at spatial scales ranging from entire continents to local populations. Given New Zealand's status as a biodiversity hotspot (Myers, Mittermeier, Mittermeier, da Fonseca, & Kent, 2000), characterizing the full extent of its endemic biota using modern, integrative taxonomic methods is also of critical importance not just for understanding its biogeographic origins and macroevolutionary patterns, but for informing conservation efforts as well.

To that end, we employed sequencing of ultraconserved elements (UCEs) (Faircloth et al., 2012) for specimens in the genera *Sorensenella* and *Karamea* and analyzed the data using phylogenomic and population genomic methods in order to assess the validity of the currently described morphospecies and understand the group's evolutionary history within New Zealand in light of the archipelago's geologic and climatic past.

4.2 Methods

4.2.1 Taxonomic sampling

79 specimens were included in this study: 22 *Karamea* specimens, 56 *Sorensenella* specimens, and 1 outgroup taxon in the genus *Triregia*. Accession information is listed in Table 4.1, and all specimens used in this work are stored at the Museum of Comparative Zoology (MCZ) and available online through MCZBase (https://mczbase.mcz.harvard.edu), or at the Natural History Museum of Denmark, University of Copenhagen (ZMUC).

Taxonomic identification was done using light microscopy examination of somatic characters (including males and females), and specimens were then selected for molecular work, focusing our sampling on representing as many species and as broad a geographic area as possible. We used multiple specimens per species and per locality whenever possible so as to test the monophyly of those taxa. Our sampling spans six (of seven) *Sorensenella* morphospecies and subspecies and four (of six) *Karamea* morphospecies and subspecies.

4.2.2 UCE library preparation

Genomic DNA was extracted from 2–4 legs per individual using the Qiagen DNeasy Blood and Tissue (Qiagen, Valencia, CA) kit with an overnight incubation. DNA concentrations were quantified using a Qubit Fluorometer (Life Technologies, Inc.) Broad Range DNA kit, and quality was assessed using an Agilent TapeStation 2200 or 4200 with Genomic DNA ScreenTapes (Agilent Technologies). Between 100 and 500 ng of genomic DNA was sheared to an average length of 500 bp on a Covaris S220 Ultrasonicator. In order to verify sonication success, select samples were run on an Agilent TapeStation using a High Sensitivity D5000 ScreenTape.

Library preparation for sequencing of ultraconserved elements (UCEs) followed established protocols using the Arachnida probe set (Derkarabetian et al., 2018; Starrett et al., 2017). Briefly,

Table 4.1 Collection information and matrix occupancy information (numbers of UCE loci per matrix) for specimens used in this study, including the outgroup.

Accession no.	*Species*	Collection date	Latitude	Longitude	M75 loci	M50 loci	Hom. loci	Mid. loci
MCZ-132838.1	*Sorensenella prehensor prehensor*	7-Jan-2016	-35.27739	174.05220	568	715	661	428
MCZ-132838.2	*Sorensenella prehensor prehensor*	7-Jan-2016	-35.27739	174.05220	583	748	690	457
MCZ-133094	*Sorensenella prehensor prehensor*	7-Jan-2016	-36.45258	174.65154	606	772	711	461
MCZ-133095	*Sorensenella prehensor prehensor*	7-Jan-2016	-36.45258	174.65154	586	742	683	442
MCZ-133097	*Sorensenella prehensor prehensor*	7-Jan-2016	-36.45258	174.65154	610	771	710	460
MCZ-133201	*Sorensenella prehensor prehensor*	9-Jan-2016	-36.94663	174.61005	533	659	604	385
MCZ-152217	*Sorensenella prehensor prehensor*	23-Jan-2019	-34.46645	172.76210	522	660	610	400
ZMUC06	*Sorensenella prehensor prehensor*	2-Feb-2011	-36.96463	174.51240	608	794	733	479
MCZ-132849	*Sorensenella* sp. "Mangamuka"	9-Jan-2016	-35.19026	173.48329	501	598	538	355
MCZ-132850.1	*Sorensenella* sp. "Mangamuka"	9-Jan-2016	-35.19026	173.48329	609	745	683	449
MCZ-132850.2	*Sorensenella* sp. "Mangamuka"	9-Jan-2016	-35.19026	173.48329	560	680	624	405
MCZ-133130	*Sorensenella* sp. "Mangamuka"	9-Jan-2016	-35.19035	173.45557	589	715	655	425
MCZ-133131	*Sorensenella* sp. "Mangamuka"	9-Jan-2016	-35.19035	173.45557	597	730	668	435
ZMUC07	*Sorensenella* sp. "Waima"	19-Mar-2011	-35.53094	173.44214	603	773	712	457
ZMUC01.1	*Sorensenella* sp. "Coromandel"	3-Jan-2011	-37.12458	175.22146	544	708	652	422
ZMUC01.2	*Sorensenella* sp. "Coromandel"	3-Jan-2011	-37.12458	175.22146	573	722	666	434
ZMUC05.2	*Sorensenella* sp. "Coromandel"	3-Apr-2011	-36.99051	175.57213	617	783	721	463
MCZ-29379.1	*Sorensenella rotara*	11-Jan-2014	-37.94336	175.63790	614	779	716	465
MCZ-29379.2	*Sorensenella rotara*	11-Jan-2014	-37.94336	175.63790	614	774	710	462
MCZ-29379.3	*Sorensenella rotara*	11-Jan-2014	-37.94336	175.63790	613	788	726	477
MCZ-29573.1	*Sorensenella rotara*	12-Jan-2014	-38.79791	177.12424	610	776	718	464
MCZ-29573.2	*Sorensenella rotara*	12-Jan-2014	-38.79791	177.12424	609	771	709	460
MCZ-148131	*Sorensenella rotara*	12-Jan-2014	-38.64738	176.90794	584	743	682	441
MCZ-152234	*Sorensenella rotara*	26-Jan-2019	-38.11843	176.20060	615	788	726	474
ZMUC03	*Sorensenella rotara*	2-Apr-2011	-37.06210	175.67149	598	762	701	452
ZMUC05.1	*Sorensenella rotara*	3-Apr-2011	-36.99051	175.57213	619	780	717	463
MCZ-152237	*Sorensenella prehensor nitida*	27-Jan-2019	-37.69055	178.54572	567	721	660	437
MCZ-29288	*Sorensenella* sp. "Central"	12-Jan-2014	-38.64738	176.90794	596	709	647	423
MCZ-29374	*Sorensenella* sp. "Central"	11-Jan-2014	-37.94336	175.63790	603	711	655	421
MCZ-29373.1	*Sorensenella* sp. "Central"	10-Jan-2014	-37.84185	174.77342	614	745	683	441
MCZ-29373.2	*Sorensenella* sp. "Central"	10-Jan-2014	-37.84185	174.77342	601	715	655	422
MCZ-133366	*Sorensenella* sp. "Central"	11-Jan-2016	-38.25976	175.09675	619	742	681	439
MCZ-133368.1	*Sorensenella* sp. "Central"	11-Jan-2016	-39.32930	175.49646	584	689	634	404
MCZ-133368.2	*Sorensenella* sp. "Central"	11-Jan-2016	-39.32930	175.49646	603	719	660	421
MCZ-133376.1	*Sorensenella* sp. "Central"	13-Jan-2016	-39.46544	175.09003	598	710	650	433
MCZ-133376.2	*Sorensenella* sp. "Central"	13-Jan-2016	-39.46544	175.09003	610	736	673	442
MCZ-133378.1	*Sorensenella* sp. "Central"	13-Jan-2016	-39.46544	175.09003	606	718	656	429
MCZ-133378.2	*Sorensenella* sp. "Central"	13-Jan-2016	-39.46544	175.09003	601	720	661	434
MCZ-133380	*Sorensenella* sp. "Central"	13-Jan-2016	-39.46544	175.09003	552	654	597	384
MCZ-133428	*Sorensenella* sp. "Central"	11-Jan-2016	-38.25995	175.09980	506	587	527	345
MCZ-133429	*Sorensenella* sp. "Central"	11-Jan-2016	-38.25995	175.09980	618	743	678	443
MCZ-133430	*Sorensenella* sp. "Central"	11-Jan-2016	-38.25995	175.09980	614	739	679	436
MCZ-133433	*Sorensenella* sp. "Central"	13-Jan-2016	-39.41640	175.21866	562	674	618	396
MCZ-135456.1	*Sorensenella* sp. "Central"	24-Feb-2008	-38.67772	176.68847	615	747	684	444
MCZ-135456.2	*Sorensenella* sp. "Central"	24-Feb-2008	-38.67772	176.68847	613	753	692	448
MCZ-135459	*Sorensenella* sp. "Central"	24-Feb-2008	-38.67569	176.69900	496	574	516	326
MCZ-135462.1	*Sorensenella* sp. "Central"	25-Feb-2008	-37.59739	175.86158	583	711	653	426
MCZ-135462.2	*Sorensenella* sp. "Central"	25-Feb-2008	-37.59739	175.86158	608	728	668	426
MCZ-147579	*Sorensenella* sp. "Central"	12-Jan-2014	-39.35609	175.47643	481	558	499	320
MCZ-147581	*Sorensenella* sp. "Central"	12-Jan-2014	-39.35609	175.47643	594	710	650	422
ZMUC04	*Sorensenella* sp. "Central"	11-Jun-2011	-36.90355	174.93510	617	743	679	437
MCZ-58956	*Sorensenella* sp. "Southern"	18-Feb-2008	-39.93770	175.63930	592	739	683	446
MCZ-58970	*Sorensenella* sp. "Southern"	18-Feb-2008	-39.93770	175.63930	598	726	667	426
MCZ-133417	*Sorensenella* sp. "Southern"	14-Jan-2016	-39.93466	175.63977	520	605	546	350
MCZ-152054	*Sorensenella bicornis bicornis*	8-Jan-2019	-43.78107	172.77835	600	729	668	438
MCZ-152060	*Sorensenella bicornis parva*	9-Jan-2019	-43.89477	171.25862	614	766	704	466
MCZ-64653.1	*Karamea tricerata*	7-Mar-2003	-40.83258	172.96897	577	706	647	421

Table 4.1 (Continued)

MCZ-64653.2	*Karamea tricerata*	7-Mar-2003	-40.83258	172.96897	484	618	568	370
MCZ-135510	*Karamea tricerata*	19-Dec-2009	-40.88297	172.81083	593	728	670	437
MCZ-64590	*Karamea* cf. *tricerata*	31-Jan-2003	-42.33225	172.17127	568	684	624	407
MCZ-135523	*Karamea* cf. *tricerata*	19-Dec-2009	-41.27003	172.13325	452	575	526	350
MCZ-135527	*Karamea* cf. *tricerata*	19-Dec-2009	-41.27003	172.13325	476	612	564	361
MCZ-135529	*Karamea* cf. *tricerata*	19-Dec-2009	-41.27003	172.13325	575	713	656	430
MCZ-136006	*Karamea* cf. *tricerata*	11-Feb-2008	-41.78667	172.36833	585	721	661	430
MCZ-152164	*Karamea* cf. *tricerata*	17-Jan-2019	-43.57770	169.81547	595	735	674	441
MCZ-29299.1	*Karamea lobata lobata*	16-Jan-2014	-41.79553	172.04624	518	625	572	372
MCZ-29299.2	*Karamea lobata lobata*	16-Jan-2014	-41.79553	172.04624	591	715	653	426
MCZ-29301	*Karamea lobata lobata*	17-Jan-2014	-42.38096	172.40260	547	644	589	384
MCZ-136011.1	*Karamea lobata lobata*	11-Feb-2008	-41.79667	172.04944	542	653	597	395
MCZ-136011.2	*Karamea lobata lobata*	11-Feb-2008	-41.79667	172.04944	589	722	664	427
MCZ-136012	*Karamea lobata lobata*	11-Feb-2008	-41.79667	172.04944	542	645	590	391
MCZ-152313	*Karamea lobata lobata*	05-Feb-2019	-41.27187	172.14267	588	735	678	446
MCZ-136027	*Karamea lobata australis*	12-Feb-2008	-42.03694	171.38972	586	713	656	426
MCZ-136031	*Karamea lobata australis*	12-Feb-2008	-42.03694	171.38972	600	741	681	434
MCZ-149153	*Karamea lobata australis*	21-Dec-2009	-42.10922	171.34250	583	729	671	436
MCZ-29556.1	*Karamea tuthulli*	20-Jan-2014	-43.73794	170.09549	574	694	632	411
MCZ-29556.2	*Karamea tuthulli*	20-Jan-2014	-43.73794	170.09549	569	689	628	404
MCZ-29556.3	*Karamea tuthulli*	20-Jan-2014	-43.73794	170.09549	575	708	647	421
MCZ-152215	*Triregia fairburni fairburni*	22-Jan-2019	-35.70618	174.33577	511	616	563	368

sheared DNA was purified using Ampure XP beads (Beckman Coulter) or lab-made SPRI beads (Rohland & Reich, 2012). 5 μM universal adapter stubs (Glenn et al., 2019) were ligated to libraries following end-repair and A-tailing steps performed with a KAPA Hyper Prep kit (Kapa Biosystems). Libraries were then amplified in a 50 μl reaction using KAPA HiFi HotStart ReadyMix, at which point Illumina TruSeq dual-indexed primers (i5 and i7) with modified 8-bp indexes (Glenn et al., 2019) were added. Cycling conditions were 98 ºC for 45 s, 16–18 cycles of 98 ºC for 15 s, 60 ºC for 30 s, 72 ºC for 60 s, and a final extension of 72 ºC for 5 min. Amplified libraries were quantified using a Qubit fluorometer High Sensitivity DNA kit, and 125 ng of DNA from eight equimolar samples were combined to produce 1000 ng DNA pools.

Pooled libraries underwent hybridization using the Arbor Biosciences myBaits kit version 4 kit (arborbiosci.com) and the Arachnida probe set (Faircloth, 2017; Starrett et al., 2017) in a 24-hour hybridization protocol at 60 ºC. Pooled, enriched libraries were then amplified with 16–18 PCR cycles to add TruSeq primers, and sequenced on an Illumina NovaSeq with 150 bp paired end reads at the Bauer Core Facility at Harvard University.

4.2.3 UCE locus assembly

Raw, demultiplexed reads for each sample were trimmed to remove adapter content and low-quality reads using the Illumiprocessor function of the program PHYLUCE (Faircloth, 2016). Assemblies for each individual were created using Trinity v2.1.1 (Grabherr et al., 2011) and Velvet 1.2.1 (Zerbino & Birney, 2008) using default settings. Assembled reads were then matched to the Arachnida probes using a modified version of the PHYLUCE program "phyluce_assembly_match_contigs_to_probes" to allow for multiple matches to single probes. Loci were aligned using MAFFT (Katoh & Standley, 2014) and trimmed with gblocks (Talavera & Castresana, 2007) using lenient parameters (–b1 0.5 –b2 0.5 –b3 10 –b4 4) to maximize signal for shallower phylogenetic questions. Alignments with 50% taxon occupancy or greater were imported into Geneious (Kearse et al., 2012) for manual inspection, wherein we removed non-orthologous samples (i.e. highly divergent sequences) and fixed obvious alignment errors (Hedin, Derkarabetian, Alfaro, Ramírez, & Bond, 2019).

As mitochondrial reads are commonly sequenced as by-products with UCE libraries, we also searched for reads corresponding to cytochrome *c* oxidase subunit I (hereafter 'COI') in our assemblies using the PHYLUCE program "phyluce_assembly_match_contigs_to_barcodes". Previously published COI sequences for specimens of *Sorensenella* and *Karamea* were used as reference barcodes. Recovered COI sequences for each individual were aligned using MAFFT and manually inspected to ensure open reading frames. Due to the conserved length of COI across our samples, we did not employ gblocks to trim the alignment.

4.2.4 Matrix assembly

We created two matrices allowing for variable amounts of missing data: one containing only loci with at least 50% taxon occupancy (i.e. all loci with at least 39 taxa represented, "M50"); and one

containing loci with at least 75% taxon occupancy (loci with at least 59 taxa represented, "M75"). To account for the potential effect of heterogeneous nucleotide composition across samples biasing our phylogenetic reconstructions, we ran a chi-squared test on all loci in M50 with the program BaCoCa (Kuck & Struck, 2014) and created a matrix consisting of only the loci that passed the compositional homogeneity test with a *p*-value of > 0.95 ("Hom."). Finally, to account for the possibility of extreme evolutionary rates biasing reconstructions, we created a matrix ("Mid.") that excluded the fastest and slowest 20% of loci in M50, with the evolutionary rates calculated in TrimAl (Capella-Gutiérrez, Silla-Martínez, & Gabaldón, 2009).

4.2.5 Phylogenetic analysis

For all matrices, we performed a series of phylogenetic analyses covering maximum likelihood (ML), Bayesian inference (BI), and species tree methods. For ML and BI analyses, loci for each matrix were concatenated together in PHYLUCE using the program "phyluce_align_format_nexus_files_for_raxml". ML analysis was performed in IQ-TREE-MPI v1.6.10 (Nguyen, Schmidt, von Haeseler, & Minh, 2015), partitioned by UCE locus (Chernomor, von Haeseler, & Minh, 2016) with nodal support assessed using 1500 ultrafast bootstrap (UFBoot) replicates (Hoang, Chernomor, von Haeseler, Minh, & Vinh, 2018). Model and partition testing were done using ModelFinder (-m MFP+MERGE) (Kalyaanamoorthy, Minh, Wong, von Haeseler, & Jermiin, 2017), and each partition was allowed its own set of branch lengths to account for heterotachy (-sp flag). BI tree searches were run in ExaBayes 1.5 (Aberer, Kobert, & Stamatakis, 2014) using two runs of two chains and up to 2 million generations, until the average standard deviation of split frequencies was below 5%. A consensus of both runs was created, discarding the first 25% of trees as burn-in. Finally, we used the concatenation-free species tree method ASTRAL 4.10.12 (Mirarab et al., 2014) to account for the potential biasing effect of concatenating loci with

conflicting gene genealogies. Individual gene trees for ASTRAL input were generated for each UCE locus using RAxML v 8.2.11 (Stamatakis, 2014) under the GTRGAMMAX model.

Due to inconsistent relationships between some major clades of *Sorensenella* when analyzed under different inference methods, we also performed an approximately unbiased (AU) topology test (Shimodaira, 2002) in IQ-TREE to assess whether one of the possible tree topologies was significantly worse than the other. First, we generated a guide tree (without branch lengths) whose interspecific relationships in *Sorensenella* were constrained to follow the alternative branching pattern. We then performed an ML tree search under that constrained topology in IQ-TREE (-g flag) for the M50 dataset. Finally, we compared the unconstrained M50 ML tree to the constrained tree using the AU test and 10,000 RELL (Kishino, Miyata, & Hasegawa, 1990) replicates.

4.2.6 Molecular dating

Because there are no known triaenonychid fossils with which to calibrate a phylogeny, and because of the shallower nature of this phylogenetic study, we employed a divergence dating strategy using published substitution rates of COI for spiders (family Dysderidae; Bidegaray-Batista & Arnedo, 2011) and insects (tenebrionid beetles; Papadopoulou, Anastasiou, & Vogler, 2010). These rates constitute the phylogenetically closest comparisons available to *Sorensenella* and *Karamea*, and while mitochondrial substitution rates in at least some groups of harvestmen (Cyphophthalmi) are known to be accelerated (e.g. Boyer, Baker, & Giribet, 2007; Clouse & Wheeler, 2014; Fernández & Giribet, 2014; Young & Hebert, 2015), we believed it preferable to employ at least one method of divergence dating rather than forgo it entirely, as Laniatores do not seem to have unusual mitochondrial evolutionary rates.

We used an iterative strategy to identify the best clock model and tree prior for our COI dataset using the Path sampler application in BEAST 2.4.7 (Bouckaert et al., 2014; Xie, Lewis, Fan,

Kuo, & Chen, 2011). First, we ran three path sampling analyses all under a Yule tree prior with 100 steps of 1 million generations, corresponding to a strict clock, an exponential relaxed clock, and a lognormal relaxed clock. Marginal likelihood estimates were compared using Bayes Factors to select the best clock model. We then ran another path sampling analysis under the best clock model, but under a birth-death speciation tree prior. Marginal likelihood estimates of the two analyzed tree priors were again compared with Bayes Factors. For all path sampling analyses, we applied the optimal site substitution model identified under BIC in the program ModelFinder (Kalyaanamoorthy et al., 2017).

Finally, we estimated lineage ages in BEAST 2 under the best clock model and tree speciation prior, with three different clock rates. For the spider-derived rate, we set the clock rate prior (ucld.mean) to 0.0199 (lower: 0.0136; upper: 0.027), corresponding to the mean lognormal clock estimate and 95% highest density probability (HPD) from Bidegaray-Batista and Arnedo (2011). However, for the insect-derived rate, Papadopoulou et al. (2010) provide two COI rates: one for unpartitioned analyses, and a second for partitioned analyses in which the first and second codon positions are separated from the third position. This is their preferred strategy, as the separate partition for position three should mitigate potentially negative effects of saturation when applying a molecular clock. For the unpartitioned insect rate we specified the clock rate as 0.0169 (95% HPD: 0.015–0.0188), and for the partitioned arthropod rate the clock rate was set to 0.0178 (95% HPD: 0.0159–0.0197). The site substitution models applied to the partitioned analysis were chosen under BIC in ModelFinder. Four runs of 200 million generations each were launched for the three different clock rate analyses (hereafter "spider", "insect", and "partitioned"). Stationarity and convergence of runs was confirmed in Tracer v1.6 (Rambaut & Drummond, 2009), with all ESS values >200.

4.2.7 Calling SNPs from UCE loci

SNP datasets were assembled for both *Sorensenella* and *Karamea* from the cleaned M50 dataset, largely following the methods of Zarza et al. (2018) and Derkarabetian, Castillo, Koo, Ovchinnikov, and Hedin (2019). We used the majority-rule consensus sequence for each UCE locus in M50, generated in Geneious, as the reference genome. Adapter-trimmed and sanitized paired-end reads were aligned to the reference using bwa (Li & Durbin, 2009), and the resulting BAM files were sorted with SAMtools (Li et al., 2009). Picard (http://broadinstitute.github.io/picard) was used to identify and remove PCR duplicates and merge BAM files. This resulted in two merged BAM files: one for *Sorensenella* only, and one for *Karamea* only. We then used the Genome Analysis Toolkit (GATK) v 3.2 (McKenna et al., 2010) to search for indels and SNPs, realign reads, remove indels, and output SNPs with a Phred quality threshold of 30 or higher for each dataset. This workflow followed the recommendations of van der Auwera et al. (2013), including running a second pass through the GATK pipeline to ensure high-quality SNP calling. VCFtools was used to create SNP datasets with 75% taxon coverage, and one random SNP per locus was chosen using the script "rand_var_per_chr.pl" (github.com/caballero/Scripts). Resulting VCF files were converted to STRUCTURE format using the script "adegenet_from_vcf.py" (github.com/mgharvey/seqcap_pop) for use in subsequent species delimitation methods.

4.2.8 STRUCTURE

In order to characterize population substructure within each genus, we ran ParallelStructure (Besnier & Glover, 2013; Pritchard, Stephens, & Donnelly, 2000) via the CIPRES Science Gateway (Miller, Pfeiffer, & Schwartz, 2010). We specified an ancestry model allowing admixture and correlated allele frequencies, as we believed this model configuration would best reflect the turbulent geologic history of New Zealand and the resulting episodic changes in harvestman population connectivity through

time (following the recommendations of Porras-Hurtado et al., 2013). To determine the optimal number of groups within the species, we tested values of K = 1–12 for *Sorensenella* and K = 1–8 for *Karamea*, using 20 iterations for each K value and 100,000 Markov chain Monte Carlo (MCMC) generations following a burn-in of 50,000 generations. Optimal K value was determined using the deltaK method of Evanno, Regnaut, and Goudet (2005) implemented in STRUCTURE HARVESTER (Earl & vonHoldt, 2011), which compares the value of K to the rate of change of the likelihood function, and visual inspection of the change in *Ln P(D)* for each K value. In initial tests, we included the two South Island *Sorensenella* specimens (*S. bicornis bicornis* and *S. bicornis parva*). However, their inclusion largely obscured any other signal of genetic structure, likely due to the deep divergence between the North and South Island clades (see Sections 4.3.1 and 4.3.4), so these two samples were removed for all remaining species delimitation analyses.

As a second test of individual assignment to STRUCTURE group, a principal components analysis (PCA) was performed in the program GenoDive v3.03 (Meirmans & Van Tienderen, 2004) for each genus. Results were then imported into R for visualization.

4.2.9 VAE: Unsupervised machine learning clustering

Many methods to delimit species with genetic data are based on the multispecies coalescent model (e.g. Yang & Rannala, 2010). However, the application of these models has recently been called into question for delimiting population structure rather than species limits (Sukumaran & Knowles, 2017). This problem of disentangling species divergences from population structure is even more pronounced in short-range endemic (SRE) taxa (sensu Harvey, 2002), where ecological constraints and fragmented habitats lend dispersal-limited organisms an exceptionally high level of population structure (e.g. Fernández & Giribet, 2014; Hedin, Carlson, & Coyle, 2015; Thomas & Hedin, 2008).

To that end, we employed an unsupervised machine learning approach – a variational autoencoder (VAE) – to delimit species within *Sorensenella* and *Karamea*. This approach has previously been shown to accurately delimit closely related species of harvestmen with high population substructure (Derkarabetian, Castillo, et al., 2019). In this method, recoded SNP data is passed through a neural network (the "encoder"), which compresses the dimensionality of those data down into a reduced representation, wherein each sample has a mean (μ) and standard deviation (σ). This representation is then run through another neural net (the "decoder"), which generates a reconstruction of your input SNP data in the form of a two-dimensional plot.

VAE was implemented using the Keras python deep learning library (Chollet, 2015) and the TensorFlow machine learning framework (Abadi et al., 2016), utilizing a python script from Derkarabetian, Castillo, et al. (2019) to construct the VAE model and plot the results. SNP data matrices were translated to "one-hot" encoding such that each nucleotide was given a unique binary variable: A was coded as 1,0,0,0; C was 0,1,0,0; G was 0,0,1,0; and T was 0,0,0,1. Ambiguities from heterozygous sites were also considered, assigning 0.5 to each possible nucleotide (e.g. Y, which could be C or T, was coded as 0, 0.5, 0, 0.5). Missing data and indels (N or -) were coded as 0,0,0,0 and ignored by the model so as to prevent clustering of specimens solely based on the absence of data.

4.2.10 Population genomics

Basic population genetic statistics of the STRUCTURE- and VAE-identified species, as well as all individuals within each genus, were calculated in GenoDive (number of alleles observed per species [Num], observed [H_o] and expected [H_s] heterozygosity, inbreeding coefficients [G_{is}]). Population differentiation (F_{ST}) was also calculated for all species pairs with >1 individual in GenoDive, using 10,000 permutations to assess significance. Finally, a hierarchical analysis of molecular variance

(AMOVA) was performed in GenoDive using an infinite allele model and 1,000 permutations to assess significance. This was done in order to determine the relative amounts of genetic variation within individuals, species, and each genus as a whole.

4.3 Results

4.3.1 Phylogenetic relationships

UCE analysis included 79 specimens, and taxonomic coverage across each matrix is shown in Table 4.1. We recovered the reciprocal monophyly of both *Karamea* and *Sorensenella* in all analyses with full support (Figure 4.3). Within *Karamea*, we also found a highly stable topology between its major clades across all analyses with full support. These clades for the most part reflected the described morphospecies, with *K. tuthilli* constituting the sister group of all other species, with a deep divergence. However, specimens of the morphospecies *K. tricerata* were relatively deeply divided into two clades, which potentially could correspond to a species-level separation. Likewise, the two subspecies *K. lobata lobata* and *K. lobata australis* were recovered as each other's sister group, though whether this constituted a species-level divergence was unclear.

In *Sorensenella*, we similarly found multiple clades whose composition was stable across analyses, some of which corresponded to described morphospecies and others of which represented undescribed species. However, the relationships between some clades varied depending on inference method. In all analyses we recovered the two South Island species *S. bicornis bicornis* and *S. bicornis parva* as sister taxa. This clade was reciprocally monophyletic with the North Island *Sorensenella* species and separated by a very long branch, indicating an ancient divergence in the genus.

Within the North Island, we recovered a clade of (*S. rotara*, (*S. prehensor nitida*, (*S.* n. sp. "Southern", *S.* n. sp. "Central")))) where evert species-level node received maximal support in all analyses. All four of these species are distributed across the central and southern North Island (see

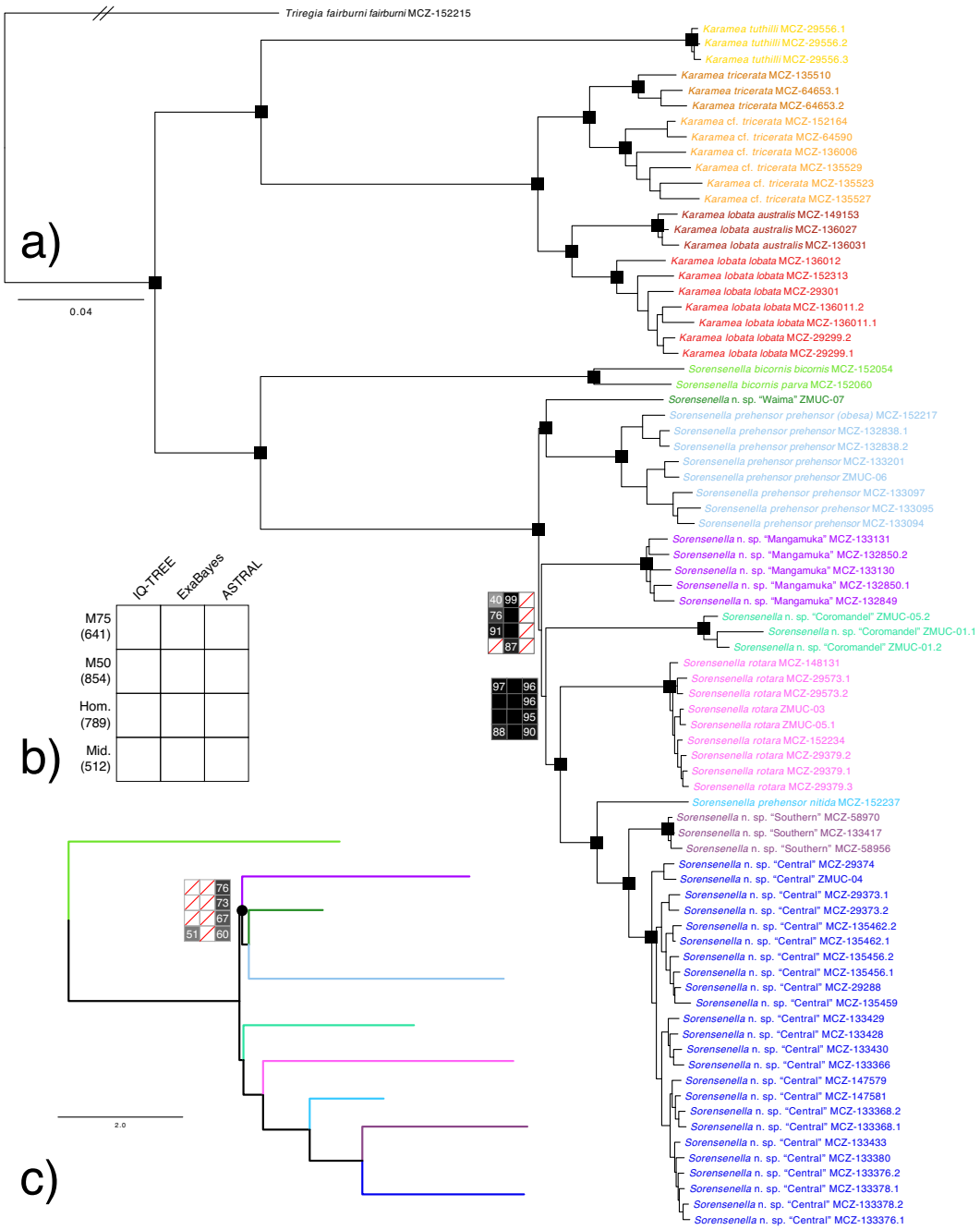

Figure 4.3 Phylogeny of *Sorensenella* and *Karamea* inferred from the largest matrix of UCE loci (M50) in ExaBayes. (a) Small black squares represent nodes which received maximal support in all analyses. Nodes in which at least one analysis did not give full support are shown with a plot, colored in grey scale by strength of support. Squares with red lines indicate analyses which did not recover the shown topology. Terminals colored by species, as in Figure 4.2. (b) Explanation of nodal support plot, as shown in (a) and (c). Numbers below matrix names refer to the total number of loci in the matrix. (c) Phylogeny of *Sorensenella* inferred from M50 in ASTRAL, with intraspecific branches collapsed and colored as in (a). Support plot drawn for the node that conflicted with the topology of (a), marked with a black circle.

Figure 4.2). We found another four genetic species that were all restricted to the Northland peninsula: *S. prehensor prehensor*, *Sorensenella* n. sp. "Waima", *Sorensenella* n. sp. "Mangamuka", and *Sorensenella* n. sp. "Coromandel". Notably, the morphologically distinct[2] subspecies *S. prehensor obesa* (MCZ-152217), which Forster (1954) described as restricted to the northernmost point of Cape Reinga on the Northland peninsula, resolved squarely inside the clade of *S. prehensor prehensor* with full support in all analyses. We therefore treat *S. prehensor obesa* as a junior synonym of *S. prehensor prehensor*. In all analyses, we recovered a sister-group relationship between the species from Waima and *S. prehensor prehensor*. In our ASTRAL analyses and the IQ-TREE analysis of "Mid.", we found this clade of *prehensor prehensor* + Waima as the sister group to the species from Mangamuka with moderate support (Figure 4.3c). However, in the ExaBayes and all other IQ-TREE analyses we recovered a grade in which the Waima + *prehensor prehensor* clade diverged first, followed by the species from Mangamuka. The AU test found the ASTRAL and IQ-TREE "Mid." topology to be significantly worse than the alternative topology, though (delta$L$ = 509.34; p-AU = 0.00567). Finally, all analyses placed *Sorensenella* n. sp. "Coromandel" as the sister group to the clade from central-southern North Island, with generally high support.

4.3.2 Species delimitation

Our SNP-calling pipeline resulted in final matrices of 387 SNPs in *Karamea* (22 individuals, 9.49% missing data) and 715 SNPs in *Sorensenella* (North Island only) (54 individuals, 5.49% missing data).

STRUCTURE analysis of *Karamea* identified an optimal K value of 2, separating out *K. tuthilli* from all other specimens, likely due to their deep phylogenetic split (see Figure 4.3). However, a

[2] *Sorensenella p. obesa* is differentiated from *S. p. prehensor* by its larger body size (scute length 4.18 mm vs. 3.17 mm, respectively), enlarged anterio-median tubercles, reduced anterior corner tubercles, and missing lateral tubercles (Figure 1a, b). However, there are no appreciable differences in their genitalia, which tend to be a source of reliable morphological characters for differentiating species within Triaenonychidae specifically and Laniatores generally.

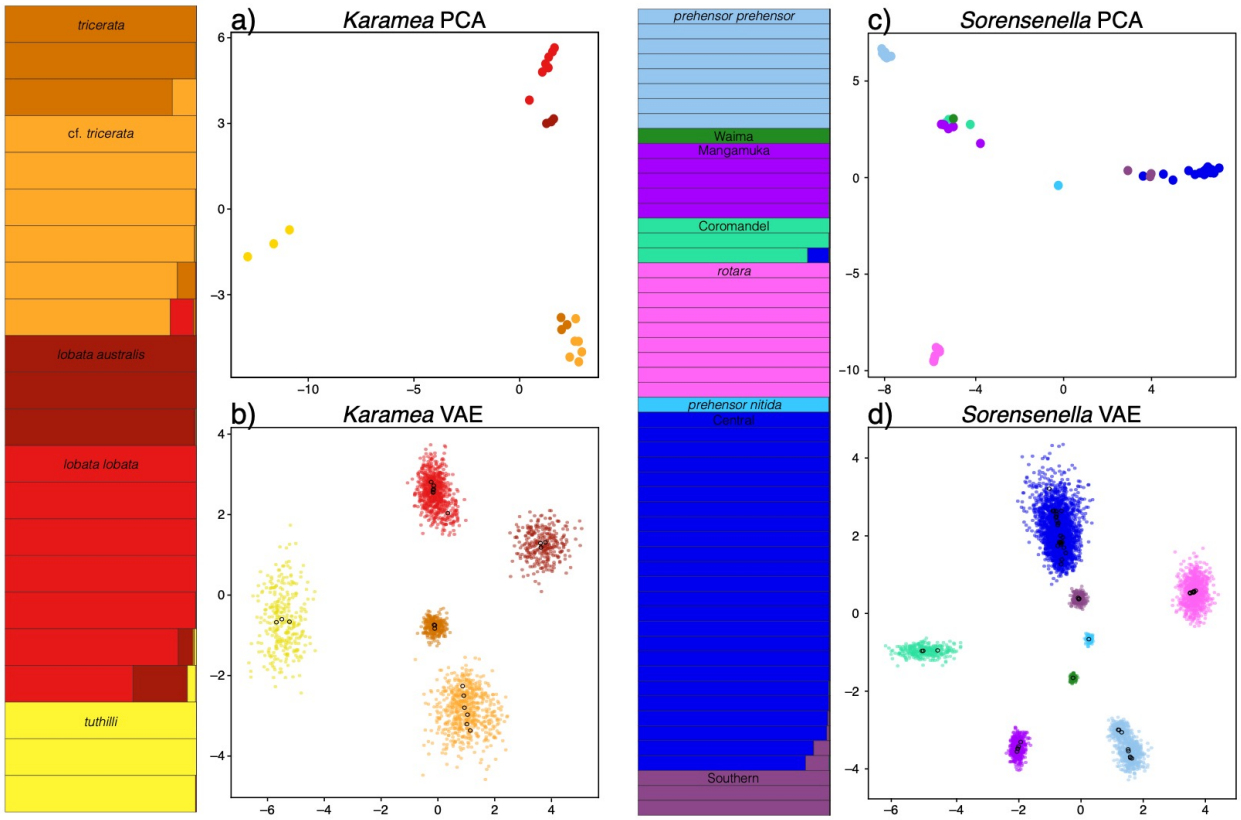

Figure 4.4 Results of species delimitation analyses for *Sorensenella* and *Karamea* from SNPs derived from UCE loci. STRUCTURE plots for each genus colored by cluster, as in Figures 4.2 and 4.3. (a) PCA plot for *Karamea* showing PC1 (32.79%) vs. PC2 (26.48%), with points colored by putative species. (b) VAE plot for *Karamea*, with standard deviations (σ, colored by species) and averages (μ, shown as open black circles) drawn for each specimen. (c) PCA plot for *Sorensenella* showing PC1 (35.53%) and PC2 (20.14%), with points colored by putative species. (d) VAE plot for *Sorensenella*, with standard deviations (σ, colored by species) and averages (μ, shown as open black circles) drawn for each specimen.

subsequent STRUCTURE analysis excluding *K. tuthilli* identified K=4 as optimal, separating out *K. lobata lobata*, *K. lobata australis*, and splitting *K. tricerata* in two groups (Figure B.1a). As such, we show the results for K=5 in Figure 4.4. Low levels of admixture were identified between *K. lobata lobata* and *K. lobata australis*, as well as between *K. tricerata* and *K.* cf. *tricerata*. A single specimen of *K.* cf. *tricerata* (MCZ-136006) showed small amounts of admixture with *K. lobata lobata* as well. Overall, though, samples were easily classified into one of the five clusters. This clustering scheme was corroborated by the VAE output, which clearly showed the samples separating into five distinct

groups with nonoverlapping standard deviations (σ, Figure 4.4b). The PCA plot of PC1 (32.79%) and PC2 (26.48%) showed this result less clearly, with *K. tuthilli*, *K. tricerata* + *K.* cf. *tricerata*, and *K. lobata lobata* + *K. lobata australis* forming well-separated clusters (Figure 4.4a). However, both *K. tricerata* and *K.* cf. *tricerata* as well as *K. lobata lobata* and *K. lobata australis* were more clearly differentiated when PC3 (9.98%, Figure B.1b) was considered.

Pairwise genetic differentiation (F_{ST}) between all putative species of *Karamea* was generally high (range of 0.438–0.955, Table 4.2), though given the small sample sizes (three individuals each) of *K. tricerata*, *K. lobata australis*, and *K. tuthilli*, all pairwise F_{ST} calculations between those three groups were non-significant. The one major exception to the generally high F_{ST} values was between *K. tricerata* and *K.* cf. *tricerata*, where F_{ST} was 0.438 ($p = 0.013$). This result is corroborated by the STRUCTURE plot, wherein they displayed moderate mutual signatures of admixture.

Table 4.2 Pairwise F_{ST} for *Karamea* species. Numbers below the diagonal show F_{ST} values, with significant values marked by an asterisk (*). Numbers above the diagonal show *p*-values for F_{ST} comparisons.

	tricerata	**cf. *tricerata***	***l. lobata***	***l. australis***	***tuthilli***
tricerata	—	0.013	0.007	0.100	0.098
cf. *tricerata*	0.438*	—	0.001	0.012	0.013
l. lobata	0.725*	0.666*	—	0.009	0.007
l. australis	0.749	0.652*	0.606*	—	0.097
tuthilli	0.915	0.879*	0.900*	0.955	—

STRUCTURE analysis of the North Island *Sorensenella* identified K=8 as the optimal number of clusters. Low levels of admixture were identified between *Sorensenella* n. sp. "Central" and *Sorensenella* n. sp. "Coromandel", as well as between *Sorensenella* n. sp. "Central" and *Sorensenella* n. sp. "Southern". All other species showed no signal of admixture. The VAE output recapitulated the STRUCTURE-identified clusters, all of which were well-defined with nonoverlapping standard deviations (Figure 4.4d). However, as in *Karamea*, these clusters were less obvious in the PCA plot of PC1 (35.53%) and PC2 (20.14%), displaying overlap between *Sorensenella* n. sp. "Central" and

Sorensenella n. sp. "Southern", as well as between *Sorensenella* n. sp. "Mangamuka", *Sorensenella* n. sp. "Coromandel", and *Sorensenella* n. sp. "Waima" (Figure 4.4c). Again, these STRUCTURE- and VAE-identified clusters were more clearly differentiated when additional PCs were considered (data not shown).

Table 4.3 Pairwise F_{ST} for *Sorensenella* species. Numbers below the diagonal show F_{ST} values, with significant values marked by an asterisk (*). Numbers above the diagonal show *p*-values for F_{ST} comparisons.

	p. prehensor	**Mangamuka**	**Coromandel**	***rotara***	**Central**	**Southern**
p. prehensor	—	0.001	0.007	0.000	0.000	0.006
Mangamuka	0.771*	—	0.018	0.001	0.000	0.018
Coromandel	0.792*	0.875*	—	0.004	0.001	0.100
rotara	0.859*	0.926*	0.950*	—	0.000	0.004
Central	0.855*	0.886*	0.895*	0.895*	—	0.000
Southern	0.797*	0.891*	0.932	0.958*	0.690*	—

Pairwise genetic differentiation between all species of *Sorensenella* with > 1 individual were high (F_{ST} range from 0.690–0.958, Table 4.3). The least differentiated species pair was *Sorensenella* n. sp. "Southern" and *Sorensenella* n. sp. "Central", again corroborating the results of STRUCTURE and PCA. Interestingly, despite showing some admixture in the STRUCTURE plot with *Sorensenella* n. sp. "Central", and overlapping with *Sorensenella* n. sp. "Mangamuka" in the PCA plot, *Sorensenella* n. sp. "Coromandel" was quite highly differentiated from all species (F_{ST} range =0.792–0.950). As in *Karamea*, the F_{ST} calculation between *Sorensenella* n. sp. "Southern" and *Sorensenella* n. sp. "Coromandel" was non-significant due to small sample sizes in each species.

Taken together, these results imply that the "subspecies" identified by Forster (1954) are in fact distinct species (e.g. *K. lobata lobata* and *K. lobata australis*; *S. prehensor prehensor* and *S. prehensor nitida*). While we were only able to include single exemplars of *S. prehensor nitida* and *Sorensenella* n. sp. "Waima", these two individuals were recovered as distinct species across multiple methods, and their species-level separation is further supported by the fact that these specimens are both males and exhibit unique morphologies. (As is the case for nearly all harvestman species, the morphospecies in

Forster (1954) are diagnosed by secondary sexual characters of males.) Indeed, for the recovered species "Waima", "Mangamuka", and "Central", we sequenced male specimens for our phylogeny, all of which do not correspond morphologically to any described species. The clades we are calling *Sorensenella* n. sp. "Coromandel" and *Sorensenella* n. sp. "Southern", however, were only represented in this study by females or juveniles. Therefore, future work will not only focus on formally describing the new species identified here, but will also target additional samples from those geographic areas in the hopes of finding males of those species.

Table 4.4 Indices of genetic diversity for all species as well as for both genera in aggregate. N: number of individuals sampled in each species; Num: number of alleles observed per species; H_o: observed heterozygosity; H_s: expected heterozygosity under equilibrium; G_{is}: inbreeding coefficient.

	n	Num	H_o	H_s	G_{is}
p. prehensor	8	1.164	0.014	0.058	0.759
Mangamuka	5	1.087	0.024	0.032	0.272
Coromandel	3	1.081	0.029	0.030	0.024
rotara	9	1.022	0.001	0.007	0.931
Central	24	1.129	0.008	0.026	0.706
Southern	3	1.012	0.006	0.006	-0.042
All *Sorensenella*	54	1.912	0.015	0.029	0.470
tricerata	3	1.158	0.054	0.069	0.222
cf. *tricerata*	6	1.287	0.056	0.093	0.396
l. lobata	7	1.245	0.037	0.064	0.417
l. australis	3	1.088	0.026	0.037	0.298
tuthilli	3	1.021	0.007	0.009	0.200
All *Karamea*	22	1.879	0.037	0.059	0.381

4.3.3 Genetic diversity within species

Within *Karamea*, the number of observed alleles (Num) was similar for all species (range: 1.021–1.287) (Table 4.4). Observed heterozygosity (H_o, the frequency of heterozygotes within each species) was low in all species, though substantially lower in *K. tuthilli* (0.007) compared to the other species (which ranged from 0.026–0.056). Expected heterozygosity (H_s, expected heterozygosity assuming Hardy-Weinberg equilibrium and corrected for sampling size) showed a similar pattern, where *K. tuthilli* again had a much lower value (0.009) compared to all other species (0.037–0.093). Despite this range in observed and expected heterozygosity values, inbreeding coefficients (G_{is}) were

similarly low in all species (range: 0.200–0.417), suggesting fairly low levels of inbreeding for each species. However, given the small sample sizes (especially for *K. tuthilli*, *K. tricerata*, and *K. lobata australis*), it is difficult to determine whether these results truly reflect higher levels of genetic diversity or simply limited data.

A hierarchical analysis of molecular variance (AMOVA), conducted to assess the partitioning of genetic variation between species of *Karamea*, within each species, and within individuals, indicated that a significant proportion of the total genetic diversity was found between species (75.9%, $p = 0.001$) (Table 4.5).

Table 4.5 Results of analysis of molecular variance (AMOVA) for *Karamea* species.

Source of variation	Nested in	%var	*F*-stat	*F*-value	Std. dev.	*p*-value
Within individual	—	0.149	F_{IT}	0.851	0.012	—
Between individuals	Species	0.092	F_{IS}	0.383	0.032	0.001
Between species	—	0.759	F_{ST}	0.759	0.016	0.001

We recovered a somewhat different pattern in the genetic diversity of *Sorensenella*. The number of observed alleles was similar in all species (range: 1.012–1.164, Table 4.4), and in line with our results for this metric in *Karamea*. However, observed heterozygosity was very low in all species, with an average H_o across all species of 0.015 (range: 0.001–0.029) compared to the average H_o of 0.037 in *Karamea*, and inbreeding coefficients for the different *Sorensenella* species showed dramatic variation (range: -0.042–0.931). The species *S. prehensor prehensor* and *Sorensenella* n. sp. "Central" had high G_{is} values (0.759 and 0.706, respectively), indicating high levels of inbreeding and/or isolation. This was somewhat surprising, given the fact that these two species are the most geographically widespread *Sorensenella* species (aside from *S. rotara*, see Discussion). But, given their low H_o and high G_{is} values, these species could have experienced previous population bottlenecks – a plausible hypothesis given the turbulent history of New Zealand. By contrast, G_{is} was lower and H_o was higher in the geographically restricted species from Mangamuka and Coromandel when compared to

other species of *Sorensenella*. It is worth noting, though, that while such low inbreeding coefficients may indeed reflect species with large, randomly mating populations, it is also possible that they are imprecise estimates due to limited sampling. Finally, the species *S. rotara* had a G_{is} value of 0.931, indicating extremely high levels of isolation and inbreeding. It also had the lowest observed and expected heterozygosity values of any species. Importantly, *S. rotara* is known only to contain females and juveniles, and this is unlikely to be an artefact of limited sampling, as dozens of specimens of this species have been collected and deposited in museum lots over the past century (Forster, 1954). This fact, coupled with its extremely low genetic diversity across a fairly broad geographic range, suggests that *S. rotara* may be parthenogenetic, a phenomenon reported in a few harvestman species (Burns, Hedin, & Tsurusaki, 2018; Wachter et al., 2016) but never before in Triaenonychidae.

Table 4.6 Results of analysis of molecular variance (AMOVA) for *Sorensenella* species.

Source of variation	Nested in	%var	*F*-stat	*F*-value	Std. dev.	*p*-value
Within individual	—	0.050	F_{IT}	0.950	0.004	—
Between individuals	Species	0.083	F_{IS}	0.627	0.025	0.001
Between species	—	0.867	F_{ST}	0.867	0.010	0.001

AMOVA analysis of *Sorensenella* indicated that the largest proportion of genetic diversity was attributable to variation between species (86.7%, $p = 0.001$, Table 4.6). The next largest source of genetic variation was found between individuals of the same species (8.3 %, $p = 0.001$), followed by 5% of variation found within individuals. These results support the idea of *Sorensenella* species as short-range endemics with very low dispersal abilities.

4.3.4 Divergence dating of *Sorensenella* and *Karamea*

Path sampling analysis of the COI alignment for *Sorensenella* and *Karamea* in BEAST identified a lognormal clock model and a birth-death tree as the optimal priors for the dataset, with decisive

support from Bayes Factors (BF = 69.31 compared to the next-highest model's marginal *L* estimate).

In our time-calibrated COI phylogeny, the estimated time of initial diversification of *Sorensenella* + *Karamea* was 40.4 Ma (95% HDP inclusive of all three clock rates: 21.6–66.4 Ma) (Figure 4.5). This age largely predates the end of the OMT (which peaked ~23 mya), though not in the 95% HPD of the chronogram calibrated with the spider substitution rate, which was the fastest rate we employed. This age somewhat contrasts with the results from Chapter 2, in which this clade was estimated to be 66.3 Ma (95% HPD: 41.4–90.5 Ma) based on fossil-derived calibrations of outgroup nodes, though the 95% confidence intervals do overlap over a period of about 20 Ma.

Karamea started diversifying ~ 27.6 mya (95% HPD: 12.3–48.7 mya), corresponding to the split between *K. tuthilli* and all other species. *Karamea tuthilli* itself was subtended by a long branch. *Karamea tricerata* + *K.* cf. *tricerata* diverged from *K. lobata lobata* + *K. lobata australis* ~16.8 mya (95% HPD: 7–29 mya), *K. lobata lobata* and *K. lobata australis* separated ~8 mya (95% HPD: 2.8–14.6 mya), and *K. tricerata* and *K.* cf. *tricerata* diverged ~5.3 mya (95% HPD: 2–9.5 mya). The median ages of the sampled specimens of *K. tricerata*, *K.* cf. *tricerata*, *K. lobata lobata*, and *K. lobata australis* were recovered as 0.72 Ma, 3.75 Ma, 0.47 Ma, and 2.9 Ma, respectively.

Sorensenella started diversifying *ca.* 33.7 Ma (95% HPD: 17.4–55.4 Ma), corresponding to the split between North Island and South Island species. The South Island species of *S. bicornis bicornis* and *S. bicornis parva* were found to have diverged ~13.6 mya (95% HPD: 2.9–28.7 mya), and the North Island *Sorensenella* was estimated to start diversifying at 17.4 Ma (95% HPD: 9.8–27.6 Ma). The relationships between North Island species in the COI chronogram showed some discordance with the topology supported by UCEs: while the COI tree recovered a monophyletic group of the species found in the Northland peninsula (*S. prehensor prehensor*, *Sorensenella* n. sp. "Waima", *Sorensenella* n. sp. "Mangamuka", and *Sorensenella* n. sp. "Coromandel") (albeit with posterior

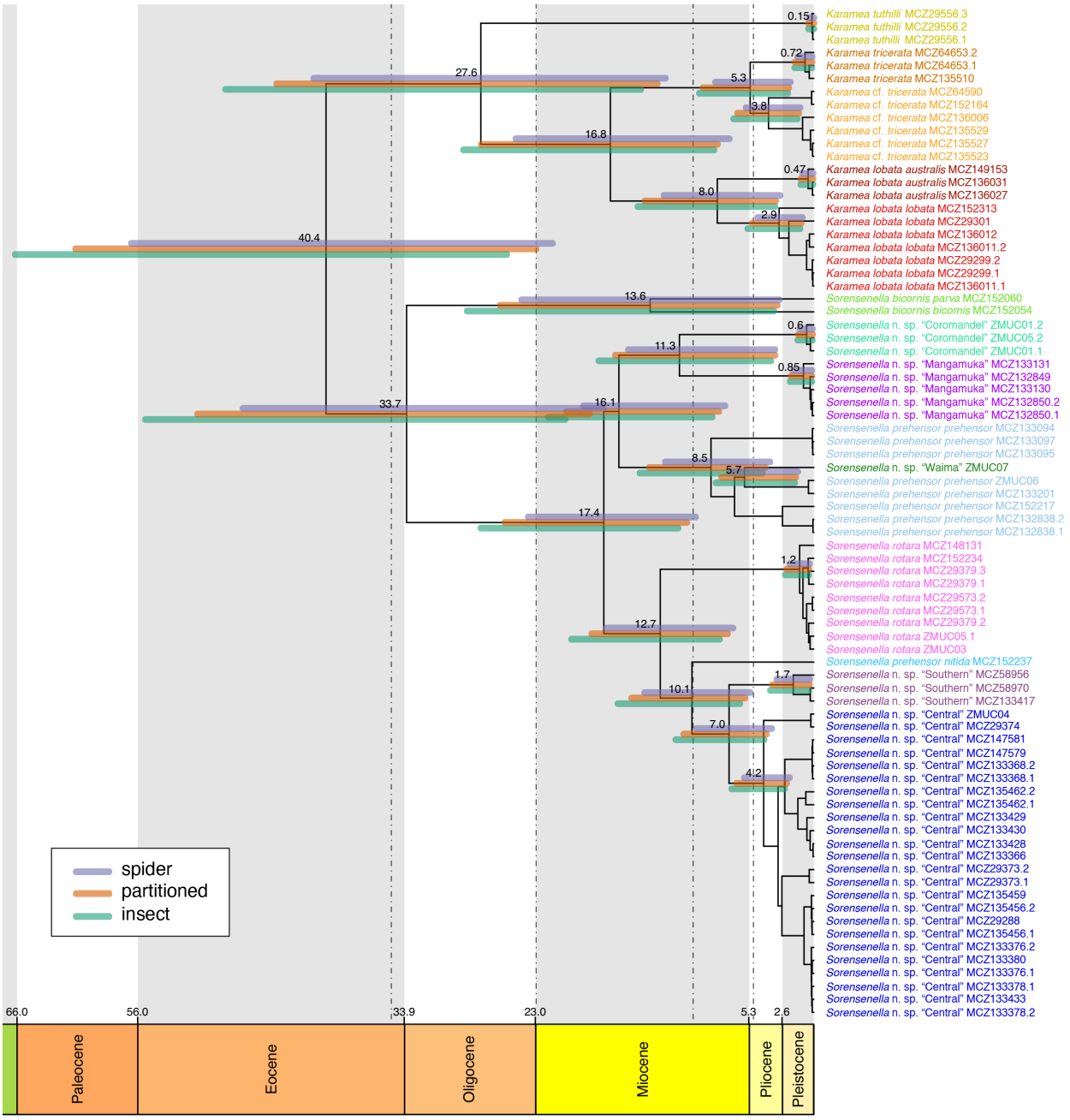

Figure 4.5 Dated COI phylogeny for *Sorensenella* and *Karamea*. Blue bars correspond to the 95% highest probability density (HPD) regions of the spider substitution rate, orange bars correspond to the 95% HPD regions of the partitioned substitution rate, and green bars correspond to the 95% HPD regions of the insect substitution rate. Terminals colored by species, as in Figures 4.2–4.4. Vertical dotted lines indicate major events in New Zealand's history: 35 Ma (start of the OMT); 23 Ma (ending peak of the OMT); 10 Ma (start of Southern Alps uplift); 5 Ma (end of major period of alpine uplift). Numbers at nodes refer to median inferred ages from the partitioned substitution rate analysis in millions of years.

probabilities < 0.95 in all relevant nodes), the UCE tree instead reconstructed these species as a grade (see Figures 4.3 and 4.5). Additionally, the COI tree placed *Sorensenella* n. sp. "Waima" inside *S. prehensor prehensor*, again with low support, limiting our ability to determine when those species diverged. Despite those limitations, we found that the taxa from Northland were estimated to have started diversifying in the Miocene, *ca.* 16.1 mya (95% HPD: 7.4–21.9 mya). *Sorensenella* n. sp. "Mangamuka" and *Sorensenella* n. sp. "Coromandel", both of which are known only from two geographically proximate localities, were recovered as very recent lineages (median ages 0.85 Ma and 0.6 Ma, respectively). By contrast, the clade comprising *S. prehensor prehensor* and *Sorensenella* n. sp. "Waima" had an estimated median age of 8.5 Ma. The group of species from central and southern North Island (*S. rotara*, *S. prehensor nitida*, *Sorensenella* n. sp. "Central" and *Sorensenella* n. sp. "Southern"), was in turn estimated to be 12.7 Ma (95% HPD: 6.7–20.1 Ma), with those species showing a variety of estimated ages: *Sorensenella* n. sp. "Central" was 4.2 Ma (95% HPD: 2–6.8 Ma); *Sorensenella* n. sp. "Southern" was 1.7 Ma (95% HPD: 0.4–3.6 Ma), and *S. rotara* was 1.2 Ma (95% HPD: 0.4–2.34 Ma).

4.4 Discussion

4.4.1 Diversification and biogeography of *Karamea*

The timing of major cladogenetic splits within *Karamea* (e.g. divergence between *K. tricerata* and *K.* cf. *tricerata* ~5.3 mya; divergence between *K. lobata lobata* and *K. lobata australis* ~8 mya) correspond to the start of the activation of the Alpine fault and subsequent uplift of the Southern Alps (10–5 mya) (Wallis & Trewick, 2009). Those four putative species are found in the mountainous northwest region of the South Island, and during the Pliocene and Pleistocene this area was exposed as high-elevation land and subjected to repeated glacial-interglacial cycling (Trewick & Bland, 2012). Their diversification may therefore be attributable to persistence in refugia as forests expanded and

contracted in response to climatic changes. *Karamea tuthilli*, which is known only from Aoraki/Mt. Cook (Forster, 1954), has a distant relationship with the other *Karamea* species (diverging ~27.6 mya) and low heterozygosity, and could therefore represent a relictual lineage that managed to survive through rampant extinction as the Southern Alps formed and then experienced extensive glaciation (Wallis & Trewick, 2009). This contrasts with *K.* cf. *tricerata* MCZ-152164, whose southernmost representative is found nearby to *K. tuthilli* (see Figure 4.2), but which diverged from its geographically distant sister taxon (MCZ-64590, separated by a linear distance of 236 km) only ~180 kya.

The morphospecies *K. lobata aurea* (from northwest South Island) and *K. trailli* (from the southernmost reaches of South Island and Stewart Island) were not available for inclusion in this study, but future work will attempt to incorporate UCE sequence data from museum material (Derkarabetian, Benavides, & Giribet, 2019) of these species to see how they relate to other species of *Karamea*. In particular, it will be interesting to see whether *K. trailli* appears to be a relictual lineage similar to *K. tuthilli*.

4.4.2 Diversification and biogeography of *Sorensenella*

The North Island and South Island *Sorensenella* clades diverged *ca.* 33.7 Ma, coinciding with the OMT and predating the severing of direct terrestrial connections between the North and South Islands from the early Miocene until the Pleistocene (Buckley et al., 2015; Bunce et al., 2009; Trewick & Bland, 2012). Within the South Island, the divergence between *S. bicornis bicornis* and *S. bicornis parva* (~13.6 mya) may have been driven by uplift of the Southern Alps. However, as we only have one exemplar per species we can make no claims about the potential roles of the South Island precipitation gradient, Pleistocene glaciation, and/or increased erosion across the Canterbury Plains as potential drivers of within-species diversification (Wallis & Trewick, 2009). Additionally, we were

not able to include the morphospecies *S. bicornis waikanae* in this study, which is hypothesized to be closely related to the species from the South Island despite being known from the southernmost portion of the North Island. As in *Karamea*, future work will attempt the sequencing of UCEs from museum specimens of this species to see how it is related to other *Sorensenella* species, particularly if it forms a clade with *S. bicornis bicornis* and *S. bicornis parva*, as suspected based on morphology (Forster, 1954).

With an estimated age of ~17.4 Ma, the clade of North Island *Sorensenella* largely post-dates the OMT, after which land area in the North Island expanded substantially (Cooper & Cooper, 1995). It therefore seems plausible that such a sudden expansion of habitable land and open niches allowed *Sorensenella* to rapidly diversify in the Northland peninsula and the Bay of Plenty area (i.e. the northernmost areas of the central North Island) during the mid- to late-Miocene. The phylogeny of the group suggests a general north-to-south colonization pattern, with a grade of early-branching species restricted to Northland and a derived clade of species from the central and southern North Island (Figure 4.3). The Northland peninsula has long been recognized as one of the most stable regions in New Zealand, harboring an increased level of endemism in both plants (McGlone, 1985) and insects (Buckley et al., 2015), and it is differentiated from the remainder of the North Island across the Kauri Line (Ellis et al., 2015), a taxonomically widespread phylogeographic break characterized by decreased genetic diversity to its south. Proposed mechanisms driving the reduced diversity south of the Kauri Line include extinction due to glaciation and/or volcanic eruptions in the last 100,000 years (Ellis et al., 2015). While those events completely post-date the estimated ages for *Sorensenella*, we do see a similar pattern in our data: the species from Northland (*S. prehensor prehensor*, *Sorensenella* n. sp. "Coromandel", and *Sorensenella* n. sp. "Mangamuka") exhibit overall higher genetic diversity as measured by observed heterozygosity (H_o: 0.014–0.029) compared to the central-southern species (*S. rotara*, *Sorensenella* n. sp. "Central", *Sorensenella* n. sp. "Southern"; H_o: 0.001–

0.008) (Table 4.4). A more plausible mechanism driving extinction and population bottlenecks in the central-southern species instead could be the formation of a wide marine seaway across much of the central North Island in the Pliocene (Bunce et al., 2009; Ellis et al., 2015; Trewick & Bland, 2012). This sea strait gradually retreated south, expanding the available land on the North Island until ~1 mya, when the North and South Islands regained a (brief) terrestrial connection. Our chronogram reflects such a pattern: *Sorensenella* n. sp. "Central" was estimated to have started diversifying ~4.2 mya, and its constituent lineages began diversifying ~2.6 mya or later, likely moving south into the newly available land after the bottleneck (Figure B.2).

Within the species that are represented by multiple populations and individuals, many divergences are estimated to be very recent (e.g. *Sorensenella* n. sp. "Mangamuka", *Sorensenella* n. sp. "Coromandel", *Sorensenella* n. sp. "Southern", *S. rotara*). These recent dates could potentially reflect the influence of Pleistocene glacial cycles causing forest habitat to expand and contract through time. Given the imprecision of our dating analyses and complete lack of fossils in the group, this is difficult to prove with certainty. That being said, the species *S. rotara* stands out among the listed examples due to its comparatively widespread distribution, with samples having been collected from places over 400 km apart across the North Island (not all of which were included in this study). This widespread distribution despite its quite recent origin, complete lack of discovered males, and extremely low genetic diversity all support the hypothesis that *S. rotara* is parthenogenetic (see Section 4.3.3). Many parthenogenetic species, including harvestmen, are often found in marginal or disturbed habitats (Burns et al., 2018; Cuellar, 1977; Peck, Yearsley, & Waxman, 1998; Wachter et al., 2016). Indeed, two species in the harvestman genus *Megabunus* are believed to have evolved parthenogenesis in response to Pleistocene glaciations across the European Alps; that is, given their doubly high intrinsic rate of increase, parthenogens could establish populations in recently unglaciated areas via longer-distance overland dispersal, thereby outcompeting bisexual lineages

(Wachter et al., 2016). *Sorensenella rotara* is sympatrically distributed with both *Sorensenella* n. sp. "Central" and *Sorensenella* n. sp. "Coromandel", and has even been collected in the same patch of leaf litter as these other *Sorensenella* species, undercutting the idea that they are restricted to marginal habitats. Nevertheless, the ecological niche of *S. rotara*, and indeed all species of *Sorensenella*, should be investigated.

4.5 Conclusions

In this study, we used UCE sequencing to delimit species and resolve the phylogeny of the New Zealand triaenonychid genera *Sorensenella* and *Karamea*. We found evidence of multiple undescribed species, particularly in *Sorensenella*, and found that an unsupervised machine learning approach to species delimitation worked effectively in this group of short-range endemics, confirming that many of the subspecies from Forster (1954) are in fact species. The biogeographic history of the group retains signatures of many major geologic and climatic events in New Zealand's history, including the OMT, formation of the Southern Alps, Pliocene sea level changes, and likely Pleistocene glacial cycles (though more precise dating estimates would be needed to confirm this hypothesis). This study points to several directions for future work on this group, including describing new species and exploring the ecological niche of the putative parthenogen *S. rotara*.

Appendix A

Supplement for Chapter 3

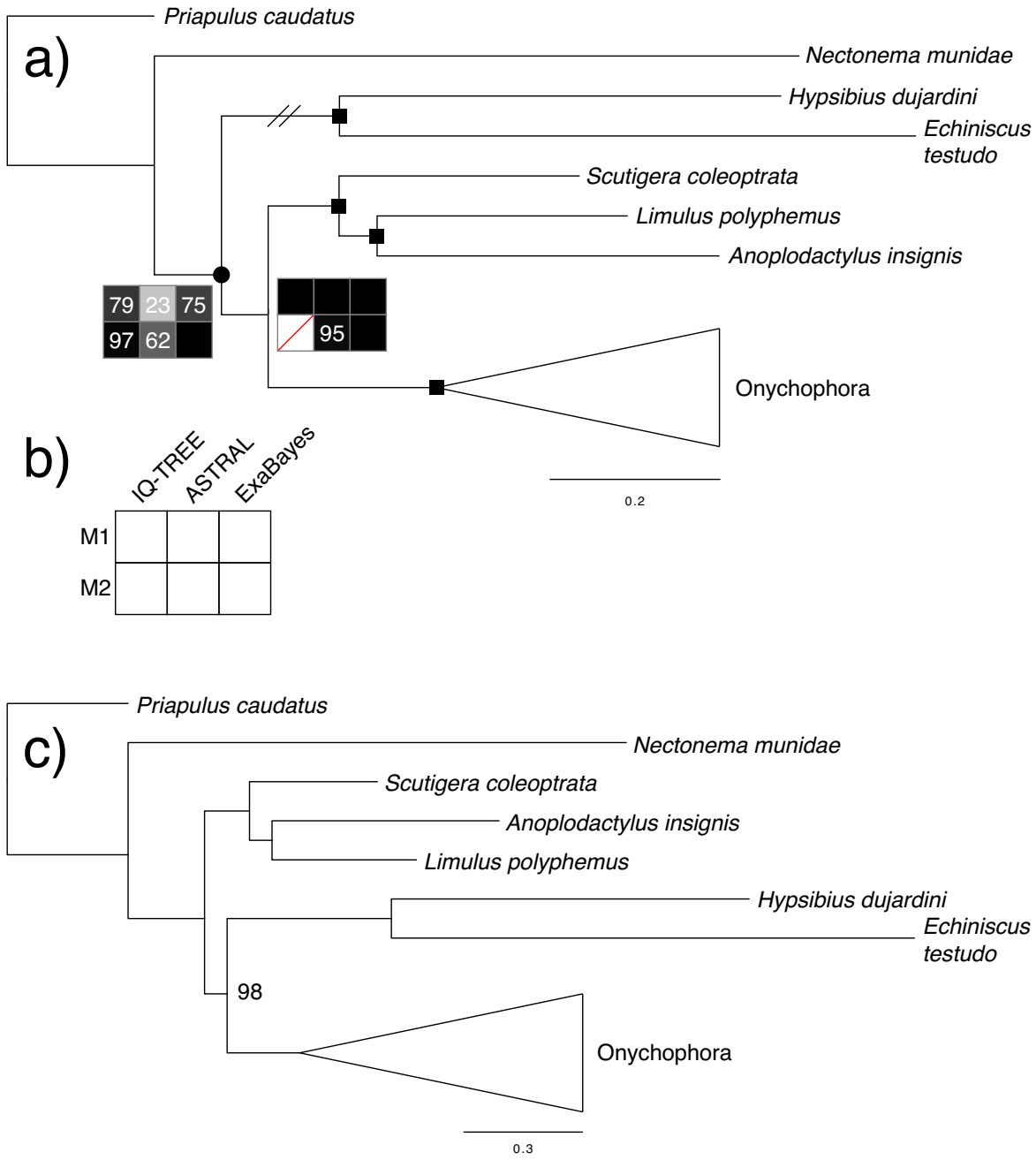

Figure A.1. Phylogenetic relationships of ecdysozoan outgroup taxa. (a) Phylogeny inferred from IQ-TREE analysis of M1. Small black squares indicate nodes that were recovered in all analyses with strong support (IQ-TREE and ASTRAL > 90, ExaBayes > 0.95). Support plots drawn at nodes that did not receive high support in all treatments. A white square with a red line through it indicates that relationship was not recovered in an analysis. (b) Explanation of support plot, as shown in (a). (c) Phylogeny inferred from IQ-TREE analysis of M2, showing alternative sister group relationship between Onychophora and Tardigrada. Number at node shows the ultrafast bootstrap support value.

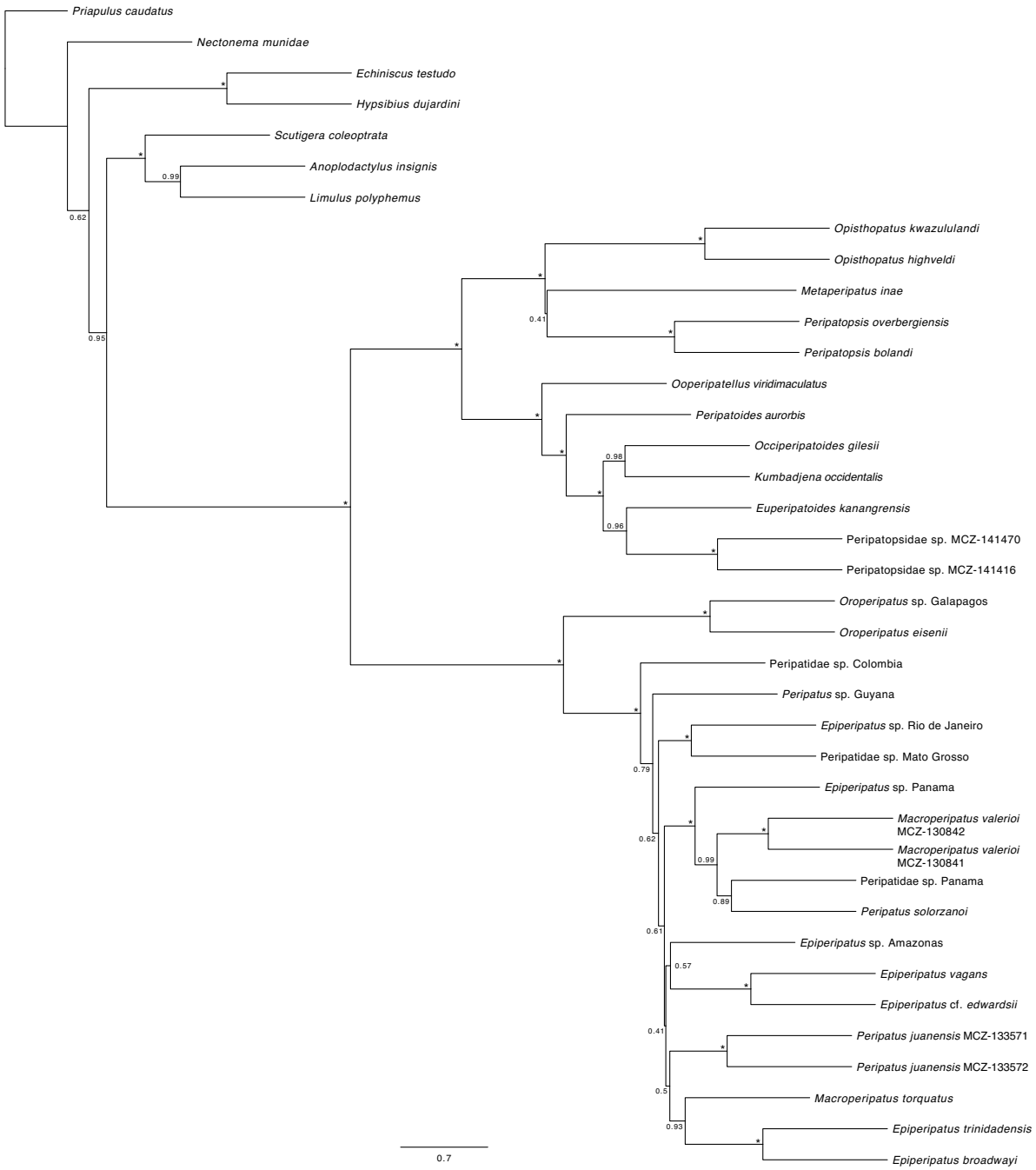

Figure A.2. Phylogeny inferred from ASTRAL analysis of M2. Asterisks (*) mark nodes with full support; remaining nodes show the proportion of quartets in the input gene trees that are congruent with the recovered species tree.

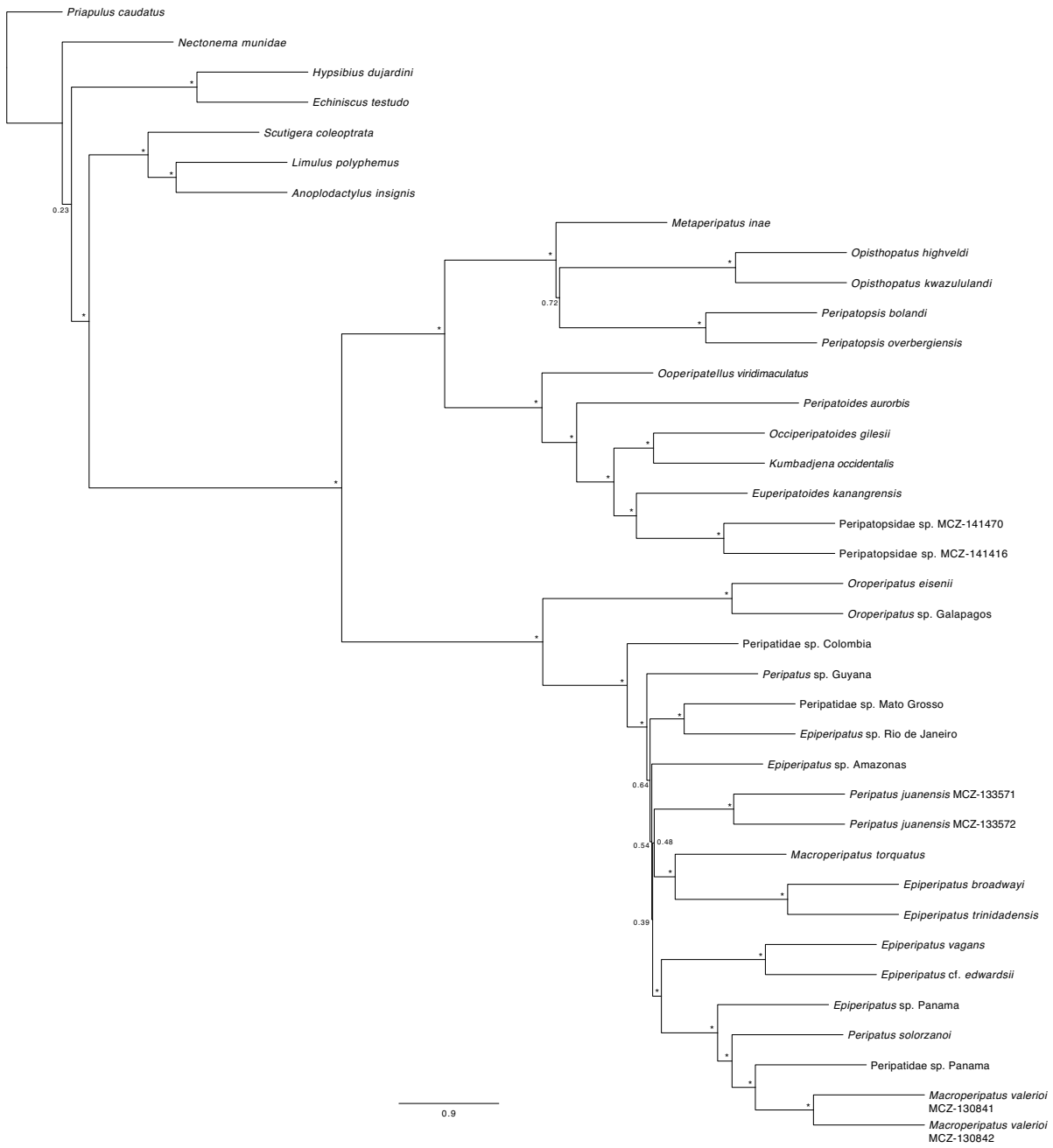

Figure A.3. Phylogeny inferred from ASTRAL analysis of M1. Asterisks (*) mark nodes with full support; remaining nodes show the proportion of quartets in the input gene trees that are congruent with the recovered species tree.

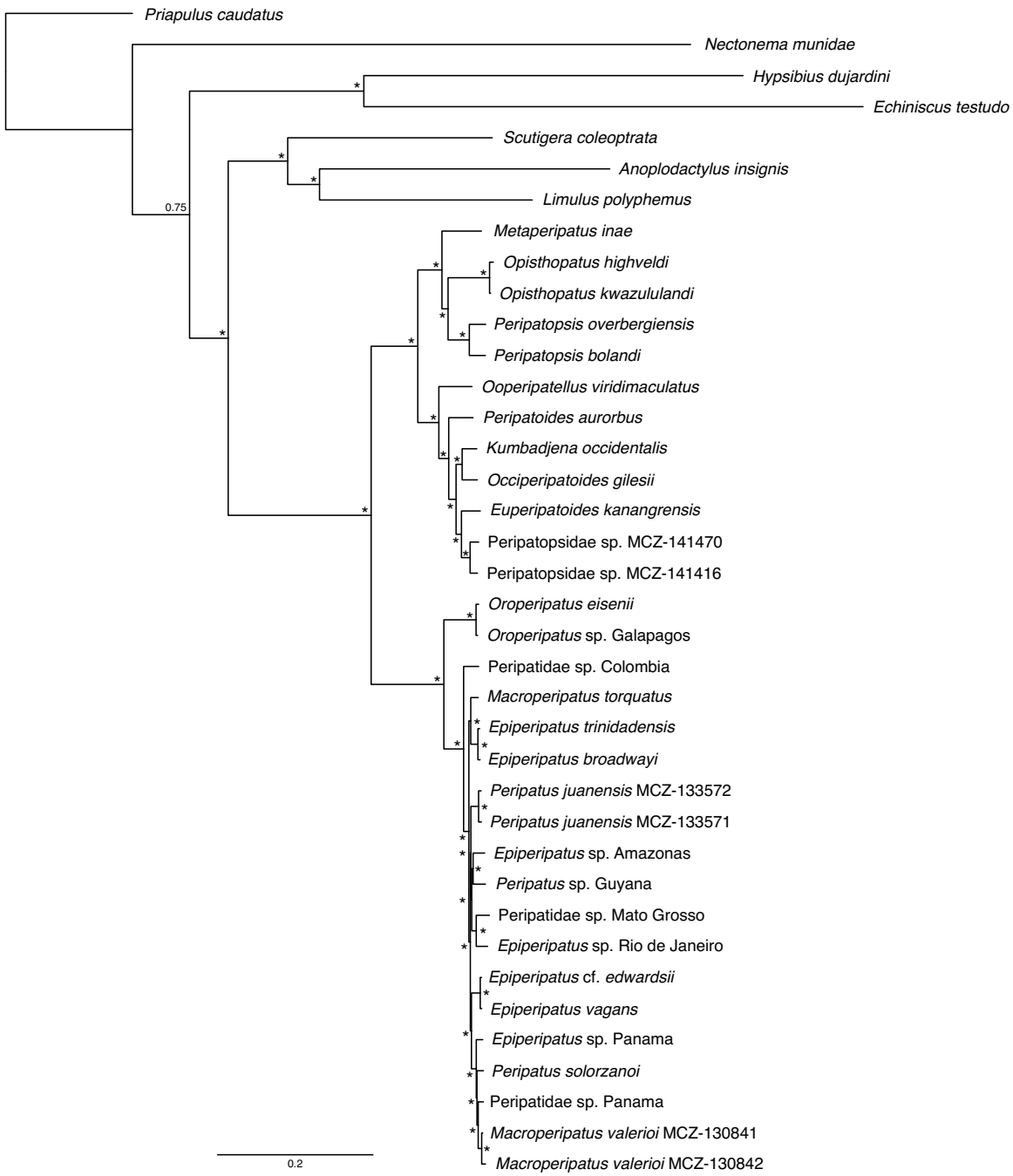

Figure A.4. Phylogeny inferred from ExaBayes analysis of M1. Asterisks (*) mark nodes with full support; remaining nodes show the posterior probability.

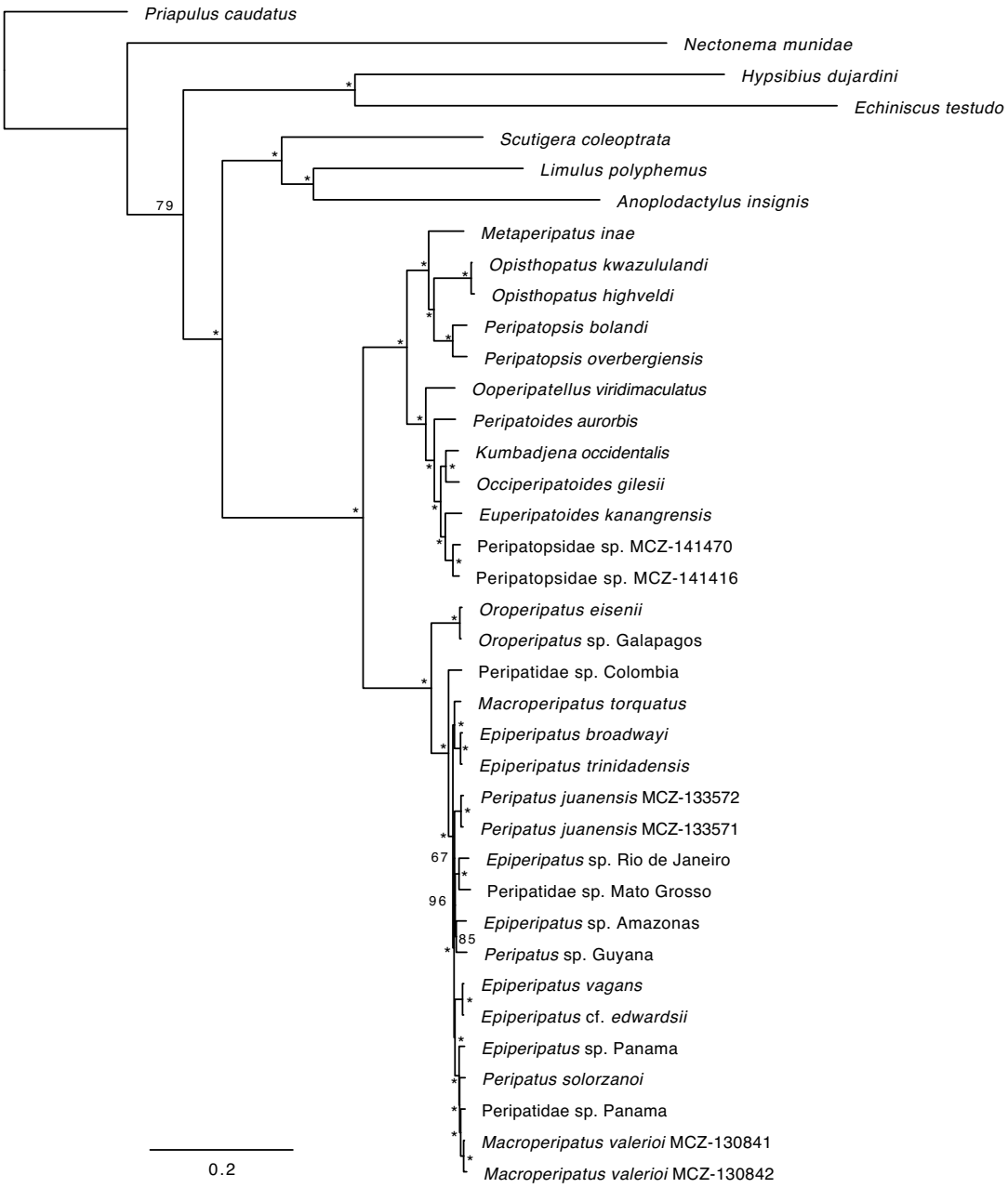

Figure A.5. Phylogeny inferred from IQ-TREE analysis of M1. Asterisks (*) mark nodes with full support; remaining nodes show the ultrafast bootstrap support value.

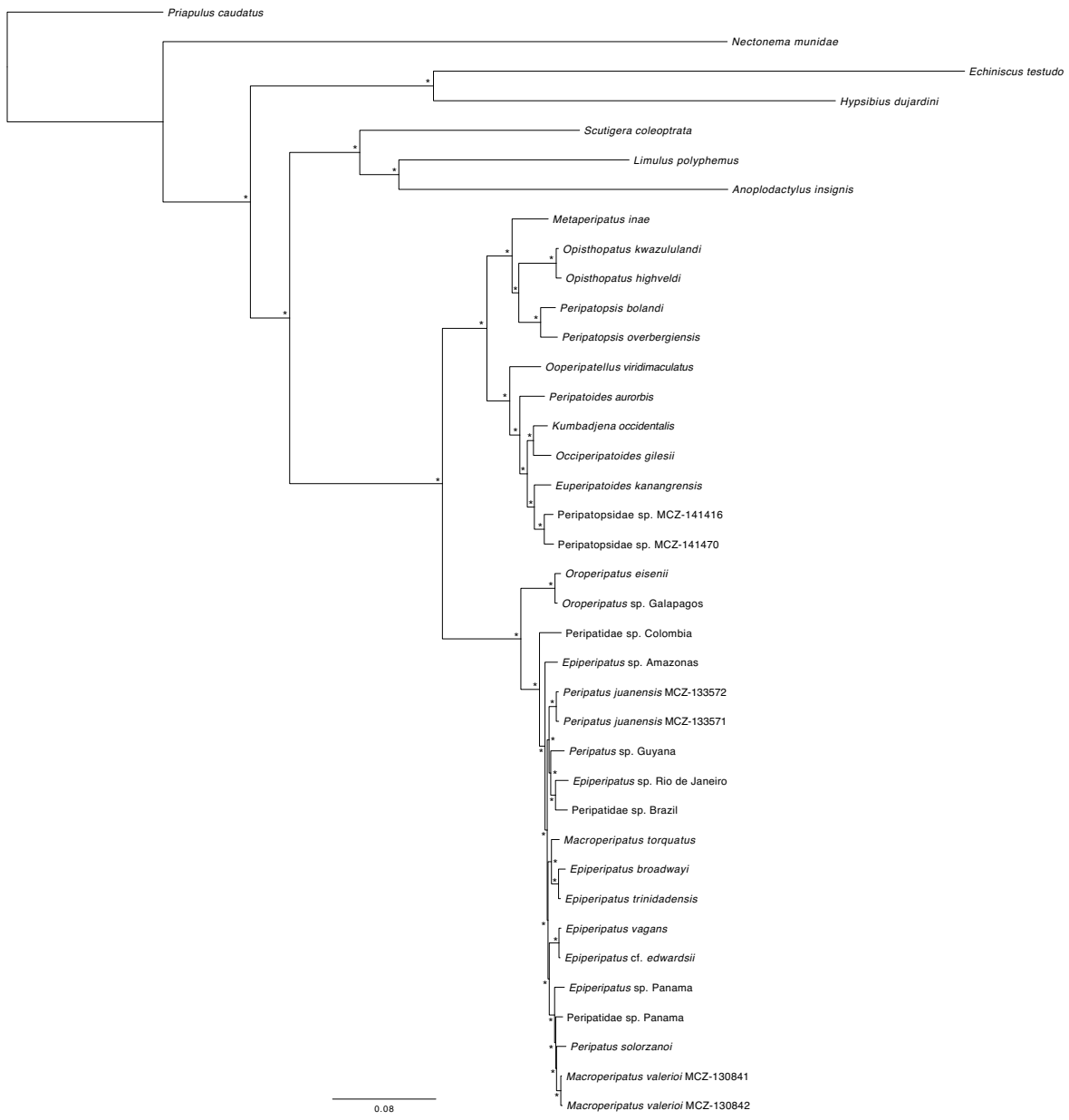

Figure A.6. Phylogeny inferred from ExaBayes analysis of M2. Asterisks (*) mark nodes with full support.

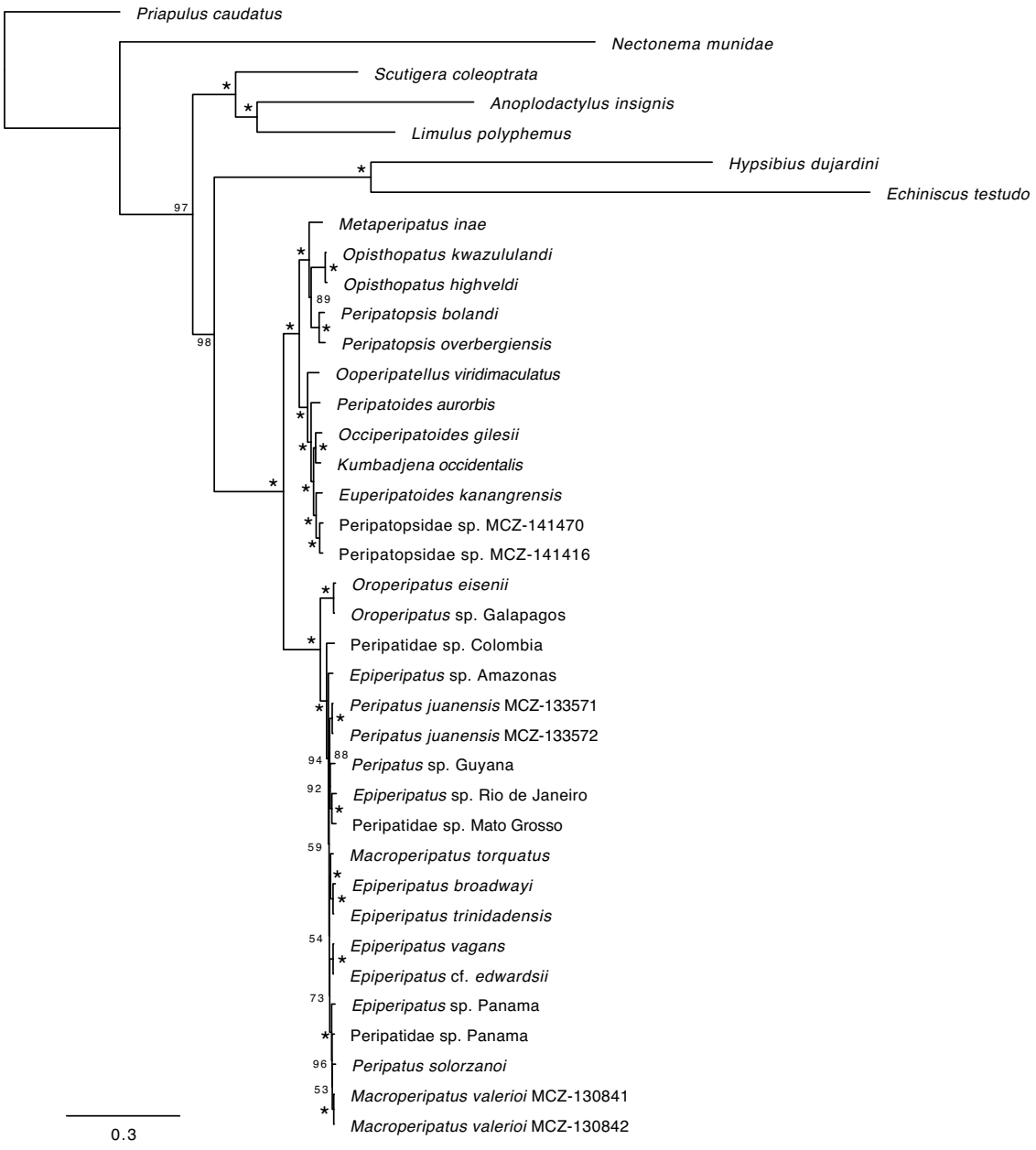

Figure A.7. Phylogeny inferred from IQ-TREE analysis of M2. Asterisks (*) mark nodes with full support; remaining nodes show the ultrafast bootstrap support value.

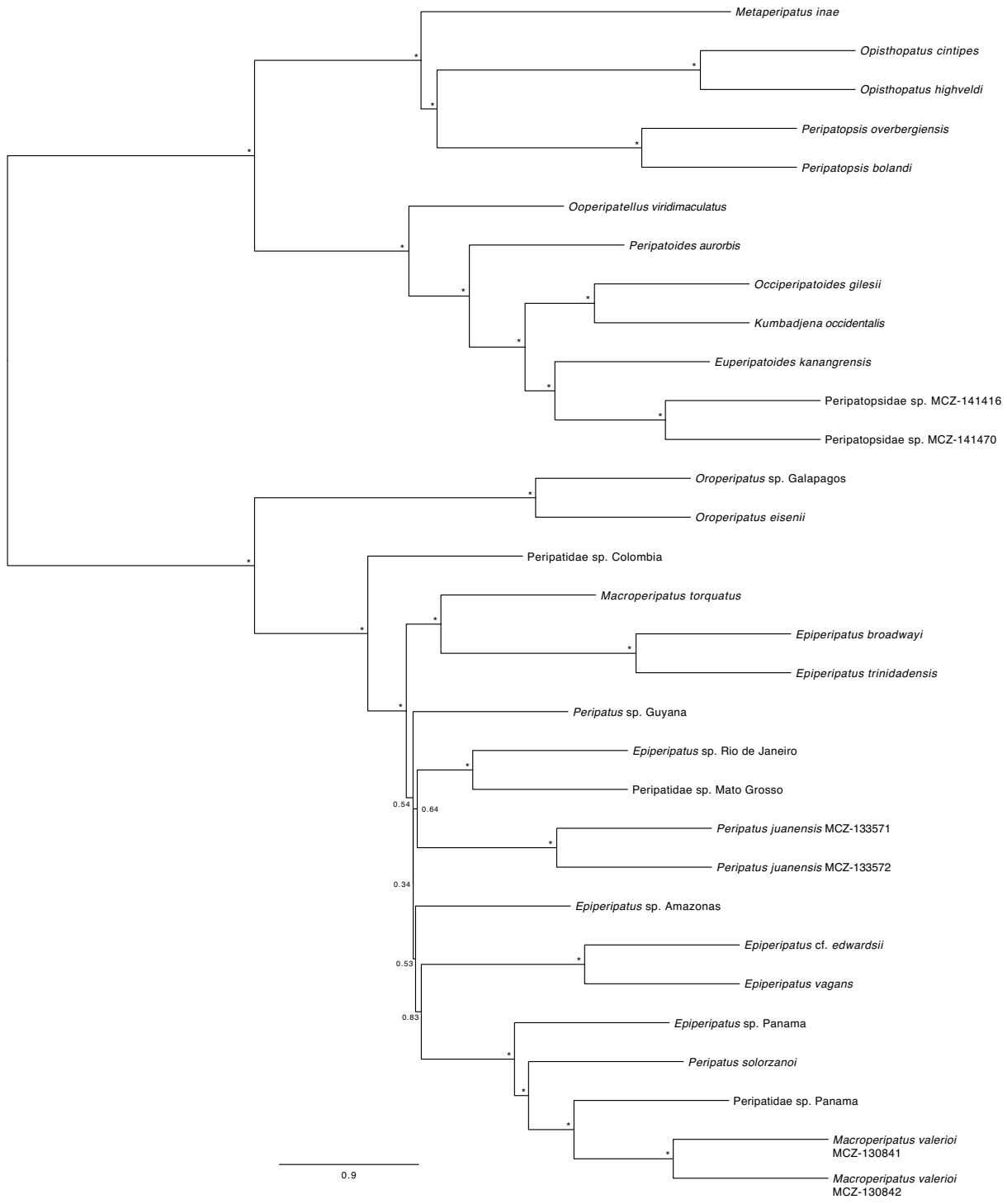

Figure A.8. Phylogeny inferred from ASTRAL analysis of M3. Asterisks (*) mark nodes with full support; remaining nodes show the proportion of quartets in the input gene trees that are congruent with the recovered species tree.

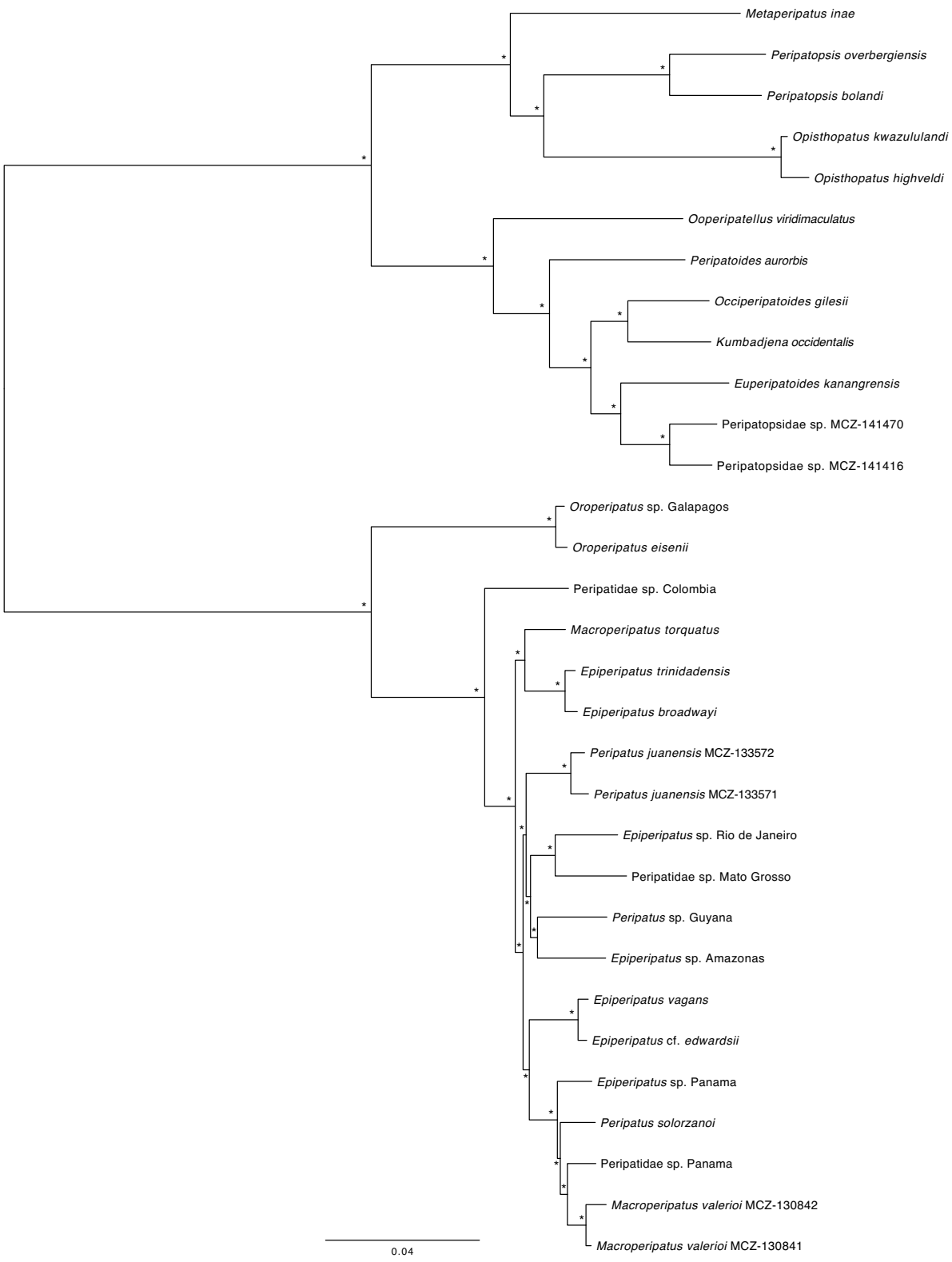

Figure A.9. Phylogeny inferred from ExaBayes analysis of M3. Asterisks (*) mark nodes with full support.

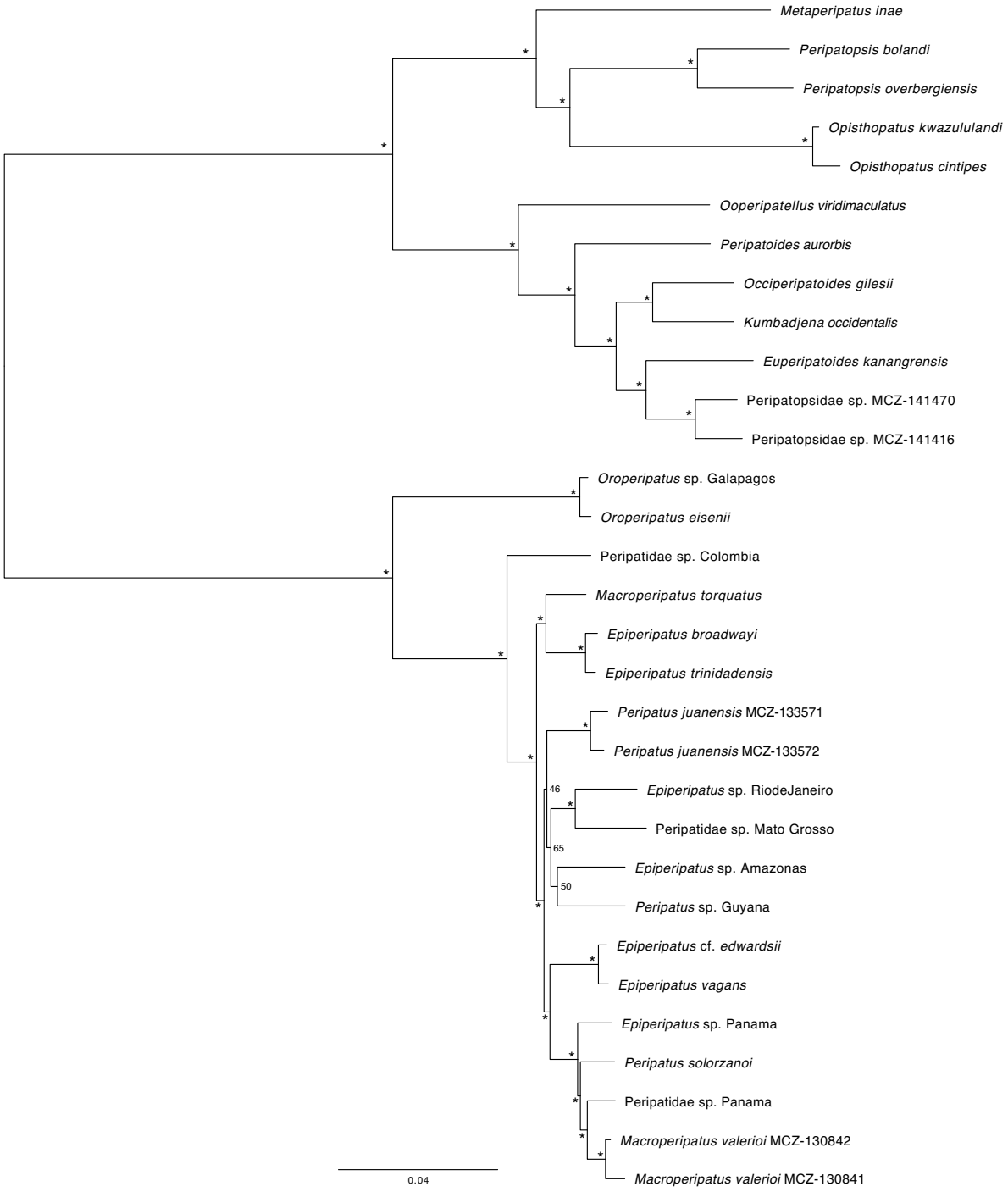

Figure A.10. Phylogeny inferred from IQ-TREE analysis of M3. Asterisks (*) mark nodes with full support; remaining nodes show the ultrafast bootstrap support value.

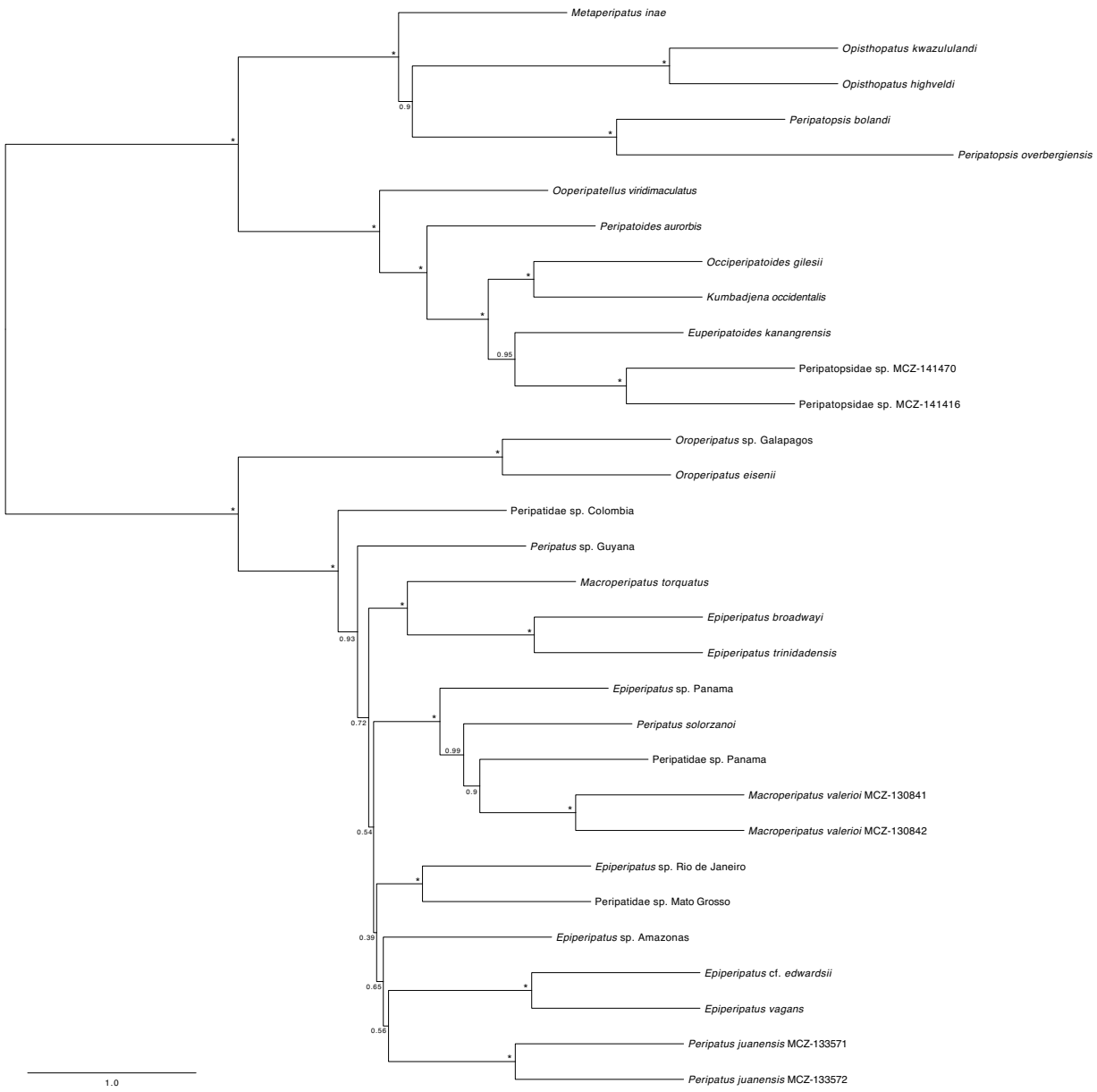

Figure A.11. Phylogeny inferred from ASTRAL analysis of M4. Asterisks (*) mark nodes with full support; remaining nodes show the proportion of quartets in the input gene trees that are congruent with the recovered species tree.

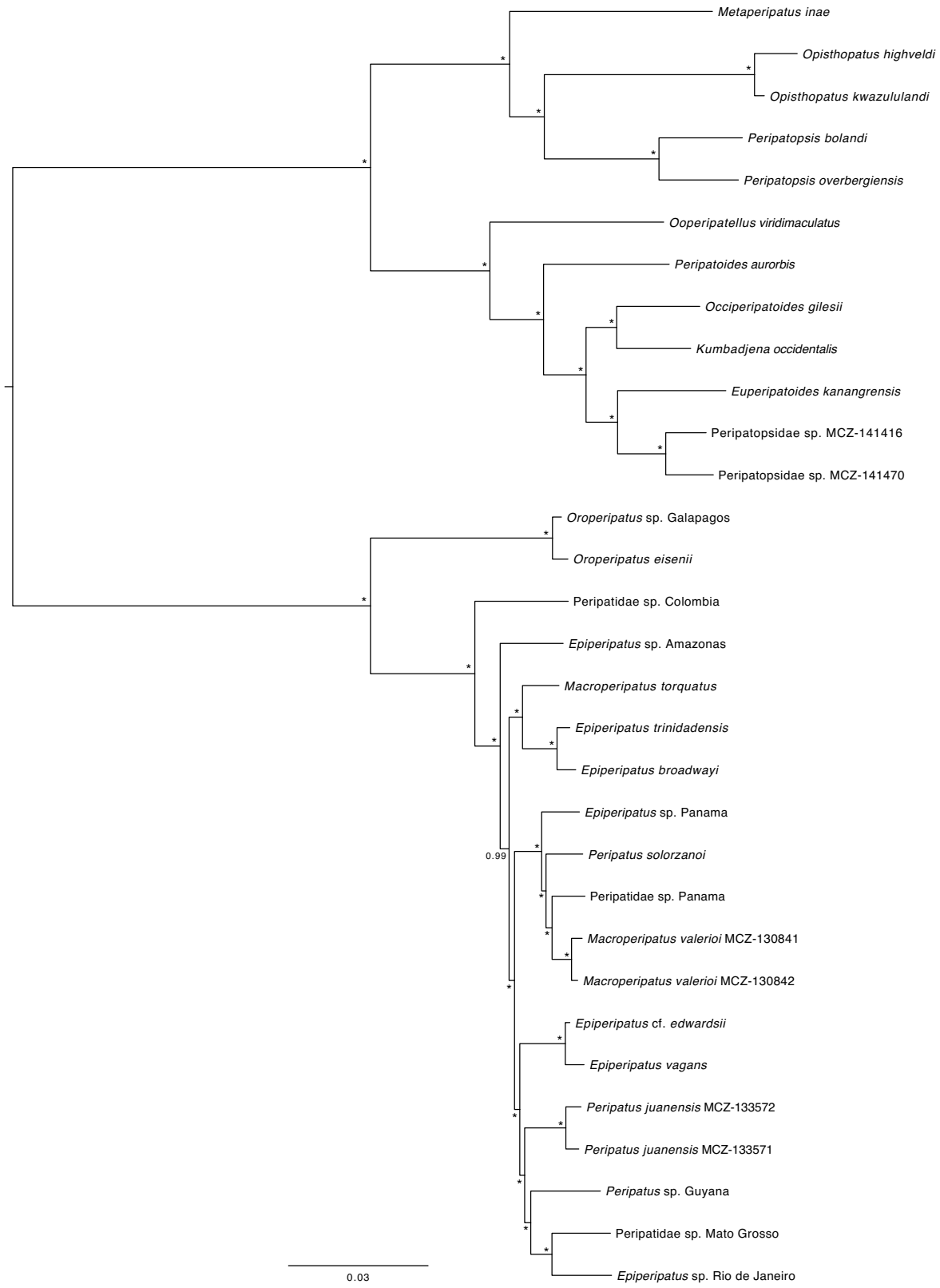

Figure A.12. Phylogeny inferred from ExaBayes analysis of M4. Asterisks (*) mark nodes with full support; remaining nodes show the posterior probability.

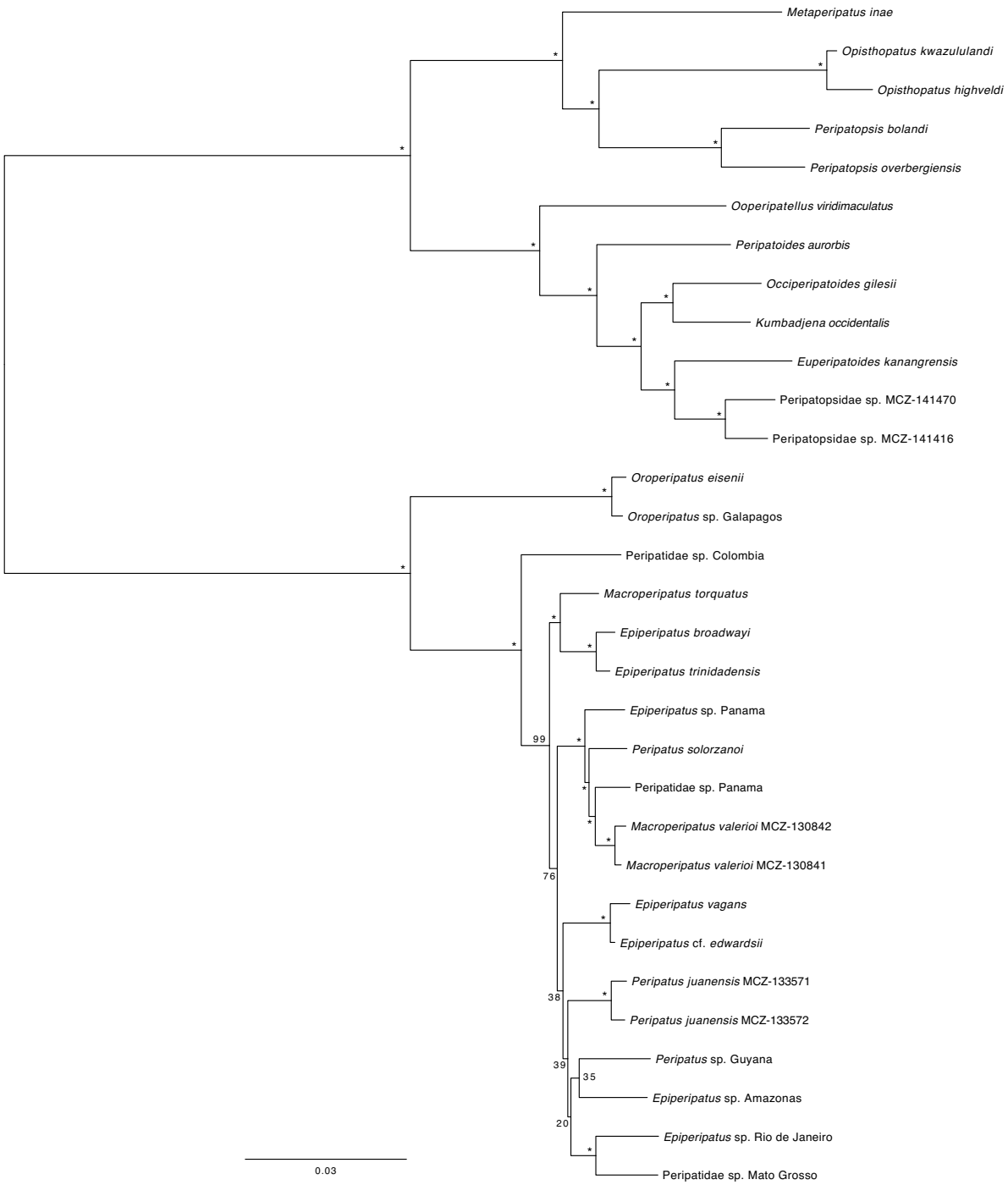

Figure A.13. Phylogeny inferred from IQ-TREE analysis of M4. Asterisks (*) mark nodes with full support; remaining nodes show the ultrafast bootstrap support value.

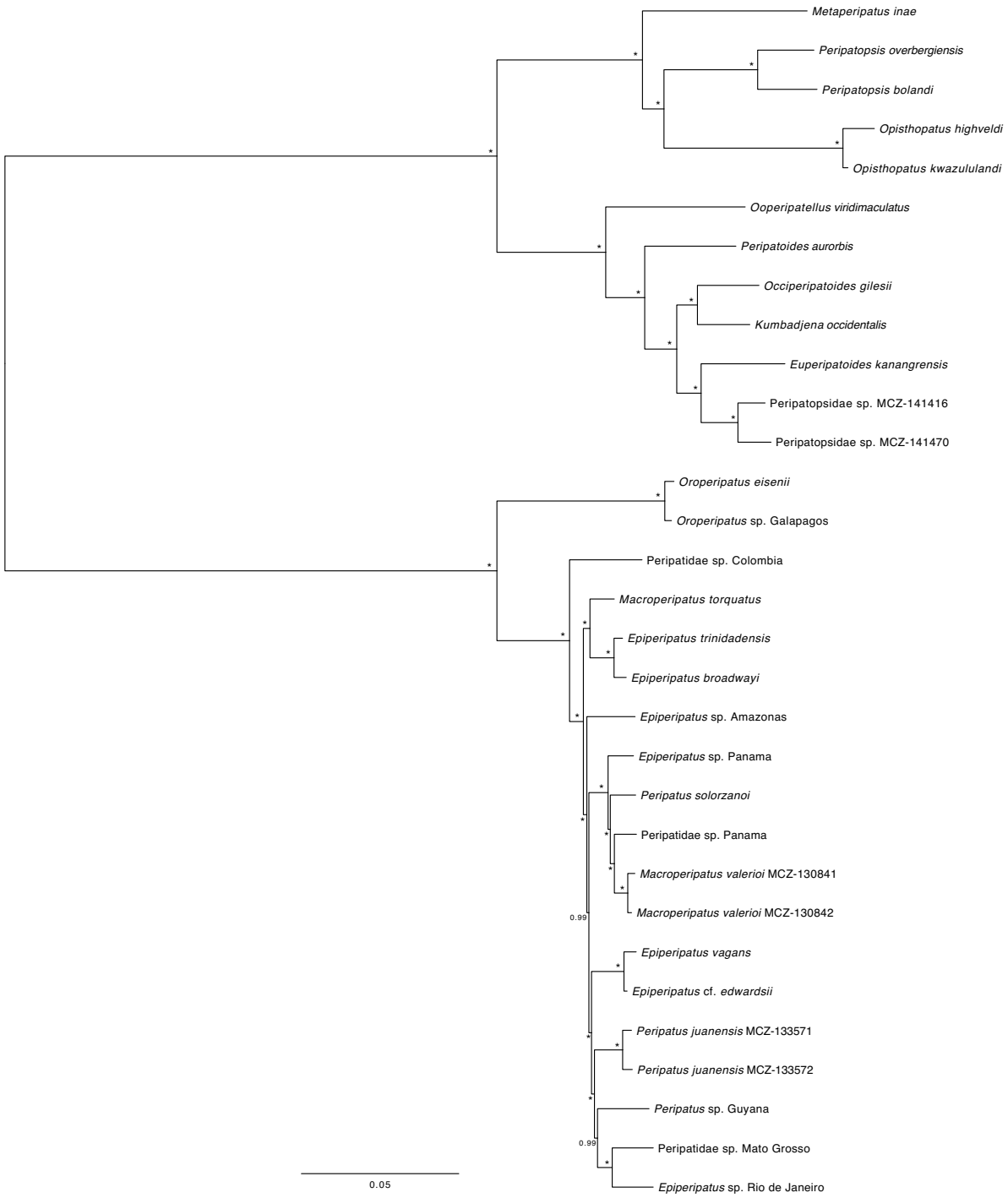

Figure A.14. Phylogeny inferred from PhyloBayes analysis of M4. Asterisks (*) mark nodes with full support; remaining nodes show the posterior probability.

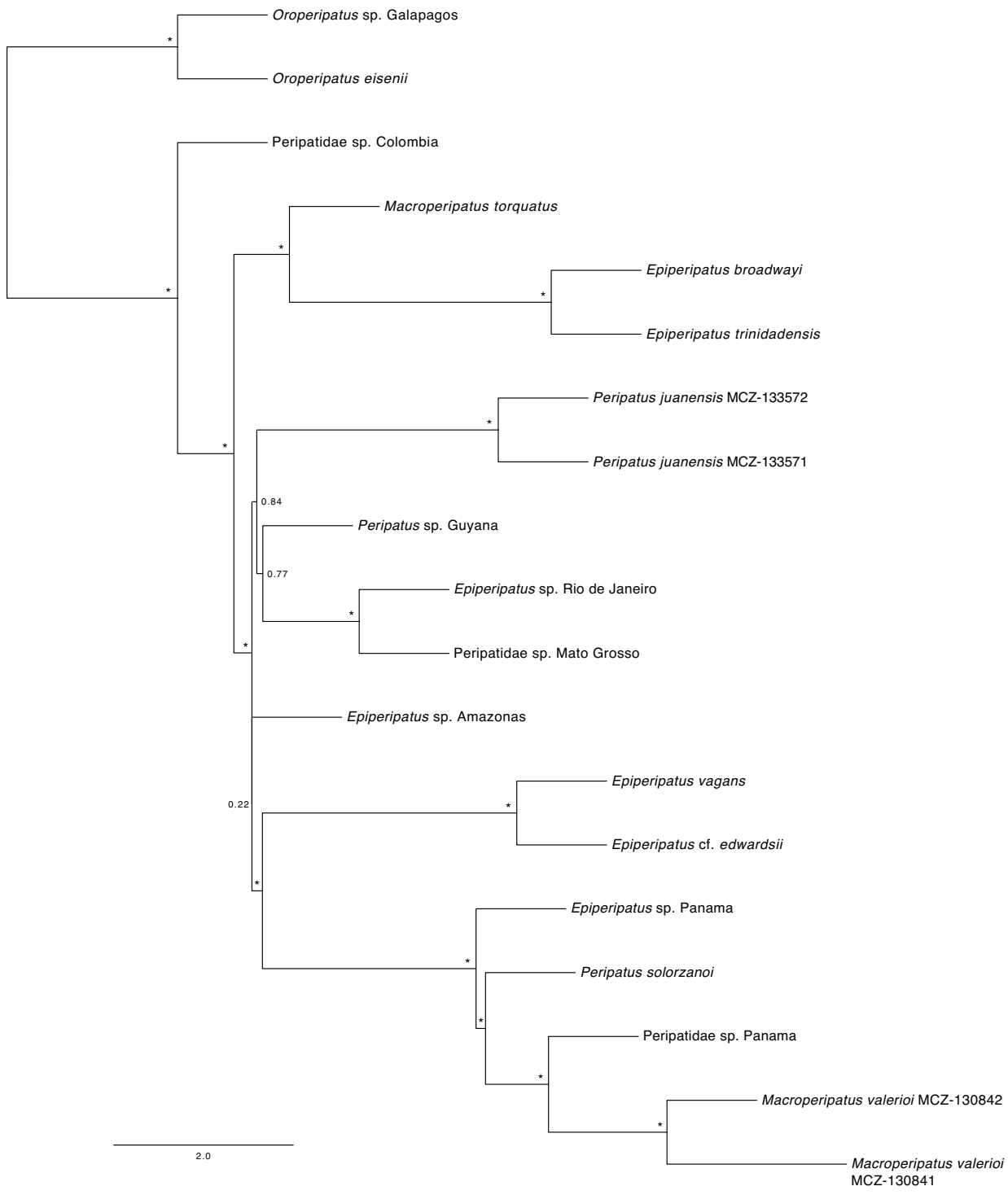

Figure A.15. Phylogeny of Neopatida inferred from ASTRAL analysis of M5. Asterisks (*) mark nodes with full support; remaining nodes show the proportion of quartets in the input gene trees that are congruent with the recovered species tree.

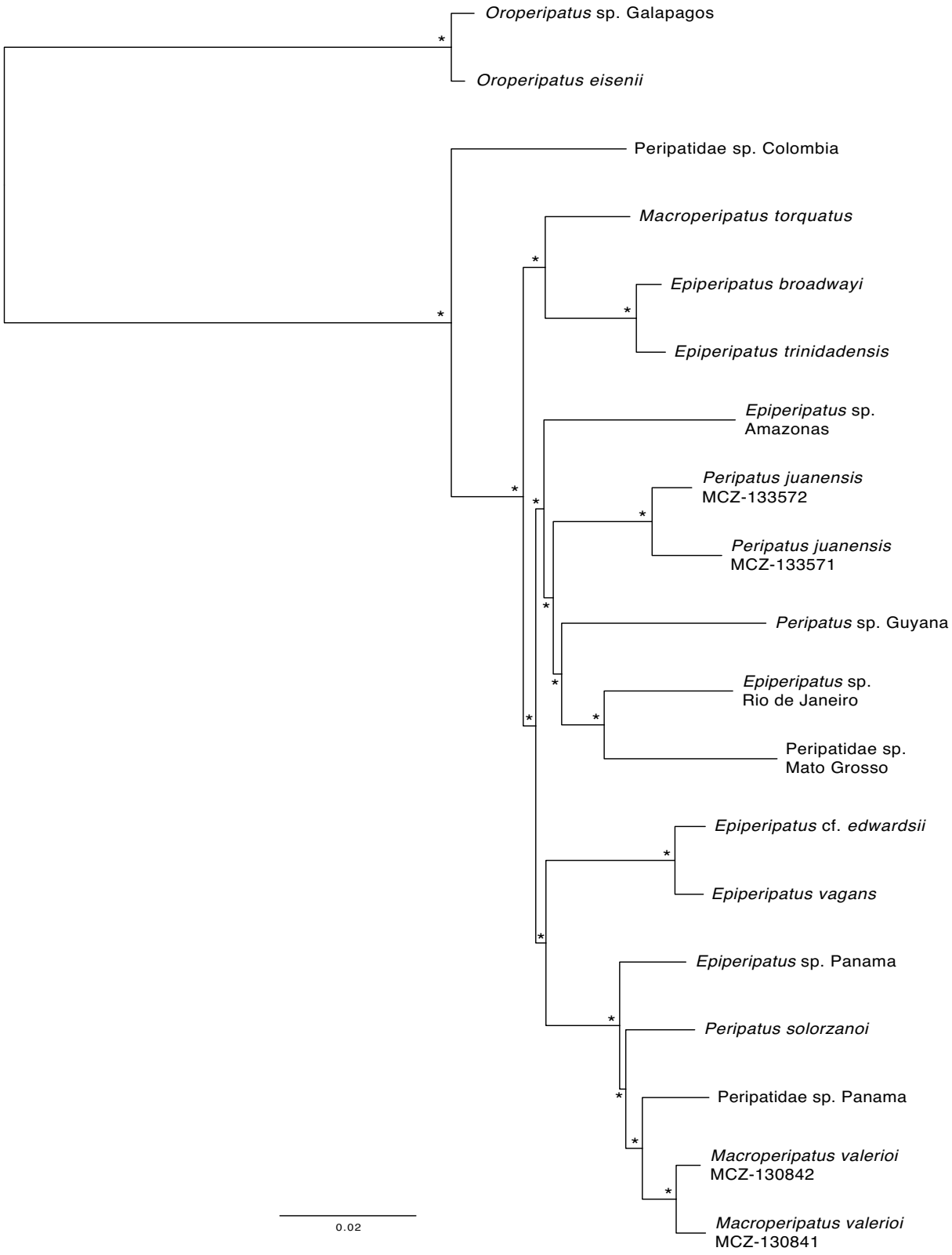

Figure A.16. Phylogeny of Neopatida inferred from ExaBayes analysis of M5. Asterisks (*) mark nodes with full support.

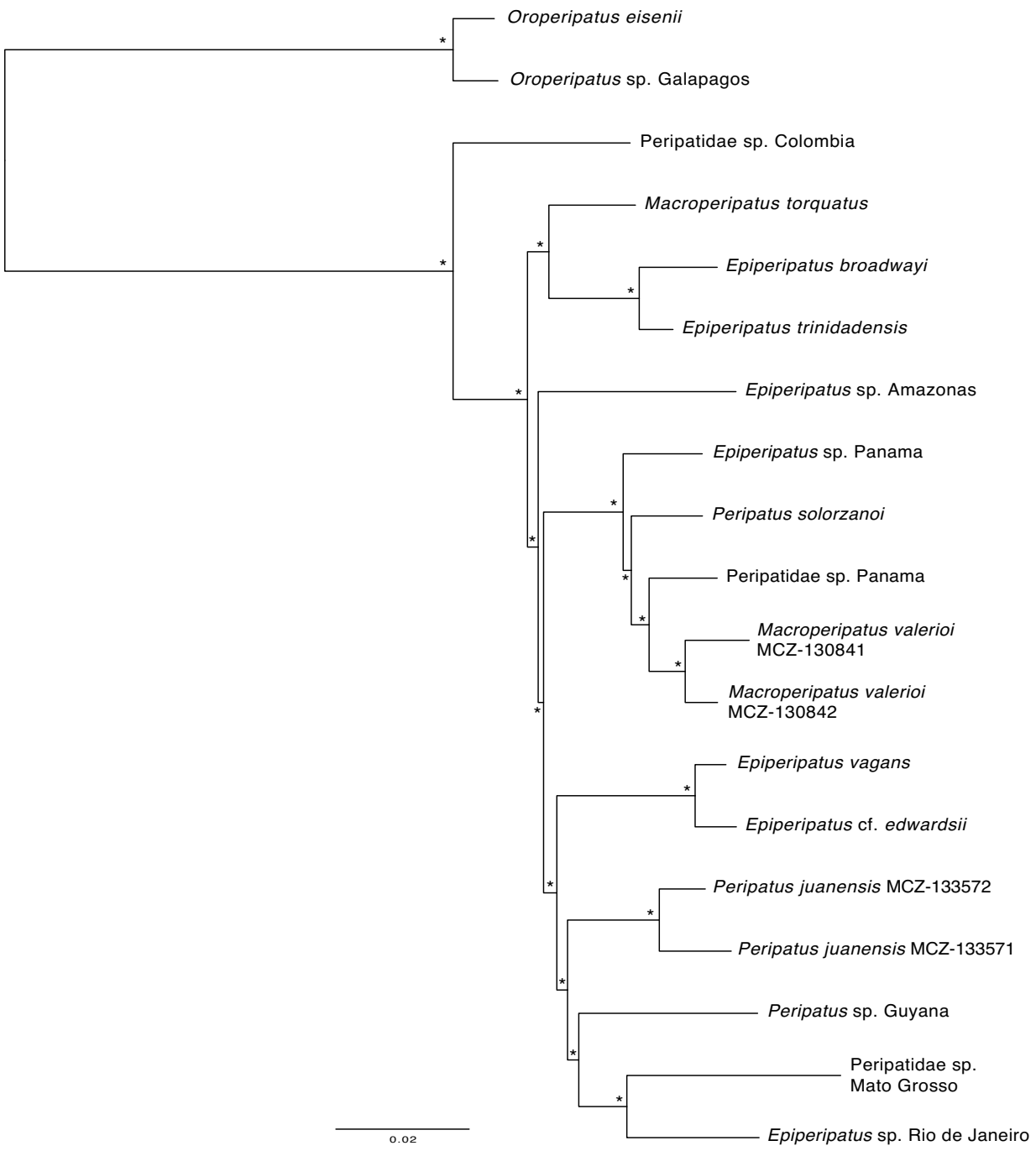

Figure A.17. Phylogeny of Neopatida inferred from IQ-TREE analysis of M5. Asterisks (*) mark nodes with full support.

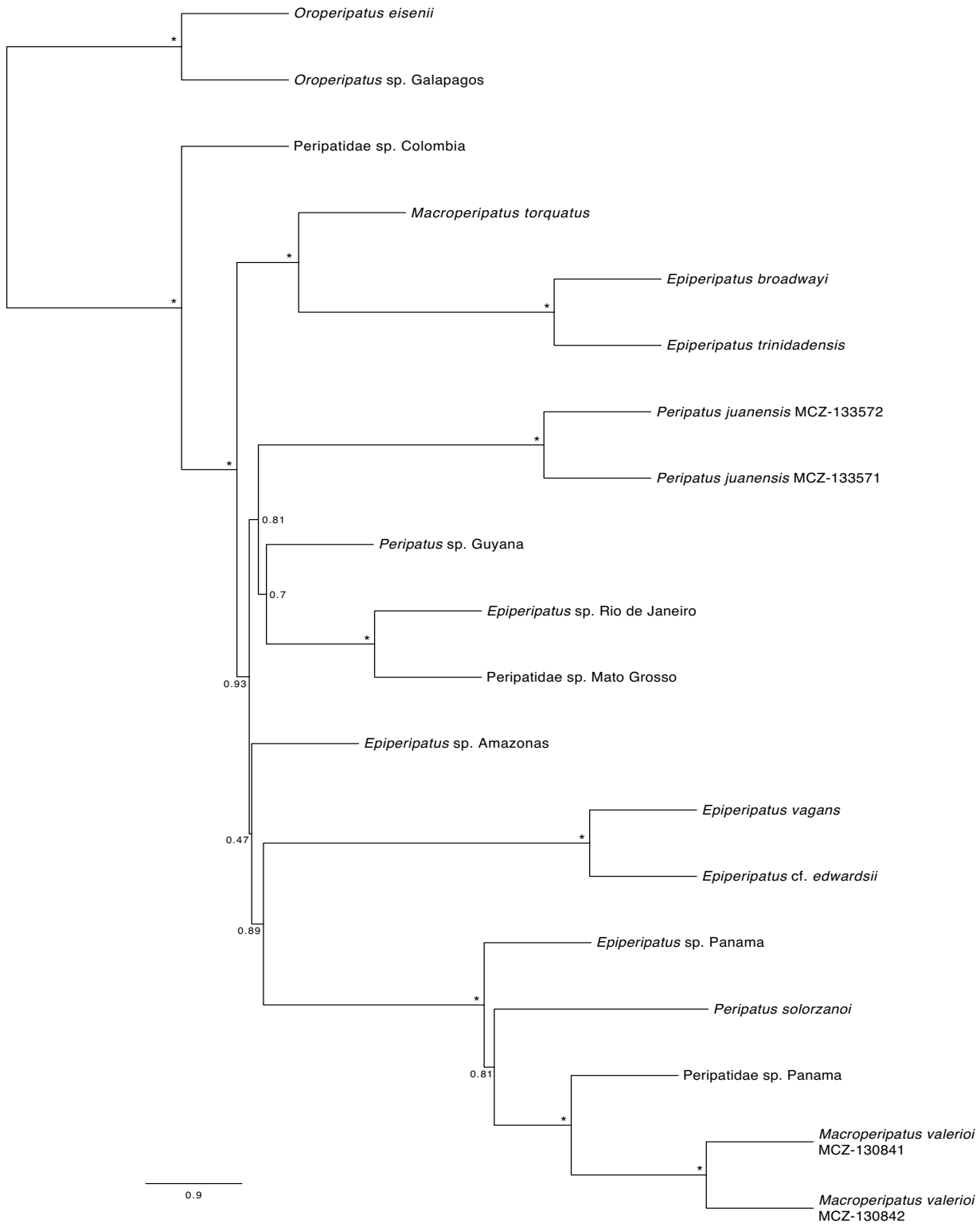

Figure A.18. Phylogeny of Neopatida inferred from ASTRAL analysis of M6. Asterisks (*) mark nodes with full support; remaining nodes show the proportion of quartets in the input gene trees that are congruent with the recovered species tree.

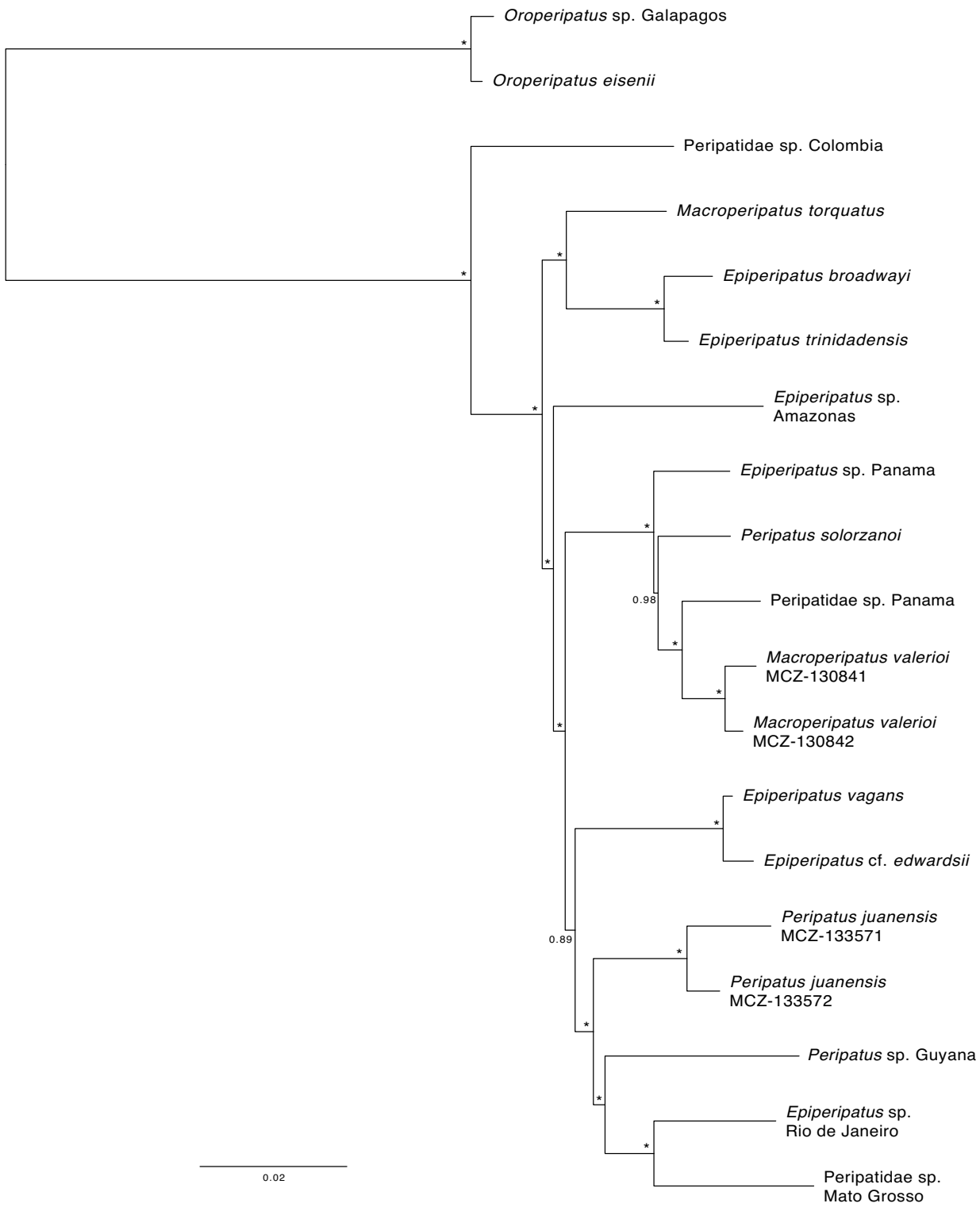

Figure A.19. Phylogeny of Neopatida inferred from ExaBayes analysis of M6. Asterisks (*) mark nodes with full support; remaining nodes show the posterior probability.

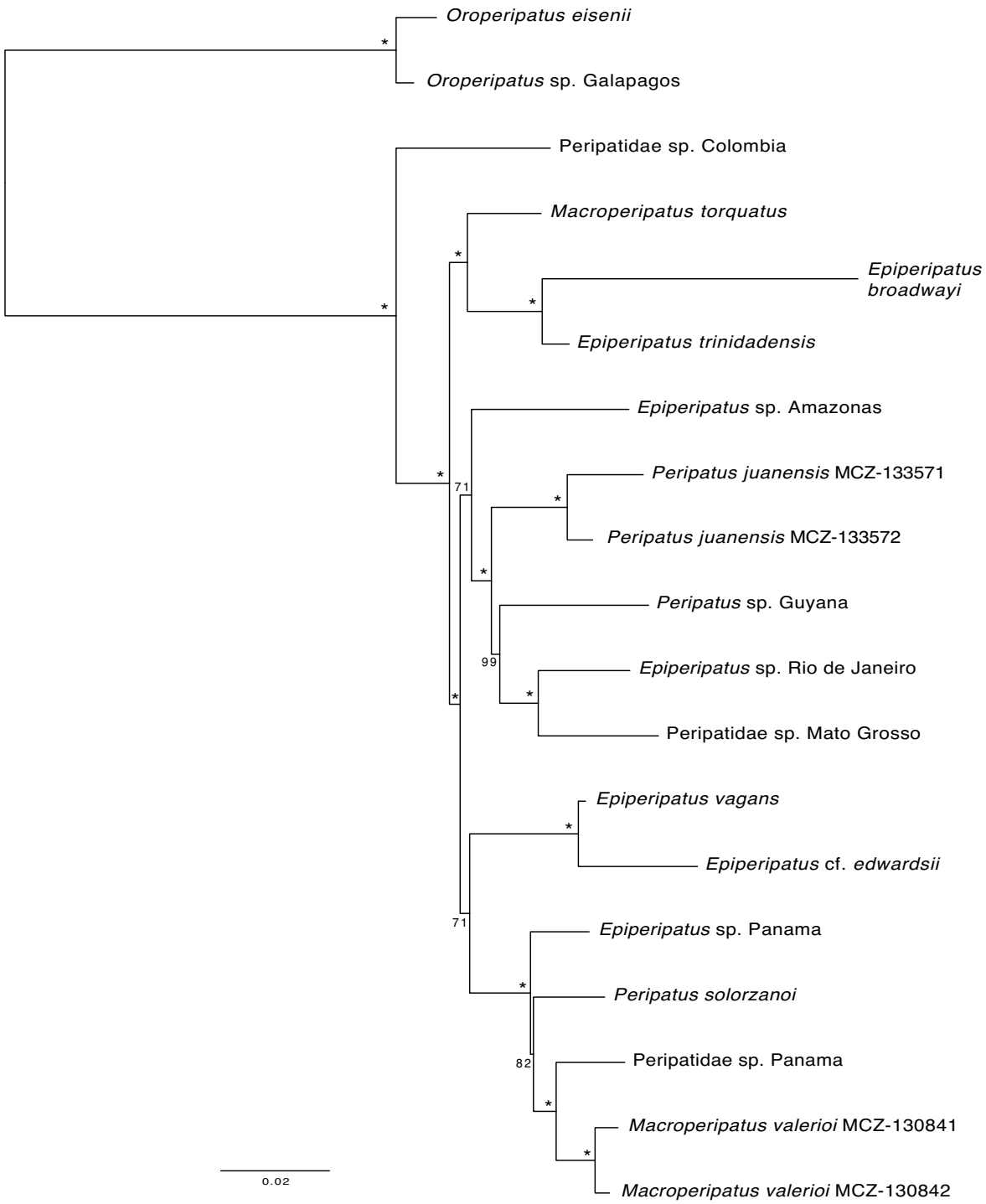

Figure A.20. Phylogeny of Neopatida inferred from IQ-TREE analysis of M6. Asterisks (*) mark nodes with full support; remaining nodes show the ultrafast bootstrap support value.

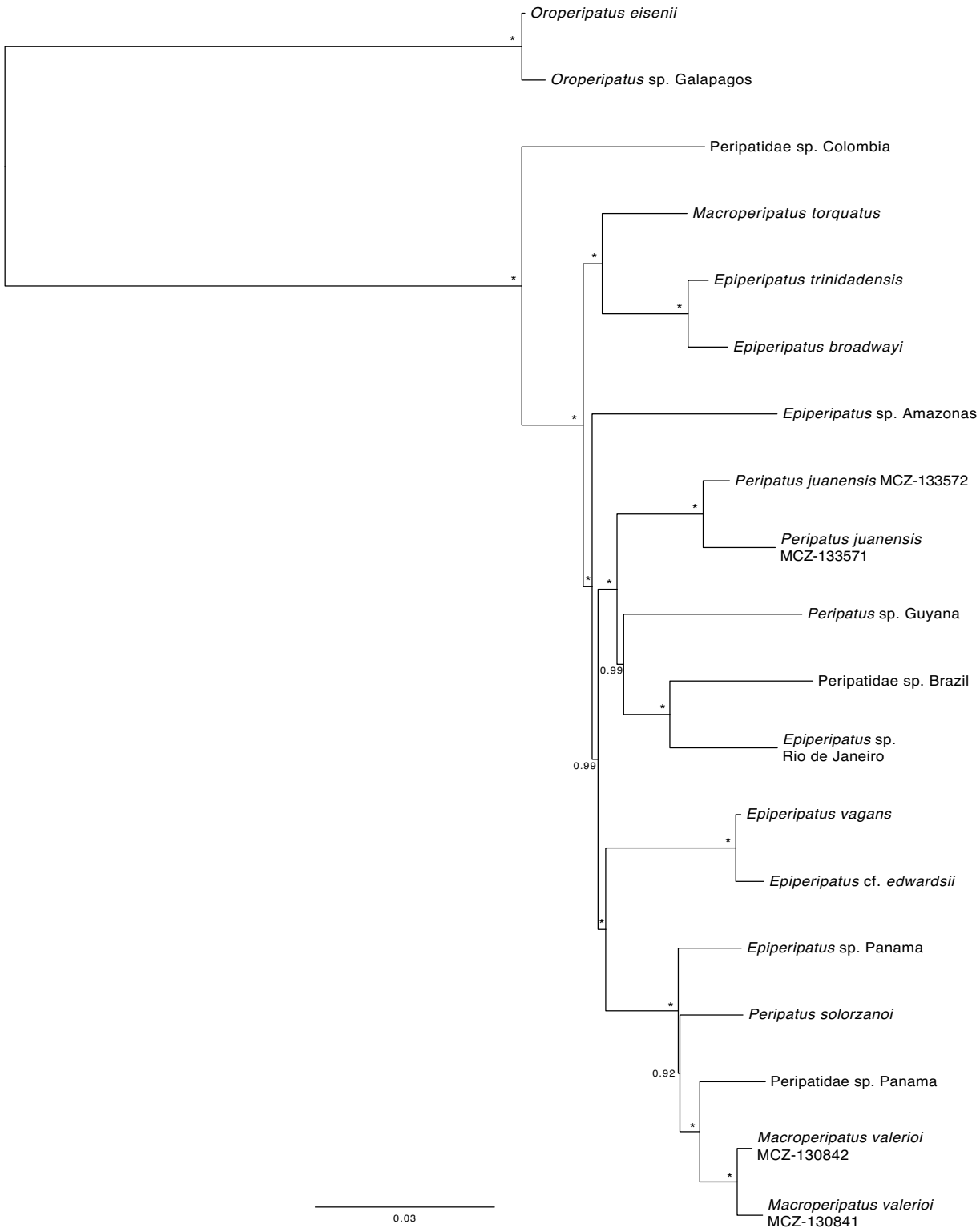

Figure A.21. Phylogeny inferred from PhyloBayes analysis of M6. Asterisks (*) mark nodes with full support; remaining nodes show the posterior probability.

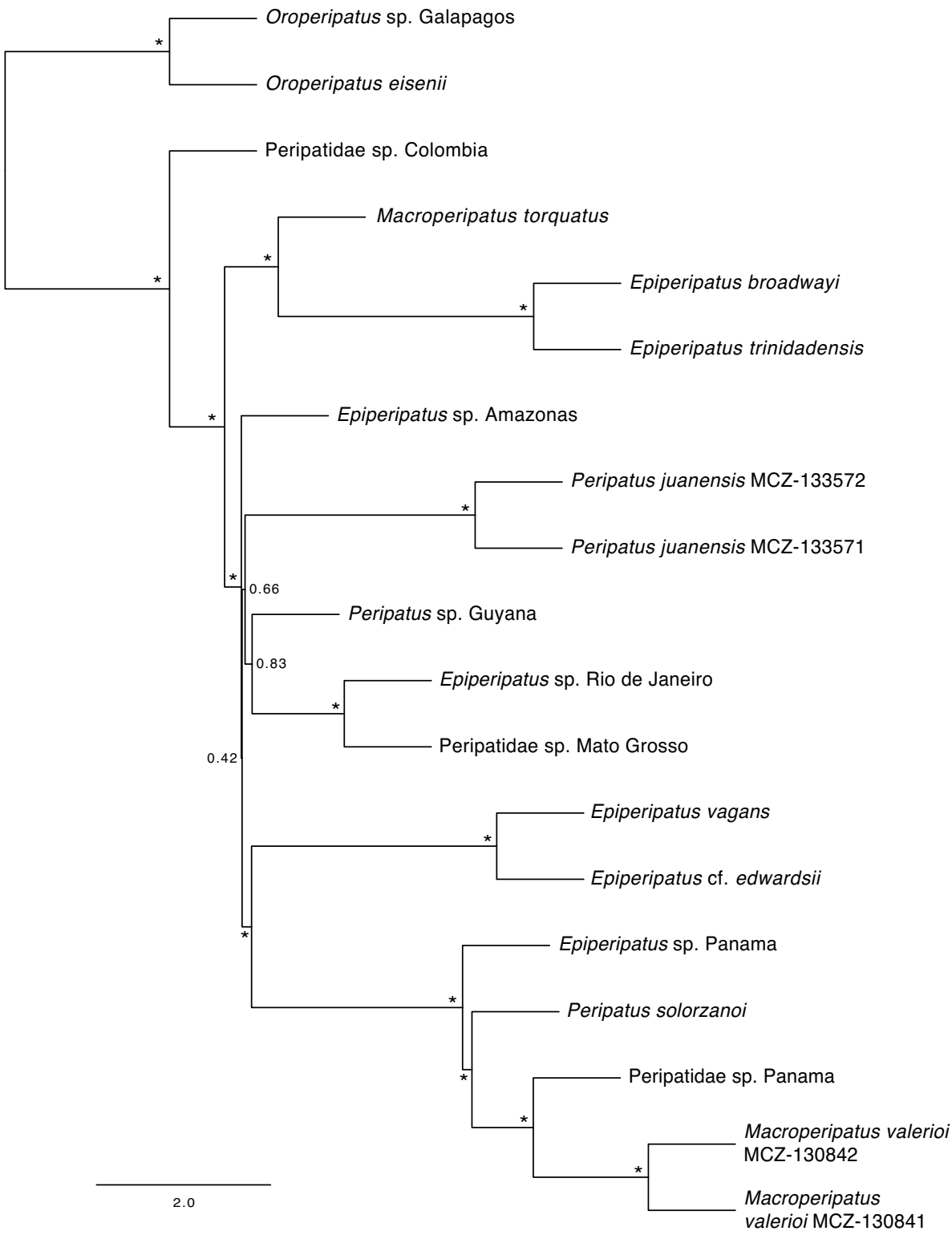

Figure A.22. Phylogeny of Neopatida inferred from ASTRAL analysis of M7. Asterisks (*) mark nodes with full support; remaining nodes show the proportion of quartets in the input gene trees that are congruent with the recovered species tree.

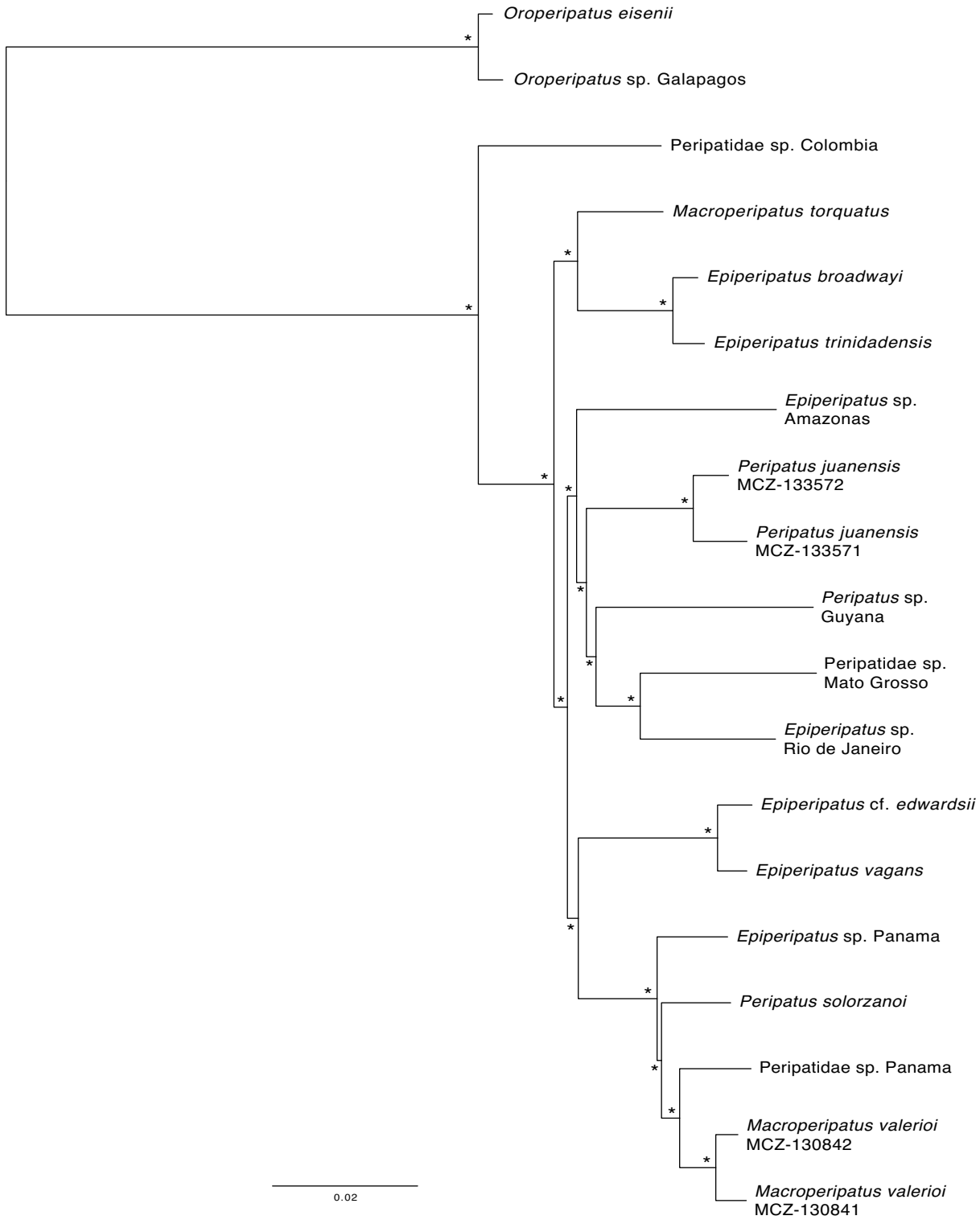

Figure A.23. Phylogeny of Neopatida inferred from ExaBayes analysis of M7. Asterisks (*) mark nodes with full support.

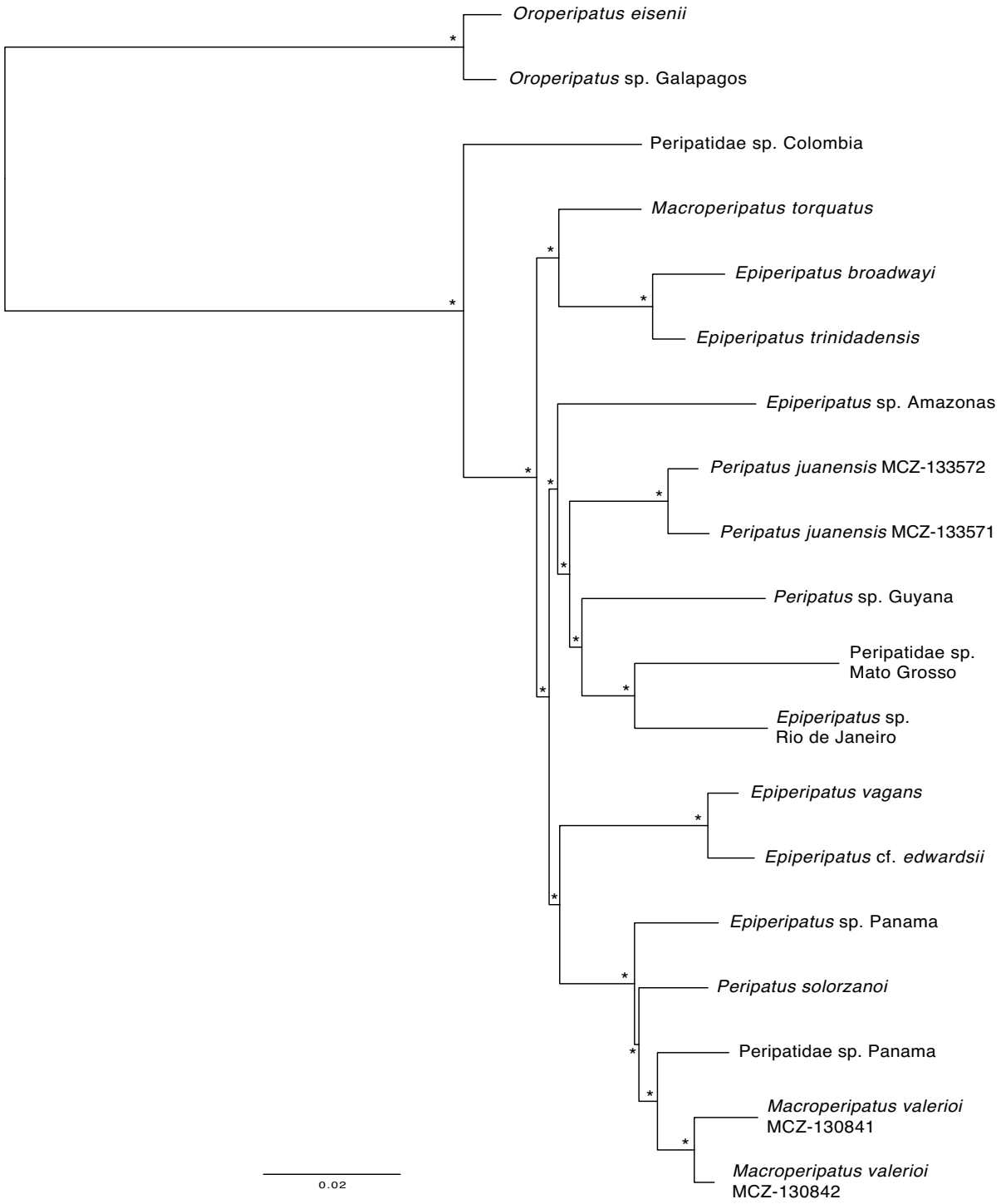

Figure A.24. Phylogeny of Neopatida inferred from IQ-TREE analysis of M7. Asterisks (*) mark nodes with full support.

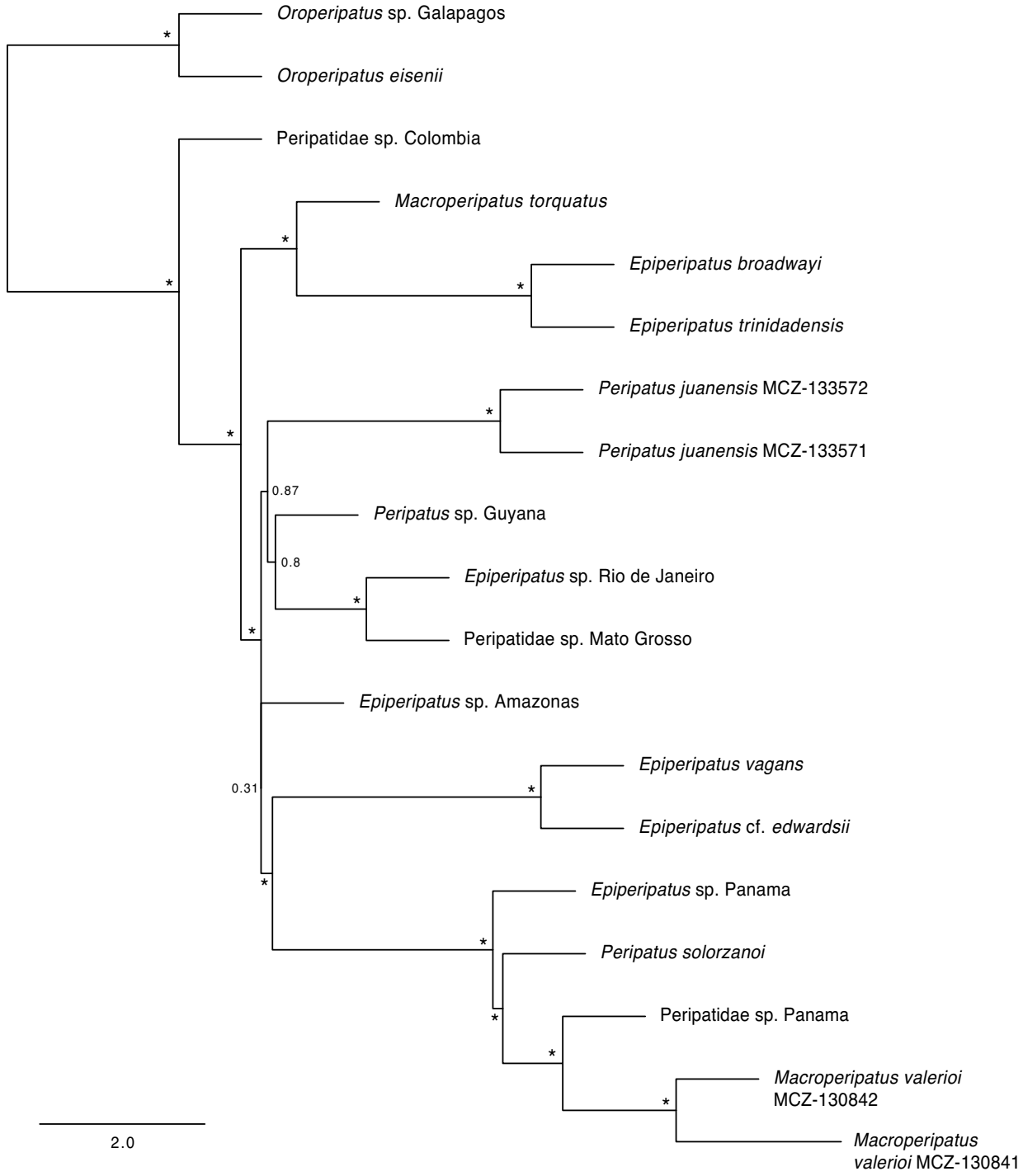

Figure A.25. Phylogeny of Neopatida inferred from ASTRAL analysis of M8. Asterisks (*) mark nodes with full support; remaining nodes show the proportion of quartets in the input gene trees that are congruent with the recovered species tree.

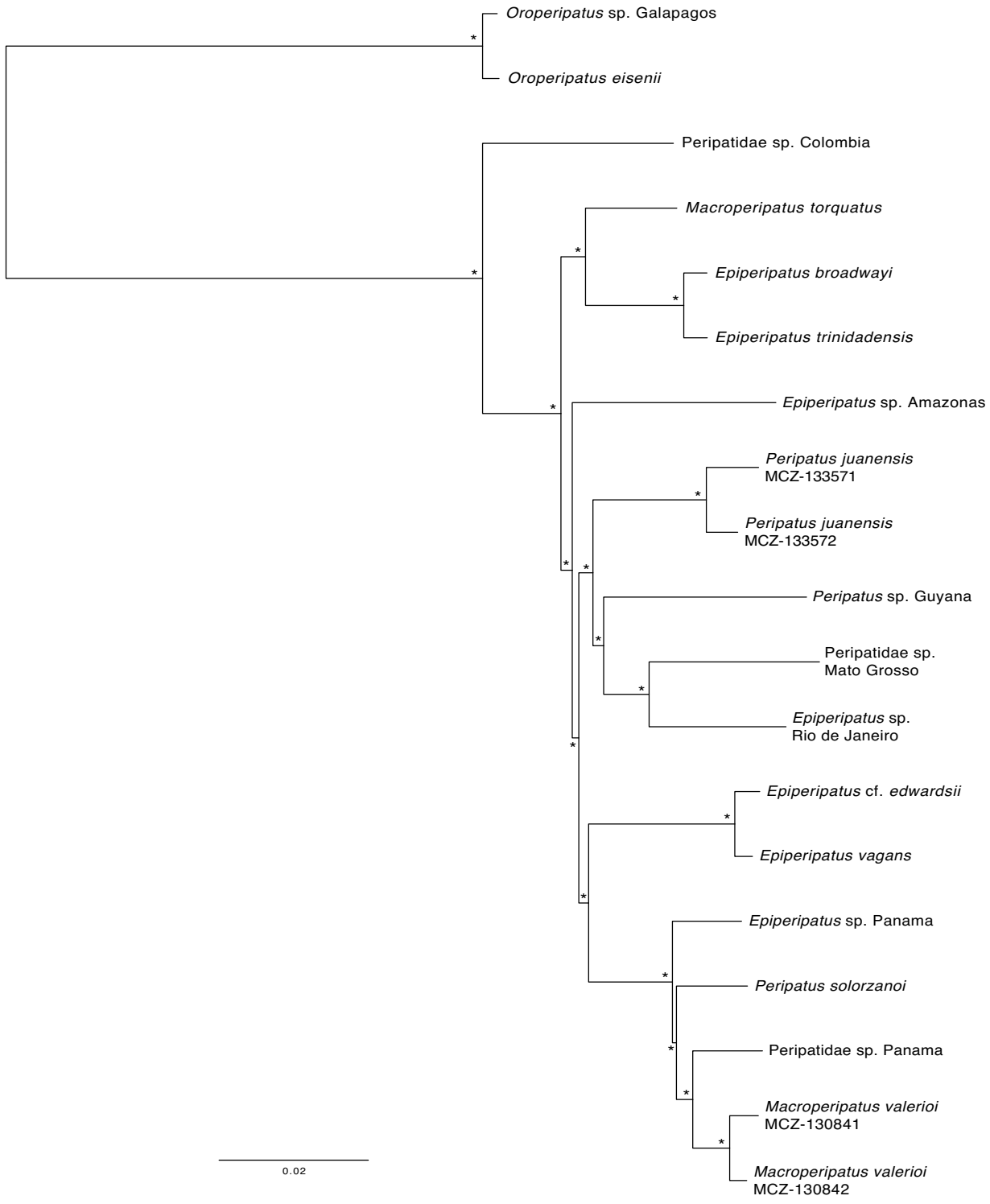

Figure A.26. Phylogeny of Neopatida inferred from ExaBayes analysis of M8. Asterisks (*) mark nodes with full support.

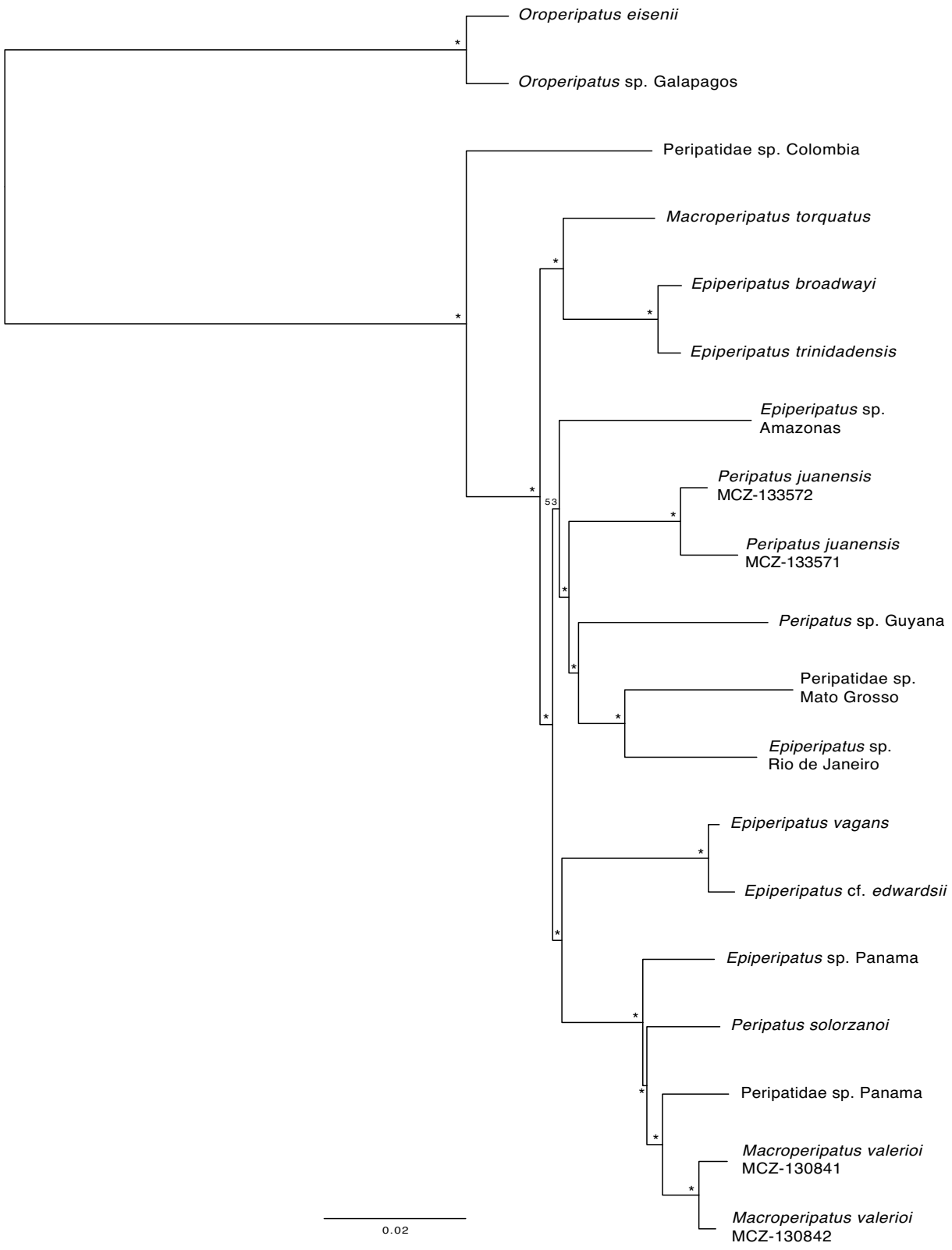

Figure A.27. Phylogeny of Neopatida inferred from IQ-TREE analysis of M8. Asterisks (*) mark nodes with full support.

Table A.1. Composition of Neopatida-specific matrices M5–M8. New transcriptomes in bold. See sections 3.2.2, 3.3.2, and 3.3.3 for details.

Species	Catalog number	Country	M5 %	M6 %	M7 %	M8 %
Oroperipatus eisenii	**MCZ-74293**	**Mexico**	**0.73**	**0.93**	**0.73**	**0.75**
***Oroperipatus* sp.**	**MCZ-133614**	**Galapagos**	**0.27**	**0.66**	**0.28**	**0.26**
Peripatidae sp.	**MCZ-141458**	**Colombia**	**0.86**	**0.94**	**0.87**	**0.87**
Epiperipatus trinidadensis	**MCZ-143926**	**Trinidad**	**0.89**	**0.91**	**0.89**	**0.91**
Epiperipatus broadwayi	**MCZ-143935**	**Tobago**	**0.85**	**0.87**	**0.85**	**0.85**
Macroperipatus torquatus	**MCZ-143928**	**Trinidad**	**0.87**	**0.91**	**0.87**	**0.88**
Epiperipatus sp.	MCZ-136557	Brazil (Amazonas)	0.73	0.9	0.73	0.73
***Epiperipatus* sp.**	**MCZ-141131**	**Brazil (Rio de Janeiro)**	**0.75**	**0.93**	**0.76**	**0.76**
Peripatidae sp.	**MCZ-141132**	**Brazil (Mato Grosso)**	**0.56**	**0.73**	**0.56**	**0.58**
***Peripatus* sp.**	**MCZ-46445**	**Guyana**	**0.28**	**0.74**	**0.28**	**0.28**
Peripatus juanensis	**MCZ-133572**	**Puerto Rico**	**0.32**	**0.79**	**0.32**	**0.3**
Peripatus juanensis	**MCZ-133571**	**Puerto Rico**	**0.2**	**0.58**	**0.2**	**0.19**
Epiperipatus sp.	MCZ-141126	Panama	0.8	0.86	0.8	0.8
Epiperipatus vagans	**MCZ-141130**	**Panama**	**0.76**	**0.84**	**0.77**	**0.79**
Peripatidae sp.	**MCZ-141128**	**Panama**	**0.78**	**0.82**	**0.79**	**0.78**
Peripatus solorzanoi	**MCZ-130840**	**Costa Rica**	**0.77**	**0.92**	**0.77**	**0.77**
Macroperipatus valerioi	**MCZ-130841**	**Costa Rica**	**0.78**	**0.91**	**0.78**	**0.79**
Macroperipatus valerioi	**MCZ-130842**	**Costa Rica**	**0.42**	**0.88**	**0.42**	**0.4**
Epiperipatus* cf. *edwardsii	**MCZ-49455**	**Panama**	**0.39**	**0.8**	**0.39**	**0.37**

Appendix B

Supplement for Chapter 4

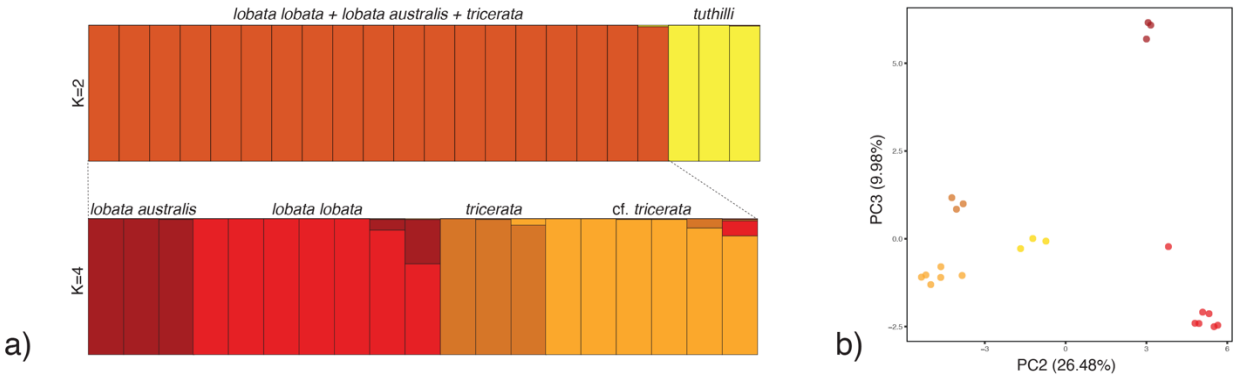

Figure B.1. (a) STRUCTURE analysis of *Karamea* species, where K=2 was recovered as the optimal value using the deltaK method of Evanno et al. (2005). When *K. tuthilli* is excluded from consideration, K=4 was recovered as the optimal clustering value. See section 4.3.2 for details. (b) PCA plot generated from analysis of *Karamea*-specific SNPs in GenoDive, showing PC2 (20.14%) vs. PC3 (9.98%) and the segregation of *K. lobata lobata* from *K. lobata australis*, as well as the separation of *K. tricerata* from *Karamea* cf. *tricerata*. Points are colored by species cluster.

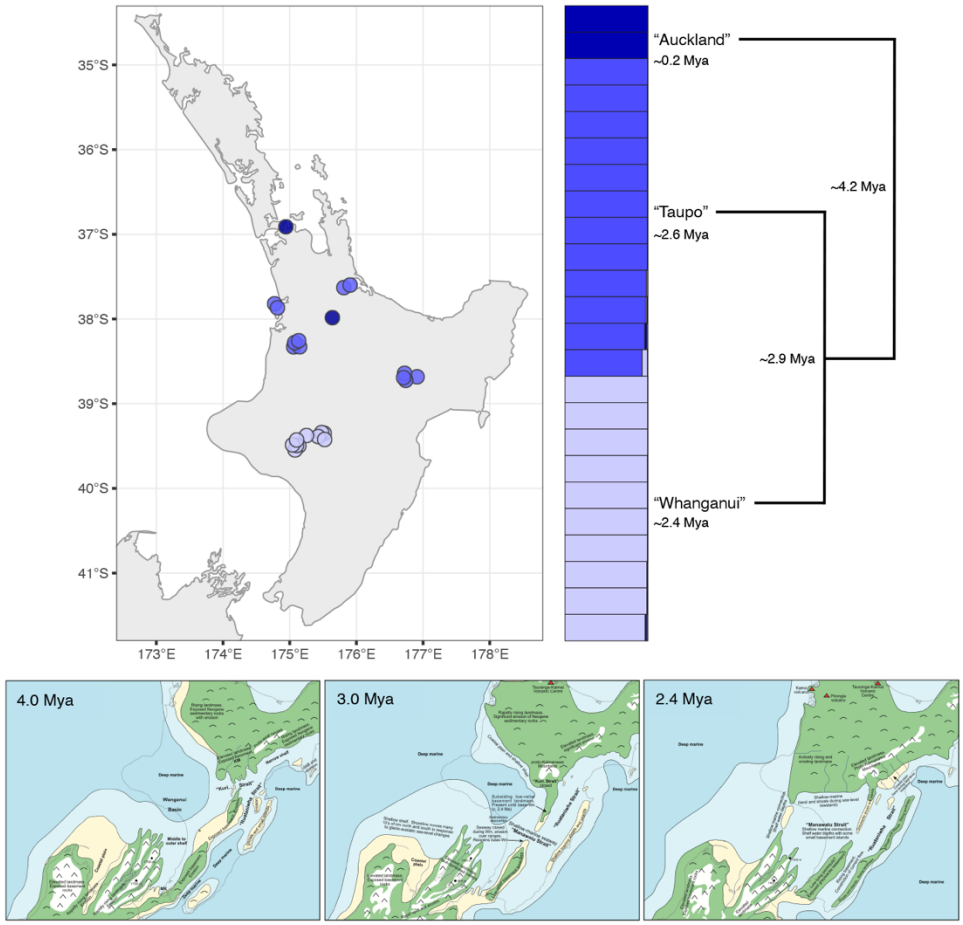

Figure B.2. Results of STRUCTURE analysis of *Sorensenella* n. sp. "Central", where the optimal K value was 3. Map shows the distribution of the different populations of the species across the central region of New Zealand's North Island. Schematic phylogeny at right depicts the estimated divergence times between populations, and estimated initial diversification times for each population, as inferred in BEAST 2 using the partitioned COI substitution rate. The Pliocene divergence times and low genetic diversity for the species (see section 4.3.3, Table 4.4, and section 4.4.2) may reflect a recent geographic expansion following the retreat of a sea strait that covered much of the central North Island, as depicted above in the images modified from Trewick & Bland (2012).

Bibliography

Abadi, M., Barham, P., Chen, J., Chen, Z., Davis, A., Dean, J., . . . Brain, G. (2016). TensorFlow: a system for large-scale machine learning. *12th USENIX Symposium on Operating Systems Design and Implementation (OSDI '16)*. Retrieved from www.tensorflow.org

Aberer, A. J., Kobert, K., & Stamatakis, A. (2014). ExaBayes: massively parallel bayesian tree inference for the whole-genome era. *Molecular Biology and Evolution, 31*(10), 2553–2556. doi:10.1093/molbev/msu236

Absolon, K., & Kratochvíl, J. (1932). Peltaeonychidae, nova čeled slepých opilionidu z jeskýn jihoillyrské oblasti. *Príroda, 25*(5), 153–156.

Aguinaldo, A. M., Turbeville, J. M., Linford, L. S., Rivera, M. C., Garey, J. R., Raff, R. A., & Lake, J. A. (1997). Evidence for a clade of nematodes, arthropods and other moulting animals. *Nature, 387*(6632), 489–493. doi:10.1038/387489a0

Ali, J. R. (2012). Colonizing the Caribbean: is the GAARlandia land-bridge hypothesis gaining a foothold? *Journal of Biogeography, 39*(3), 431–433. doi:10.1111/j.1365-2699.2011.02674.x

Ali, J. R., & Aitchison, J. C. (2008). Gondwana to Asia: plate tectonics, paleogeography and the biological connectivity of the Indian sub-continent from the Middle Jurassic through latest Eocene (166–35 Ma). *Earth-Science Reviews, 88*(3-4), 145–166. doi:10.1016/j.earscirev.2008.01.007

Allwood, J., Gleeson, D., Mayer, G., Daniels, S., Beggs, J. R., & Buckley, T. R. (2010). Support for vicariant origins of the New Zealand Onychophora. *Journal of Biogeography, 37*(4), 669–681. doi:10.1111/j.1365-2699.2009.02233.x

Altenhoff, A. M., Glover, N. M., Train, C. M., Kaleb, K., Warwick Vesztrocy, A., Dylus, D., . . . Dessimoz, C. (2018). The OMA orthology database in 2018: retrieving evolutionary relationships among all domains of life through richer web and programmatic interfaces. *Nucleic Acids Research, 46*(D1), D477–D485. doi:10.1093/nar/gkx1019

Antonelli, A., Nylander, J. A., Persson, C., & Sanmartín, I. (2009). Tracing the impact of the Andean uplift on Neotropical plant evolution. *Proceedings of the National Academy of Sciences of the USA, 106*(24), 9749–9754. doi:10.1073/pnas.0811421106

Bacon, C. D., Silvestro, D., Jaramillo, C., Smith, B. T., Chakrabarty, P., & Antonelli, A. (2015). Biological evidence supports an early and complex emergence of the Isthmus of Panama. *Proceedings of the National Academy of Sciences of the USA, 112*(19), 6110–6115. doi:10.1073/pnas.1423853112

Baker, C. M., Boyer, S. L., & Giribet, G. (2020). A well-resolved transcriptomic phylogeny of the mite harvestman family Pettalidae (Arachnida, Opiliones, Cyphophthalmi) reveals signatures of Gondwanan vicariance. *Journal of Biogeography, 47*. doi:10.1111/jbi.13828

Beaulieu, J. M., Tank, D. C., & Donoghue, M. J. (2013). A Southern hemisphere origin for campanulid angiosperms, with traces of the break-up of Gondwana. *BMC Evolutionary Biology, 13*, 80. doi:10.1186/1471-2148-13-80

Benavides, L. R., Cosgrove, J. G., Harvey, M. S., & Giribet, G. (2019). Phylogenomic interrogation resolves the backbone of the Pseudoscorpiones tree of life. *Molecular Phylogenetics and Evolution, 139*, 106509. doi:10.1016/j.ympev.2019.05.023

Benkendorff, K., Beardmore, K., Gooley, A. A., Packer, N. H., & Tait, N. N. (1999). Characterisation of the slime gland secretion from the peripatus, *Euperipatoides kanangrensis* (Onychophora: Peripatopsidae). *Comparative Biochemistry and Physiology Part B: Biochemistry and Molecular Biology, 124*(4), 457–465. doi:10.1016/s0305-0491(99)00145-5

Besnier, F., & Glover, K. A. (2013). ParallelStructure: a R package to distribute parallel runs of the population genetics program STRUCTURE on multi-core computers. *PLoS One, 8*(7), e70651. doi:10.1371/journal.pone.0070651

Bidegaray-Batista, L., & Arnedo, M. A. (2011). Gone with the plate: the opening of the Western Mediterranean basin drove the diversification of ground-dweller spiders. *BMC Evolutionary Biology, 11*, 317. doi:10.1186/1471-2148-11-317

Borner, J., Rehm, P., Schill, R. O., Ebersberger, I., & Burmester, T. (2014). A transcriptome approach to ecdysozoan phylogeny. *Molecular Phylogenetics and Evolution, 80*, 79–87. doi:10.1016/j.ympev.2014.08.001

Bouckaert, R., Heled, J., Kuhnert, D., Vaughan, T., Wu, C.-H., Xie, D., . . . Drummond, A. J. (2014). BEAST 2: a software platform for Bayesian evolutionary analysis. *PLoS Computational Biology, 10*(4), e1003537. doi:10.1371/journal.pcbi.1003537

Bouvier, E.-L. (1899a). Contributions a l'histoire des Péripates américains. *Bulletin de la Société Entomologique de France, 68*, 385–450.

Bouvier, E.-L. (1899b). Nouvelles observations sur les Péripates américains. *Comptes Rendus Hebdomadaires des Séances de l'Académie des Sciences, 129*, 1029–1031. doi:doi:10.5962/bhl.part.26693

Boyer, S. L., Baker, J. M., & Giribet, G. (2007). Deep genetic divergences in *Aoraki denticulata* (Arachnida, Opiliones, Cyphophthalmi): a widespread 'mite harvestman' defies DNA taxonomy. *Molecular Ecology, 16*(23), 4999–5016. doi:10.1111/j.1365-294X.2007.03555.x

Boyer, S. L., Clouse, R. M., Benavides, L. R., Sharma, P. P., Schwendinger, P. J., Karunarathna, I., & Giribet, G. (2007). Biogeography of the world: a case study from cyphophthalmid Opiliones, a globally distributed group of arachnids. *Journal of Biogeography, 34*(12), 2070–2085. doi:10.1111/j.1365-2699.2007.01755.x

Boyer, S. L., & Giribet, G. (2007). A new model Gondwanan taxon: systematics and biogeography of the harvestman family Pettalidae (Arachnida, Opiliones, Cyphophthalmi), with a

taxonomic revision of genera from Australia and New Zealand. *Cladistics, 23*(4), 337–361. doi:10.1111/j.1096-0031.2007.00149.x

Boyer, S. L., Markle, T. M., Baker, C. M., Luxbacher, A. M., & Kozak, K. H. (2016). Historical refugia have shaped biogeographical patterns of species richness and phylogenetic diversity in mite harvestmen (Arachnida, Opiliones, Cyphophthalmi) endemic to the Australian Wet Tropics. *Journal of Biogeography, 43*(7), 1400–1411. doi:10.1111/jbi.12717

Braband, A., Cameron, S. L., Podsiadlowski, L., Daniels, S. R., & Mayer, G. (2010). The mitochondrial genome of the onychophoran *Opisthopatus cinctipes* (Peripatopsidae) reflects the ancestral mitochondrial gene arrangement of Panarthropoda and Ecdysozoa. *Molecular Phylogenetics and Evolution, 57*(1), 285–292. doi:10.1016/j.ympev.2010.05.011

Braband, A., Podsiadlowski, L., Cameron, S. L., Daniels, S., & Mayer, G. (2010). Extensive duplication events account for multiple control regions and pseudo-genes in the mitochondrial genome of the velvet worm *Metaperipatus inae* (Onychophora, Peripatopsidae). *Molecular Phylogenetics and Evolution, 57*(1), 293–300. doi:10.1016/j.ympev.2010.05.012

Briscoe, D. A., & Tait, N. N. (1995). Allozyme evidence for extensive and ancient radiations in Australian Onychophora. *Zoological Journal of the Linnean Society, 114*(1), 91–102. doi:10.1111/j.1096-3642.1995.tb00114.x

Buchs, D. M., Arculus, R. J., Baumgartner, P. O., Baumgartner-Mora, C., & Ulianov, A. (2010). Late Cretaceous arc development on the SW margin of the Caribbean Plate: Insights from the Golfito, Costa Rica, and Azuero, Panama, complexes. *Geochemistry, Geophysics, Geosystems, 11*(7), Q07S24. doi:10.1029/2009gc002901

Buckley, T. R., James, S., Allwood, J., Bartlam, S., Howitt, R., & Prada, D. (2011). Phylogenetic analysis of New Zealand earthworms (Oligochaeta: Megascolecidae) reveals ancient clades and cryptic taxonomic diversity. *Molecular Phylogenetics and Evolution, 58*(1), 85–96. doi:10.1016/j.ympev.2010.09.024

Buckley, T. R., Krosch, M., & Leschen, R. A. B. (2015). Evolution of New Zealand insects: summary and prospectus for future research. *Austral Entomology, 54*(1), 1–27. doi:10.1111/aen.12116

Bull, J. K., Sands, C. J., Garrick, R. C., Gardner, M. G., Tait, N. N., Briscoe, D. A., . . . Sunnucks, P. (2013). Environmental complexity and biodiversity: the multi-layered evolutionary history of a log-dwelling velvet worm in montane temperate Australia. *PLoS One, 8*(12), e84559. doi:10.1371/journal.pone.0084559

Bunce, M., Worthy, T. H., Phillips, M. J., Holdaway, R. N., Willerslev, E., Haile, J., . . . Cooper, A. (2009). The evolutionary history of the extinct ratite moa and New Zealand Neogene paleogeography. *Proceedings of the National Academy of Sciences of the USA, 106*(49), 20646–20651. doi:10.1073/pnas.0906660106

Burns, M., Hedin, M., & Tsurusaki, N. (2018). Population genomics and geographical parthenogenesis in Japanese harvestmen (Opiliones, Sclerosomatidae, *Leiobunum*). *Ecology and Evolution, 8*(1), 36–52. doi:10.1002/ece3.3605

Cantrill, D. J., & Poole, I. (2012). Icehouse to hothouse: the Permian–Triassic crisis and Triassic vegetation. In *The Vegetation of Antarctica through Geological Time* (pp. 105–160).

Capella-Gutiérrez, S., Silla-Martínez, J. M., & Gabaldón, T. (2009). trimAl: a tool for automated alignment trimming in large-scale phylogenetic analyses. *Bioinformatics, 25*(15), 1972–1973. doi:10.1093/bioinformatics/btp348

Chen, Y. W., Wu, J., & Suppe, J. (2019). Southward propagation of Nazca subduction along the Andes. *Nature, 565*(7740), 441–447. doi:10.1038/s41586-018-0860-1

Chernomor, O., von Haeseler, A., & Minh, B. Q. (2016). Terrace aware data structure for phylogenomic inference from supermatrices. *Systematic Biology, 65*(6), 997–1008. doi:10.1093/sysbio/syw037

Chollet, F. (2015). Keras. Retrieved from https://keras.io

Chousou-Polydouri, N., Carmichael, A., Szűts, T., Saucedo, A., Gillespie, R., Griswold, C., & Wood, H. M. (2019). Giant Goblins above the waves at the southern end of the world: The biogeography of the spider family Orsolobidae (Araneae, Dysderoidea). *Journal of Biogeography, 46*(2), 332–342. doi:10.1111/jbi.13487

Clark, A. H. (1913). A revision of the American species of *Peripatus*. *Proceedings of the Biological Society of Washington, 26*, 15–19.

Clouse, R. M., & Wheeler, W. C. (2014). Descriptions of two new, cryptic species of *Metasiro* (Arachnida: Opiliones: Cyphophthalmi: Neogoveidae) from South Carolina, USA, including a discussion of mitochondrial mutation rates. *Zootaxa*(3814), 177–201. doi:10.11646/zootaxa.3814.2.2

Cluzel, D., Maurizot, P., Collot, J., & Sevin, B. (2012). An outline of the Geology of New Caledonia; from Permian–Mesozoic Southeast Gondwanaland active margin to Cenozoic obduction and supergene evolution. *Episodes, 35*(1), 72–86. doi:10.18814/epiiugs/2012/v35i1/007

Colloff, M. J. (2013). Species-groups and biogeography of the oribatid mite family Malaconothridae (Oribatida: Malaconothroidea), with new species from the south-western Pacific region. *Zootaxa, 3722*, 401–438. doi:10.11646/zootaxa.3722.4.1

Concha, A., Mellado, P., Morera-Brenes, B., Sampaio Costa, C., Mahadevan, L., & Monge-Najera, J. (2015). Oscillation of the velvet worm slime jet by passive hydrodynamic instability. *Nature Communications, 6*(6292), 1–6. doi:10.1038/ncomms7292

Cook, L. G., & Crisp, M. D. (2005). Not so ancient: the extant crown group of *Nothofagus* represents a post-Gondwanan radiation. *Proceedings of the Royal Society B: Biological Sciences, 272*(1580), 2535–2544. doi:10.1098/rspb.2005.3219

Cooper, A., & Cooper, R. A. (1995). The Oligocene bottleneck and New Zealand biota: genetic record of a past environmental crisis. *Proceedings of the Royal Society of London B, 261*(1362), 293–302. doi:10.1098/rspb.1995.0150

Cuellar, O. (1977). Animal parthenogenesis. *Science, 197*(4306), 837–843. doi:10.1126/science.887925

Cunha, W. T. R., Santos, R. C. O., Araripe, J., Sampaio, I., Schneider, H., & Rêgo, P. S. (2017). Molecular analyses reveal the occurrence of three new sympatric lineages of velvet worms (Onychophora: Peripatidae) in the eastern Amazon basin. *Genetics and Molecular Biology, 40*(1), 147–152. doi:10.1590/1678-4685-GMB-2016-0037

Daniels, S. R., Dambire, C., Klaus, S., & Sharma, P. P. (2016). Unmasking alpha diversity, cladogenesis and biogeographical patterning in an ancient panarthropod lineage (Onychophora: Peripatopsidae: *Opisthopatus cinctipes*) with the description of five novel species. *Cladistics, 32*(5), 506–537. doi:10.1111/cla.12154

Daniels, S. R., Picker, M. D., Cowlin, R. M., & Hamer, M. L. (2009). Unravelling evolutionary lineages among South African velvet worms (Onychophora: *Peripatopsis*) provides evidence for widespread cryptic speciation. *Biological Journal of the Linnean Society, 97*(1), 200–216. doi:10.1111/j.1095-8312.2009.01205.x

Derkarabetian, S., Benavides, L. R., & Giribet, G. (2019). Sequence capture phylogenomics of historical ethanol-preserved museum specimens: Unlocking the rest of the vault. *Molecular Ecology Resources, 19*(6), 1531–1544. doi:10.1111/1755-0998.13072

Derkarabetian, S., Burns, M., Starrett, J., & Hedin, M. (2016). Population genomic evidence for multiple Pliocene refugia in a montane-restricted harvestman (Arachnida, Opiliones, *Sclerobunus robustus*) from the southwestern United States. *Molecular Ecology, 25*(18), 4611–4631. doi:10.1111/mec.13789

Derkarabetian, S., Castillo, S., Koo, P. K., Ovchinnikov, S., & Hedin, M. (2019). A demonstration of unsupervised machine learning in species delimitation. *Molecular Phylogenetics and Evolution, 139*, 106562. doi:10.1016/j.ympev.2019.106562

Derkarabetian, S., Starrett, J., Tsurusaki, N., Ubick, D., Castillo, S., & Hedin, M. (2018). A stable phylogenomic classification of Travunioidea (Arachnida, Opiliones, Laniatores) based on sequence capture of ultraconserved elements. *Zookeys*(760), 1–36. doi:10.3897/zookeys.760.24937

Dunlop, J. A., Anderson, L. I., Kerp, H., & Hass, H. (2004). A harvestman (Arachnida: Opiliones) from the Early Devonian Rhynie cherts, Aberdeenshire, Scotland. *Transactions of the Royal Society of Edinburgh: Earth Sciences, 94*(04), 341–354. doi:10.1017/s0263593300000730

Dunn, C. W., Hejnol, A., Matus, D. Q., Pang, K., Browne, W. E., Smith, S. A., . . . Giribet, G. (2008). Broad phylogenomic sampling improves resolution of the animal tree of life. *Nature, 452*(7188), 745–749. doi:10.1038/nature06614

Eagles, G. (2007). New angles on South Atlantic opening. *Geophysical Journal International, 168*(1), 353–361. doi:10.1111/j.1365-246X.2006.03206.x

Earl, D. A., & vonHoldt, B. M. (2011). STRUCTURE HARVESTER: a website and program for visualizing STRUCTURE output and implementing the Evanno method. *Conservation Genetics Resources, 4*(2), 359–361. doi:10.1007/s12686-011-9548-7

Edgecombe, G. D., & Giribet, G. (2008). A New Zealand species of the trans-Tasman centipede order Craterostigmomorpha (Arthropoda : Chilopoda) corroborated by molecular evidence. *Invertebrate Systematics, 22*(1), 1–15. doi:10.1071/is07036

Elias, M., Joron, M., Willmott, K., Silva-Brandao, K. L., Kaiser, V., Arias, C. F., . . . Jiggins, C. D. (2009). Out of the Andes: patterns of diversification in clearwing butterflies. *Molecular Ecology, 18*(8), 1716–1729. doi:10.1111/j.1365-294X.2009.04149.x

Ellis, E. A., Marshall, D. C., Hill, K. B. R., Owen, C. L., Kamp, P. J. J., & Simon, C. (2015). Phylogeography of six codistributed New Zealand cicadas and their relationship to multiple biogeographical boundaries suggest a re-evaluation of the Taupo Line. *Journal of Biogeography, 42*(9), 1761–1775. doi:10.1111/jbi.12532

Enderlein, G. (1909). Die Spinnen der Crozet-Inseln und von Kergueken. *Deutsche Südpolar-Expedition 1901-3, 10*(Zool. 2), 535–540.

Espinasa, L., Garvey, R., Espinasa, J., Fratto, C. A., Taylor, S., Toulkeridis, T., & Addison, A. (2015). Cave dwelling Onychophora from a lava tube in the Galapagos. *Subterranean Biology, 15*, 1–10. doi:10.3897/subtbiol.15.8468

Evanno, G., Regnaut, S., & Goudet, J. (2005). Detecting the number of clusters of individuals using the software STRUCTURE: a simulation study. *Molecular Ecology, 14*(8), 2611–2620. doi:10.1111/j.1365-294X.2005.02553.x

Fage, L. B. (1945). Arachnides cavernicoles nouveaux de Madagascar. *Bulletin du Muséum national d'histoire naturelle, 17*(4), 301–307.

Faircloth, B. C. (2016). PHYLUCE is a software package for the analysis of conserved genomic loci. *Bioinformatics, 32*(5), 786–788. doi:10.1093/bioinformatics/btv646

Faircloth, B. C. (2017). Identifying conserved genomic elements and designing universal bait sets to enrich them. *Methods in Ecology and Evolution, 8*(9), 1103–1112. doi:10.1111/2041-210x.12754

Faircloth, B. C., McCormack, J. E., Crawford, N. G., Harvey, M. G., Brumfield, R. T., & Glenn, T. C. (2012). Ultraconserved elements anchor thousands of genetic markers spanning multiple evolutionary timescales. *Systematic Biology, 61*(5), 717–726. doi:10.1093/sysbio/sys004

Fernández, R., Edgecombe, G. D., & Giribet, G. (2016). Exploring phylogenetic relationships within Myriapoda and the effects of matrix composition and occupancy on phylogenomic reconstruction. *Systematic Biology, 65*(5), 871–889. doi:10.1093/sysbio/syw041

Fernández, R., Edgecombe, G. D., & Giribet, G. (2018). Phylogenomics illuminates the backbone of the Myriapoda Tree of Life and reconciles morphological and molecular phylogenies. *Scientific Reports, 8*(83), 1–7. doi:10.1038/s41598-017-18562-w

Fernández, R., & Giribet, G. (2014). Phylogeography and species delimitation in the New Zealand endemic, genetically hypervariable harvestman species, *Aoraki denticulata* (Arachnida, Opiliones, Cyphophthalmi). *Invertebrate Systematics, 28*, 401–414. doi:10.1071/IS14009

Fernández, R., Laumer, C. E., Vahtera, V., Libro, S., Kaluziak, S., Sharma, P. P., . . . Giribet, G. (2014). Evaluating topological conflict in centipede phylogeny using transcriptomic data sets. *Molecular Biology and Evolution, 31*(6), 1500–1513. doi:10.1093/molbev/msu108

Fernández, R., Sharma, P. P., Tourinho, A. L., & Giribet, G. (2017). The Opiliones tree of life: shedding light on harvestmen relationships through transcriptomics. *Proceedings of the Royal Society of London B, 284*, 20162340. doi:10.1098/rspb.2016.2340

Folmer, O., Black, M., Hoeh, W., Lutz, R., & Vrujenhoek, R. C. (1994). DNA primers for amplification of mitochondrial cytochrome *c* oxidase subunit I from diverse metazoan invertebrates. *Molecular marine biology and biotechnology, 3*, 294–299.

Forster, R. R. (1948). A new sub-family and species of New Zealand Opiliones. *Records of the Auckland Institute and Museum, 3*(4/5), 313–318.

Forster, R. R. (1952). Western Australian Opiliones. *Journal of the Royal Society of Western Australia, 36*, 23–29.

Forster, R. R. (1954). *The New Zealand harvestmen (sub-order Laniatores).* Christchurch: Canterbury Museum bulletin.

Gamble, T., Bauer, A. M., Greenbaum, E., & Jackman, T. R. (2008). Evidence for Gondwanan vicariance in an ancient clade of gecko lizards. *Journal of Biogeography, 35*, 88–104. doi:10.1111/j.1365-2699.2007.01770.x

Garwood, R. J., Dunlop, J. A., Giribet, G., & Sutton, M. D. (2011). Anatomically modern Carboniferous harvestmen demonstrate early cladogenesis and stasis in Opiliones. *Nature Communications, 2*, 444. doi:10.1038/ncomms1458

Garwood, R. J., Edgecombe, G. D., Charbonnier, S., Chabard, D., Sotty, D., & Giribet, G. (2016). Carboniferous Onychophora from Montceau-les-Mines, France, and onychophoran terrestrialization. *Invertebrate Biology, 135*(3), 179–190. doi:10.1111/ivb.12130

Garwood, R. J., Sharma, P. P., Dunlop, J. A., & Giribet, G. (2014). A Paleozoic stem group to mite harvestmen revealed through integration of phylogenetics and development. *Current Biology, 24*(9), 1017–1023. doi:10.1016/j.cub.2014.03.039

Gellatly, A., Chinn, T., & Rothlisberger, F. (1988). Holocene glacier variations in New Zealand: A review. *Quaternary Science Reviews, 7*(2), 227–242. doi:10.1016/0277-3791(88)90008-x

Ghiselin, M. T. (1984). *Peripatus* as a Living Fossil. In N. Eldredge & S. M. Stanley (Eds.), *Living Fossils* (pp. 214–217): Springer-Verlag.

Gillespie, R. G., & Roderick, G. K. (2002). Arthropods on islands: colonization, speciation, and conservation. *Annual Review of Entomology, 47*, 595–632. doi:10.1146/annurev.ento.47.091201.145244

Giribet, G., & Baker, C. M. (2019). Further discussion on the Eocene drowning of New Caledonia: Discordances from the point of view of zoology. *Journal of Biogeography, 46*, 1912–1918. doi:10.1111/jbi.13635

Giribet, G., & Boyer, S. L. (2010). 'Moa's Ark' or 'Goodbye Gondwana': is the origin of New Zealand's terrestrial invertebrate fauna ancient, recent or both? *Invertebrate Systematics, 24*(1), 1–8. doi:10.1071/is10009

Giribet, G., Boyer, S. L., Baker, C. M., Fernández, R., Sharma, P. P., de Bivort, B. L., . . . Griswold, C. E. (2016). A molecular phylogeny of the temperate Gondwanan family Pettalidae (Arachnida, Opiliones, Cyphophthalmi) and the limits of taxonomic sampling. *Zoological Journal of the Linnean Society, 178*(3), 523–545. doi:10.1111/zoj.12419

Giribet, G., Buckman-Young, R. S., Costa, C. S., Baker, C. M., Benavides, L. R., Branstetter, M. G., . . . Pinto-da-Rocha, R. (2018). The 'Peripatos' in Eurogondwana? — Lack of evidence that southeast Asian onychophorans walked through Europe. *Invertebrate Systematics, 32*(4), 842–865. doi:10.1071/is18007

Giribet, G., Carranza, S., Baguñà, J., Riutort, M., & Ribera, C. (1996). First molecular evidence for the existence of a Tardigrada + Arthropoda clade. *Molecular Biology and Evolution, 13*(1), 76–84. doi:10.1093/oxfordjournals.molbev.a025573

Giribet, G., & Edgecombe, G. D. (2006). The importance of looking at small-scale patterns when inferring Gondwanan biogeography: a case study of the centipede *Paralamyctes* (Chilopoda, Lithobiomorpha, Henicopidae). *Biological Journal of the Linnean Society, 89*(1), 65–78. doi:10.1111/j.1095-8312.2006.00658.x

Giribet, G., & Edgecombe, G. D. (2017). Current understanding of Ecdysozoa and its internal phylogenetic relationships. *Integrative and Comparative Biology, 57*(3), 455–466. doi:10.1093/icb/icx072

Giribet, G., Sharma, P. P., Benavides, L. R., Boyer, S. L., Clouse, R. M., De Bivort, B. L., . . . Schwendinger, P. J. (2012). Evolutionary and biogeographical history of an ancient and global group of arachnids (Arachnida: Opiliones: Cyphophthalmi) with a new taxonomic arrangement. *Biological Journal of the Linnean Society, 105*(1), 92–130. doi:10.1111/j.1095-8312.2011.01774.x

Giribet, G., & Shear, W. A. (2010). The genus *Siro* Latreille, 1796 (Opiliones, Cyphophthalmi, Sironidae), in North America with a phylogenetic analysis based on molecular data and the description of four new species. *Bulletin of the Museum of Comparative Zoology, 160*(1), 1–33. doi:10.3099/0027-4100-160.1.1

Giribet, G., Vogt, L., González, A. P., Sharma, P. P., & Kury, A. B. (2010). A multilocus approach to harvestman (Arachnida: Opiliones) phylogeny with emphasis on biogeography and the systematics of Laniatores. *Cladistics, 26*(4), 408–437. doi:10.1111/j.1096-0031.2009.00296.x

Giribet, G., & Wheeler, W. C. (2001). Some unusual small-subunit ribosomal RNA sequences of metazoans. *American Museum Novitates, 3337*, 1–14.

Gleeson, D. M., Rowell, D. M., Tait, N. N., Briscoe, D. A., & Higgins, A. V. (1998). Phylogenetic relationships among onychophora from Australasia inferred from the mitochondrial cytochrome oxidase subunit I gene. *Molecular Phylogenetics and Evolution, 10*(2), 237–248. doi:10.1006/mpev.1998.0512

Glenn, T. C., Nilsen, R. A., Kieran, T. J., Sanders, J. G., Bayona-Vasquez, N. J., Finger, J. W., . . . Faircloth, B. C. (2019). Adapterama I: universal stubs and primers for 384 unique dual-indexed or 147,456 combinatorially-indexed Illumina libraries (iTru & iNext). *PeerJ, 7*, e7755. doi:10.7717/peerj.7755

Grabherr, M. G., Haas, B. J., Yassour, M., Levin, J. Z., Thompson, D. A., Amit, I., . . . Regev, A. (2011). Full-length transcriptome assembly from RNA-Seq data without a reference genome. *Nature Biotechnology, 29*(7), 644–652. doi:10.1038/nbt.1883

Grandcolas, P., Murienne, J., Robillard, T., Desutter-Grandcolas, L., Jourdan, H., Guilbert, E., & Deharveng, L. (2008). New Caledonia: a very old Darwinian island? *Philosophical Transactions of the Royal Society of London Series B, Biological Sciences, 363*(1508), 3309–3317. doi:10.1098/rstb.2008.0122

Grimaldi, D. A., Engel, M. S., & Nascimbene, P. C. (2002). Fossiliferous Cretaceous amber from Myanmar (Burma): its rediscovery, biotic diversity, and paleontological significance. *American Museum Novitates, 3361*, 1–71. doi:10.1206/0003-0082(2002)361<0001:fcafmb>2.0.co;2

Grünewald, S., Spillner, A., Bastkowski, S., Bogershausen, A., & Moulton, V. (2013). SuperQ: computing supernetworks from quartets. *IEEE/ACM Transactions on Computational Biology and Bioinformatics, 10*(1), 151–160. doi:10.1109/TCBB.2013.8

Haas, B. J., Papanicolaou, A., Yassour, M., Grabherr, M., Blood, P. D., Bowden, J., . . . Regev, A. (2013). *De novo* transcript sequence reconstruction from RNA-seq using the Trinity platform for reference generation and analysis. *Nature Protocols, 8*(8), 1494-1512. doi:10.1038/nprot.2013.084

Harvey, M. S. (2002). Short-range endemism among the Australian fauna: some examples from non-marine environments. *Invertebrate Systematics, 16*(4), 555–570. doi:10.1071/is02009

Harvey, M. S., Rix, M. G., Harms, D., Giribet, G., Vink, C. J., & Walter, D. E. (2017). The Biogeography of Australasian Arachnids. In M. C. Ebach (Ed.), *Handbook of Australasian Biogeography* (pp. 241–268). Boca Raton, Florida: CRC Press.

Hedges, S. B. (2006). Paleogeography of the Antilles and origin of West Indian terrestrial vertebrates. *Annals of the Missouri Botanical Garden, 93*(2), 231–244. doi:10.3417/0026-6493(2006)93[231:Potaao]2.0.Co;2

Hedges, S. B., Hass, C. A., & Maxson, L. R. (1992). Caribbean biogeography: molecular evidence for dispersal in West Indian terrestrial vertebrates. *Proceedings of the National Academy of Sciences of the USA, 89*, 1909–1913.

Hedin, M., Carlson, D., & Coyle, F. (2015). Sky island diversification meets the multispecies coalescent - divergence in the spruce-fir moss spider (*Microhexura montivaga*, Araneae, Mygalomorphae) on the highest peaks of southern Appalachia. *Molecular Ecology, 24*(13), 3467–3484. doi:10.1111/mec.13248

Hedin, M., Derkarabetian, S., Alfaro, A., Ramírez, M. J., & Bond, J. E. (2019). Phylogenomic analysis and revised classification of atypoid mygalomorph spiders (Araneae, Mygalomorphae), with notes on arachnid ultraconserved element loci. *PeerJ, 7*, e6864. doi:10.7717/peerj.6864

Hedin, M., & McCormack, M. (2017). Biogeographical evidence for common vicariance and rare dispersal in a southern Appalachian harvestman (Sabaconidae, *Sabacon cavicolens*). *Journal of Biogeography, 44*(7), 1665–1678. doi:10.1111/jbi.12973

Heenan, P. B., & Smissen, R. D. (2013). Revised circumscription of *Nothofagus* and recognition of the segregate genera *Fuscospora*, *Lophozonia*, and *Trisyngyne* (Nothofagaceae). *Phytotaxa, 146*(1), 1–31. doi:10.11646/phytotaxa.146.1.1

Hejnol, A., Obst, M., Stamatakis, A., Ott, M., Rouse, G. W., Edgecombe, G. D., . . . Dunn, C. W. (2009). Assessing the root of bilaterian animals with scalable phylogenomic methods. *Proceedings of the Royal Society of London B, 276*(1677), 4261–4270. doi:10.1098/rspb.2009.0896

Hickman, V. V. (1939). Opiliones and Araneae. *Reports: British and New Zealand Antarctic Research Expedition 1929–1931, 4*(5), 159–187.

Hickman, V. V. (1958). Some Tasmanian harvestmen of the family Triaenonychidae (sub-order Laniatores). *Papers and Proceedings of the Royal Society of Tasmania, 92*, 1–116.

Hoang, D. T., Chernomor, O., von Haeseler, A., Minh, B. Q., & Vinh, L. S. (2018). UFBoot2: Improving the Ultrafast Bootstrap Approximation. *Molecular Biology and Evolution, 35*(2), 518–522. doi:10.1093/molbev/msx281

Hogg, H. R. (1920). Some Australian Opiliones. *Proceedings of the Zoological Society of London*, 31–48.

Huang, D., Hormiga, G., Cai, C., Su, Y., Yin, Z., Xia, F., & Giribet, G. (2018). Origin of spiders and their spinning organs illuminated by mid-Cretaceous amber fossils. *Nature Ecology & Evolution, 2*(4), 623–627. doi:10.1038/s41559-018-0475-9

Hunt, G. S. (1990). *Hickmanoxyomma*, a new genus of cavernicolous harvestmen from Tasmania (Opiliones: Triaenonychidae). *Records of the Australian Museum, 42*(1), 45–68. doi:10.3853/j.0067-1975.42.1990.106

Hunt, G. S. (1996). A preliminary phylogenetic analysis of Australian Triaenonychidae (Arachnida: Opiliones). *Revue Suisse de Zoologie*, 295–308.

Hunt, G. S., & Hickman, J. L. (1993). A revision of the genus *Lomanella* Pocock and its implications for family level classification in the Travunioidea (Arachnida: Opiliones: Triaenonychidae). *Records of the Australian Museum, 45*, 81–119.

Huson, D. H., & Bryant, D. (2006). Application of phylogenetic networks in evolutionary studies. *Molecular Biology and Evolution, 23*(2), 254–267. doi:10.1093/molbev/msj030

Iturralde-Vinent, M., & MacPhee, R. D. E. (1999). Paleogeography of the Caribbean region: implications for Cenozoic biogeography. *Bulletin of the American Museum of Natural History, 238*, 1–95.

Jeffery, N. W., Oliveira, I. S., Gregory, T. R., Rowell, D. M., & Mayer, G. (2012). Genome size and chromosome number in velvet worms (Onychophora). *Genetica, 140*(10-12), 497–504. doi:10.1007/s10709-013-9698-5

Kalyaanamoorthy, S., Minh, B. Q., Wong, T. K. F., von Haeseler, A., & Jermiin, L. S. (2017). ModelFinder: fast model selection for accurate phylogenetic estimates. *Nature Methods, 14*(6), 587–589. doi:10.1038/nmeth.4285

Kamei, R. G., San Mauro, D., Gower, D. J., Van Bocxlaer, I., Sherratt, E., Thomas, A., . . . Biju, S. D. (2012). Discovery of a new family of amphibians from northeast India with ancient links to Africa. *Proceedings of the Royal Society B: Biological Sciences, 279*(1737), 2396–2401. doi:10.1098/rspb.2012.0150

Karaman, I. (2019). A redescription and family placement of *Buemarinoa patrizii* Roewer, 1956 (Opiliones, Laniatores, Triaenonychidae). *Biologia Serbica, 41*(1), 67–77. doi:10.5281/zenodo.3373487

Karsch, F. A. F. (1880). Arachnologische Blätter (Decas I). IX. Neue Phalangiden des Berliner Museums. *Zeitschrift für die gesammten Naturwissenschaften, 53*(6), 400–404.

Katoh, K., & Standley, D. M. (2014). MAFFT: iterative refinement and additional methods. *Methods in Molecular Biology, 1079*, 131–146. doi:10.1007/978-1-62703-646-7_8

Kauri, H. (1961). Opiliones. In B. Hanström, P. Brinck, & G. Rudebeck (Eds.), *South African Animal Life: Results of the Lund University Expedition in 1950-1951* (Vol. 8, pp. 9–197). Uppsala: Almquist & Wiksell.

Kearse, M., Moir, R., Wilson, A., Stones-Havas, S., Cheung, M., Sturrock, S., . . . Drummond, A. (2012). Geneious Basic: an integrated and extendable desktop software platform for the organization and analysis of sequence data. *Bioinformatics, 28*(12), 1647–1649. doi:10.1093/bioinformatics/bts199

Kishino, H., Miyata, T., & Hasegawa, M. (1990). Maximum likelihood inference of protein phylogeny and the origin of chloroplasts. *Journal of Molecular Evolution, 31*(2), 151–160. doi:10.1007/bf02109483

Kocot, K. M., Struck, T. H., Merkel, J., Waits, D. S., Todt, C., Brannock, P. M., . . . Halanych, K. M. (2017). Phylogenomics of Lophotrochozoa with consideration of systematic error. *Systematic Biology, 66*(2), 256–282. doi:10.1093/sysbio/syw079

Krosch, M. N., Baker, A. M., Mather, P. B., & Cranston, P. S. (2011). Systematics and biogeography of the Gondwanan Orthocladiinae (Diptera: Chironomidae). *Molecular Phylogenetics and Evolution, 59*(2), 458–468. doi:10.1016/j.ympev.2011.03.003

Kuck, P., & Struck, T. H. (2014). BaCoCa--a heuristic software tool for the parallel assessment of sequence biases in hundreds of gene and taxon partitions. *Molecular Phylogenetics and Evolution, 70*, 94–98. doi:10.1016/j.ympev.2013.09.011

Kury, A. B. (2004). A new genus of Triaenonychidae from South Africa (Opiliones, Laniatores). *Revista Ibérica de Aracnología, 9*, 205–210.

Kury, A. B. (2017). When the Danish diacritic evaporates: nomenclatural considerations on the generic name *Sorensenella* Pocock, 1903 (Opiliones: Insidiatores: Triaenonychidae). *Arachnida – Revisita Arachnologica Italiana, 14*.

Kury, A. B., Mendes, A. C., & Souza, D. R. (2014). World checklist of Opiliones species (Arachnida). Part 1: Laniatores - Travunioidea and Triaenonychoidea. *Biodiversity Data Journal, 2*, e4094. doi:10.3897/BDJ.2.e4094

Lagomarsino, L. P., Condamine, F. L., Antonelli, A., Mulch, A., & Davis, C. C. (2016). The abiotic and biotic drivers of rapid diversification in Andean bellflowers (Campanulaceae). *New Phytologist, 210*(4), 1430–1442. doi:10.1111/nph.13920

Lambeck, K., & Chappell, J. (2001). Sea level change through the last glacial cycle. *Science, 292*(5517), 679–686.

Landis, C. A., Campbell, H. J., Begg, J. G., Mildenhall, D. C., Paterson, A. M., & Trewick, S. A. (2008). The Waipounamu Erosion Surface: questioning the antiquity of the New Zealand land surface and terrestrial fauna and flora. *Geological Magazine, 145*(02), 173–197. doi:10.1017/s0016756807004268

Lartillot, N., Lepage, T., & Blanquart, S. (2009). PhyloBayes 3: a Bayesian software package for phylogenetic reconstruction and molecular dating. *Bioinformatics, 25*(17), 2286–2288. doi:10.1093/bioinformatics/btp368

Lartillot, N., Rodrigue, N., Stubbs, D., & Richer, J. (2013). PhyloBayes MPI: phylogenetic reconstruction with infinite mixtures of profiles in a parallel environment. *Systematic Biology, 62*(4), 611–615. doi:10.1093/sysbio/syt022

Laumer, C. E., Fernandez, R., Lemer, S., Combosch, D., Kocot, K. M., Riesgo, A., . . . Giribet, G. (2019). Revisiting metazoan phylogeny with genomic sampling of all phyla. *Proceedings of the Royal Society B: Biological Sciences, 286*(1906), 20190831. doi:10.1098/rspb.2019.0831

Laumer, C. E., Hejnol, A., & Giribet, G. (2015). Nuclear genomic signals of the 'microturbellarian' roots of platyhelminth evolutionary innovation. *Elife, 4*. doi:10.7554/eLife.05503

Lawrence, R. F. (1931). The harvest-spiders (Opiliones) of South Africa. *Annals of the South African Museum, 29*(2), 341–508.

Lawrence, R. F. (1933). The harvest-spiders (Opiliones) of Natal. *Annals of the Natal Museum, 7*(2), 211–241.

Lawrence, R. F. (1934). New South African Opiliones. *Annals of the South African Museum, 30*(4), 549–586.

Lawrence, R. F. (1959). Arachnides – Opilions. *Faune de Madagascar, 9*, 1–121.

Lee, M. S., Soubrier, J., & Edgecombe, G. D. (2013). Rates of phenotypic and genomic evolution during the Cambrian explosion. *Current Biology, 23*(19), 1889–1895. doi:10.1016/j.cub.2013.07.055

Lewis, K. B., Carter, L., & Davey, F. J. (1994). The opening of Cook Strait: Interglacial tidal scour and aligning basins at a subduction to transform plate edge. *Marine Geology, 116*(3-4), 293–312. doi:10.1016/0025-3227(94)90047-7

Li, H., & Durbin, R. (2009). Fast and accurate short read alignment with Burrows-Wheeler transform. *Bioinformatics, 25*(14), 1754–1760. doi:10.1093/bioinformatics/btp324

Li, H., Handsaker, B., Wysoker, A., Fennell, T., Ruan, J., Homer, N., . . . Genome Project Data Processing, S. (2009). The Sequence Alignment/Map format and SAMtools. *Bioinformatics, 25*(16), 2078–2079. doi:10.1093/bioinformatics/btp352

Loman, J. C. C. (1898). Neue Opilioniden von Süd-Afrika und Madagaskar. Ergebnisse einer Reise von Prof. Max Weber im Jahre 1894. *Zoologische Jahrbücher, Abteilung für Systematik, Ökologie und Geographie der Tiere, 11*(6), 515–530.

Loman, J. C. C. (1901). Ueber die geographische Verbreitung der Opilioniden. *Zoologische Jahrbücher, Abteilung für Systematik, Ökologie und Geographie der Tiere, 13*, 71–104.

Loman, J. C. C. (1902). Neue aussereuropäische Opilioniden. *Zoologische Jahrbücher, Abteilung für Systematik, Ökologie und Geographie der Tiere, 16*(2), 163–216.

Lozano-Fernandez, J., Giacomelli, M., Fleming, J. F., Chen, A., Vinther, J., Thomsen, P. F., . . . Olesen, J. (2019). Pancrustacean evolution illuminated by taxon-rich genomic-scale data sets with an expanded remipede sampling. *Genome Biology and Evolution, 11*(8), 2055–2070. doi:10.1093/gbe/evz097

Machado, G. (2007). Maternal or paternal egg guarding? Revisiting parental care in triaenonychid harvestmen (Opiliones). *Journal of Arachnology, 35*(1), 202–204. doi:10.1636/sh06-14.1

Mao, K., Milne, R. I., Zhang, L., Peng, Y., Liu, J., Thomas, P., . . . Renner, S. S. (2012). Distribution of living Cupressaceae reflects the breakup of Pangea. *Proceedings of the National Academy of Sciences of the USA, 109*(20), 7793–7798. doi:10.1073/pnas.1114319109

Mapalo, M. A., Arakawa, K., Baker, C. M., Persson, D. K., Mirano-Bascos, D., & Giribet, G. (2020). The unique antimicrobial recognition and signaling pathways in Tardigrades with a comparison across Ecdysozoa. *G3: Genes, Genomes, Genetics, 10*(3), 1137–1148. doi:10.1534/g3.119.400734

Marske, K. A., Leschen, R. A., & Buckley, T. R. (2011). Reconciling phylogeography and ecological niche models for New Zealand beetles: Looking beyond glacial refugia. *Molecular Phylogenetics and Evolution, 59*(1), 89–102. doi:10.1016/j.ympev.2011.01.005

Martin, H. A. (2006). Cenozoic climatic change and the development of the arid vegetation in Australia. *Journal of Arid Environments, 66*(3), 533–563. doi:10.1016/j.jaridenv.2006.01.009

Maury, E. A. (1988). Triaenonychidae sudamericanos III. Descripción de los nuevos géneros *Nahuelonyx* y *Valdivionyx* (Opiliones, Laniatores). *Journal of Arachnology, 16*, 71–83.

Maury, E. A. (1990). Triaenonychidae Sudamericanos. VI. Tres nuevas especies del género *Nuncia* Loman 1902 (Opiliones, Laniatores). *Boletin de la Sociedad de Biología de Concepción, 61*, 103–119.

May, M. R., Höhna, S., Moore, B. R., & Cooper, N. (2016). A Bayesian approach for detecting the impact of mass-extinction events on molecular phylogenies when rates of lineage diversification may vary. *Methods in Ecology and Evolution, 7*(8), 947–959. doi:10.1111/2041-210x.12563

Mayer, G. (2007). *Metaperipatus inae* sp. nov. (Onychophora: Peripatopsidae) from Chile with a novel ovarian type and dermal insemination. *Zootaxa, 1440*, 21–37.

Mayer, G., Franke, F. A., Treffkorn, S., Gross, V., & de Sena Oliveira, I. (2015). Onychophora. In A. Wanninger (Ed.), *Evolutionary Developmental Biology of Invertebrates 3* (pp. 53–98): Springer-Verlag.

Mayer, G., Whitington, P. M., Sunnucks, P., & Pfluger, H. J. (2010). A revision of brain composition in Onychophora (velvet worms) suggests that the tritocerebrum evolved in arthropods. *BMC Evolutionary Biology, 10*, 255. doi:10.1186/1471-2148-10-255

McGlone, M. S. (1985). Plant biogeography and the late Cenozoic history of New Zealand. *New Zealand Journal of Botany, 23*(4), 723–749. doi:10.1080/0028825x.1985.10434240

McGlone, M. S. (2005). Goodbye Gondwana. *Journal of Biogeography, 32*(5), 739–740. doi:10.1111/j.1365-2699.2005.01278.x

McGuire, J. A., Witt, C. C., Remsen, J. V., Jr., Corl, A., Rabosky, D. L., Altshuler, D. L., & Dudley, R. (2014). Molecular phylogenetics and the diversification of hummingbirds. *Current Biology, 24*(8), 910–916. doi:10.1016/j.cub.2014.03.016

McKenna, A., Hanna, M., Banks, E., Sivachenko, A., Cibulskis, K., Kernytsky, A., . . . DePristo, M. A. (2010). The Genome Analysis Toolkit: a MapReduce framework for analyzing next-generation DNA sequencing data. *Genome Research, 20*(9), 1297–1303. doi:10.1101/gr.107524.110

McLoughlin, S. (2001). The breakup history of Gondwana and its impact on pre-Cenozoic floristic provincialism. *Australian Journal of Botany, 49*(3), 271–300. doi:10.1071/bt00023

McLoughlin, S., & Kear, B. P. (2010). The Australasian Cretaceous scene. *Alcheringa: An Australasian Journal of Palaeontology, 34*(3), 197–203. doi:10.1080/03115518.2010.497264

Meirmans, P. G., & Van Tienderen, P. H. (2004). GENOTYPE and GENODIVE: two programs for the analysis of genetic diversity of asexual organisms. *Molecular Ecology Notes, 4*(4), 792–794. doi:10.1111/j.1471-8286.2004.00770.x

Mendes, A. C. (2009). *Avaliação do status sistemático dos táxons supragenéricos da infra-ordem Insidiatores Loman, 1902 (Arachnida, Opiliones, Laniatores).* (Ph.D.). Universidade Federal do Rio de Janeiro.

Mendes, A. C., & Kury, A. B. (2008). Intercontinental Triaenonychidae—the case of *Ceratomontia* (Opiliones, Insidiatores). *Journal of Arachnology, 36*(2), 273–279. doi:10.1636/ch07-93.1

Miller, M. A., Pfeiffer, W., & Schwartz, T. (2010). Creating the CIPRES Science Gateway for inference of large phylogenetic trees. *Proceedings of the Gateway Computing Environments Workshop (GCE)*, 1–8.

Mirarab, S., Reaz, R., Bayzid, M. S., Zimmermann, T., Swenson, M. S., & Warnow, T. (2014). ASTRAL: genome-scale coalescent-based species tree estimation. *Bioinformatics, 30*(17), i541–i548. doi:10.1093/bioinformatics/btu462

Misof, B., Liu, S., Meusemann, K., Peters, R. S., Donath, A., Mayer, C., . . . Zhou, X. (2014). Phylogenomics resolves the timing and pattern of insect evolution. *Science, 346*(6210), 763–767. doi:10.1126/science.1257570

Mitchell, K. J., Llamas, B., Soubrier, J., Rawlence, N. J., Worthy, T. H., Wood, J., . . . Cooper, A. (2014). Ancient DNA reveals elephant birds and kiwi are sister taxa and clarifies ratite bird evolution. *Science, 344*(6186), 898–900. doi:10.1126/science.1251981

Monge-Nájera, J. (1995). Phylogeny, biogeography and reproductive trends in the Onychophora. *Zoological Journal of the Linnean Society, 114*(1), 21–60. doi:10.1111/j.1096-3642.1995.tb00111.x

Monge-Nájera, J., Barrientos, Z., & Aguilar, F. (1993). Behavior of *Epiperipatus biolleyi* (Onychophora: Peripatidae) under laboratory conditions. *Revista de Biologia Tropical, 41*(3), 689–696.

Mora, M., Herrera, A., & León, P. (1994). The genome of *Epiperipatus biolleyi* (Perpatidae), a Costa Rican onychophoran. *Revista de Biologia Tropical, 44*(1), 153–157.

Mortimer, N., Campbell, H. J., Tulloch, A. J., King, P. R., Stagpoole, V. M., Wood, R. A., . . . Seton, M. (2017). Zealandia: Earth's Hidden Continent. *GSA Today*, 27–35. doi:10.1130/gsatg321a.1

Muñoz-Cuevas, A. (1972). Presencia de la tribu Triaenobunini en Chile. Descripción del nuevo género y de la nueva especie *Americobunus ringueleti* (Arachnida, Opiliones, Triaenonychidae). *Physis, 31*(82), 1–7.

Muñoz-Cuevas, A. (1973). Descripción de *Araucanobunus juberthiei* gen. et sp. nov. de Triaenobunini del Chile (Arachnida, Opiliones, Triaenonychidae). *Physis, 32*(84), 173–179.

Murienne, J., Daniels, S. R., Buckley, T. R., Mayer, G., & Giribet, G. (2014). A living fossil tale of Pangaean biogeography. *Proceedings of the Royal Society of London B, 281*(1775), 20132648. doi:10.1098/rspb.2013.2648

Myers, N., Mittermeier, R. A., Mittermeier, C. G., da Fonseca, G. A., & Kent, J. (2000). Biodiversity hotspots for conservation priorities. *Nature, 403*(6772), 853–858. doi:10.1038/35002501

Nattier, R., Pellens, R., Robillard, T., Jourdan, H., Legendre, F., Caesar, M., . . . Grandcolas, P. (2017). Updating the phylogenetic dating of New Caledonian biodiversity with a meta-analysis of the available evidence. *Scientific Reports, 7*(1), 3705. doi:10.1038/s41598-017-02964-x

Nguyen, L.-T., Schmidt, H. A., von Haeseler, A., & Minh, B. Q. (2015). IQ-TREE: A fast and effective stochastic algorithm for estimating maximum-likelihood phylogenies. *Molecular Biology and Evolution, 32*(1), 268–274. doi:10.1093/molbev/msu300

O'Dea, A., Lessios, H. A., Coates, A. G., Eytan, R. I., Restrepo-Moreno, S. A., Cione, A. L., . . . Jackson, J. B. (2016). Formation of the Isthmus of Panama. *Science Advances, 2*(8), e1600883. doi:10.1126/sciadv.1600883

Oliveira, I. d. S., Bai, M., Jahn, H., Gross, V., Martin, C., Hammel, J. U., . . . Mayer, G. (2016). Earliest onychophoran in amber reveals Gondwanan migration patterns. *Current Biology, 26*(19), 2594–2601. doi:10.1016/j.cub.2016.07.023

Oliveira, I. d. S., Franke, F. A., Hering, L., Schaffer, S., Rowell, D. M., Weck-Heimann, A., . . . Mayer, G. (2012). Unexplored character diversity in onychophora (velvet worms): A comparative study of three peripatid species. *PLoS One, 7*(12), e51220. doi:10.1371/journal.pone.0051220

Oliveira, I. d. S., Lacorte, G. A., Fonseca, C. G., Wieloch, A. H., & Mayer, G. (2011). Cryptic speciation in Brazilian *Epiperipatus* (Onychophora: Peripatidae) reveals an underestimated diversity among the peripatid velvet worms. *PLoS One, 6*(6), e19973. doi:10.1371/journal.pone.0019973

Oliveira, I. d. S., Lacorte, G. A., Weck-Heimann, A., Cordeiro, L. M., Wieloch, A. H., & Mayer, G. (2014). A new and critically endangered species and genus of Onychophora (Peripatidae) from the Brazilian savannah – a vulnerable biodiversity hotspot. *Systematics and Biodiversity, 13*(3), 211–233. doi:10.1080/14772000.2014.985621

Oliveira, I. d. S., & Mayer, G. (2017). A new giant egg-laying onychophoran (Peripatopsidae) reveals evolutionary and biogeographical aspects of Australian velvet worms. *Organisms Diversity & Evolution, 17*(2), 375–391. doi:10.1007/s13127-016-0321-3

Oliveira, I. d. S., Read, V. M., & Mayer, G. (2012). A world checklist of Onychophora (velvet worms), with notes on nomenclature and status of names. *Zookeys*(211), 1–70. doi:10.3897/zookeys.211.3463

Oliveira, I. d. S., Ruhberg, H., Rowell, D. M., & Mayer, G. (2018). Revision of Tasmanian viviparous velvet worms (Onychophora : Peripatopsidae) with descriptions of two new species. *Invertebrate Systematics, 32*(4), 909–932. doi:10.1071/is17096

Oliveira, I. d. S., Schaffer, S., Kvartalnov, P. V., Galoyan, E. A., Palko, I. V., Weck-Heimann, A., . . . Mayer, G. (2013). A new species of *Eoperipatus* (Onychophora) from Vietnam reveals novel morphological characters for the South-East Asian Peripatidae. *Zoologischer Anzeiger, 252*(4), 495–510. doi:10.1016/j.jcz.2013.01.001

Oliveira, I. d. S., Wieloch, A. H., & Mayer, G. (2010). Revised taxonomy and redescription of two species of the Peripatidae (Onychophora) from Brazil: a step towards consistent terminology of morphological characters. *Zootaxa, 2493*(16–34).

Ortega-Hernández, J. (2016). Making sense of 'lower' and 'upper' stem-group Euarthropoda, with comments on the strict use of the name Arthropoda von Siebold, 1848. *Biological Reviews, 91*(1), 255–273. doi:10.1111/brv.12168

Ortiz-Juareguizar, E., & Pascual, R. (2011). The tectonic setting of the Caribbean region and the K/T turnover of the South American land-mammal fauna. *Boletín Geológico y Minero, 122*(3), 333–344.

Papadopoulou, A., Anastasiou, I., & Vogler, A. P. (2010). Revisiting the insect mitochondrial molecular clock: the mid-Aegean trench calibration. *Molecular Biology and Evolution, 27*(7), 1659–1672. doi:10.1093/molbev/msq051

Peck, J. R., Yearsley, J. M., & Waxman, D. (1998). Explaining the geographic distributions of sexual and asexual populations. *Nature, 391*(6670), 889–892. doi:10.1038/36099

Phillips, W. J., & Grimmett, R. E. R. (1932). Some new Opiliones from New Zealand. *Proceedings of the Zoological Society of London*, 731–740.

Pocock, R. I. (1903a). Fifteen new species and two new genera of tropical and southern Opiliones. *The Annals and Magazine of Natural History, Séries 7, 11*, 433–450.

Pocock, R. I. (1903b). On some new harvest-spiders of the order Opiliones from the southern continents. *Proceedings of the Zoological Society of London, 2*(2), 392–413.

Podsiadlowski, L., Braband, A., & Mayer, G. (2008). The complete mitochondrial genome of the onychophoran *Epiperipatus biolleyi* reveals a unique transfer RNA set and provides further support for the ecdysozoa hypothesis. *Molecular Biology and Evolution, 25*(1), 42–51. doi:10.1093/molbev/msm223

Porras-Hurtado, L., Ruiz, Y., Santos, C., Phillips, C., Carracedo, A., & Lareu, M. V. (2013). An overview of STRUCTURE: applications, parameter settings, and supporting software. *Frontiers in Genetics, 4*, 98. doi:10.3389/fgene.2013.00098

Porto, W., & Pérez-Gonázlez, A. (2019). Redescription of the New Zealand harvestman *Nuncia obesa obesa* (Opiliones: Laniatores: Triaenonychidae) and implications for the supposed transcontinental distribution of *Nuncia*. *Journal of Arachnology, 47*, 370–376.

Pritchard, J. K., Stephens, M., & Donnelly, P. (2000). Inference of population structure using multilocus genotype data. *Genetics, 155*, 954–959.

Pyron, R. A. (2014). Biogeographic analysis reveals ancient continental vicariance and recent oceanic dispersal in amphibians. *Systematic Biology, 63*(5), 779–797. doi:10.1093/sysbio/syu042

Rabosky, D. L. (2014). Automatic detection of key innovations, rate shifts, and diversity-dependence on phylogenetic trees. *PLoS One, 9*(2), e89543. doi:10.1371/journal.pone.0089543

Rambaut, A., & Drummond, A. J. (2009). Tracer v. 1.6. Program and documentation available at < http://tree.bio.ed.ac.uk/software/tracer/ >.

Ranwez, V., Harispe, S., Delsuc, F., & Douzery, E. J. (2011). MACSE: Multiple Alignment of Coding SEquences accounting for frameshifts and stop codons. *PLoS One, 6*(9), e22594. doi:10.1371/journal.pone.0022594

Reid, A. L. (1996). Review of the Peripatopsidae (Onychophora) in Australia, with comments on peripatopsid relationships. *Invertebrate Taxonomy, 10*(4), 663–936. doi:10.1071/it9960663

Ritchie, A. M., Lo, N., & Ho, S. Y. W. (2017). The impact of the tree prior on molecular dating of data sets containing a mixture of inter- and intraspecies sampling. *Systematic Biology, 66*(3), 413–425. doi:10.1093/sysbio/syw095

Rix, M. G., Edwards, D. L., Byrne, M., Harvey, M. S., Joseph, L., & Roberts, J. D. (2015). Biogeography and speciation of terrestrial fauna in the south-western Australian biodiversity hotspot. *Biological Reviews, 90*(3), 762–793. doi:10.1111/brv.12132

Rix, M. G., & Harvey, M. S. (2012). Phylogeny and historical biogeography of ancient assassin spiders (Araneae: Archaeidae) in the Australian mesic zone: evidence for Miocene speciation within Tertiary refugia. *Molecular Phylogenetics and Evolution, 62*(1), 375–396. doi:10.1016/j.ympev.2011.10.009

Roewer, C. F. (1914). Opilioniden von Neu-Caledonien. In: Sarasin, F. & J. Roux (eds). *Nova Caledonia, 1*(4,12), 439–443.

Roewer, C. F. (1915). Die Familie der Triaenonychidae der Opiliones – Laniatores. *Archiv für Naturgeschichte, 80*(12), 61–168.

Roewer, C. F. (1931). Über Triaenonychiden (6. Ergänzung der "Weberknechte der Erde", 1923). *Zeitschrift für wissenschaftliche Zoologie, 138*(1), 137–185.

Roewer, C. F. (1956). Cavernicole Arachniden aus Sardinien II. *Fragmenta Entomologica, 2*(9), 97–104.

Roewer, C. F. (1961). Opiliones aus Süd-Chile. *Senckenbergiana Biologica, 42*(1/2), 99–105.

Rohland, N., & Reich, D. (2012). Cost-effective, high-throughput DNA sequencing libraries for multiplexed target capture. *Genome Research, 22*(5), 939–946. doi:10.1101/gr.128124.111

Rota-Stabelli, O., Daley, A. C., & Pisani, D. (2013). Molecular timetrees reveal a Cambrian colonization of land and a new scenario for ecdysozoan evolution. *Current Biology, 23*(5), 392–398. doi:10.1016/j.cub.2013.01.026

Ruhberg, H. (1985). Die Peripatopsidae (Onychophora). Systematik, Ökologie, Chorologie und phylogenetische Aspekte. *Zoologica, 46*, 1–183.

Sampaio Costa, C. (2016). *Sistemática e análise filogenética de Epiperipatus Clark, 1913 baseada em dados moleculares e morfológicos (Onychophora: Peripatidae).* (Ph.D.). Universidade de São Paulo.

Sanmartín, I., & Ronquist, F. (2004). Southern hemisphere biogeography inferred by event-based models: plant versus animal patterns. *Systematic Biology, 53*(2), 216–243. doi:10.1080/10635150490423430

Sato, S., Buckman-Young, R. S., Harvey, M. S., & Giribet, G. (2018). Cryptic speciation in a biodiversity hotspot: multilocus molecular data reveal new velvet worm species from Western Australia (Onychophora : Peripatopsidae : Kumbadjena). *Invertebrate Systematics, 32*(6), 1249–1264. doi:10.1071/is18024

Schwentner, M., Combosch, D. J., Pakes Nelson, J., & Giribet, G. (2017). A phylogenomic solution to the origin of insects by resolving crustacean-hexapod relationships. *Current Biology, 27*(12), 1818–1824. doi:10.1016/j.cub.2017.05.040

Scotese, Christopher R. (2004). A continental drift flipbook. *The Journal of Geology, 112*(6), 729-741. doi:10.1086/424867

Selden, P. A., Dunlop, J. A., Giribet, G., Zhang, W., & Ren, D. (2016). The oldest armoured harvestman (Arachnida: Opiliones: Laniatores), from Upper Cretaceous Myanmar amber. *Cretaceous Research, 65*, 206–212. doi:10.1016/j.cretres.2016.05.004

Sharma, P. P., Baker, C. M., Cosgrove, J. G., Johnson, J. E., Oberski, J. T., Raven, R. J., . . . Giribet, G. (2018). A revised dated phylogeny of scorpions: phylogenomic support for ancient

divergence of the temperate Gondwanan family Bothriuridae. *Molecular Phylogenetics and Evolution, 122*, 37–45. doi:10.1016/j.ympev.2018.01.003

Sharma, P. P., & Giribet, G. (2011). The evolutionary and biogeographic history of the armoured harvestmen – Laniatores phylogeny based on ten molecular markers, with the description of two new families of Opiliones (Arachnida). *Invertebrate Systematics, 25*(2), 106–142. doi:10.1071/is11002

Sharma, P. P., & Giribet, G. (2014). A revised dated phylogeny of the arachnid order Opiliones. *Frontiers in Genetics, 5*, 255. doi:10.3389/fgene.2014.00255

Sharma, P. P., Kaluziak, S. T., Perez-Porro, A. R., Gonzalez, V. L., Hormiga, G., Wheeler, W. C., & Giribet, G. (2014). Phylogenomic interrogation of Arachnida reveals systemic conflicts in phylogenetic signal. *Molecular Biology and Evolution, 31*(11), 2963–2984. doi:10.1093/molbev/msu235

Shear, W. A. (1977). *Fumontana deprehendor*, n. gen., n. sp., the first triaenonychid opilionid from eastern North America (Opiliones: Laniatores: Triaenonychidae). *Journal of Arachnology, 3*, 177–183.

Shear, W. A. (1980). A review of the Cyphophthalmi of the United States and Mexico, with a proposed reclassification of the suborder (Arachnida, Opiliones). *American Museum Novitates, 2705*, 1–34.

Shimodaira, H. (2002). An approximately unbiased test of phylogenetic tree selection. *Systematic Biology, 51*(3), 492–508. doi:10.1080/10635150290069913

Simão, F. A., Waterhouse, R. M., Ioannidis, P., Kriventseva, E. V., & Zdobnov, E. M. (2015). BUSCO: assessing genome assembly and annotation completeness with single-copy orthologs. *Bioinformatics, 31*(19), 3210-3212. doi:10.1093/bioinformatics/btv351

Simon, E. (1899). Ergebnisse einer Reise nach dem Pacific (Schauinsland 1896–1897). *Zoologische Jahrbücher, 12*(4), 411–437.

Smith, M. R., & Ortega-Hernández, J. (2014). *Hallucigenia*'s onychophoran-like claws and the case for Tactopoda. *Nature, 514*(7522), 363–366. doi:10.1038/nature13576

Smith, S. A., & Dunn, C. W. (2008). Phyutility: a phyloinformatics tool for trees, alignments and molecular data. *Bioinformatics, 24*(5), 715–716. doi:10.1093/bioinformatics/btm619

Soares, H. E. M. (1968). Contribuição ao estudo dos opiliões do Chile (Opiliones: Gonyleptidae, Triaenonychidae). *Papéis avulsos de zoologia, 21*(27), 259–272.

Sørensen, W. E. (1886). Opiliones. In L. Koch & E. v. Keyserling (Eds.), *Die Arachniden Australiens nach der Natur bechrieben und abgebildt* (Vol. 2, pp. 53–86).

Sørensen, W. E. (1902). Gonyleptiden (Opiliones, Laniatores). *Ergebnisse der Hamburger Magalhaensischen Sammelreise, 6*(5), 1–36.

Stamatakis, A. (2014). RAxML version 8: a tool for phylogenetic analysis and post-analysis of large phylogenies. *Bioinformatics, 30*(9), 1312–1313. doi:10.1093/bioinformatics/btu033

Starrett, J., Derkarabetian, S., Hedin, M., Bryson, R. W., Jr., McCormack, J. E., & Faircloth, B. C. (2017). High phylogenetic utility of an ultraconserved element probe set designed for Arachnida. *Molecular Ecology Resources, 17*(4), 812–823. doi:10.1111/1755-0998.12621

Strand, E. (1932). Miscellanea nomenclatorica zoologica et palaeontologica III. *Nochmals: Nomenklatur und Ethik*, 133–196.

Strimmer, K., & von Haeseler, A. (1997). Likelihood-mapping: A simple method to visualize phylogenetic content of a sequence alignment. *Proceedings of the National Academy of Sciences, 94*(13), 6815–6819. doi:10.1073/pnas.94.13.6815

Sukumaran, J., & Knowles, L. L. (2017). Multispecies coalescent delimits structure, not species. *Proceedings of the Natlional Academy of Sciences of the USA, 114*(7), 1607–1612. doi:10.1073/pnas.1607921114

Sutherland, R., Dickens, G. R., Blum, P., Agnini, C., Alegret, L., Asatryan, G., . . . Zhou, X. (2020). Continental-scale geographic change across Zealandia during Paleogene subduction initiation. *Geology, 48*, 1–6. doi:10.1130/g47008.1

Tait, N. N., & Briscoe, D. A. (1995). Genetic differentiation within New Zealand Onychophora and their relationships to the Australian fauna. *Zoological Journal of the Linnean Society, 114*(1), 103–113. doi:10.1006/zjls.1995.0019

Talavera, G., & Castresana, J. (2007). Improvement of phylogenies after removing divergent and ambiguously aligned blocks from protein sequence alignments. *Systematic Biology, 56*(4), 564–577. doi:10.1080/10635150701472164

Taylor, C. K. (2011). Revision of the genus *Megalopsalis* (Arachnida: Opiliones: Phalangioidea) in Australia and New Zealand and implications for phalangioid classification. *Zootaxa, 2773*, 1–65.

Thomas, S. M., & Hedin, M. (2008). Multigenic phylogeographic divergence in the paleoendemic southern Appalachian opilionid *Fumontana deprehendor* Shear (Opiliones, Laniatores, Triaenonychidae). *Molecular Phylogenetics and Evolution, 46*(2), 645–658. doi:10.1016/j.ympev.2007.10.013

Thorell, T. T. T. (1876). Sopra alcuni Opilioni (Phalangidea) d'Europa e dell' Asia occidentale, con un quadro dei generi europei di quest' Ordine. *Annali del Museo Civico di Storia Naturale di Genova, 8*, 452–508.

Toussaint, E. F. A., Bloom, D., & Short, A. E. Z. (2017). Cretaceous West Gondwana vicariance shaped giant water scavenger beetle biogeography. *Journal of Biogeography, 44*(9), 1952–1965. doi:10.1111/jbi.12977

Trewick, S. A. (1998). Sympatric cryptic species in New Zealand Onychophora. *Biological Journal of the Linnean Society, 63*(3), 307–329. doi:10.1111/j.1095-8312.1998.tb01520.x

Trewick, S. A. (2000). Mitochondrial DNA sequences support allozyme evidence for cryptic radiation of New Zealand *Peripatoides* (Onychophora). *Molecular Ecology, 9*(3), 269–281. doi:10.1046/j.1365-294x.2000.00873.x

Trewick, S. A., & Bland, K. J. (2012). Fire and slice: palaeogeography for biogeography at New Zealand's North Island/South Island juncture. *Journal of the Royal Society of New Zealand, 42*(3), 153–183. doi:10.1080/03036758.2010.549493

Trewick, S. A., Paterson, A. M., & Campbell, H. J. (2006). Hello New Zealand. *Journal of Biogeography, 34*(1), 1–6. doi:10.1111/j.1365-2699.2006.01643.x

Vaidya, G., Lohman, D. J., & Meier, R. (2011). SequenceMatrix: concatenation software for the fast assembly of multi-gene datasets with character set and codon information. *Cladistics, 27*(2), 171–180. doi:10.1111/j.1096-0031.2010.00329.x

van der Auwera, G. A., Carneiro, M. O., Hartl, C., Poplin, R., Del Angel, G., Levy-Moonshine, A., . . . DePristo, M. A. (2013). From FastQ data to high confidence variant calls: the Genome Analysis Toolkit best practices pipeline. *Current Protocols in Bioinformatics, 43*, 11.1011–1011.1010.1033. doi:10.1002/0471250953.bi1110s43

Vélez, S. (2011). *Biogeography and speciation of arthropods across the Tasman Sea: Craterostigmus tasmanianus (Chilopoda: Craterostigmomorpha: Craterostigmidae), Monoscutidae (Opiliones: Eupnoi: Phalangioidea), and Triaenonychidae (Opiliones: Laniatores).* (PhD Ph.D.). Harvard University.

Vélez, S., Fernández, R., & Giribet, G. (2014). A molecular phylogenetic approach to the New Zealand species of Enantiobuninae (Opiliones : Eupnoi : Neopilionidae). *Invertebrate Systematics, 28*(6), 565–589. doi:10.1071/is14030

Wachter, G. A., Papadopoulou, A., Muster, C., Arthofer, W., Knowles, L. L., Steiner, F. M., & Schlick-Steiner, B. C. (2016). Glacial refugia, recolonization patterns and diversification forces in Alpine-endemic *Megabunus* harvestmen. *Molecular Ecology, 25*(12), 2904–2919. doi:10.1111/mec.13634

Wallis, G. P., & Jorge, F. (2018). Going under down under? Lineage ages argue for extensive survival of the Oligocene marine transgression on Zealandia. *Molecular Ecology, 27*(22), 4368–4396. doi:10.1111/mec.14875

Wallis, G. P., & Trewick, S. A. (2009). New Zealand phylogeography: evolution on a small continent. *Molecular Ecology, 18*(17), 3548–3580. doi:10.1111/j.1365-294X.2009.04294.x

Wang, B., Dunlop, J. A., Selden, P. A., Garwood, R. J., Shear, W. A., Muller, P., & Lei, X. (2018). Cretaceous arachnid *Chimerarachne yingi* gen. et sp. nov. illuminates spider origins. *Nature Ecology & Evolution, 2*(4), 614–622. doi:10.1038/s41559-017-0449-3

Wei, W. (2004). Opening of the Australia–Antarctica Gateway as dated by nannofossils. *Marine Micropaleontology, 52*(1-4), 133–152. doi:10.1016/j.marmicro.2004.04.008

Werth, A., & Shear, W. (2014). The evolutionary truth about living fossils. *American Scientist, 102*(6), 434–443. doi:10.1511/2014.111.434

Wesener, T., Raupach, M. J., & Decker, P. (2011). Mountain refugia play a role in soil arthropod speciation on Madagascar: a case study of the endemic giant fire-millipede genus *Aphistogoniulus*. *PLoS One, 6*(12), e28035. doi:10.1371/journal.pone.0028035

Wesener, T., Raupach, M. J., & Sierwald, P. (2010). The origins of the giant pill-millipedes from Madagascar (Diplopoda: Sphaerotheriida: Arthrosphaeridae). *Molecular Phylogenetics and Evolution, 57*(3), 1184–1193. doi:10.1016/j.ympev.2010.08.023

Whiting, M. F., Carpenter, J. C., Wheeler, Q. D., & Wheeler, W. C. (1997). The Strepsiptera problem: phylogeny of the holometabolous insect orders inferred from 18S and 28S ribosomal DNA sequences and morphology. *Systematic Biology, 46*(1), 1–68. doi:10.1093/sysbio/46.1.1

Wolfe, J. M., Daley, A. C., Legg, D. A., & Edgecombe, G. D. (2016). Fossil calibrations for the arthropod Tree of Life. *Earth-Science Reviews, 160*, 43–110. doi:10.1016/j.earscirev.2016.06.008

Wood, H. M., Matzke, N. J., Gillespie, R. G., & Griswold, C. E. (2013). Treating fossils as terminal taxa in divergence time estimation reveals ancient vicariance patterns in the palpimanoid spiders. *Systematic Biology, 62*(2), 264–284. doi:10.1093/sysbio/sys092

Wu, M., Chatterji, S., & Eisen, J. A. (2012). Accounting for alignment uncertainty in phylogenomics. *PLoS One, 7*(1), e30288. doi:10.1371/journal.pone.0030288

Xie, W., Lewis, P. O., Fan, Y., Kuo, L., & Chen, M. H. (2011). Improving marginal likelihood estimation for Bayesian phylogenetic model selection. *Systematic Biology, 60*(2), 150–160. doi:10.1093/sysbio/syq085

Yang, J., Ortega-Hernandez, J., Gerber, S., Butterfield, N. J., Hou, J. B., Lan, T., & Zhang, X. G. (2015). A superarmored lobopodian from the Cambrian of China and early disparity in the evolution of Onychophora. *Proceedings of the National Academy of Sciences of the USA, 112*(28), 8678–8683. doi:10.1073/pnas.1505596112

Yang, Z., & Rannala, B. (2010). Bayesian species delimitation using multilocus sequence data. *Proceedings of the National Academy of Sciences of the USA, 107*(20), 9264–9269. doi:10.1073/pnas.0913022107

Yoshida, Y., Koutsovoulos, G., Laetsch, D. R., Stevens, L., Kumar, S., Horikawa, D. D., . . . Arakawa, K. (2017). Comparative genomics of the tardigrades *Hypsibius dujardini* and *Ramazzottius varieornatus*. *PLoS Biology, 15*(7), e2002266. doi:10.1371/journal.pbio.2002266

Young, M. R., & Hebert, P. D. (2015). Patterns of protein evolution in cytochrome *c* oxidase 1 (COI) from the Class Arachnida. *PLoS One, 10*(8), e0135053. doi:10.1371/journal.pone.0135053

Zarza, E., Connors, E. M., Maley, J. M., Tsai, W. L. E., Heimes, P., Kaplan, M., & McCormack, J. E. (2018). Combining ultraconserved elements and mtDNA data to uncover lineage diversity in a Mexican highland frog (*Sarcohyla*; Hylidae). *PeerJ, 6*, e6045. doi:10.7717/peerj.6045

Zerbino, D. R., & Birney, E. (2008). Velvet: algorithms for de novo short read assembly using de Bruijn graphs. *Genome Research, 18*(5), 821–829. doi:10.1101/gr.074492.107